ZooKeys 1109: 1–15 (2022)
doi: 10.3897/zookeys.1109.85565
https://zookeys.pensoft.net

RESEARCH ARTICLE

A peer-reviewed open-access journal
ZooKeys
Launched to accelerate biodiversity research

Lepocranus and *Valalyllum* gen. nov. (Orthoptera, Tetrigidae, Cladonotinae), endangered Malagasy dead-leaf-like grasshoppers

Maks Deranja[1], Niko Kasalo[1], Karmela Adžić[1], Damjan Franjević[1], Josip Skejo[1]

1 *University of Zagreb, Faculty of Science, Department of Biology, Division of Zoology, Evolution Lab, Rooseveltov trg 6, HR-10000 Zagreb, Croatia*

Corresponding authors: Maks Deranja (maks.deranja@gmail.com), Niko Kasalo (niko.kasalo5@gmail.com)

Academic editor: Zhu-Qing He | Received 19 April 2022 | Accepted 18 May 2022 | Published 1 July 2022

http://zoobank.org/FC606834-C259-4254-B8CA-9C5A6007246B

Citation: Deranja M, Kasalo N, Adžić K, Franjević D, Skejo J (2022) *Lepocranus* and *Valalyllum* gen. nov. (Orthoptera, Tetrigidae, Cladonotinae), endangered Malagasy dead-leaf-like grasshoppers. ZooKeys 1109: 1–15. https://doi.org/10.3897/zookeys.1109.85565

Abstract

Only two leaf-like pygmy grasshopper species and specimens are known from Madagascar: the Leatherback Pygmy Grasshopper (*Lepocranus fuscus* Devriese, 1991) —which has a relatively low median carina of the pronotum; and the Malagasy Litterhopper (*Valalyllum folium* **gen. et. sp. nov.**), herein described — which has a high median carina. *Lepocranus fuscus* is known from the rainforests around Tampolo, Manakambahiny, and Mahavelona (Foulpointe). The new taxon, *Valalyllum folium* **gen. et. sp. nov.** is known only from the Belanono forest. Both species inhabit northeastern Madagascar. The new species could be rare or not-easy-to-spot in the rainforest leaf litter, where it most probably lives. A new tribe, Valalyllini **trib. nov.**, is described for the two mentioned genera because its members are different from the Caribbean leaf-like Choriphyllini Cadena-Castañeda & Silva, 2019, from the African leaf-like Xerophyllini Günther, 1979, and from the Asian leaf-like Cladonotini Bolívar, 1887. A tabular key to the tribes of Cladonotinae with leaf-like representatives is provided, together with photographs of type specimens of both species belonging to the newly described tribe. The holotype of the new species belongs to the Muséum national d'Histoire naturelle Orthoptera collection, Paris.

Keywords

Gondwana, identification traits, mimicry, new genus, new species, new tribe, phylogenetic position, rainforest, taxonomy, Valalyllini

Introduction

Leaf mimicry in animals has evolved independently a number of times (Skejo et al. 2019). From the leaf-like satanic leaf-tailed gecko (*Uroplatus phantasticus* Boulenger, 1888) to the Indian oakleaf (*Kallima inachus* Boisduval, 1836), this curious morphology certainly survived as an adaptation for avoiding diurnal predators. Anyone who has visited a tropical rainforest will know how unlikely it is to spot a leaf-like critter in diverse leaf litter. Among the pygmy grasshoppers (Tetrigidae), there are several leaf-like species, mostly belonging to the subfamily Cladonotinae (Tumbrinck 2014). Katydids are well-known for their various leaf-like forms (Nickle and Castner 1995) as well.

Until now, only a single leaf-like species of Tetrigidae was known to inhabit Madagascar—the Leatherback Pygmy Grasshopper, *Lepocranus fuscus* (Devriese 1991) (Fig. 1). This species has been known from several individuals, of which the only digitalized one is a male holotype from the Tampolo forest, slightly northwest of Toamasina (Tamatave). The species has also been reported from the rainforests around Manakamahiny and Mahavelona (Foulpointe) (Danielczak et al. 2017). With this paper, we add one more species to the diverse Malagasy fauna, *Valalyllum folium* gen. et sp. nov. (Fig. 2). Our description is based on a single male from the Belanono rainforest, in the northernmost rainforests of Madagascar. The aim of this study is to describe *V. folium* sp. nov., compare it to *L. fuscus*, provide identification traits for the Malagasy leaf-like pygmy grasshoppers, and discuss their position in the Tetrigidae tree of life by describing a new tribe, Valalyllini trib. nov. (Fig. 3).

Materials and methods

Museum acronyms used were MNCN for Museo Nacional de Ciencias Naturales (Madrid) and MNHN for the Muséum national d'Histoire naturelle. Taxonomy follows the Orthoptera species file (Cigliano et al. 2022) and nomenclature follows the International Code of the Zoological Nomenclature. Morphology and measurements follow Devriese (1991) and Tumbrinck's (2014) capital work on the subfamily Cladonotinae; we have added a new important character, whether the anterior pronotal tip comes before the face or not. Measurements were taken in ImageJ (version 1.8.0_172) after calibration with millimetre paper. For comparison of the new tribe with already described taxa, we have consulted Devriese (1999) monograph on Xerophyllini Günther, 1979, and the Orthoptera species file (Cigliano et al. 2022) digital catalogue of museum specimens for Choriphyllini Cadena-Castañeda & Silva, 2019 and Cladonotini Bolívar, 1887. The holotype male of *Lepocranus fuscus* is deposited in MNCN and was examined and digitalized by the authors. The holotype male of *Valalyllum folium* gen. et. sp. nov. is deposited in MNHN, Paris and was examined and digitalized by the authors. Both *Lepocranus fuscus* and *Valalyllum folium* gen. et. sp. nov. holotypes are now digitalized and high-resolution photographs are uploaded to the Orthoptera species file database (Cigliano et al. 2022).

Results

Class Insecta
Order Orthoptera
Suborder Caelifera
Infraorder Acrididea
Superfamily Tetrigoidea Rambur, 1838

Family Tetrigidae Rambur, 1838

Diversity in Madagascar. Altogether, 76 Tetrigidae species (including the new one) are known to inhabit Madagascar, of which 73 (= 96%) can be found only in Madagascar and nowhere else in the world (Cigliano et al. 2022). These species are assigned to altogether 29 genera, of which 24 are endemic to the island. Hitherto, only a single leaf-like species was known from the island, *Lepocranus fuscus*. This study adds one more species with this interesting cryptic morphology, *Valalyllum folium* gen. et sp. nov.

Subfamily Cladonotinae

Composition and distribution. This diverse and polyphyletic family includes altogether 314 species assigned to 74 genera (Cigliano et al. 2022). Most genera require revision and are not adequately classified in the Tetrigidae system (Zhang et al. 2020). Within the subfamily Cladonotinae, several monophyletic tribes exist, such as Caribbean Choriphyllini (*Choriphyllum* Serville, 1838 and *Phyllotettix* Hancock, 1902), African Xerophyllini (including leaf-like *Acmophyllum* Karsch, 1890, *Seyidotettix* Rehn, 1938, *Trypophyllum* Karsch, 1890, *Xerophyllum* Fairmaire, 1846), and Asian Cladonotini (*Hymenotes* Westwood, 1837, *Holoarcus* Hancock, 1909, *Dolatettix* Hancock, 1907).

Diversity in Madagascar. Altogether, 18 Tetrigidae species of Madagascar are assigned to the subfamily Cladonotinae: two members of Valalyllini trib. nov. (*L. fuscus* and *V. folium*); 13 species of the genus *Thymochares*, which is currently not assigned to any of the tribes, and it is questionable whether it represents a genus of Cladonotinae; *Microthymochares pullus*, an endemic genus and species with the same taxonomic problem as *Thymochares*; *Epitettix spheniscus* also with the same problematic assignment; and Xerophyllini and its member *Morphopoides madagascariensis* (Cigliano et al. 2022).

Tribe Valalyllini trib. nov. [Leaf-like Cladonotinae of Madagascar]

http://zoobank.org/49EABF65-9F2F-482B-B545-B1A997AE9957
Figs 1–3; Table 1

Cladonotini (partim): Tumbrinck et al. (2020): 336 (tentatively assigned to Cladonotinae: Cladonotini).

Type genus. *Valalyllum* gen. nov., herein described (see below), type species *V. folium* sp. nov., also described herein.

Composition and distribution. Two monotypic genera, *Lepocranus* (including only *L. fuscus*) and *Valalyllum* gen. nov. (including *V. folium* sp. nov.). *Lepocranus fuscus* is endemic to the rainforests east of Mahavelona (Foulpointe) (Danielczak et al. 2017), while *V. folium* sp. nov. is endemic to northern Malagasy rainforests around Sambava and Andapa. *Lepocranus folium* sp. nov. lives 350 km more northerly than *L. fuscus*.

Descriptive diagnosis. Members of Valalyllini (*Lepocranus*, *Valalyllum* gen. nov.) are very similar to and thus most likely closely related to Asian Cladonotini (genera *Misythus* Stål, 1877, *Hymenotes* Westwood, 1837, *Holoarcus* Hancock, 1909) and Caribbean Choriphyllini (*Choriphyllum* Serville, 1838 and *Phyllotettix* Hancock, 1902). Head, pronotum and legs in these three tribes show remarkable similarity and are regarded as homologous. Superficially, the leaf-like morphology of Valalyllini trib. nov. also resembles that of leaf-like Xerophyllini, but detailed comparisons reveal no homologous parts.

Antenna shorter than hind femur; vertex very wide; vertex slightly and obliquely elevated above the compound eyes; vertex without horns; upper margin of the antennal grove in the level of the lower margin of a compound eye; pronotal tip of the pronotum projected above the head, but not before the eyes or before the face; transverse pronotal veins weak, almost unrecognizable; pronotal tip obliquely bilobate in dorsal view; legs smooth, only with weak (small) undulations and triangular projections, not toothed or sawed. Found only in Madagascar.

Table 1 shows a comparison between leaf-like Caribbean Choriphyllini (*Choriphyllum* Serville, 1838 and *Phyllotettix* Hancock, 1902), Asian Cladonotini (*Hymenotes* Westwood, 1837, *Misythus* Stål, 1877, *Holoarcus* Hancock, 1909 and *Dolatettix* Hancock, 1907), and African Xerophyllini (*Xerophyllum* Fairmaire, 1846, *Trypophyllum* Karsch, 1890, *Acmophyllum* Karsch, 1890). The leaf-like Tetrigidae were visually compared by Skejo et al. (2019). For comparison and elucidation of the mentioned characters, the reader is urged to refer to the abovementioned publication.

Table 1. Tabular key to the four Cladonotinae tribes with leaf-like representatives (Valalyllini trib. nov. from Madagascar, Choriphyllini from the Caribbean, Cladonotini from SE Asia, and Xerophyllini from Africa).

	Valalyllini trib. nov.	**Choriphyllini**	**Cladonotini**	**Xerophyllini**
Distribution	**Madagascar**	**Caribbean**	**Philippines, Papua**	**Tropical Africa**
Antenna	short	long or short	short	short
Vertex horns	absent	absent	absent	present
Upper margin of the antennal groove	on the level of the lower margin of a compound eye	on the level of the lower margin of a compound eye	on the level of the lower margin of a compound eye	below the lower margin of a compound eye
Anterior tip of the pronotum	not falling in front of the face	strongly projected in front of the face	projected in front of the eyes	variable, not falling in front of the face (*Trypophyllum*) or projected in front of the face (*Xerophyllum*)
Transverse veins on the pronotum	weak	strong	very strong	weak
Posterior tip of the pronotum	obliquely bilobate	pointed	variable (*pointed* in *Misythus*, bilobate in *Cladonotus*)	pointed
Legs texture	smooth, with small protrusions	smooth	toothed or spiky	toothed or spiky

Genus *Lepocranus* Devriese, 1991

Lepocranus: Devriese 1991

Type species. *Lepocranus fuscus*, by original designation and by the original monotypy.

Composition and distribution. A single species only (*L. fuscus*), endemic to the Malagasy rainforests east of Mahavelona (Foulpointe), such as Tampolo, where the holotype is from, and Manakambahiny (reported in Danielczak et al. 2017).

Original etymology. Complex noun, male in gender, composed of Latinized Ancient Greek "lepos" (λέπος), meaning *bark*, and "chranos" (χράνος), meaning *helmet* (Devriese 1991).

Diagnosis. Same as for the species, see below.

Lepocranus fuscus Devriese, 1991

Fig. 1

Lepocranus fuscus: Devriese 1991

Material examined. ***Holotype.*** Madagascar • 1♂; "Foret de Tampolo, Madagascar"; May. 1932; A. Seyrig leg.; MNCN 7230.

Genus and species diagnosis. Small (< 10 mm long), apterous, leaf-like, cryptic species endemic to northern Madagascar. Antennae are short and filiform, composed of 15 antennomeres. The upper margins of the antennal groove are at the lower margin of a compound eye. Frontal costa bifurcates between the eyes into rounded facial carinae (parallel in *Valalyllum* gen. nov.), between which there is a wide scutellum, as wide as a compound eye. Vertex obliquely projected above the eyes in frontal view. Vertex about 3 times wider than a compound eye. In the frontal view, a compound eye is rounded (ovoid in *Valalyllum* gen. nov.). Pronotum is leaf-like, 2.4 times as long as high (1.75 times in *Valalyllum* gen. nov.) because of the compressed and elevated median carina. In the dorsal view, the median carina of the pronotum is sulcate. Median carina of the pronotum is straight in the dorsal view (undulated in *Valalyllum* gen. nov.). Pronotum dips above the head in dorsal view, then smoothly curves upwards and gradually descends towards the posterior apex at an obtuse angle (150° slope, already reported in Devriese 1991) (posterior slope is abrupt in *Valalyllum* gen. nov. and forms a right-angle). Posterior slope of the median carina is weakly undulated (much more in *Valalyllum* gen. nov.). The posterior apex of the pronotum is bilobated in the dorsal view. Pronotum does not cover the whole abdomen, the last segments are not covered, and the subgenital plate is visible (fully covered in *Valalyllum* gen. nov.). Dorsal margin of hind femora bearing strong projections (lappets). Genicular and antegenicular teeth are large and blunt (small and angular in *Valalyllum* gen. n). Mid tibia is stout. The top margins of the mid and the fore femora undulated but lack strong tubercules. Pulvilli of the hind tarsi are rounded.

Original etymology. Latin adjective in male gender, "fuscus, -a, -um" meaning brown (Devriese 1991).

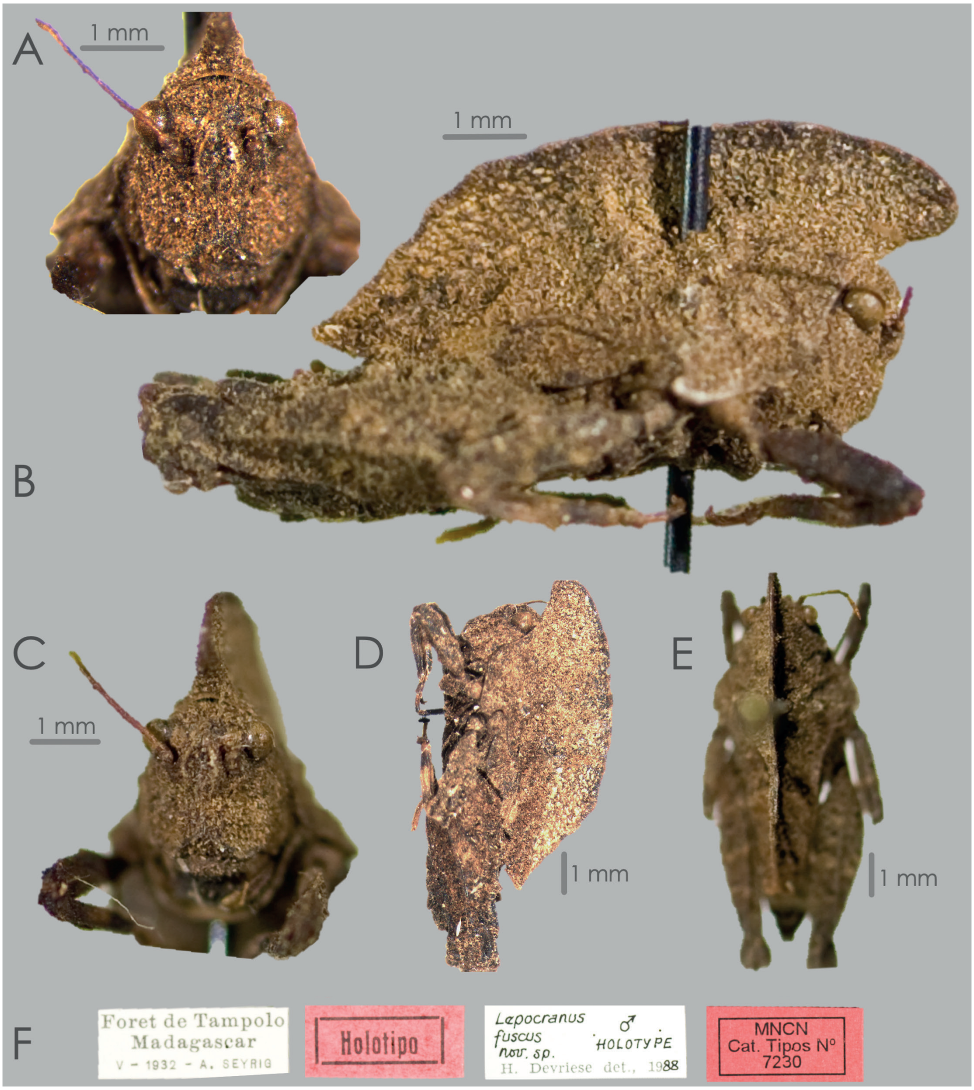

Figure 1. *Lepocranus fuscus* Devriese, 1991 **A** head detail in frontal view **B** habitus in right lateral view **C** habitus in frontal view **D** habitus in light lateral view **E** habitus in dorsal view **F** labels. Photo: J. Skejo and MNCN Madrid.

Vernacular name. Leatherback Pygmy Grasshopper (Danielczak et al. 2017).

Measurements (male holotype). ***Body length***: (from the tip of the head to the tip of the subgenital plate) 8.6 mm (cited 9.8 mm in Devriese 1999, from the tip of the pronotum to the tip of the subgenital plate). ***Pronotum length***: 8.1 mm (cited 8.2 mm in Devriese 1991). ***Pronotum maximum height***: 3.3 mm. ***Pronotum width between the lateral lobes***: 3.8 mm. ***Pronotum width between the shoulders***: 2.5 mm. ***Eye width***: 0.4 mm. ***Vertex width***: 1.2 mm. ***Fore femur length***: 2.2 mm. ***Fore femur width***: 0.5 mm. ***Mid femur length***: 2.5 mm. ***Mid femur width***: 0.8 mm. ***Hind femur***

length: 5.3 mm (cited 5.3 mm in Devriese 1991). ***Hind femur width***: 2.1 mm. ***Hind femur length/width ratio***: 2.5.

Locus typicus. Madagascar, Tampolo.

IUCN Red List Assessment. The Leatherback Pygmy Grasshopper was listed as an endangered species on the IUCN Red List because (1) the minimal geographic range it inhabits (the extent of occurrence is only about 3000 km^2), (2) the population seems to be fragmented, and (3) the decline in both the number of mature individuals and the size and quality of the range area due to inferred severe deforestation (Danielczak et al. 2017).

Genus *Valalyllum* gen. nov.

http://zoobank.org/40A42840-9E96-4ED6-8D4A-2872D80E2E70

Type species. *Valalyllum folium* gen. et sp. nov., here described, by original monotypy.

Composition and distribution. A single species only (*V. folium*), endemic to Madagascar (Belanono).

Etymology. Noun of neuter gender. From Malagasy "*valala*" or "*vahalala*"- grasshopper and Latinized Ancient Greek "*phyllum*" - leaf

Diagnosis and description. Same as for the species, see below.

Valalyllum folium sp. nov.

http://zoobank.org/0DA809A6-3F8A-48D2-8DAB-2E135114FC73

Fig. 2

Material examined. ***Holotype.*** Madagascar • 1 ♂; East Madagascar, Belanono, "30 km SW de Sambava, sur la route d'Andapa" [along the road to Andapa]; Valdon and Peyrieras leg.; MNHN.

Diagnosis. Large (> 11 mm long), apterous, leaf-like, rectangular, and cryptic species endemic to northern Madagascar. Antennae are short and filiform, composed of 15 antennomeres. Upper margins of the antennal groove in the level of the lower margin of a compound eye. Frontal costa bifurcates between the eyes into parallel facial carinae (more rounded in *Lepocranus*), between which there is a wide scutellum, as wide as a compound eye. Vertex obliquely projected above the eyes in the frontal view. Vertex about 3 times wider than a compound eye (measured at its widest part as seen in the frontal view). In the frontal view, a compound eye is ovoid (rounded in *Lepocranus*). Pronotum is rectangular and 1.75 times as long as high (2.4 times in *Lepocranus*) because of the compressed and elevated median carina. In the dorsal view, the median carina of the pronotum is sulcate. Median carina of the pronotum is undulated in a sinusoid fashion in the dorsal view (straight in *Lepocraus*). Pronotum dips above the head in dorsal view, then smoothly curves upwards and sharply descends towards the posterior apex. The posterior slope of the pronotum is abrupt (gradual in *Lepocranus*), forming a right-angle (obtuse angle in *Lepocranus*), and undulated. The posterior apex of the pronotum is bilobated in the dorsal view. Pronotum covers the whole abdomen

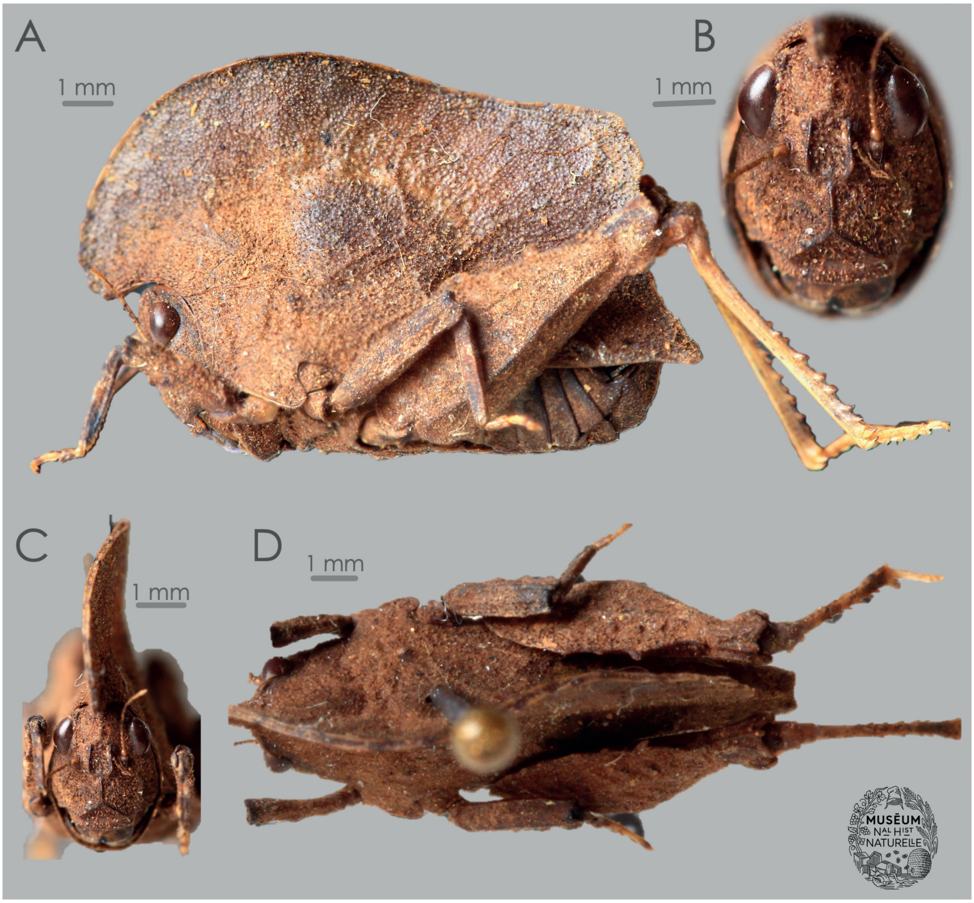

Figure 2. *Valalyllum folium* gen. et sp. nov. from Madagascar, male holotype, deposited in MNHN Paris. **A** habitus in left lateral view **B** head in frontal view **C** habitus in frontal view **D** habitus in dorsal view. Photo J. Skejo and MNHN Paris.

(last segments not covered in *Lepocranus*). Dorsal margin of the hind femora bears three small projections (lappets). Genicular and antegenicular teeth are small and angular. Mid tibia is stout. Top margins of the mid and the fore femora lack tubercules. Pulvilli of the hind tarsi are rounded.

Etymology. The specific epitheton is a noun in apposition, from Latin "*folium, -i, n.*" leaf, because of the species' leaf-like morphology.

Proposed vernacular name. Malagasy Litterhopper

Description. ***Holotype*** **(male).** ***General appearance.*** *Valalyllum folium* gen. et sp. nov. is a large (> 11 mm); smooth; rectangular; cryptic; dead-leaf-mimicking species with fine leaf-like venation on the elevated part of pronotum; uniformly brown except for the yellowish tarsi of all legs, as well as pale-yellowish hind tibiae.

Head. *Antenna* (Fig. 2B, C) short, filiform, composed of 15 antennomeres. The first segment is the largest scapus, second is a barrel-like pedicel, both circular in cross-section, while the remaining 13 antennomeres make up the flagellum. Segments 3rd to 6th are basal segments of the flagellum and they are robust, about two times as long as wide. Segments 7th to 10th are the central segments, and they are elongated, from four to five times as long as wide. Segments 11th to 13th are the subapical segments, shorter and bulkier than the mid segments. Last two antennomeres, i.e., 14th and 15th are reduced apical antennomeres. In the frontal view (Fig. 2B, C), the vertex is 3 times wider than the width of the compound eye (1.2 mm wide vertex, 0.4 mm wide compound eye); the vertex tip is above the top margin of the compound eyes, forming a smooth convex bulge. Frontal costa is smooth before the bifurcation, without visible projections or teeth. Bifurcation of the frontal costa is situated just below the line connecting the mid portion of the compound eyes. Height of the compound eye is greater than the height of the scutellum. Compound eye is ovoid. Width of the compound eye is the same as the width of the scutellum. Scutellum in its widest part and at the level of antennal groove is significantly wider than the antennal groove. Facial carinae are visible, and run straight after the bifurcation. Facial carinae are however, slightly sub-parallel, so the scutellum is slightly widened at the level of the median ocellus. Facial carinae are compressed and elevated but smooth. Paired ocelli are situated below the line connecting the mid portion of the compound eyes, but above the lower margin of compound eyes. Top margin of the antennal groove is placed at the level of the bottom margin of the compound eyes. In the lateral view (Fig. 2A), both vertex and face are visible around an ovoid compound eye. Fastigium protrudes beyond the furthest margin of the compound eyes for a half of the compound eye width. Occipital area is visible and narrow. In the dorsal view (Fig. 2D), the vertex is 3 times wider than the width of the compound eye. However, in this view, the vertex is also visibly very short and reaches to about a third of the compound eye length, i.e., it is not projected, but indrawn. Lateral and transverse carinae are slightly visible and elevated. Medial carina not visible due to pronotal occlusion.

Pronotum In the frontal view (Fig. 2C), the pronotum is visible above the head as a large, compressed and elevated and undulated projection with sulcated (ditched) ridge. In lateral view (Fig. 2A), the pronotum has the appearance of a dead leaf, because of the strongly compressed and elevated median carina of the pronotum. Prozonal and extralateral carinae are invisible. The pronotum is long (13.4 mm) and high (7.6 mm), giving a rectangular shape to the insect. Tip of the median carina of the pronotum has striped pale-dark-pale-dark coloration. Anterior margin is projected above the head as an oblique projection and then goes in circular fashion towards the dorsal portion, where it becomes the highest in the level of the mid coxae. After its highest portion, the dorsal margin of the median carina slowly decreases in height, and then in the level of the subgenital plate it abruptly falls in almost rectangular angle. The whole distal portion of the pronotum after this abrupt slope is finely toothed and undulated. Ventral sinus of the pronotum is large and visible, while tegminal sinus lacks because of the absence of wings. Infrascapular area, covered by the hind femora, is wide, smooth and

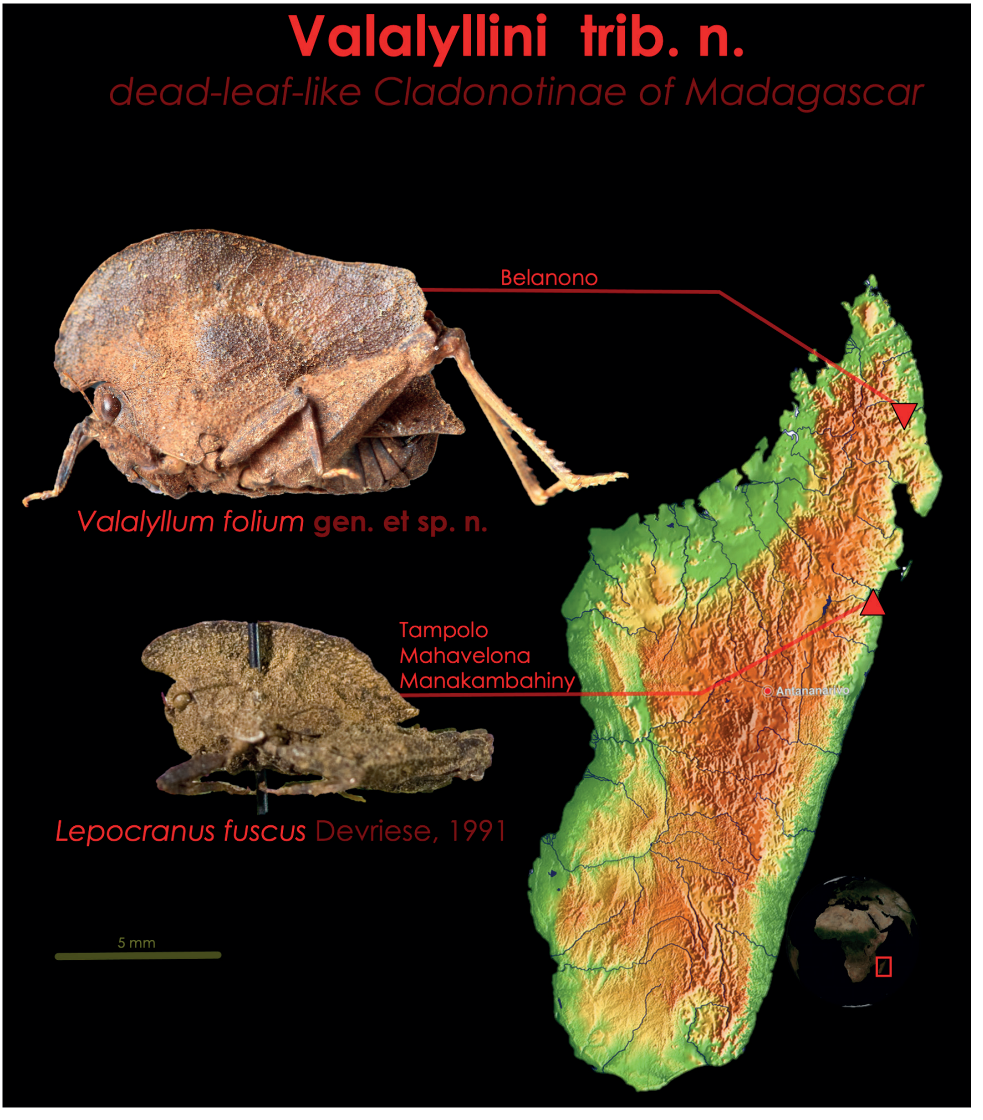

Figure 3. The diversity and the distribution of the tribe Valalyllini trib. nov. (*Valalyllum folium* gen. et sp. nov. in the north, and *Lepocranus fuscus* in the south), the Malagasy dead-leaf-like Cladonotinae. Both species are endemic to small areas and are likely endangered because of deforestation. Both species most probably inhabit rainforest leaf litter.

convex. The compressed dorsum of pronotum is finely granulated and intercepted with many fine veins (carinulae), giving an insect even more credible dead-leaf mimicry. Paranota are triangular, with truncate-oblique apex. In the dorsal view (Fig. 2D), the median carina has a sulcated ridge and forms a sinusoid undulation from the head caudad. The pronotum is finely granulated. Prozonal and extralateral carinae are absent, not visible. No pronotal projections visible. Shoulders (humeral angles) oblique, not projected outwards. Posterior apex of the pronotum is widely bilobate.

Legs. Fore legs (Fig. 2A, C, D). The fore femur is stouter than the mid one, length/width ratio is about 3.1. The dorsal margin of the fore femur has a continuous carina without tubercles. Ventral margin with the same femur has one tubercle close to the femur's distal end. The fore tibia is finely serrated and rectangular in cross-section. Distal segment of the fore tarsus is much longer than the proximal one. ***Mid legs*** (Fig. 2A, D). Dorsal and ventral margins of the mid femur bear continuous carinae, but ventral carina also has three small tubercles. Length/width ratio of the mid femur is 3.7. The mid tibia is finely tuberculated and rectangular in cross-section. Distal segment of the fore tarsus is much longer than the proximal one. ***Hind legs*** (Fig. 2A, D). The dorsal margin of the hind femur bears three large, but relatively blunt teeth. Ventral margin with continuous carina. Length/width ratio of the hind femur is 2.7. The hind tibia bears numerous strong teeth, but otherwise has a very smooth surface. First segment of the tarsus bears three strongly protruding, smooth and rounded pulvilli. First tarsal segment is much longer than the third.

Measurements (male holotype). ***Body length*** (from the tip of head to the tip of the subgenital plate) 11.3 mm. ***Pronotum length*** 13.4 mm. ***Pronotum maximum height*** 7.6 mm. ***Pronotum width between lateral lobes*** 5.2 mm. ***Pronotum width between the shoulders*** 3.5 mm. ***Eye width*** 0.4 mm. ***Vertex width*** 1.2 mm. ***Fore femur length*** 2.5 mm. ***Fore femur width*** 0.8 mm. ***Mid femur length*** 3.3 mm. ***Mid femur width*** 0.9 mm. ***Hind femur length*** 7.5 mm. ***Hind femur width*** 2.8 mm. ***Hind femur length/width ratio*** 2.7.

Locus typicus. Madagascar, Sava region, Belanono (rainforest between Sambava and Adapa).

Proposed IUCN Red List Assessment. Similar to the Leatherback Pygmy Grasshopper (*Lepocranus fuscus*) (Danielczak et al. 2017), the Malagasy Litterhopper (*Valalyllum folium* gen. et sp. nov.) should be immediately listed as an endangered species in the IUCN Red List because (1) of a very small geographic range it inhabits (known from a single locality, (2) the population might be fragmented and (3) the decline in both the number of mature individuals and the size and quality of the range because of expected severe deforestation.

Discussion

Despite its relatively small area, Madagascar is one of the richest biodiversity hotspots on Earth, boasting a high number of endemic taxa from the species level and above. This fact characterizes Madagascar as a high-priority area for conservation (Myers et al. 2000). Even at the level of Tetrigidae we find unbelievable diversity, with the new genus being the 24th endemic genus of the total number of 29 (Cigliano et al. 2022). Tragically, Madagascar has a long tradition of deforestation. Only 15% of the island remains forested, with the northern rainforest being the healthiest (Ganzhorn et al. 2001; Harper et al. 2007;

Vieilledent et al. 2018). The deforestation continues despite efforts to stop it (Tabor et al. 2017). Undescribed species can hardly be protected (Liu et al. 2022) and our models hinge on abundant and reliable data (Tedesco et al. 2014; Régnier et al. 2015). The nomenclatural acts we perform reflect our endeavor to assist in preservation of biodiversity.

The two members of the Valalyllini trib. nov. are similar but can be readily separated by several characters, namely the size and the shape of the eyes, the size of the leaf-like crest, and the general size of the body. Although these features can be variable individually, *L. fuscus* as a whole appears as a neotenic form of *V. folium* gen. et sp. nov. and is thus likely closely related to it but morphologically consistently separate. A remarkable similarity between the leaf-like tribes Valalyllini trib. nov. (Madagascar), Cladonotini (Asia), and Choriophyllini (Caribbean) is evident, so it is reasonable to hypothesize that those characters represent homologies and reflect the common ancestry on the ancient continent of Gondwana, which is a pattern that has been observed in numerous other taxa (Turner 2004; Gray et al. 2009; Reguero and Goin 2021). Cladonotinae are polyphyletic; their taxonomy is still far from resolved (Zhang et al. 2020). There is a strong possibility that more tribes could be defined within the subfamily and that some of the defined ones could contain genera that better fit elsewhere. The broad picture we present could lead to the solution, but there is more work to be done.

Both *Lepocranus fuscus* and *Valalyllum folium* gen. et sp. nov. are known only from a small area. A single digitalized specimen of *L. fuscus* is not exceptionally well preserved due to the presence of mould (Devriese 1991) and the new species is known only from a single specimen. Clearly, this situation is not ideal as the identity of both species remains incomplete. *Lepocranus fuscus* is already considered endangered (Danielczak et al. 2017), and could become extinct before we know anything about it. The same could be true for *V. folium* sp. nov. Considering the previously discussed points, a clear distinction between two Malagasy dead-leaf-mimic genera is presented. It is certainly going to be updated in the light of new findings as it is definitely incomplete, but it serves as a valuable starting point for future research.

Conclusions

A new dead-leaf-like genus and species of Malagasy Tetrigidae, *Valalyllum folium* gen. et sp. nov. is described and compared to *Lepocranus fuscus*, the only species of the genus *Lepocranus*. The two species are similar, but clearly separable by the general size, the shape of the pronotal crest and the shape of the eyes. *Valalyllum folium* gen. et sp. nov. and *Lepocranus fuscus* are assigned to the newly described tribe Valalyllini trib. nov. as the only Malagasy tetrigids with leaf-like pronotal crests. The comparison of the present tribe with others of similar morphology has revealed several likely homologies, which imply common ancestry. As the taxonomy of Cladonotinae is not resolved yet, new groups within the subfamily are certainly going to be defined, which will help in elucidating their evolutionary relationships.

Lepocranus fuscus is already considered endangered according to the IUCN Red List and, following the same pattern, we propose that the new species should be considered endangered as well.

Both species from the newly described tribe are defined only by a single specimen each, which is a fact that obscures the variability of the species. However, considering the rampant deforestation of Madagascar and the fact that the species can be differentiated by intraspecifically invariable characters homologous with other leaf-like tribes, we find it vital to describe the new, likely endangered, species and thus assist the efforts to classify and protect the rich Malagasy biodiversity.

Acknowledgements

Thanks to Josef Tumbrinck (Germany) and Hendrik Devriese (Belgium), without them it would have been impossible to get all the literature. Many thanks to Mercedes París (Spain), Laure Desutter and Simon Poulain (France) for the help with specimens' digitalization. Thank you to Barbara Anđelić (Croatia) for the help with photography and measurements. Thank you to anonymous and non-anonymous reviewers for their time and comments. This work was funded by Orthoptera Species File 2016 and 2017 grants to Josip Skejo and Josef Tumbrinck ("Digitalization of Tetrigidae types in European Musea", and "Revision of Ignacio Bolívar's Tetrigidae collection in MNCN"). Maks Deranja, Niko Kasalo, Karmela Adžić, and Josip Skejo are authors of equal contribution.

References

Boisduval J-A (1836) Histoire naturelle des insectes. Spécies général des Lépidoptères. Tome premier. Roret, Paris, 690 pp. https://doi.org/10.5962/bhl.title.9194

Bolívar I (1887) Essai sur les Acridiens de la tribu des Tettigidae. Annales de la Société Entomologique de Belgique 31: 175–313.

Cigliano MM, Braun H, Eades DC, Otte D (2022) Orthoptera Species File. Version 5.0/5.0. http://Orthoptera.SpeciesFile.org [accessed 11 Apr. 2022]

Danielczak A, Devriese H, Hochkirch, A (2017) *Lepocranus fuscus*. The IUCN Red List of Threatened Species 2017: e.T103898314A103900710. http://doi.org/10.2305/IUCN.UK.2017-2.RLTS.T103898314A103900710.en

Devriese H (1991) Contribution à l'étude des Tetrigidae de Madagascar (Orthoptera). Bulletin & annales de la Société royale belge d'entomologie 127(5–6): 119–131.

Devriese H (1999) Révision des Xerophyllini d'Afrique (Orthoptera Tetrigidae). Belgian Journal of Entomology 1: 21–99.

Fairmaire L (1846) Revue de la tribu des Membracides. Annales de la Société Entomologique de France 4(2): 235–320, 479–531.

Ganzhorn JU, Lowry PP II, Schatz GE, Sommer S (2001) The biodiversity of Madagascar: One of the world's hottest hotspots on its way out. Oryx 35(4): 346–348. https://doi.org/10.1046/j.1365-3008.2001.00201.x

Gray DP, Harding JS, Winterbourn MJ (2009) *Namanereis tiriteae*, New Zealand's freshwater polychaete: New distribution records and review of biology. New Zealand Natural Sciences 34: 29–38.

Günther K (1979) Die Tetrigoidea von Afrika südlich der Sahara (Orthoptera: Caelifera). Beiträge zur Entomologie 29(1): 7–183.

Hancock JL (1902) Tettigidae of North America. Chicago, 188 pp.

Hancock JL (1907) Orthoptera Fam. Acridiidae. Subfam. Tetriginae In: Verteneuil V, Desmet L (Eds) Genera Insectorum. Vol. 48, Bruxelles, 1–79.

Hancock JL (1909) Further studies of the Tetriginae (Orthoptera) in the Oxford University Museum. The Transactions of the Entomological Society of London 56(3–4): 387–426. https://doi.org/10.1111/j.1365-2311.1909.tb02160.x

Harper GJ, Steininger MK, Tucker CJ, Juhn D, Hawkins F (2007) Fifty years of deforestation and forest fragmentation in Madagascar. Environmental Conservation 34(4): 325–333. https://doi.org/10.1017/S0376892907004262

Karsch FAF (1890) Über die von Herrn Dr. R. Büttner in Westafrika gesammelten Tettigiden-Arten. Entomologisches Nachrichtenblatt (Vienna, Austria) 16(2): 17–27.

Liu J, Slik F, Zheng S, Lindenmayer DB (2022) Undescribed species have higher extinction risk than known species. Conservation Letters: e12876. https://doi.org/10.1111/conl.12876

Myers N, Mittermeier RA, Mittermeier CG, Da Fonseca GA, Kent J (2000) Biodiversity hotspots for conservation priorities. Nature 403(6772): 853–858. https://doi.org/10.1038/35002501

Nickle DA, Castner JL (1995) Strategies utilized by katydids (Orthoptera: Tettigoniidae) against diurnal predators in rainforests of northeastern Peru. Journal of Orthoptera Research 4(4): 75–88. https://doi.org/10.2307/3503461

Régnier C, Achaz G, Lambert A, Cowie RH, Bouchet P, Fontaine B (2015) Mass extinction in poorly known taxa. Proceedings of the National Academy of Sciences of the United States of America 112(25): 7761–7766. https://doi.org/10.1073/pnas.1502350112

Reguero MA, Goin FJ (2021) Paleogeography and biogeography of the Gondwanan final breakup and its terrestrial vertebrates: New insights from southern South America and the "double Noah's Ark" Antarctic Peninsula. Journal of South American Earth Sciences 108: e103358. https://doi.org/10.1016/j.jsames.2021.103358

Rehn JAG (1938) Studies in African Acrydiinae (Orthoptera, Acrididae). Part 2. New genera and species, and critical notes on previously-known forms. Proceedings. Academy of Natural Sciences of Philadelphia 90: 361–387.

Serville JGA (1838) Histoire naturelle des insectes. Orthoptères. Librairie encylopédique de Roret, Paris, 776 pp. https://doi.org/10.5962/bhl.title.95609

Skejo J, Gupta SK, Chandra K, Panhwar WA, Franjević D (2019) Oriental macropterous leaf-mimic pygmy grasshoppers—genera *Oxyphyllum* and *Paraphyllum* (Orthoptera: Tetrigidae) and their taxonomic assignment. Zootaxa 4590(5): 546–560. https://doi.org/10.11646/zootaxa.4590.5.3

Stål C (1855) Nya Orthoptera. Öfversigt af Kongliga Vetenskaps–Akademiens Förhandlinger 12: 348–353.

Tabor K, Jones KW, Hewson J, Rasolohery A, Rambeloson A, Andrianjohaninarivo T, Harvey CA (2017) Evaluating the effectiveness of conservation and development investments in reducing deforestation and fires in Ankeniheny-Zahemena Corridor, Madagascar. PLoS ONE 12(12): e0190119. https://doi.org/10.1371/journal.pone.0190119

Tedesco PA, Bigorne R, Bogan AE, Giam X, Jézéquel C, Hugueny B (2014) Estimating how many undescribed species have gone extinct. Conservation Biology 28(5): 1360–1370. https://doi.org/10.1111/cobi.12285

Tumbrinck J (2014) Taxonomic revision of the Cladonotinae (Orthoptera: Tetrigidae) from the islands of South–East Asia and from Australia, with general remarks to the classification and morphology of the Tetrigidae and descriptions of new genera and species from New Guinea and New Caledonia. Biodiversity. Biogeography and Nature Conservation in Wallacea and New Guinea 2: 345–396.

Tumbrinck J, Deranja M, Adžić K, Pavlović M, Skejo J (2020) Cockscomb-shaped twighopper, *Cladonotus bhaskari* sp. nov., a new and rare pygmy grasshopper species from Sri Lanka (Orthoptera: Tetrigidae: Cladonotinae). Zootaxa 4821(2): 333–342. https://doi.org/10.11646/zootaxa.4821.2.5

Turner AH (2004) Crocodyliform biogeography during the Cretaceous: Evidence of Gondwanan vicariance from biogeographical analysis. Proceedings of the Royal Society of London – Series B, Biological Sciences 271(1552): 2003–2009. https://doi.org/10.1098/rspb.2004.2840

Vieilledent G, Grinand C, Rakotomalala FA, Ranaivosoa R, Rakotoarijaona JR, Allnutt TF, Achard F (2018) Combining global tree cover loss data with historical national forest cover maps to look at six decades of deforestation and forest fragmentation in Madagascar. Biological Conservation 222: 189–197. https://doi.org/10.1016/j.biocon.2018.04.008

Westwood JO (1837) Characters of new insects from Manila. Proceedings of the Zoological Society of London 5: 127–130.

Zhang RJ, Zhao CL, Wu FP, Deng WA (2020) Molecular data provide new insights into the phylogeny of Cladonotinae (Orthoptera: Tetrigoidea) from China with the description of a new genus and species. Zootaxa 4809(3): 547–559. https://doi.org/10.11646/zootaxa.4809.3.8

ZooKeys 1109: 17–48 (2022)
doi: 10.3897/zookeys.1109.83863
https://zookeys.pensoft.net

RESEARCH ARTICLE

A peer-reviewed open-access journal
ZooKeys
Launched to accelerate biodiversity research

A new systematic arrangement for the blister beetle genus *Eurymeloe* (Meloini, Meloidae, Coleoptera) with the description of a new species from Spain

Alberto Sánchez-Vialas[1], José L. Ruiz[2], Ernesto Recuero[1,3], Felipe Gutiérrez-Pérez[4], Mario García-París[1]

1 *Museo Nacional de Ciencias Naturales (MNCN-CSIC), calle José Gutiérrez Abascal 2, 28006, Madrid, Spain* **2** *Instituto de Estudios Ceutíes, Paseo del Revellín 30, 51001 Ceuta, Spain* **3** *Department of Plant & Environmental Sciences, Clemson University, Clemson, SC 29634, USA* **4** *Avenida Francisco Javier Sauquillo 22, 28944, Madrid, Spain*

Corresponding author: Alberto Sánchez-Vialas (albertosv@mncn.csic.es)

Academic editor: Aaron Smith | Received 16 March 2022 | Accepted 23 May 2022 | Published 1 July 2022

https://zoobank.org/6A9F48F5-C156-421C-815A-DC6D1E07742A

Citation: Sánchez-Vialas A, Ruiz JL, Recuero E, Gutiérrez-Pérez F, García-París M (2022) A new systematic arrangement for the blister beetle genus *Eurymeloe* (Meloini, Meloidae, Coleoptera) with the description of a new species from Spain. ZooKeys 1109: 17–48. https://doi.org/10.3897/zookeys.1109.83863

Abstract

The taxonomic status and subgeneric arrangement of the genus *Eurymeloe* have been debated for decades. In this work, the internal taxonomy of *Eurymeloe* is redefined by recognising three subgenera: *Eurymeloe* for the former *Eurymeloe brevicollis* species group, *Coelomeloe* for *Eurymeloe tuccia*, and *Bolognaia* Ruiz, García-París, Sánchez-Vialas & Recuero, **subgen. nov**., to accommodate the species of the formerly recognised *Eurymeloe rugosus* species group. Additionally, a new species of the newly described subgenus *Bolognaia* is described from the Iberian Peninsula based on molecular and morphological traits. The new species, *Eurymeloe* (*Bolognaia*) *orobates* **sp. nov.**, can be distinguished from all other species of *Eurymeloe* by the following combination of morphological traits: dispersed brownish setae over the body that are arranged in small tufts on the abdominal terga; a small, very transverse pronotum that presents a unique macrosculpture; a deeply and densely punctured integument of the head and pronotum; and the very rugose elytra. The characters displayed by *E. orobates* suggest that the species groups that were previously defined and recognised for *Eurymeloe*, and that are now integrated within the newly erected subgenus *Bolognaia*, are non-monophyletic.

Keywords

Bolognaia subgen. nov., *Coelomeloe*, Iberian Peninsula, new species, phylogeny, systematics

Introduction

The taxonomy of *Eurymeloe* Reitter, 1911, originally described as a subgenus of *Meloe* Linnaeus, 1758, has been controversial due to both its differential use at the genus (Selander 1985; Sánchez-Vialas et al. 2021) or the sub-genus level (see Bologna 1988, 1991, 2008, 2020a; Bologna et al. 1989; Bologna and Pinto 2001; García-París et al. 2010) and its relationship with the monospecific *Coelomeloe* Reitter, 1911, which has been considered a synonym of *Eurymeloe* (Selander 1985; Bologna 2020b; Sánchez-Vialas et al. 2021) or as a separate but closely related subgenus (Bologna 1988, 1991; Bologna et al. 1989; Bologna and Pinto 2001; Di Giulio et al. 2013). Based on morphology, *Eurymeloe* was defined and recognised as two clearly diagnosable species groups, "*E. brevicollis*" and "*E. rugosus*" [Bologna, 1988; as *Meloe* (*Eurymeloe*)]. However, according to recent molecular phylogenetic analyses (Sánchez-Vialas et al. 2021), *Coelomeloe* (a former subgenus of *Meloe*) and the species of the "*E. brevicollis* species group" sensu Bologna (1988) constitute a monophyletic assemblage that is the sister clade of the "*E. rugosus* species group" (sensu Bologna 1988). These analyses have highlighted that, although the generic taxonomic status of *Eurymeloe* is well supported by molecular and morphological data (Selander 1985; Sánchez-Vialas et al. 2021), its internal taxonomic structure remains in need of reassessment.

The *Eurymeloe rugosus* species group was comprehensively revised by Bologna (1988), who established two main subgroups based on several morphological traits. The first one, subgroup A or the "*E. rugosus* subgroup", was formed by species presenting black (or partially brownish) pilosity over the body, an opaque or shiny black integument, deep punctures on the head and pronotum, and rugose elytra. The species forming the second one, subgroup B or the "*E. murinus* subgroup", were characterised by having a general brownish yellow pilosity, greyish black or brownish black (exceptionally pale brown) integument with a matte or satin appearance, shallow punctures on the surface of the head and pronotum, and elytra that are less rugose than those of the first subgroup. In addition to these two subgroups, Ruiz et al. [2010; as *Meloe* (*Eurymeloe*)] proposed a third one, the "*E. saharensis* subgroup", which includes *Eurymeloe saharensis* (Chobaut, 1898) (widely distributed from the Canary Islands to the Arabian Peninsula) and a closely related species, *E. vignai* (Bologna, 1990). Compared to the first two subgroups, this last one presents distinctive morphological characters such as a slender appearance, long antennae and legs (especially tarsi), silky black integument, pilosity consisting of short reddish setae, thick but sparse punctures on the head and pronotum, and a very shallow elytral rugosity. To date, ca. 20 Palaearctic species have been included in the *E. rugosus* species group (Bologna 1988; Ruiz and García-París 2009, 2015; Ruiz et al. 2010). However, very few studies have examined the phylogenetic relationships among them.

Recently, Sánchez-Vialas et al. (2021) showed that the clade corresponding to the *E. rugosus* species group is comprised of at least three main lineages: one represented by *Eurymeloe fernandezi* (Pardo Alcaide, 1951) with the other two corresponding generally to Bologna's (1988) subgroups A (*E. rugosus* subgroup) and B (*E. murinus* subgroup). However, as pointed by Ruiz and García-París (2009), the morphological traits defining these groups require further study as the specific composition of each is unclear. Moreover, although Sánchez-Vialas et al. (2021) included several representatives of Bologna's (1988) two subgroups, their study lacked specimens of *E. rugosus* (Marsham, 1802), i.e., the primary species characterising subgroup A, as well as those of the *M. saharensis* subgroup.

We recently collected specimens representing a new distinctive species of the *E. rugosus* species group from central Spain. The new species, which can be easily diagnosed by both conspicuous morphological characters and molecular data, is characterised by a combination of morphological traits present in either one or the other of Bologna's (1988) subgroups, suggesting that these subgroups are not monophyletic and that some of the characters used to distinguish them (e.g., body setae colouration) are not diagnostic.

In this study, we (1) describe the new species of *Eurymeloe* and analyse its phylogenetic relationships by using the Meloini molecular framework of Sánchez-Vialas et al. (2021), together with other published (Rulik et al. 2017; Ohnishi et al. 2021) and unpublished data, including sequences of *E. rugosus*; (2) describe a new subgenus within *Eurymeloe*, *Bolognaia* subgen. nov., to accommodate the species of the *E. rugosus* species group (sensu Bologna 1988, 1991); (3) redefine, in a more restricted sense, the subgenus *Eurymeloe*; and (4) discuss the internal taxonomic structures within the new subgenus.

Materials and methods

We studied the external morphology of a total of 326 specimens belonging to 17 species of *Eurymeloe*. All specimens are listed in either Ruiz and García-París (2009, 2015) or Sánchez-Vialas et al. (2021), and housed in collections at the Museo Nacional de Ciencias Naturales (**MNCN-CSIC**), Madrid, Spain; the Museu de Zoologia, Barcelona, Spain (**MZB**); and the Natural History Museum, London, England (**NHMUK**); or in the personal collections of M. A. Bologna, University "Roma Tre", Rome, Italy (**MAB**); and J. L. Ruiz, Ceuta, Spain (**JLR**). A specimen from Biel (Zaragoza) recorded as *Meloe rugosus* (currently *Eurymeloe rugosus*, see Sánchez-Vialas et al. 2021) by Recalde et al. (2002) and Pérez-Moreno et al. (2003) and housed in the entomological collection of the Sociedad Entomológica Aragonesa (**SEA**) [Maynar-Duplá Collection], Zaragoza, Spain, was also studied. In addition, we examined specimens of *Eurymeloe gomari* (Ruiz and García-París 2009) from Morocco, *E. ganglbaueri* (Apfelbeck, 1907) from Sardinia (Italy), and a new species of *Eurymeloe* from central Spain. Comparisons with the remaining species included in Bologna's (1988) *E. rugosus* species group (i.e., those distributed in the Middle East and the eastern Mediterranean) were made using diagnostic morphological traits extracted from the literature (mainly Kaszab 1958, 1983; Bologna 1988, 1991; Ruiz and García-París 2009, 2015; Ruiz et al. 2010). The geographic distributions of the studied species were also extracted from the literature, mostly from studies by Bologna (1988, 1991, 2008, 2020a).

The description of the new species of *Eurymeloe* is based on a total of five specimens (one male, dried preserved, and four females, ethanol-preserved), all belonging to the type series. These specimens were collected from the mountains of central Spain, at Puerto de la Quesera (Province of Guadalajara, Autonomous Community of Castilla-La Mancha). The type series is held at MNCN-CSIC.

For the morphological study, dry-mounted specimens were examined under a stereomicroscope. The male specimen was rehydrated in water before the extraction of the genital structures, which was subsequently mounted on a piece of cardboard using dimethylhydantoin formaldehyde (DMHF) resin and pinned adjacent to the specimen. Measurements were taken using a micrometre that was coupled to one of the microscope eyepieces. Digital images of live, dry-mounted specimens, and of male and female genital structures, were taken with a reflex camera (Canon 77D) fitted with a macro-lens (Sigma 105 mm F2.8) and two external flashes. We used the terminology suggested by Selander (1966) to describe the various parts of the male genitalia.

For the molecular analyses, we used sequences of *Eurymeloe* available from GenBank and those of four new specimens that we had collected and preserved in ethanol (now housed at the MNCN-CSIC), including one from Morocco corresponding to *Eurymeloe gomari*, one from Sardinia (Italy) corresponding to *E. ganglbaueri*, and two from central Spain corresponding to the new species, *Eurymeloe* sp. nov. From GenBank, we downloaded the sequences of 31 specimens belonging to 13 species of *Eurymeloe* (Rulik et al. 2017; Ohnishi et al. 2021; Sánchez-Vialas et al. 2021) (Table 1). A total of 31 specimens of 16 species from ten genera of Meloidae was used as the outgroup (Sánchez-Vialas et al. 2021) (Table 1). Tissue sampling, DNA extraction, sequencing, and alignments were performed as described by Sánchez-Vialas et al. (2021).

The molecular data set consisted of two mitochondrial (COI and 16S rRNA) and two nuclear (Wg and 18S rRNA) gene fragments from 66 specimens (including the four new ones). All sequences were compiled and revised using Sequencer v. 4.9 and aligned with MAFFT (Katoh and Toh 2008). Final alignments were visually inspected with Mesquite v. 3.04 (Maddison and Maddison 2019). Phylogenetic analyses using a Bayesian inference approach, as implemented in MrBayes v. 3.2.3 (Ronquist et al. 2012), were performed on a combined data set consisting of 2917 bp from the four mitochondrial and nuclear sequences (COI, 16S, Wg, 18S) (Table 1). Analyses, which started with a randomly generated tree, consisted of four Metropolis-coupled Markov chains Monte Carlo (one cold, three heated) and two simultaneous runs of 10×10^6 generations each, sampling every 1000 generations. We discarded the first 25% of the obtained trees as burn-in and generated the consensus tree in MrBayes. Posterior clade probabilities were used to assess nodal support.

To delimit species, we adopted the evolutionary species concept (Wiley 1978; Wiley and Mayden 2000) in which a species is considered “a single lineage of ancestral descendant populations of organisms which maintains its identity from other such lineages and which has its own evolutionary tendencies and historical fate” (Wiley 1978: 18). This concept combines implications derived from the phylogenetic species concept, such as reciprocal monophyly, with additional subjective properties (e.g., phenetic distinguishability and reproductive isolation, among other lines of evidence) that can be used to assess the historical fate of lineages (Ruiz and García-París 2015; Sánchez-Vialas et al. 2020).

Table 1. Specimen identity, collection locality, voucher number, and GenBank accession numbers of the new and previously published sequences analysed in this work.

Taxon	Locality	Voucher number	GenBank # CoxI	GenBank # 16S	GenBank # Wg	GenBank # 18S
Eurymeloe apivorus	Morocco: Fès-Meknès: Ifrane, 2 km South of Cedro Gouran, Middle Atlas	**mel 81009**	MW158218	MW158046	MW157964	MW158119
Eurymeloe apivorus	Morocco: Fès-Meknès: Ifrane, 2 km South of Cedro Gouran, Middle Atlas	**mel 81013**	MW158220	MW158048	MW157966	MW158121
Eurymeloe apivorus	Morocco: Fès-Meknès: Ifrane, 2 km South of Cedro Gouran, Middle Atlas	**mel 81054**	MW158219	MW158047	MW157965	MW158120
Eurymeloe brevicollis	Spain: Cantabria: Brañavieja, Pico Tres Mares	**mel 04107**	MW158305	MW158088	MW157987	MW158142
Eurymeloe brevicollis	Andorra: Arinsal	**mel 07092**	MW158306	MW158089	MW157988	MW158143
Eurymeloe corvinus	Japan: Niigata, Sado, Kitaushima	**9060**	LC583106.1			
Eurymeloe corvinus	Japan: Saga, Karatsu, Hirose	**11881**	LC583105.1			
Eurymeloe corvinus	Japan: Nagano, Iriyamabe	**10521**	LC583104.1			
Eurymeloe fernandezi	Spain: Islas Canarias: La Palma, Los Sauces	**mel 07045**	MW158266	MW158068	MW157972	MW158127
Eurymeloe fernandezi	Spain: Islas Canarias: La Palma, Los Sauces	**mel 07048**	MW158267	MW158069	MW157973	MW158128
Eurymeloe ganglbaueri	Italy: Lazio: Tarquinia	**mel 81064**	MW158268	MW158070	MW157974	MW158129
Eurymeloe ganglbaueri	Italy: Lazio: Tarquinia	**mel 81065**	MW158269	MW158071	MW157975	MW158130
Eurymeloe ganglbaueri	Italy: Sardinia: 4 km North-West of Orgosolo	**ASV19011**		OM918705		OM925566
Eurymeloe glazunovi	Romania: Dobruja: Istria	**mel 07001**	MW158265	MW158067	MW157971	MW158126
Eurymeloe gomari	Morocco: 9 km South-West of Moulay Abdeselam	**ASV18019**	OM936883	OM918704		OM925565
Eurymeloe gomari	Morocco: Tangier-Tetouan: Chaouen, Talassemtane National Park	**mel 81063**	MW158275	MW158076	MW157981	MW158136
Eurymeloe ibericus	Spain: Ávila: Villanueva del Campillo, Puerto de Villatoro	**mel 06039**	MW158307	MW158090	MW157989	MW158144
Eurymeloe ibericus	Spain: Ávila: Hoyos del Espino, Plataforma de Gredos	**mel 81039**	MW158308	MW158091	MW157990	MW158145
Eurymeloe mediterraneus	Spain: Cádiz: Puerto Real	**mel 04255**	MW158221	MW158049	MW157967	MW158122
Eurymeloe mediterraneus	Morocco: Moulay Abdelsalam	**mel 07010**	MW158222	MW158050	MW157968	MW158123
Eurymeloe mediterraneus	Spain: Cuenca: Saelices	**mel 07147**	MW158224	MW158052	MW157970	MW158125
Eurymeloe mediterraneus	Morocco: Tetouan: Agnan, Sierra del Haus	**mel 81066**	MW158223	MW158051	MW157969	MW158124
Eurymeloe murinus	Morocco: Marrakesh-Safi: 2 km North of Aguelmouse, Tizi n'Tichka, High Atlas	**mel 81018**	MW158270	MW158072	MW157976	MW158131
Eurymeloe murinus	Spain: Madrid: Colmenar Viejo	**mel 81053**	MW158271		MW157977	MW158132
Eurymeloe nanus	Spain: Madrid: 7 km South of Tielmes	**mel 01028**	MW158273	MW158074	MW157979	MW158134
Eurymeloe nanus	Spain: Madrid: Tielmes	**mel 81042**	MW158274	MW158075	MW157980	MW158135
Eurymeloe nanus	Spain: Toledo: Villacañas, Sierra del Romeral	**mel 05001**	MW158272	MW158073	MW157978	MW158133
Eurymeloe orobates sp. nov.	Spain: Guadalajara: Puerto de la Quesera	**ASV18002**	OM936884		OM925567	
Eurymeloe orobates sp. nov.	Spain: Guadalajara: Puerto de la Quesera	**ASV18003**	OM936885		OM925568	
Eurymeloe rugosus	Germany: Saxony-Anhalt	**ZFMK-TIS-2003300**	KU918912.1			
Eurymeloe tuccia	Spain: Menorca: 2 km South of Binimella	**mel 06034**	MW158276	MW158077	MW157982	MW158137

Taxon	Locality	Voucher number	GenBank # CoxI	GenBank # 16S	GenBank # Wg	GenBank # 18S
Eurymeloe tuccia	Spain: Islas canarias: La Palma: Don Pedro	**mel 07058**	MW158277	MW158078	MW157983	MW158138
Eurymeloe tuccia	Spain: Almería: La Mela	**mel 81001**	MW158278	MW158079	MW157984	MW158139
Eurymeloe tuccia	Portugal: Algarve: Sagres, Praia do Martinhal	**mel 81002**	MW158279	MW158080	MW157985	MW158140
Eurymeloe tuccia	Morocco: Larache: Lixus	**mel 81006**	MW158280	MW158081	MW157986	MW158141
Lampromeloe aff. variegatus	Morocco: Marrakesh-Safi: 5.5 km North-East of Aguelmouse, Tizi n'Tichka, High Atlas	**mel 81010**	MW158202	MW158033	MW157953	MW158108
Lampromeloe cavensis	Morocco: Casablanca-Settat: Ouled Bahmad	**mel 06011**	MW158201	MW158032	MW157952	MW158107
Lampromeloe variegatus	Spain: Salamanca: 5 km West of Palencia de Negrilla	**mel 05015**	MW158203	MW158034	MW157954	MW158109
Lampromeloe variegatus	Hungary: Komárom-Esztergom: Vèrtesszölös	**mel 81068**	MW158204	MW158035	MW157955	MW158110
Meloe (Anchomeloe) autumnalis	Spain: Guadalajara: Villanueva de la Torre	**mel 04246**	MW158189	MW158025	MW157949	MW158104
Meloe (Anchomeloe) autumnalis	Spain: Zaragoza: El Frago	**mel 10070a**	MW158191	MW158027	MW157951	MW158106
Meloe (Anchomeloe) autumnalis	Morocco: Tangier-Tetouan: Chaouen, Djebel Tissouka	**mel 81071**	MW158190	MW158026	MW157950	MW158105
Meloe (Meloe) proscarabaeus	Spain: Menorca: 3.5 km South-West of Fornells	**mel 06026**	MW158148	MW157993	MW157939	MW158094
Meloe (Meloe) proscarabaeus	Morocco: Souss-Massa: 2 km South of Chafarni	**mel 81007**	MW158150	MW157995	MW157941	MW158096
Meloe (Meloe) proscarabaeus	Hungary: Tolna: Bátaapáti	**mel 06004**	MW158151	MW157996	MW157942	MW158097
Meloe (Meloe) proscarabaeus	Italy: Tuscany: Alberese	**mel 81082**	MW158149	MW157994	MW157940	MW158095
Meloe (Meloe) tropicus	Guatemala: El Quiché: 9 km North-East of Santa Cruz Quiché	**mel 81075**	MW158188	MW158024	MW157948	MW158103
Meloe (Meloe) cf. *violaceus*	Hungary: Tolna: Mőcsény	**mel 07033**	MW158186	MW158022	MW157946	MW158101
Meloe (Meloe) cf. *violaceus*	Hungary: Vas: Csákánydoroszló	**mel 07036**	MW158187	MW158023	MW157947	MW158102
Meloe (Meloe) violaceus	Spain: Ávila: Hoyos del Espino	**mel 05024**	MW158183	MW158019	MW157943	MW158098
Meloe (Meloe) violaceus	Spain: León: Correcillas: Pico Polvareda	**mel 81051**	MW158185	MW158021	MW157945	MW158100
Meloe (Meloe) violaceus	Spain: León: Correcillas: Pico Polvareda	**mel 81052**	MW158184	MW158020	MW157944	MW158099
Meloegonius cicatricosus	Hungary: Pest: Tatárszentzgyörgy	**mel 06002**	MW158208	MW158038	MW157959	MW158114
Meloegonius cicatricosus	Hungary: Komárom-Esztergom: Vèrtesszölös	**mel 81069**	MW158209	MW158039	MW157960	MW158115
Mesomeloe coelatus	Morocco: Guelmine-Smara: Reg Labyad	**Mcoelatus_labyad**	MW805179			
Mesomeloe coelatus	Morocco: Guelmine-Smara: Jbel Ouarkziz	**Mcoelatus_ouarkziz**	MW805180			
Mesomeloe ottomerkli	Qatar: 1.8 km West of Al Marrawnah	**mel Qatar1**	HG003653	MW158044	MW157962	MW158117
Mesomeloe ottomerkli	Qatar: 1.8 km West of Al Marrawnah	**mel Qatar2**	HG003654	MW158045	MW157963	MW158118
Physomeloe corallifer	Spain: Madrid: 5 km South-East of Agustín de Guadalix, 618 m asl	**mel 09051**	MW158210	MW158040	MW157961	MW158116
Taphromeloe erythrocnemus	Morocco: 2.5 km North-West of Douar Azerzou	**ASV18007**	MW158309	MW158092	MW157991	MW158146
Treiodous gracilicornis	Guatemala: El Quiché: 3.4 km North of Uspantán	**mel 81077**	MW158205	MW158036	MW157956	MW158111
Treiodous gracilicornis	Mexico: Guerrero: 5 km West of Carrizal de Bravo	**mel 874**	MW158206		MW157957	MW158112

Taxon	Locality	Voucher number	GenBank # CoxI	GenBank # 16S	GenBank # Wg	GenBank # 18S
Treiodous laevis	Mexico: Guanajuato: Dolores Hidalgo	**mel 08094**	MW158207	MW158037	MW157958	MW158113
Lytta vessicatoria	Spain: Ourense: A Acea	**mel 05073**	MW158147	MW157992		MW158093
Phodaga alticeps	Mexico: Baja California Norte: Ejido Luchadores del Desierto, Northwest of Laguna Salada	**KRN14**	MK024506	MK024642		MK024601
Cordylospasta fulleri	USA: California: 4.8 km North-East of Big Pine	**KRN23**	MK024478	MK024619		MK024572

Results

Phylogenetic relationships within *Eurymeloe*

Our Bayesian phylogenetic tree, which has a topology similar to the one presented by Sánchez-Vialas et al. (2021), recovered three major lineages within the genus *Eurymeloe* (Fig. 1). The first lineage is represented by the type species of the genus *Eurymeloe*, *E. brevicollis* (Panzer, 1793), plus the species *E. ibericus* (Reitter, 1895) and *E. corvinus* (Marseul, 1877), which together form a clade with *E. tuccia* (Rossi, 1790), the type species of the subgenus *Coelomeloe*. These two clades together form the sister group of the clade comprising the remaining species of *Eurymeloe* that were previously included in the *E. rugosus* species group (sensu Bologna 1988).

With respect to the internal taxonomic structure of *Eurymeloe* (sensu Sánchez-Vialas et al. 2021), it consists of three main clades, all morphologically diagnosable, with the following subgeneric status: (1) *Coelomeloe*; (2) *Eurymeloe sensu stricto* (s. str.), which includes the species in Bologna's (1988) *E. brevicollis* species group, and (3) the lineage including all species within the *E. rugosus* species group (Fig. 1). As the name-bearing type species of *Eurymeloe* (*E. brevicollis*) lies within the *E. brevicollis* species group, *Eurymeloe* (s. str.), the clade formed by the *E. rugosus* species group requires a new subgeneric name (as there is no name available for this group). We propose and describe herein a new subgenus of *Eurymeloe* to accommodate the species of Bologna's *M. rugosus* species group (sensu Bologna 1988): *Bolognaia* subgen. nov. We also redefine the subgenus *Eurymeloe*.

Bolognaia is comprised of three main lineages: one represented by *E. fernandezi*, an endemic of the Canary Islands, which resolved as the sister taxon to the other two lineages formed, respectively, by *E. mediterraneus* (Müller, 1925) and its closely related species and by *E. murinus* (Brandt and Erichson 1832) and its related species, including the new species of *Eurymeloe* from central Spain. The sequences of the new samples from Spain resolved as a distinctive lineage that is the sister taxon to the clade formed by *E. murinus* and *E. ganglbaueri*. This new lineage is not morphologically congruent with any other described species of *Eurymeloe* (Fig. 2).

Lastly, our molecular phylogenetic analysis confirmed the species identification of the other two newly sequenced specimens as *E. gomari* and *E. ganglbaueri*, and their relationship with the other specimens. As a result, the northern limit of

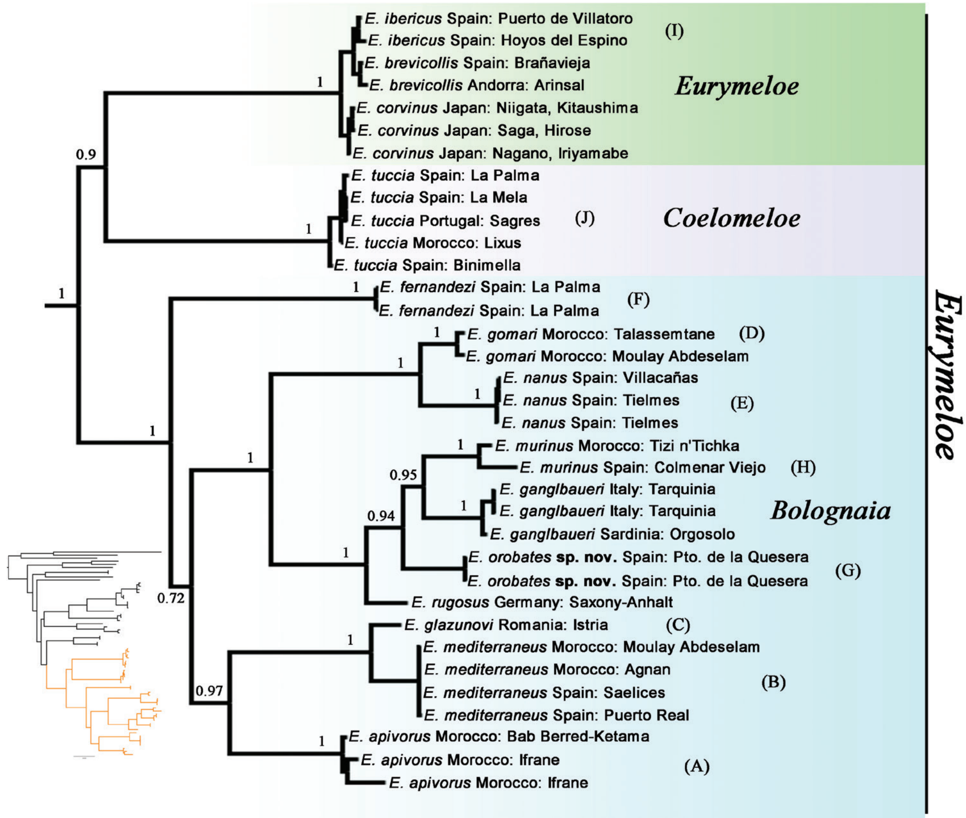

Figure 1. Bayesian phylogeny of the genus *Eurymeloe* based on the concatenated matrix of mitochondrial and nuclear genes (COI, 16S, Wg, 18S). The three subgeneric taxonomic categories are indicated as follows: *Eurymeloe* (in green), *Coelomeloe* (in violet) and *Bolognaia* (in blue). Numbers on the nodes represent the posterior probabilities of the clades. Letters in parentheses (**A–J**) correspond to the species portrayed in Fig. 2. Phylogeny in lower left shows the outgroups (black) and the lineage of *Eurymeloe* (orange). Additional information for each specimen is provided in Table 1.

the distribution range of the Moroccan endemic *E. gomari*, which was previously known only from its type locality, has been expanded by approximately 37 km to the northwest along the Rif Mountains. The new specimen of *E. ganglbaueri* from Sardinia resolved, as expected, within the same clade as the conspecific Italian continental samples.

Redefinition of the genus *Eurymeloe*

Given the new systematic arrangement proposed here for *Eurymeloe* as three subgenera (*Eurymeloe*, *Coelomeloe*, and *Bolognaia* subgen. nov.), we consider it necessary to present a revised diagnosis of *Eurymeloe* based on the morphology of adult specimens.

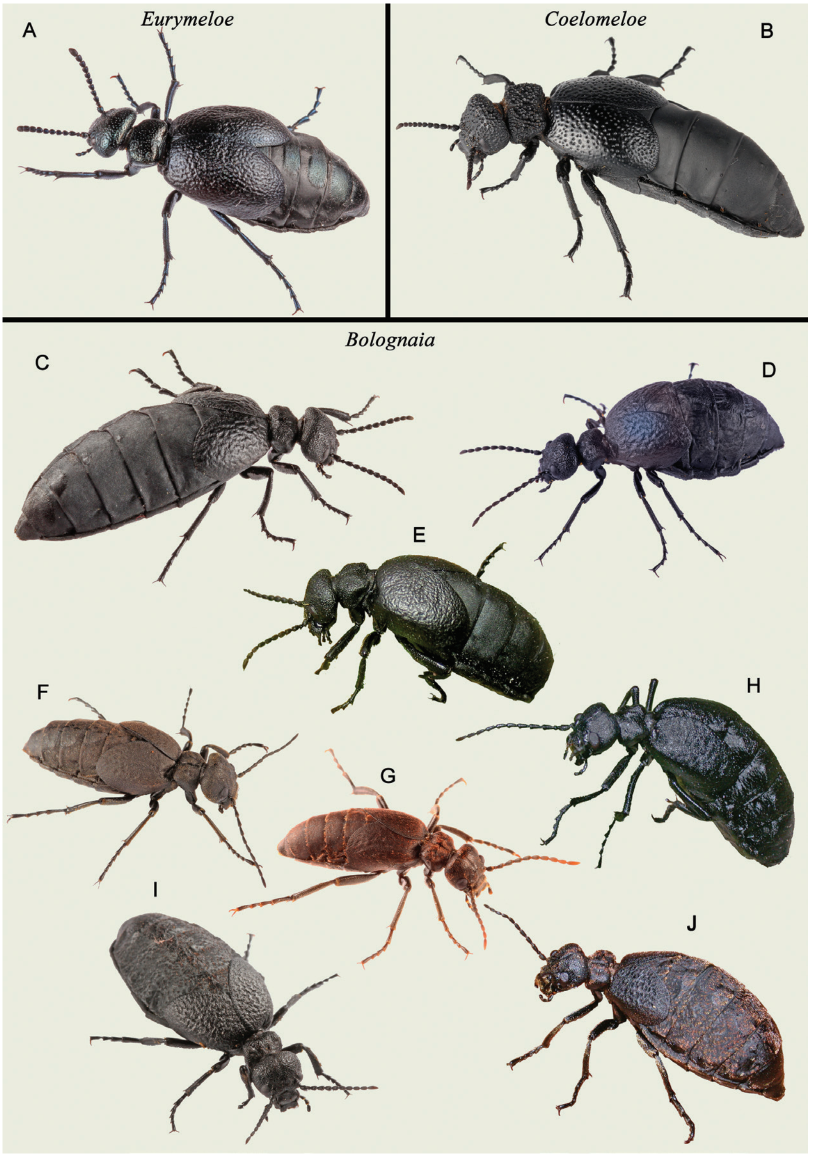

Figure 2. Habitus of some living adult specimens of the current subgenera of *Eurymeloe* **A** subgenus *Eurymeloe*, represented by a specimen of *Eurymeloe* (*Eurymeloe*) *ibericus* from Puebla de la Sierra, northern Madrid, Spain **B** subgenus *Coelomeloe*, represented by a specimen of *Eurymeloe* (*Coelomeloe*) *tuccia* found 3 km east of Celín, Sierra de Gádor, Almería, Spain **C–I** subgenus *Bolognaia* **C** *Eurymeloe* (*Bolognaia*) *affinis* from the surroundings of Bab Taza, Rif Mountains, Morocco **D** *E.* (*Bolognaia*) *mediterraneus* (type species of the subgenus *Bolognaia*) from Puebla de la Sierra, northern Madrid, Spain **E** *E.* (*Bolognaia*) *glazunovi* from Istria, Romania **F** *E.* (*Bolognaia*) *gomari* from the surroundings of Bab Taza, Rif Mountains, Morocco **G** *E.* (*Bolognaia*) *nanus* from Alcázar de San Juan, Ciudad Real, Spain **H** *E.* (*Bolognaia*) *fernandezi* from Los Sauces, La Palma, Canary Islands **I** *Eurymeloe orobates* sp. nov., from Puerto de la Quesera, Guadalajara, Spain **J** *Eurymeloe* (*Bolognaia*) *murinus* from Tizi n`Tichka, High Atlas, Morocco. Photographs: **A–C, F, G, I** (ASV) **E, H, J** (MGP) **D** (J. Aznar González de Rueda).

Genus *Eurymeloe* Reitter, 1911

Type species. *Meloe brevicollis* Panzer, 1793, by subsequent designation of Pinto and Selander (1970).

Description (adult). Size small to medium (6–36 mm), with diverse appearance, ranging from very robust to comparatively slender. Body integument colour variable, black, dull grey or dark brown (exceptionally sandy brown) to moderately metallic blue, opaque, bright, silky or sometimes with an oily shininess (Fig. 2A). Body pubescence short, sometimes quite distinct (*Bolognaia*) or very short, recumbent, often almost imperceptible (subgenus *Eurymeloe*) or absent dorsally (*Coelomeloe*; Fig. 2B), variable in colour, from yellowish to reddish brown and black. Head rounded, sides straight to arched, convergent to eyes. Eyes small or medium, usually subreniform, variably protruding, without longitudinal depressions behind them. Antennae unmodified in males, moniliform or submoniliform, robust or slender, short to moderate length, not reaching posterior margin of pronotum (*Eurymeloe*, *Coelomeloe*) or often reaching or even surpassing it (*Bolognaia*). Antennomeres subcylindrical or subconical, relatively robust or slender, highly variable width/length ratio, V to VII neither enlarged nor geniculated. Clypeus transverse, approximately twice as wide as long. Frontoclypeal suture angulated. Labrum wide, fore margin broadly emarginate. Maxillary and labial palpomeres unmodified. Mandibles robust, regularly and strongly curved on the outer margins. Pronotum from flat (*Coelomeloe*) to moderately convex (*Eurymeloe*, *Bolognaia*), subrectangular (*Coelomeloe*, *Eurymeloe*), subhexagonal or trapezoidal (*Bolognaia*), transverse or very transverse, usually equal to or more than 1.5 × as wide as long (exceptionally, 1.2–1.3 × as wide as long), with sides subparallel or converging backward; posterior margin usually broadly emarginated, with base not incised in the middle. Head and pronotum punctation from fine and scattered, sometimes almost absent (*Eurymeloe*), to somewhat deep and dense (*Bolognaia*), even very broad, dense, and deep, foveate in appearance (*Coelomeloe*). Hind margin of mesonotum straight or weakly arcuate. Metanotum short and barely visible, covered by the base of the elytra. Mesosternum short and wide, lacking scutum. Mesepisterna meet or not at the midline of the body. Elytra short and dehiscent, imbricate basally, not completely covering abdomen, smooth to densely coriaceous, rugose (*Eurymeloe*, *Bolognaia*) or with a surface densely foveate (*Coelomeloe*). Hind wings absent. Legs normal, unmodified in male, robust or more or less slender, pilose. Tibiae with two spurs at apex; outer spur of metatibiae widened and obliquely truncate, spoon-shaped. Tarsomeres with or without hair pads or dense setose pubescence on the inferior sides. Tarsal claws smooth, with distinct lower blades. Abdomen large, inflated, hypertrophied. Abdominal terga with medium or small highly sclerotised central plates. Last abdominal ventrite broadly emarginated at hind margin in males. Male genitalia: gonoforceps evenly sclerotised with gonostyli from moderately short to elongate, with distal regions more or less wide, usually digitiform (in lateral view), rounded at apex; gonocoxal plate broadly widened at the middle (in dorsal view); aedeagus robust (*Eurymeloe*, *Coelomeloe*) or relatively slender (*Bolognaia*), usually shorter than or approximately equal in length to the gonoforceps (in some species of *Bolognaia*, sometimes a little longer than the gonoforceps), with two dorsal hooks and one endophallic hook.

Larva. The morphological traits of previously known first instar larvae of *Eurymeloe* (triungulines), including *Coelomeloe*, and the descriptions of the triungulines of several additional species of *Eurymeloe*, have been synthesised and studied by Di Giulio et al. (2013, 2014). We herein refer to these works for larval morphological traits.

Taxonomic remarks. The adult instar of species of the genus *Eurymeloe* is morphologically diverse, and the three subgenera can be recognised based on this diversity. Adults of the subgenera *Eurymeloe*, *Coelomeloe*, and the newly described *Bolognaia* are distinguishable particularly by the shape of the antennae and the pronotum, the macrosculpture of the pronotum, body integument and pilosity, and the punctation of the head, pronotum, and elytra, among other traits.

Description of the subgenus

***Bolognaia* Ruiz, García-París, Sánchez-Vialas & Recuero, subgen. nov.**
https://zoobank.org/6B062E01-EF30-47F3-8ED2-42394FE7D532

Type species. *Meloe mediterraneus* Müller, 1925, by present designation.

Description (adult). Size small or medium to large (8–36 mm). Body integument black, dull grey or dark brown, occasionally sandy brown [*E. pallidicolor* (Martínez de la Escalera, 1909)], with an opaque, silky or bright appearance, never bluish or metallic (Fig. 2C–J). Body pubescence quite distinct, black, yellowish, whitish or golden, short or very short. Head rounded, temples usually forming a regular arc, except in *E. murinus* (Brandt and Erichson 1832) and *E. affinis* (Lucas, 1847), which have strongly enlarged temples; occiput usually weakly concave. Medium-sized eyes [smaller in *E. affinis* and *E. apivorus* (Reitter, 1895)], subreniform, moderately protruding, without a longitudinal depression behind them. Antennae moniliform, normally slender, not thickened towards the apex; long or medium in length, usually reaching the posterior margin of the pronotum or exceeding it; unmodified in males, straight. Antennomeres IV–IX subcylindrical, always longer than wide. Clypeus transverse, approximately twice as wide as long. Labrum wide, fore margin broadly emarginate. Mandibles robust, regularly curved along the outer margins. Pronotum slightly convex, transverse, mainly subhexagonal or subtrapezoidal, wider than long, usually 1.4–2.1 × as wide as long [in *E. fernandezi*, 1.2–1.3 × as wide as long], sides not parallel, converging backward, posterior margin broadly emarginated, posterior corners rounded. Pronotum surface variable, with or without a depressed area or groove in the middle, frequently with two depressed or smooth areas, diffuse, on both sides of the disc. Head and pronotum punctation fine to coarse, of variable density, always with pubescence. Posterior margin of mesonotum straight or weakly arcuate. Mesepisterna usually not meeting at the midline of the body. Elytra short and dehiscent, smooth to strongly rough, usually rugulose. Legs normal, usually slender, pubescent. Tarsomeres without hair pads on the inferior side, though some species [e.g., *E. nanus* (Lucas, 1847), *E. baudueri* (Grenier, 1863), *E. gomari*] have fairly dense setose pubescence that appears as small and short brushes. Last abdominal ventrite broadly and deeply emarginated at the hind margin in males. Male genitalia: Gonostyli usually elongate, distal regions narrow with their apices acuminate or digitiform in lateral view; gonocoxal plate long, usually narrow and slightly widened at the middle in dorsal view; aedeagus usually elongate, equally long as or longer than gonoforceps.

Etymology. The name *Bolognaia*, formed by the noun "Bologna" plus the Italian suffix "–aia" derived from the Latin "–aria" (used, in this case, to form a word meaning an animal associated with the specified noun Bologna), is in honour of Marco A. Bologna, a distinguished Italian entomologist specialising in the Meloidae and a friend who, among other excellent works, was able to clarify, for the first time, the complex taxonomy of the small-sized species of *Eurymeloe* related to *E. rugosus* for which the new subgenus is here erected.

Taxonomic remarks. We selected *M. mediterraneus* as the type species of *Bolognaia* because it is a morphologically well-characterised species, with low morphological or genetic intraspecific geographic differentiation (Bologna 1988, 1991; Sánchez-Vialas et al. 2021), and without nomenclatural or identity problems associated to synonyms (García-París et al. 2010; Bologna 2020a). *Bolognaia*, a monophyletic subgenus, largely corresponds to the *E. rugosus* species group of *Eurymeloe* defined by Bologna (1988, 1991). It includes species whose adults are characterised mainly by the following traits: small or medium body size; black, dull grey, or dark brown body colour; a distinctive black or pale-coloured (yellowish, whitish, or golden) pilosity; elongated and subcylindrical antennomeres that are longer than wide; and generally marked punctation and rugosity.

Based on molecular data (this work) and adult morphology (see Reitter 1895; Martínez de la Escalera 1909; Pliginskij 1910; Pardo Alcaide 1951; Kaszab 1958, 1983; Bologna 1988, 1991, 1994a, 1994b; Ruiz and García-París 2009, 2015; García-París and Ruiz 2011; Di Giulio et al. 2013), we include within the subgenus *Bolognaia* the following species: *Eurymeloe* (*Bolognaia*) *affinis* (Lucas, 1847), *E.* (*B.*) *apivorus* (Reitter, 1895), *E.* (*B.*) *apenninicus* (Bologna, 1988), *E.* (*B.*) *baamarani* (Ruiz and García-París 2015), *E.* (*B.*) *baudii* (Leoni, 1907), *E.* (*B.*) *baudueri* (Grenier, 1863), *E.* (*B.*) *fernandezi*, *E.* (*B.*) *flavicomus* (Wollaston, 1854), *E.* (*B.*) *ganglbaueri*, *E.* (*B.*) *glazunovi* (Pliginskij, 1910), *E.* (*B.*) *gomari*, *E.* (*B.*) *kandaharicus* (Kaszab, 1958), *E.* (*B.*) *mediterraneus*, *E.* (*B.*) *murinus*, *E.* (*B.*) *nanus*, *E.* (*B.*) *omanicus* (Kaszab, 1983), *E.* (*B.*) *pallidicolor*, and *E.* (*B.*) *rugosus*.

According to our molecular analyses (Fig. 1), three sublineages can be recognised within *Bolognaia*: two generally corresponding to Bologna's (1988) subgroups A and B, defined by presenting, respectively, an entirely black body pilosity (in our analyses, *E. mediterraneus*, *E. apivorus*, and *E. glazunovi*) or a pale-coloured (whitish, yellowish, reddish yellow, or golden) pilosity over the entire body or parts of it [in our analyses, *E. ganglbaueri*, *E. murinus*, *E. nanus*, *E. gomari*, *E. rugosus*, and *Eurymeloe orobates* sp. nov. from central Spain]. Notably, based on our molecular analyses, *E. rugosus*, which was included in Bologna's (1988) subgroup A, appears to be genetically more related to the species included in his subgroup B. In this regard, following a detailed examination of some specimens belonging to *E. rugosus*, we observed that several have inconspicuous brownish and reddish to yellowish setae (but not tufts) on their abdominal tergites, similar to those observed on the morphologically related species *E. apenninicus* (JLR, pers. obs.). In fact, Escherich (1890) and Bologna (1988, 1991) pointed out that some specimens of *E. rugosus* show yellowish brown setae on the last abdominal tergites; these correspond to the named var. *abdominalis* (Escherich 1890) (which has even been confused with *E. ganglbaueri*, see Bologna 1988: 247). Likewise, *E. ganglbaueri*, which presents a golden-yellow pilosity on a part of the body, resolved as genetically more related to species in subgroup B. The third sublineage diverged from its sister group, the A and B sublineages, during the Middle Miocene (Sánchez-Vialas et al. 2021). This sublineage is composed of only one species, *E. fernandezi*, an endemic of the Canary Islands that is morphologically singular and isolated within the subgenus (Pardo Alcaide 1951; Bologna 1988, 1991, 1994a; Ruiz and García-París 2015).

For practical purposes, but also supported by our analyses and some morphological traits (mainly, pilosity colour, integument aspect, pronotum punctation, and elytra rugosity; see Bologna 1988; Ruiz and García-París 2009, 2015), we redefine the specific composition of the subgroups established by Bologna (1988) within *Bolognaia* (defined as the *E. rugosus* species group by Bologna 1988) as follows:

(1) group A or *E. mediterraneus* group (now renamed), characterised mainly by a dark body pilosity (black or dark brown) and a black body integument that is usually glossy, semi-glossy, or silky in appearance [exceptionally, it is matte as in *E.* (*B.*) *baamarani*]. This group integrates the following species: *E.* (*B.*) *affinis*, *E.* (*B.*) *apivorus*, *E.* (*B.*) *baamarani*, *E.* (*B.*) *baudii*, *E.* (*B.*) *glazunovi*, and *E.* (*B.*) *mediterraneus*. In some specimens of *E.* (*B.*) *mediterraneus*, particularly those from Sardinia (Bologna 1988, 1991), the pilosity of the temples, pronotum and, sometimes, abdomen, is brown. The unstudied *E.* (*B.*) *affinis setosus* Escherich, 1890 from Algeria, which differs from the typical form of the species by the presence of isolated yellowish setae along the abdominal tergites, among other traits (e.g., smaller size, constant frontal furrow, and different elytral sculpture) (Escherich 1890; Bologna 1988, 1991; Di Giulio et al. 2013), possibly constitutes a distinct species, as mentioned by Di Giulio et al. (2013) and previously suggested by Escherich (1890) and Peyerimhoff (in Cros 1934: 90).

(2) group B or *E. murinus* group, characterised mainly by a pale-coloured (reddish, golden, brownish, yellowish, or whitish) body pilosity, either over the entire body or parts of it, and a body integument that is usually greyish, greyish black, or dark brown and opaque; exceptionally, it is glossy black as in *E.* (*B.*) *apenninicus* and *E.* (*B.*) *rugosus*. This group comprises the following species: *E.* (*B.*) *apenninicus*, *E.* (*B.*) *baudueri*, *E.* (*B.*) *flavicomus*, *E.* (*B.*) *ganglbaueri*, *E.* (*B.*) *gomari*, *E.* (*B.*) *kandaharicus*, *E.* (*B.*) *murinus*, *E.* (*B.*) *nanus*, *E.* (*B.*) *omanicus*, *E.* (*B.*) *pallidicolor*, and *E.* (*B.*) *rugosus*. Within this group, *E.* (*B.*) *apenninicus* and *E.* (*B.*) *rugosus* can be clearly differentiated from the others by having a glossy black body integument and dark reddish brown

(sometimes almost black) body setation, with scattered and sparse yellowish brown short setae on the abdominal tergites that are often barely noticeable.

(3) group C, composed by only *E.* (*B.*) *fernandezi*, well characterised morphologically within *Bolognaia* (see Pardo Alcaide 1951; Ruiz and García-París 2015).

Bologna (1988, 1990) integrated *M. saharensis* (= *M. otini* Peyerimhoff, 1949, *M. marianii* Kaszab, 1983; see Ruiz et al. 2010; Bologna 2020a) and *M. vignai* in the *E. rugosus* species group. Ruiz et al. (2010) considered the closely related *E. saharensis* and *E. vignai* as morphologically isolated and proposed a new group for them. As neither *E. saharensis* nor *E. vignai* have been studied at the molecular level, we have tentatively ascribed them to *Bolognaia* as *Eurymeloe* (*Bolognaia*) *saharensis* (Chobaut, 1898) and *E.* (*B*). *vignai* (Bologna, 1990).

Sánchez-Vialas et al. (2021) considered the six Asian species that Bologna (1988) included in the *E. rugosus* species group as belonging to *Eurymeloe*. These species are *Eurymeloe heptapotamicus* (Pliginski, 1910), *E. primaeveris* (Kaszab, 1958), *E. punjabensis* (Kaszab, 1958), *E. schmidi* (Kaszab, 1978), *E. scutellatus* (Reitter, 1895), and *E. subsetosus* (Reitter, 1895). However, the available information on these taxa is currently insufficient to assign them to the subgenus *Bolognaia*; therefore, they require further study at both the morphological and the molecular levels.

Redefinition of the subgenus

***Eurymeloe* Reitter, 1911**

Type species. *Meloe brevicollis* Panzer, 1793 (by subsequent designation of Pinto and Selander, 1970).

Description (adult). Size small or medium (6–30 mm), usually robust in appearance. Body integument colour black to moderately metallic blue, bright, silky, or with an oily shininess (Fig. 2I). Body pubescence very short, recumbent, or absent on the head and pronotum. Head rounded, sides almost straight, convergent to the eyes. Eyes small, subreniform, weakly protruding, and without longitudinal depression behind them. Antennae submoniliform, robust, short or medium in length, usually not reaching the posterior margin of the pronotum, smoothly thickened towards the apex in some species (e.g., *E. brevicollis*); in males, unmodified. Antennomeres subcylindrical or subconical, V to VII (in some species IV to IX, e.g., *E. brevicollis*), wider than long or, at most, as wide as long. Clypeus transverse, approximately twice as wide as long. Labrum wide, fore margin broadly emarginate. Mandibles robust, often curved along the outer margin. Pronotum slightly or moderately convex, very transverse, usually more than 1.7 × wider than long, sides not parallel and obtusely rounded, posterior margin broadly emarginated, posterior corners rounded. Pronotum surface slightly variable, moderately convex, usually with a weak, diffuse, median longitudinal groove. Head and pronotum punctation from fine and scattered, sometimes almost absent, to deep and dense, with or without (*E. brevicollis*) very short pubescence. Hind margin of mesonotum straight or weakly arcuate. Elytra short and dehiscent, smooth to densely coriaceous or rugose. Legs normal, robust, pilose. Tarsomeres without hair pads or dense setose pubescence on the inferior side. Last abdominal ventrite broadly emarginated in males. Male genitalia: Gonostyli moderately short, distal regions wide, usually digitiform in lateral view, rounded at apex; gonocoxal plate broadly widened at the middle in dorsal view; aedeagus robust, relatively shorter than the gonoforceps or, at most, similar in length.

Taxonomic remarks. According to the present definition of the subgenus *Eurymeloe*, it is correlated with the *E. brevicollis* species group defined by Bologna (1988). It comprises a heterogeneous group of species characterised mainly by the following features in adults: small or medium in size, with a robust appearance; metallic blue or black body colour; reduced pilosity that is very scarce and short, often almost absent; wide antennomeres with V–VII usually wider than long; and variable head and pronotum punctation and elytral rugosity (see Bologna 1988, 1991).

Bologna (1988) tentatively included 22 species in the *E. brevicollis* species group. However, as this author pointed out, most of these species are very poorly known and, in some cases, the only morphological information on them is from the original description. As a result, the internal taxonomy of *Eurymeloe* s. str. is very complex and unclear (Bologna 1988).

On the basis of the molecular and morphological data (Reitter 1895, 1911; Escherich 1896; Martínez de la Escalera 1914; Peyerimhoff 1926; Bologna 1988, 1991, 1994a, 1994b; García-París et al. 2010; Di Giulio et al. 2013; this study), we ascribe to *Eurymeloe* s. str. the following species: *Eurymeloe* (*Eurymeloe*) *algiricus* (Escherich, 1890) (or *E. brevicollis algiricus*, see Bologna 2008), *E.* (*E.*) *austrinus* (Wollaston, 1854), *E.* (*E.*) *brevicollis*, *E.* (*E.*) *corvinus* (possibly co-specific with the previous species according to Di Giulio et al. 2013), *E.* (*E.*) *crosi* (Peyerimhoff, 1926), *E.* (*E.*) *curticornis* (Martínez de la Escalera, 1914) (or *E. brevicollis curticornis*, see Bologna 2008, 2020a), *E.* (*E.*) *ibericus*, and *E.* (*E.*) *lederi* (Reitter, 1895). The taxonomic positions of *E. luctuosus* (Brandt & Erichson, 1832) (related to *E. crosi*) and *E. scabriusculus* (Brandt & Erichson, 1832) (morphologically similar to *E. baudii* and *E. glazunovi*, both now included in *Bolognaia*) are still uncertain (Bologna 1988, 1991), and their assignment to *Eurymeloe* s. str. requires further studies.

Another 13 species [from Palaearctic Asia, except *E. aleuticus* (Borchmann, 1942), from the Aleutian Islands] were provisionally assigned by Bologna (1988) to the *E. brevicollis* species group: *Eurymeloe aleuticus*, *E. curticollis* (Kraatz, 1882), *E. escherichi* (Reitter, 1889), *E. frontalis* (Reitter, 1905), *E. gaberti* (Reitter, 1907), *E. laevipennis* (Brandt & Erichson, 1832), *E. lobicollis* (Fairmaire, 1891), *E. mandli* (Borchmann, 1942), *E. mathiesseni* (Reitter, 1905), *E. primulus* (Semenow, 1903), *E. servulus* (Bates, 1879), *E. transversicollis* (Fairmaire, 1891), and *E. zolotarevi* (Pliginskij, 1914). As in the previous case, additional molecular and morphological studies are required to determine the subgeneric assignment of these species.

Regarding other species of *Eurymeloe*, Shapovalov (2012) described *Meloe* (*Eurymeloe*) *sarmaticus* Shapovalov, 2012 from Russia and Central Kazakhstan and considered it closely related to the Russian-Kazakh *E. aeneus* (Tauscher, 1812). The last species, together with *E. pusio* (Wellman, 1910) and *E. asperatus* (Tan, 1981), were considered *incertae sedis* by Bologna (1988). However, recently, Bologna (2020a) integrated them into *Eurymeloe* (at the subgenus level), although he still considers *E. aeneus* a doubtful ascription. We did not examine material of these species; therefore, we cannot add new information on their current taxonomic placement.

Key to the subgenera of *Eurymeloe*

1 Body entirely black and opaque. Body pubescence absent dorsally. Pronotum flat, subrectangular, transverse, depressed in middle of the base, with sides straight, parallel. Punctation of the head and pronotum very broad, dense, subcontiguous (less dense in Sicilian and southern Italian populations) and deep, clearly foveate in appearance (Fig. 2B). Elytral surface smooth, with punctation usually broad, dense and foveate (reduced and barely visible in Sicilian and southern Italian populations). Size medium to large (14–31 mm) .... ***Coelomeloe***

– Body black, dull grey or dark brown (exceptionally sandy brown) to moderately metallic blue, bright, silky or more seldom opaque in appearance, sometimes with an oily shininess. Body pubescence quite distinct, or very short, recumbent, often almost imperceptible. Pronotum slightly to moderately convex, wider than long, with sides not parallel, more or less converging backward, and posterior angles usually broadly rounded. Head and pronotum punctation from fine and scattered, sometimes almost absent, to somewhat deep and dense, but never foveolate (Fig. 2A, C–J). Elytral surface smooth to densely coriaceous, subrugose or rugose, not foveolate. Size small to large (6–36 mm), but usually small to medium (6–22 mm).................... **2**

2 Body colour black to moderately metallic blue, bright or silky. Overall appearance robust. Body pubescence very short, recumbent, almost imperceptible or even absent on the head and pronotum. Antennae compact, robust, sometimes smoothly thickened towards the apex, short or medium in length, not reaching the posterior margin of the pronotum. Antennomeres subcylindrical or subconical, V to VII (in some species IV to IX) wider than long or, at most, as wide as long... ***Eurymeloe***

– Body integument black, dull grey or dark brown, exceptionally sandy brown, with an opaque, silky or bright appearance, never bluish or metallic. Body pubescence quite distinct. Overall appearance more graceful, sometimes moderately robust. Antennae normally slender, not thickened towards the apex, long or medium in length, usually reaching the posterior margin of the pronotum or exceeding it. Antennomeres IV to IX subcylindrical, always longer than wide .... ***Bolognaia***

Description of a new species of *Eurymeloe* from the Iberian Peninsula

Our molecular results revealed a distinctive lineage of *Eurymeloe* nested within the clade comprising *E. rugosus*, *E. murinus*, and *E. ganglbaueri*. This lineage, morphologically distinguishable from all its congeneric species, represents a new species that we herein describe.

***Eurymeloe* (*Bolognaia*) *orobates* sp. nov.**

https://zoobank.org/509BD098-E303-406E-AAE4-052059AC1865

Holotype. adult male (Fig. 3), labelled: “Puerto de la Quesera, Guadalajara, Spain, 41°12'32.2"N, 3°24'44.2"W, 1738 m, 15-XI-2015, F. Gutiérrez-Pérez et C. Cano leg.” [white label, printed]; “Holotypus *Meloe* (*Bolognaia*) *orobates* Sánchez-Vialas, Ruiz, Recuero, Gutiérrez-Pérez & García-París des. 2022” [white label, printed]; Holotipo [red label, printed]; MNCN_Ent 324740 [greyish label, printed]. Dissected and mounted genitalia (Fig. 4A–D). Dry-preserved, held at MNCN-CSIC.

Paratypes. four adult females, labelled: two females: “Puerto de la Quesera, Guadalajara, Spain 41°11'30.11"N, 3°24'27.55"W, 1625 m, 22-V-2016, M. García París, A. Fernández Liger, A. Corral Lou leg. [white label, printed]; ASV 18002 and ASV 18003, respectively [white label, handwritten]; MNCN_Ent 325407 and MNCN_Ent 325408, respectively [white label, printed]. One adult female (Fig. 5): “Puerto de la Quesera, Guadalajara, Spain, 41°11'30.11"N, 3°24'27.55"W, 1625 m, 8-XII-2018, A. Sánchez-Vialas leg.” [white label, printed]; MNCN_Ent 325409 [white label, printed]. One adult female: “Puerto de la Quesera, Guadalajara, Spain, 41°12'58.10"N, 3°25'14.37"W, 1712 m, 28-XII-2021, A. Sánchez-Vialas leg.” [white label, printed]; MNCN_Ent 325410 [white label, printed]. –All paratypes labelled: “Paratypus, *Meloe* (*Bolognaia*) *orobates* Sánchez-Vialas, Ruiz, Recuero, Gutiérrez-Pérez & García-París des. 2022” [white labels, printed]. All paratypes are preserved in ethanol (except for the female gonostyli of the specimen MNCN_Ent 325409 [Fig. 4E], which was dissected, mounted on a piece of cardboard using DMHF, and preserved dry, bearing the following labels: “Puerto de la Quesera, Guadalajara, Spain, 41°11'30.11"N, 3°24'27.55"W, 1625 m, 8-XII-2018, A. Sánchez-Vialas leg.” [white label, printed]; “Paratypus, *Meloe* (*Bolognaia*) *orobates* Sánchez-Vialas, Ruiz, Recuero, Gutiérrez-Pérez & García-París des. 2022” [white label, printed]; Paratipo [red label, printed]), held at MNCN-CSIC.

Description of the holotype. Total length (frons to apex of the tergite VIII): 11.05 mm. Length from the frons to the posterior margin of elytra: 6.55 mm. Maximum width (located slightly anterior to the apex of the elytra): 6.81 mm. Body relatively robust, with slender appendages (Fig. 3). Voluminous abdomen. Coloration black all over body and appendages, except tibial spines and tarsal claws, which are brownish. Integument finely microreticulated, silky or semi-glossy in appearance. Setation decumbent, reddish brown, fairly dark, sometimes almost black ventrally and on

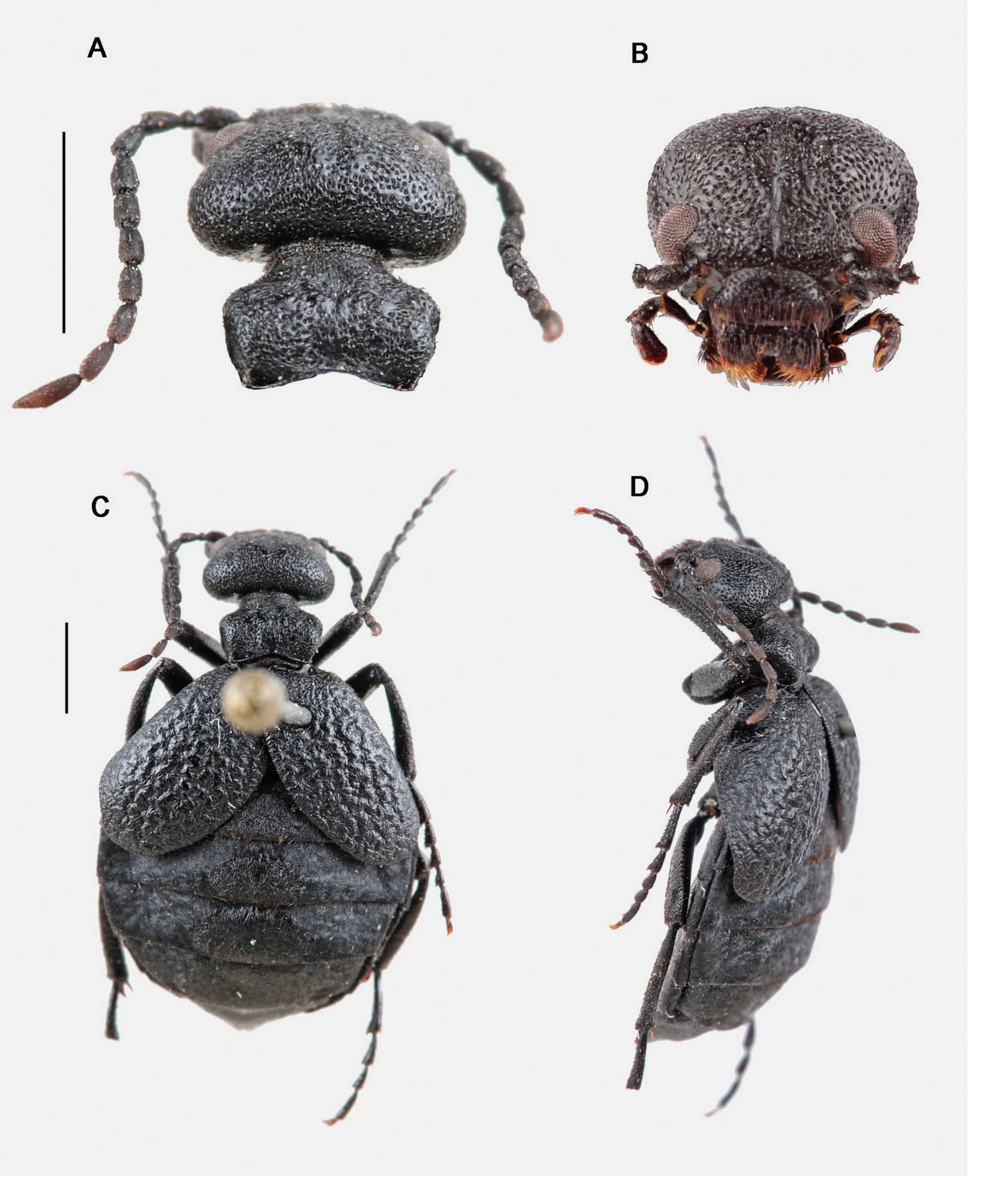

Figure 3. Holotype of *Eurymeloe orobates* sp. nov. MNCN 324740 **A** dorsal view of the head and pronotum **B** frontal view of the head **C** and **D** dorsal and dorsolateral views. Scale bars: 2 mm. Photographs: ASV.

the legs, and very short on the head, pronotum and elytra, longer on the abdominal tergites, legs, pygidium and ventral region, and arranged in relatively conspicuous tufts or single reddish yellow setae on the sclerotised plates of the abdominal tergites.

Head voluminous, broadly rounded and clearly wider than the pronotum, weakly truncated on the posterior margin of the temples, with integument black, silky

Figure 4. Genitalia of the male holotype MNCN 324740 (**A–D**) and of the female paratype MNCN 325409 (**E**) **A–C** ventral, dorsal and lateral views of the gonoforceps **D** lateral view of the aedeagus; scale bar: 1 mm **E** female gonostyli; scale bar: 0.2 mm. Photographs: ASV.

in appearance, finely microreticulated, and without longitudinal depressions behind the eyes (Fig. 3A, B). Maximum width in frontal view (at the level of the temples): 2.83 mm; minimum distance between the inner edges of the eyes: 1.83 mm; distance between the clypeus-frontal suture and the vertex (in frontal view): 1.81 mm. Temples wide and regularly rounded (Fig. 3B). Frons almost flat, with a weak and short longitudinal groove from the clypeus-frontal suture to the vertex, that is slightly deeper from the level of the eyes to the vertex; surface adjacent to the antennal insertions slightly elevated and with a weak and diffuse depression attached to the raised areas (Fig. 3B). Head punctation dense, consisting of rounded, markedly deep, closely positioned and subconfluent punctures, slightly larger in diameter in the frontal region and smaller towards the vertex, almost uniformly distributed, except on a narrow longitudinal mid-band on the frons, which is almost smooth (Fig. 3A, B). Head setation inconspicuous, short, decumbent, dark reddish brown, distributed according to the pattern of punctures in which it is inserted. Eyes medium-sized, subreniform and protruding, with upper lobes larger than the lower ones, barely notched at the level of the antennal insertions; clypeus-frontal suture deeply marked, weakly arcuate (Fig. 3B). Clypeus flat, transverse, subtrapezoidal, 2.1 × wider than long, with a brownish membranous anterior border; punctures medium-sized, separated by between 0.5 and 1 × their diameter, with the highest density on the sides; long setae homogeneously distributed, following the puncture pattern, directed forward, longest on the sides (Fig. 3B). Labrum-clypeus suture almost straight. Labrum transverse, 2.5 × wider than long, deeply emarginated in the middle, forming two clear lobes; punctures similar to those on the clypeus; setae longer on the lobes, following the punctation pattern, oriented forward and curved (Fig. 3B). Mandibles relatively robust, curved along the outer margins and notched in the distal region, glabrous at the apex, and scarcely pilose at the base. Maxillary and labial palps unmodified. Maxillary palps with palpomere I very short, subcylindrical (0.09 mm long, 0.1 mm wide); II longer, troncoconical, weakly curved in the proximal half (0.44 mm long, 0.21 mm wide); III troncoconical, shorter and wider than II (0.38 mm long, 0.23 mm wide); IV sub-trapezoidal, widened distally, broadly rounded at the apex and dorsoventrally flattened, with a narrow excavation along the distal margin (0.54 mm long, 0.3 mm wide); setae scattered and moderately long on palpomeres II and III, shorter and more scarce on palpomere IV. Labial palps short, not visible dorsally, with palpomere I subcylindrical, very short (0.11 mm long, 0.09 mm wide); II troncoconical (0.22 mm long, 0.15 mm wide); III similar in shape to the last maxillary palpomere (IV); setae as on maxillary palps.

Antennae with 11 antennomeres, moniliform, slender and long, surpassing the base of the pronotum when extended backward (Fig. 3A). Antennomeres not modified, subcylindrical or subconical, I–VIII black, semi-glossy, IX–XI dark brown, opaque but becoming reddish brown in XI. Antennomere I widened apically, subconical, ~ 1.92 × longer than wide (0.48 mm long, 0.25 mm wide); II short, subglobose, slightly wider than long (0.81 mm long, 0.82 mm wide); III–X subcylindrical, similar to each other, between 1.84 and 2.22 × longer than wide (III: 0.49 mm long, 0.22 mm wide; IV: 0.5 mm long, 0.24 mm wide; V: 0.48 mm long, 0.26 mm wide; VI: 0.46 mm long, 0.25 mm wide; VII: 0.49 mm long, 0.24 mm wide; VIII: 0.48 mm long, 0.23 mm wide; IX: 0.47 mm long, 0.21 mm wide; X: 0.48 mm long, 0.23 mm wide); XI is the longest, ~ 3.71 × longer than wide (0.78 mm long, 0.21 mm wide), subfusiform, with a blunt tip. Pilosity of antennomeres I–V comprised of short black setae, most decumbent though a few semi-erected, longer on segments I–III; antennomere VI with a mixture of short reddish brown and black setae; and antennomeres VII–XI with very short yellowish red setae, almost imperceptible.

Pronotum black, silky in appearance (Fig. 3A), small, sub-hexagonal, transverse, 1.59 × wider than long; length in the middle: 1.37 mm; maximum width (at the level of the lateral angles): 2.18 mm; lateral margins weakly converge backwards in the posterior two thirds and strongly converge forward in the anterior third, with the lateral angles well marked and rounded; fore margin almost straight; posterior margin or base broadly emarginated, with a thin flange. Dorsal surface of the pronotum clearly convex, gently sloping forward from the mid-region and steeply sloping back, with a slight and narrow depressed longitudinal-middle area with ambiguous boundaries (without a marked longitudinal midline or groove), such that two raised areas are observed on both sides of the central depression with two shallow and small rounded depressions observed anterior to the raised areas. Pronotal punctation relatively dense and unevenly distributed, consisting of relatively large, circular and deep punctures, subcontiguous, similar to those of the vertex but with a slightly larger diameter (Fig. 3A); the highest density is in the elevated areas on both sides of the midline, and the lowest densities are in the first quarter (just behind the fore margin), the depressed midband, and the central area of the base; integument surface with several fine, small and semi-wavy wrinkles between the punctures, located mainly on the sides, where they are arranged transversely and longitudinally in the middle depression. Pronotal setation inconspicuous, made up of short, curved dark reddish brown setae, mostly applied against the pronotal surface, distributed according to the pattern of punctures in which they are inserted; anterior margin, adjacent to the neck, with somewhat longer, semierect setae. Mesonotum mostly covered by the pronotum, showing, in dorsal view, only its posterior margin, which is weakly arcuate and with dense setation, consisting of setae longer than those of the pronotum, almost straight and lying backwards. Metanotum smooth, almost completely covered by the elytra. Prosternum narrow, very slightly extended posteriorly, broadly rounded at the central tip. Mesosternum relatively narrow and very transverse (width: 1.82 mm; length in the middle: 0.69 mm), with a small triangular prolongation backwards, ending in a rounded tip that extends to the level of the fore third of the mesocoxae; surface with long transverse wrinkles and dispersed punctures, similar to those of the vertex, and short setae. Metasternum subtrapezoidal, wide, covered by the mesocoxae, deep and closely notched in the middle of the posterior margin.

Elytra relatively short (length: 4.05 mm), strongly dehiscent and weakly convex, imbricated basally (the right over the left), divergent backwards and reaching the middle area of the fourth tergite, covering the first tergite, almost completely covering the second, and covering the lateral areas of the third (of which, only the central plate is clearly visible), and lateral basal portions on both sides of the fourth; elytral surface strongly rugose, corrugated, with marked wavy foveoles (Fig. 3C); punctation small, fine, shallow and scattered, confused with the roughness of the foveoles; integument with very dispersed and isolated setae, similar to those of the pronotum, although somewhat shorter.

Abdomen black, voluminous (Fig. 3C); maximum width, at level of the fourth tergite: 6.78 mm. Tergites semi-matte in appearance, with very weak and indistinct foveoles scattered on its surface; central sclerotised plates of the tergites elliptical, with a semi-glossy aspect and an integument surface that is slightly rough, with fine wrinkles, arranged transversely and concentrically. Dorsal setation decumbent, consisting of isolated and scattered short, reddish brown setae on the semi-matte sides of the tergites, and longer yellowish red (some almost golden) setae on the central plates, denser and forming inconspicuous tufts on the posterior margin of tergites II–IV. Ventrites silky in appearance, with dense punctation, made up of small, subcontiguous and slightly marked punctures that give them a finely vermiculated appearance; with short and decumbent dark brown, almost black, setae, homogeneously distributed; last ventrite clearly emarginated at the apex, with longer yellowish setae.

Legs relatively slender (Fig. 3C, D); surface with punctation fine and shallow, very dense in the tibiae and scarcer in the femurs, covered by relatively dense setation, consisting of short, dark brown (sometimes almost black) lying setae, denser on the tibiae. Length (in mm) of pro-, meso-, and metafemur as follows: 2.32, 2.6, and 3.1. Length (in mm) of pro-, meso-, and metatibia as follows: 2.25, 2.24 and 2.55. Length (in mm) of pro-, meso-, and metatarsus (and respective tarsomeres) as follow (claws excluded): 2.41 (I: 0.65; II: 0.4; III: 0.36; IV: 0.33; V: 0.67), 3.13 (I: 0.98; II: 0.53; III: 0.46; IV: 0.43; V: 0.73) and 3.56 (I: 1.36; II: 0.73; III: 0.61; IV: 0.86). Tarsi slender, clearly longer than the respective tibiae, with tarsomeres subcylindrical, slightly enlarged distally. Tarsomeres showing, on their ventral side, a small brush of very short, hirsute black setae, quite reduced in the last ones (V, V, IV). Pro- and mesotibiae with two similar distal spurs, short, narrow and straight; metatibial spurs dissimilar: outer spur spoon-shaped, inner spur similar to those of the fore- and mesotibiae but a little wider at the base and weakly curved at the apex. Coxae dense and finely punctate, with dense and short setation. Claws smooth, curved, with the lower lobe narrower than the upper one but equal in length.

Male genitalia with gonoforceps dark brown, hairless, moderately elongated, slender in dorsal, ventral, and lateral views (Fig. 4A–C). Gonostyli relatively long, ~ 4.4 × longer than wide in lateral view (1.33 mm long, 0.3 mm wide in lateral view), no excavated or depressed areas laterally in the distal regions; distal portion of each gonostylus separated dorsally by a fusiform longitudinal notch that extends to approximately the middle of the structure (Fig. 4A, B); distal lobes narrow and rounded at the apexes in lateral view (Fig. 4C). Gonocoxal plate relatively narrow and long, ~ 1.38 × longer than wide in dorsal view (1.36 mm long, 0.98 mm wide in ventral view), with the greatest width roughly in the middle of the plate, markedly emarginated at its distal margin (in ventral view) (Fig. 4A); surface almost flat. Aedeagus slender and narrow in lateral view (1.96 mm long, 0.2 mm wide in lateral view) flattened, narrowly rounded at the apex with two dorsal hooks that are similar in shape, although the distal hook is somewhat larger than the proximal one (Fig. 4D); endophallic hook small, located close to the apex and barely visible.

Variability. Female similar to the male (Fig. 5) but with the last abdominal ventrite rounded and not emarginated in its posterior margin, and with relatively shorter antennae. Morphological measurements of the studied female specimens (paratypes): total length (frons to apex of tergite VIII): 10–14 mm (mean = 12 mm; $n = 4$); body length (frons to posterior border of elytra): 6.5–9.5 mm (mean = 8.3; n = 4); body maximum width (between the elytral external borders): 6–8.1 mm (mean = 7.4; $n = 4$); pronotum length: 1.6–1.8 mm (mean = 1.7; $n = 4$); pronotum maximum

Figure 5. A–C habitus of a living female paratype (MNCN 325409) of *Eurymeloe orobates* sp. nov. **D** detail of the dorsal surface of the abdominal tergite I and the elytra. Note the brownish tufts. Photographs: ASV.

width: 2.23–2.74 mm (mean = 2.55 mm; *n* = 4); head maximum width: 2.74–3.43 mm (mean = 3.17 mm; *n* = 4); elytra length: 4–5.5 mm (mean = 5 mm; *n* = 4). Marked variability in the density of the pilose tufts on the dorsal side of the abdomen was observed: the studied females present lighter yellowish brown pilosity than that of the male, with more numerous and denser tufts located on the small, rounded depressed areas of the integument, homogeneously distributed, giving it an irregular appearance. Female gonostyli as in Fig. 4E.

Diagnosis and morphological comparisons. *Eurymeloe* (*B.*) *orobates* is characterised morphologically, with respect to all the other species of the subgenus *Bolognaia*, by the following combination of diagnostic traits: (1) body size small or medium (total length: 10–14 mm); (2) body integument entirely black, semi-glossy in appearance; (3) setation of the head, pronotum and elytra, short and decumbent, reddish brown, moderately dark, sometimes very dark (almost black) ventrally and on the legs; (4) setation of the central plates of the abdominal tergites yellowish red (some almost golden), longer and forming inconspicuous tufts; (5) antennae slender and long, surpassing the base of the pronotum when extended backwards; (6) head broadly rounded, with a weak and relatively short longitudinal median groove; (7) pronotum small, very transverse (more than 1.5 × wider than long), sub-hexagonal; (8) pronotal surface showing a weak and narrow depressed longitudinal-middle area, but without a marked groove; (9) punctation of the head and pronotum dense, forming rounded and markedly deep punctures; (10) elytral surface strongly rugose, corrugated, with marked foveoles; and (11) male genitalia with long gonostyli with no excavated or depressed areas in the distal regions and a narrow and long gonocoxal plate.

The species most similar to *E. orobates* are *E. rugosus* and *E. apenninicus* (both belonging to the group B or *E. murinus* group). Both species present dark (black or dark brown) pilosity all over the body and, on the abdominal tergites, some inconspicuous (usually barely perceptible) yellowish brown or yellow setae, but not tufts. In addition to the colour pattern of the body setation, *E. rugosus* and *E. apenninicus* differ from *E. orobates* by the shape of their pronotum, which is longer, less transverse, and flatter (less convex), and has a strong median longitudinal groove (absent in *E. orobates*). The punctation of the head and pronotum are also markedly larger, deeper, and denser in *E. rugosus* and *E. apenninicus* (see Bologna 1988, 1991). In *E. orobates*, the antennae are slenderer and longer.

Within group B (*E. murinus* group), in which *E.* (*B.*) *orobates* is integrated, the new species can be readily distinguished from *E.* (*B.*) *baudueri* (southern France, Iberian Peninsula, and northern Morocco), *E.* (*B.*) *flavicomus* (Canary Islands), *E.* (*B.*) *ganglbaueri* (mainland Italy, Sardinia, Corsica, Sicily, Greece, Albania, Bulgaria, Bosnia and Herzegovina, Montenegro, Turkey, Syria, Spain, and southern France), *E.* (*B.*) *gomari* (northern Morocco), *E.* (*B.*) *kandaharicus* (Iran and Afghanistan), *E.* (*B.*) *murinus* (Iberian Peninsula, Sicily, Sardinia, Corse, Crete, Maghreb, and Libya), *E.* (*B.*) *nanus* (Iberian Peninsula, North Africa, and Middle East), *E.* (*B.*) *omanicus* (eastern Arabian peninsula), and *E.* (*B.*) *pallidicolor* (western Morocco). For instance, in contrast to *E.* (*B.*) *orobates*, all these species present, among other specific traits, a body integument that is dull grey or dark brown, occasionally reddish brown or, rarely, sandy brown (*E. pallidicolor*) or almost black (*E. ganglbaueri*). In addition, the body integument is generally opaque or matte in appearance or, at most, silky (but never glossy or semi-glossy as in *E. orobates*). The setation of these species is also quite distinct from that of *E. orobates*: it is yellowish, whitish, or golden all over the body and usually longer, and on the abdominal tergites, the tufts of setae, when present, are highly conspicuous (see Fig. 2). Moreover, the punctation of the head and pronotum in these species is clearly finer and shallower, and the elytral sculpture is distinctly smoother (not corrugated) and without marked foveoles, except in *E. ganglbaueri*; however, in this last species, the foveoles are clearly more attenuated than in *E. orobates* (see Kaszab 1958, 1983; Bologna 1988, 1991; Ruiz and García-París 2009, 2015).

Eurymeloe (*B.*) *orobates* differs from the species of group A (*E. mediterraneus* group, composed of, at least, *E. affinis* from the Maghreb and Libya; *E. apivorus* and *E. baamarani*, which are restricted to Morocco; *E. baudii* from the Italian Peninsula, Sicily, and Croatia; *E. glazunovi* from Eastern Europe and Central Asia; and *E. mediterraneus*, which is widely distributed throughout Europe, the Mediterranean basin, the Canary

Islands, and the Middle East) by presenting reddish brown body setation and abdominal tergites with small tufts of reddish yellow setae, among other diagnostic characters (see above). By contrast, the body pilosity, including on the abdominal tergites, of species of the *E. mediterraneus* group is black (see Bologna 1988, 1991; Ruiz and García-París 2015). The Sardinian specimens of *E. mediterraneus* with brown setae can clearly be distinguished from *E. orobates* by the shape of the pronotum: in the first species, it is subrectangular and has subparallel sides; in the second, it is markedly transverse and subhexagonal and has sides that converge backwards.

The only species in group C is *E.* (*B.*) *fernandezi* (endemic to the Canary Islands). In comparison with *E.* (*B.*) *orobates*, this species presents, among other distinctive characters, an entirely black body setation; a clearly longer, not transverse pronotum with sinuous margins; an integument surface with wrinkles and parallel ridges that form eddies; and an elytral sculpture consisting of a fine zig-zag roughness (see Pardo Alcaide 1951; Ruiz and García-París 2015). Lastly, the two species tentatively assigned to *Bolognaia*, *E.* (*B.*) *saharensis* (widely distributed throughout North Africa, the Canary Islands, the Iberian Peninsula, Israel, and Saudi Arabia) and *E.* (*B.*) *vignai* (only known from Djibouti), are phenetically very different to *E.* (*B.*) *orobates*: their body setation is entirely reddish and longer, without reddish yellow setae forming tufts on the abdominal tergites; a subsquare, not transverse pronotum; relatively fine, shallow, and scattered punctation of the head and pronotum; very long legs; elytra with a soft sculpture, without foveoles or marked roughness; and highly distinctive male genitalia (Bologna 1988; Ruiz et al. 2010).

Distribution and notes on natural history. *Eurymeloe orobates* is only known from a single locality, Puerto de la Quesera (in the province of Guadalajara, Spain) in the Iberian Peninsula (Fig. 6). This site, which is at an elevation of 1738 m above sea level (a.s.l.), is within the supra-Mediterranean bioclimatic level (see Rivas-Martínez 1987; Rivas-Martínez et al. 2002). Specifically, Puerto de la Quesera is in the Sierra de Ayllón, at the eastern edge of the Sistema Central mountain range. This region is characterised predominantly by micaceous schist, slate and quartzite soils (Rivas-Martínez et al. 1990; Vera 2004). Vegetation cover around Puerto de la Quesera consists of, at lower altitudes (below 1500 m a.s.l), deciduous oak forests of *Quercus pyrenaica* Willd. and, at higher altitudes (1500–1700 m a.s.l.), formations of *Fagus sylvatica* L. Above the deciduous tree cover level, there are shrubs such as *Erica arborea* L., *Juniperus communis* L., and *Arctostaphyllos uva-ursi* L., whereas grasslands dominate at altitudes over 1800 m a.s.l (Ibáñez et al. 1982). Hostile climatic conditions including low temperatures, late spring frosts, and strong winds characterise the high-altitude areas (Ibáñez et al. 1982). Furthermore, this region has been strongly altered by human activities (e.g., deforestation and overgrazing), particularly by the establishment of terraced pinewood plantations of *Pinus sylvestris* L. (Fig. 6A) (Gil-García et al. 1995). In this region, adult specimens of *E. orobates* have been found actively wandering, under stones, and on tree barks, between November and May, usually in open areas or at the boundaries of the terraced plantations of *P. sylvestris* (authors, pers. obs.). Biological aspects of the new species remain unknown; however, we expect them to be similar to the ones described for other species of the *E. murinus* group (Bologna 1988, 1991).

Figure 6. A Puerto de la Quesera, Guadalajara, Spain. Type locality of *Eurymeloe orobates* sp. nov. **B** adult female of *Eurymeloe orobates* sp. nov. in situ (paratype MNCN 325407). Photographs **A** (ASV) **B** (MGP).

Etymology. The specific epithet *orobates* is derived from the Greek word "*oros*", meaning mountain, and "*bates*", meaning walker. This name alludes to the mountainous environment where the specimens of the new species were found, sometimes, wandering on mountain pastures and trails (Fig. 6B).

Discussion

In light of previous morphological data and recent phylogenetic analyses (Sánchez-Vialas et al. 2021; this study), we have updated the internal taxonomy of the genus *Eurymeloe*. In order to reflect the morphologically distinguishable, main monophyletic units within *Eurymeloe*, and to maintain the validity of the widely used name *Coelomeloe*, we have deemed it necessary to consider that each of the three main molecular lineages represents an independent subgenus: *Eurymeloe*, *Coelomeloe*, and *Bolognaia* subgen. nov.

Morphological traits of larvae have been traditionally considered relevant in the systematics of the group, sometimes even more informative than adult characters for phylogenetic studies (Bologna and Pinto 2001). In fact, traits of the first instar larva (triungulin) have been studied for most of the genera and subgenera of Meloini (Bologna 1988, 1991; Selander 1989; Bologna et al. 1989, 1990; Bologna and Pinto 1992, 1998; Pinto and Bologna 1993; Bologna and Aloisi 1994; Di Giulio et al. 2002; Di Giulio et al. 2013, 2014). However, not having a resolved internal taxonomy for *Eurymeloe* confuses explanations of the evolutionary history of some of these traits. For instance, a particular morphological trait related to the shape of the abdominal spiracle I that is shared between the first instar larvae of *Coelomeloe* and *Eurymeloe sensu stricto* [the *brevicollis* group of *Meloe* (*Eurymeloe*) *sensu* Bologna 1988] was previously suggested to be the result of parallel biological adaptation (Di Giulio et al. 2013). However, considering our results and consistent with those shown by Sánchez-Vialas et al. (2021), this trait can be better explained as a synapomorphic character state for these sister subgenera.

Some conspicuous adult traits are also shared between the subgenera *Eurymeloe* and *Coelomeloe*, including antennae that are submoniliform, robust, short or medium in length, and which do not usually not reach the posterior margin of the pronotum; antennomeres V to VII that are wider than long or, at most, as wide as long; and very short or not [e.g., *E.* (*E.*) *brevicollis*, *E.* (*E.*) *ibericus*, and *E.* (*C.*) *tuccia*] body pubescence. These character states differ from those of the subgenus *Bolognaia*, which usually presents antennae that are moniliform, normally slender, long or medium in length, and which usually reach or exceed the posterior margin of the pronotum; antennomeres IV-IX that are subcylindrical, always longer than wide; and distinctive short or very short (black, yellowish, whitish, or golden) body pubescence. Therefore, the close relationship between *Eurymeloe* s. str. and *Coelomeloe* is supported by both our molecular analysis (BPP = 0.9) and morphology.

Our results confirm that *E.* (*B.*) *rugosus*, a species previously assigned to Bologna's (1988) subgroup A (*E. rugosus* subgroup) on the basis of morphology, should instead be included in subgroup B (*M. murinus* subgroup). The morphology of *E. rugosus*, which presents a completely black coloration without noticeable brownish pilosity, led Bologna (1988) to separate it from subgroup B. Although both subgroups are now integrated within the subgenus *Bolognaia*, they are not monophyletic groups since, according to our molecular phylogeny, the morphological traits used to diagnose them are homoplastic. As a result, the assignation of some species to each of these groups has been controverted. For example, ambiguous morphological traits in *E. ganglbaueri* (see Ruiz & García-París 2009) has blurred its systematic allocation, as it was included in subgroup A based on morphology *sensu* Bologna (1988) but ascribed to that author's subgroup B based on molecular data (Sánchez-Vialas et al. 2021). The newly discovered species, *Eurymeloe* (*B.*) *orobates* sp. nov., notably presents a pattern of pilosity that is intermediate between *E.* (*B.*) *rugosus* and *E.* (*B.*) *murinus*-*E.* (*B.*) *ganglbaueri*, but a body integument that is more similar to *E.* (*B.*) *rugosus*.

With the addition of the new species, eight species of the subgenus *Bolognaia* are known from the Iberian Peninsula: *E.* (*B.*) *baudueri*, *E.* (*B.*) *ganglbaueri*, *E.* (*B.*) *mediterraneus*, *E.* (*B.*) *murinus*, *E.* (*B.*) *nanus*, *E.* (*B.*) *orobates*, *E.* (*B.*) *rugosus*, and *E.* (*B.*) *saharensis* (García-París et al. 2010; Bologna, 2020a; this study). The existence of a new, morphologically distinctive species of Meloidae, which was found in an apparently well surveyed area of central Spain (Puerto de la Quesera, in the province boundaries between Madrid and Guadalajara), suggests that an undefined portion of the diversity of *Bolognaia* and other secretive species of *Eurymeloe* still awaits discovery.

Acknowledgements

We are very grateful for help during the field work to E. Karen López-Estrada, Concha Cano, Andrea Corral Lou, Andrea Fernández Liger, Javier Aznar González de Rueda and Arlo Hinckley. We thank Melinda Modrell for the thorough language revision. We are also grateful to Mercedes París and Antonio Melic for providing us with the opportunity to revise the MNCN entomological collection and the Maynar Collection of the Asociación Entomológica Aragonesa, respectively. We thank Antonio Recalde for allowing us to examine an Iberian specimen of *E. rugosus*. This work was funded by the Spanish Government, project grant PID2019-110243GB-100 / AEI/10.13039/501100011033 (Ministerio de Ciencia, Innovación y Universidades, Spain) (PI: M. García-París).

References

Bologna MA (1988) Note su *Eurymeloe* e revisione delle specie euromediterranee del gruppo *rugosus* (Coleoptera, Meloidae). Fragmenta Entomologica 20(2): 233–301.

Bologna MA (1990) Faunistica e zoogeografia dei Meloidae (Coleoptera) della Somalia. Biogeographia 14(1988): 293–401. https://doi.org/10.21426/B614110400

Bologna MA (1991) Fauna d'Italia. XXVIII. Coleoptera Meloidae. Ed. Calderini, Bologna. [i–xiv] 541 pp.

Bologna MA (1994a) Meloidae from Canary and other macaronesian islands (Coleoptera). Miscel-lània Zoològica 16(1992): 73–80.

Bologna MA (1994b) I Meloidae della Grecia (Coleoptera). Fragmenta Entomologica 25 (Supplemento): 1–119.

Bologna MA (2008) Meloidae. In: Löbl I, Smetana A (Eds) Catalogue of Palaearctic Coleoptera. Vol. 5. Tenebrionoidea. Apollo Books, Stenstrup, 370–412.

Bologna MA (2020a) Meloidae. In: Iwan D, Löbl I (Eds) Catalogue of Palaearctic Coleoptera. Vol. 5. Tenebrionoidea. Revised and Updated Second Edition, Leiden, Boston, Brill, 500–562.

Bologna MA (2020b) New nomenclatural and taxonomics acts, and comments. Meloidae. In: Iwan D, Löbl I (Eds) Catalogue of Palaearctic Coleoptera. Vol. 5. Tenebrionoidea. Revised and Updated Second Edition, Leiden, Boston, Brill, 13–14.

Bologna MA, Aloisi G (1994) Systematics and bionomics of *Physomeloe* Reitter, 1911, with description of the first instar larva (Coleoptera, Meloidae). Eos 69: 45–56.

Bologna MA, Pinto JD (1992) A review of *Meloe* (*Taphromeloe*), including a description of the first-instar larva of *M.* (*T.*) *erythrocnemus* and comments on the classification of the tribe Meloini (Coleoptera: Meloidae). Proceedings of the Entomological Society of Washington 94(3): 299–308.

Bologna MA, Pinto JD (1998) A review of the Afrotropical species of *Meloe* Linnaeus 1758 (Coleoptera, Meloidae) with descriptions of first instar larvae, a key to species and an annotated catalogue. Tropical Zoology 11(1): 19–59. https://doi.org/10.1080/03946975.1998.10539352

Bologna MA, Pinto JD (2001) Phylogenetic studies of *Meloidae* (Coleoptera), with emphasis on the evolution of phoresy. Systematic Entomology 26(1): 33–72. https://doi.org/10.1046/j.1365-3113.2001.00132.x

Bologna MA, Aloisi G, Marangoni C (1989) Nuove osservazioni su *Eurymeloe* Reitter e descrizione di larve di I stadio (Coleoptera, Meloidae). Bulletin et Annales de la Société Royale Belge d'Entomologie 125: 67–75.

Bologna MA, Aloisi G, Taglianti AV (1990) Phoretic association of some African *Cyaneolytta* Péringuey 1909 with carabids, and morphology of first instar larvae in Meloini (Coleoptera Meloidae). Tropical Zoology 3(2): 159–180. https://doi.org/10.1080/03946975.1990.10539459

Cros, A. (1934) Le *Meloe affinis* Lucas var. *setosus* Escherich ses moeurs, sa larve primaire. Bulletin de la Société d'Historie naturelle de l'Afrique du Nord 21: 88–104[2 pls].

Di Giulio A, Bologna MA, Pinto JD (2002) Larval morphology of the *Meloe* subgenus *Mesomeloe*: Inferences on its phylogenetic position and a first instar larval key to the *Meloe* subgenera (Coleoptera, Meloidae). The Italian Journal of Zoology 69(4): 339–344. https://doi.org/10.1080/11250000209356479

Di Giulio A, Sciotti A, Bologna MA (2013) Revision of the first instar larvae of *Meloe*, subgenera *Eurymeloe* and *Coelomeloe*, with new descriptions and a key to the species (Coleoptera: Meloidae). The Italian Journal of Zoology 80(2): 242–254. https://doi.org/10.1080/11250003.2013.776119

Di Giulio A, Carosi M, Khodaparast R, Bologna MA (2014) Morphology of a new blister beetle (Coleoptera, Meloidae) larval type challenges the evolutionary trends of phoresy-related characters in the genus *Meloe*. Entomologia 2(164): 69–79. https://doi.org/10.4081/entomologia.2014.164

Escherich K (1890) Revision der behaarten *Meloë*-Arten der alten Welt. Wiener Entomologische Zeitung 9: 87–96.

Escherich K (1896) Meloiden-studien. IV. Theil. Wiener entomologische Zeitung 15: 27–30. https://doi.org/10.5962/bhl.part.13870

García-París M, Ruiz JL (2011) Capítulo 9. Las cantáridas y aceiteras (Coleoptera: Meloidae) en la obra de Manuel Martínez de la Escalera. In: Martín Albaladejo C, Izquierdo Moya I (Eds) Al encuentro del naturalista Manuel Martínez de la Escalera (1867–1949). Monografías del Museo Nacional de Ciencias Naturales, Consejo Superior de Investigaciones Científicas, Madrid, 173–205.

García-París M, Ruiz JL, Alonso-Zarazaga MA (2010) Catálogo sinonímico de los taxones ibero-baleares de la familia Meloidae (Coleoptera). Graellsia 66(2): 165–212. https://doi.org/10.3989/graellsia.2010.v66.018

Gil-García MJ, Tomás Las Heras R, Ruiz-Zapata MB (1995) Influencia humana sobre el paisaje vegetal pasado en el Puerto de la Quesera. Nova Acta Científica Compostelana 5: 153–160.

Ibáñez J, Almendros G, Polo A (1982) Contribución al estudio del subsistema edáfico en los ecosistemas climácicos del Sistema Central (España). I.- Características generales de los ecosistemas del Puerto de la Quesera (Macizo de Ayllón). Revue d'écologie et de biologie du sol 19(2): 135–149.

Kaszab Z (1958) Die Meloiden Afghanistan (Coleoptera). Acta Zoologica Academiae Scientiarum Hungaricae 3: 245–312.

Kaszab Z (1983) Insects of Saudi Arabia. Coleoptera: Fam. Meloidae. A synopsis of the Arabian Meloidae. In: Wittmer W, Büttiker W (Eds) Fauna of Saudi Arabia. Vol. 5. Pro Entomologia. Natural History Museum, Basle and Meteorology and Environmental Protection Administration, Jeddah, Basle (Switzerland), 144–204.

Katoh K, Toh H (2008) Recent developments in the MAFFT multiple sequence alignment program. Briefings in Bioinformatics 9(4): 286–298. https://doi.org/10.1093/bib/bbn013

Maddison WP, Maddison DR (2019) Mesquite: A Modular System for Evolutionary Analysis. Version 3.61. [Available from:] http://mesquiteproject.org [accessed on 20 January 2021]

Martínez de la Escalera M (1909) Especies nuevas de Meloidos del SW. de Marruecos. Boletín de la Real Sociedad española de Historia Natural 9: 240–244.

Martínez de la Escalera M (1914) Los Coleópteros de Marruecos. Trabajos del Museo Nacional de Ciencias Naturales, serie Zoológica 11: 1–553.

Ohnishi O, Takenaka M, Okano R, Yoshitomi H, Tojo K (2021) Wide-Scale Gene Flow, Even in Insects that Have Lost Their Flight Ability: Presence of Dispersion Due to a Unique Parasitic Ecological Strategy of Piggybacking Hosts. Zoological Science 38(2): 122–139. https://doi.org/10.2108/zs200088

Pardo Alcaide A (1951) Estudios sobre Meloidae. III. Una nueva especie de *Meloe* de la isla de Tenerife y comentarios sobre algunos meloideos de la citada isla. Eos 25: 249–255.

Pérez-Moreno I, San Martín AF, Recalde JI (2003) Aportaciones corológicas y faunísticas sobre meloidos ibéricos (Coleoptera: Meloidae). Boletin de la SEA 33: 195–217.

Peyerimhoff P (1926) Meloidae. In: Sainte-Claire Deville J, Peyerimhoff P. Nouveaux Coléoptères du Nord-Africain. Cinquante-cinquième note. Faune du Grand-Atlas marocain. Bulletin de la Société Entomologique de France 31(8): 93–96. https://doi.org/10.3406/bsef.1926.27653

Pinto JD, Bologna MA (1993) The first instar larvae of *Meloe afer* and *M. occultus*, with a clarification of antennal structure in larval *Meloe* (Coleoptera: Meloidae). The Coleopterists Bulletin 47(4): 340–348.

Pinto JD, Selander RB (1970) The bionomics of blister beetles of the genus *Meloe* and a classification of the New World species. Illinois Biology Monographs 42: 1–222. https://doi.org/10.5962/bhl.title.50239

Pliginskij VG (1910) Deux espèces nouvelles du genre *Meloë* Linn. (Coleoptera, Meloidae). Revue Russe d'Entomologie 10: 170–172.

Recalde JI, San Martín AF, Pérez-Moreno I (2002) Insecta: Coleoptera. Familia 41. Meloidae. Catalogus de la entomofauna aragonesa 26: 3–21.

Reitter E (1895) Bestimmungs-Tabellen der europaïschen Coleopteren Meloidae. I Theil: Meloini. 32. Verlag des Verfassers, Paskau, 1–13.

Reitter E (1911) Fauna Germanica. Die Käfer des Deutschen Reiches. Nach der analytischen Methode bearbeitet. Lutz, Stuttgart, 436 pp.

Rivas-Martínez S (1987) Memoria del mapa de las series de vegetación de España 1:400.000. Madrid, ICONA. 268 pp.

Rivas-Martínez S, Fernández-González F, Sánchez-Mata D, Pizarro JM (1990) Vegetación de la Sierra de Guadarrama. Itinera Geobotanica 4: 3–132.

Rivas-Martínez S, Díaz TE, Fernández-González F, Izco J, Loidi J, Lousa M, Penas A (2002) Vascular plant communities of Spain and Portugal. Addenda to the syntaxonomical checklist of 2001. Part I. Itinera Geobotanica 15: 5–432.

Ronquist F, Teslenko M, van der Mark P, Ayres DL, Darling A, Höhna S, Larget B, Liu L, Suchard LA, Huelsenbeck JP (2012) MrBayes 3.2: Efficient Bayesian phylogenetic inference and model choice across a large model space. Systematic Biology 61(3): 539–542. https://doi.org/10.1093/sysbio/sys029

Ruiz JL, García-París M (2009) Descripción de una especie nueva de *Meloe* Linnaeus, 1758 del subgénero *Eurymeloe* Reitter, 1911 (Coleoptera, Meloidae) del norte de Marruecos. Graellsia 65(2): 91–109. https://doi.org/10.3989/graellsia.2009.v65.i2.144

Ruiz JL, García-París M (2015) Una nueva especie de *Meloe* Linnaeus, 1758 del suroeste de Marruecos incluida en el grupo de *M.* (*Eurymeloe*) *rugosus* Marsham, 1802 (Coleoptera: Meloidae). Graellsia 71(1): e018. http://dx.doi.org/10.3989/graellsia.2015.v71.118

Ruiz JL, Bologna MA, García-París M (2010) Taxonomía y distribución de *Meloe* (*Eurymeloe*) *saharensis* Chobaut, 1898 (Coleoptera, Meloidae), con nuevas sinonimias y primeros registros para Europa y la Macaronesia. Graellsia 66(1): 85–96. https://doi.org/10.3989/graellsia.2010.v66.015

Rulik B, Eberle J, von der Mark L, Thormann J, Jung M, Köhler F, Ahrens D (2017) Using taxonomic consistency with semi-automated data pre-processing for high quality DNA barcodes. Methods in Ecology and Evolution 8(12): 1878–1887. https://doi.org/10.1111/2041-210X.12824

Sánchez-Vialas A, García-París M, Ruiz JL, Recuero E (2020) Patterns of morphological diversification in giant *Berberomeloe* blister beetles (Coleoptera: Meloidae) reveal an unexpected taxonomic diversity concordant with mtDNA phylogenetic structure. Zoological Journal of the Linnean Society 189(4): 1249–1312. https://doi.org/10.1093/zoolinnean/zlz164

Sánchez-Vialas A, Recuero E, Jiménez-Ruiz Y, Ruiz JL, Marí-Mena N, García-París M (2021) Phylogeny of Meloini blister beetles (Coleoptera, Meloidae) and patterns of island colonization in the Western Palaearctic. Zoologica Scripta 50(3): 358–375. https://doi.org/10.1111/zsc.12474

Selander RB (1966) A classification of the genera and higher taxa of the meloid subfamily Eleticinae (Coleoptera). Canadian Entomologist 98(5): 449–481. https://doi.org/10.4039/Ent98449-5

Selander RB (1985) *Spastomeloe*, a new genus of Meloini from Peru (Coleoptera: Meloidae). Journal of the Kansas Entomological Society 58: 668–685.

Selander RB (1989) The triungulin larva of *Meloe cicatricosus* Leach (Col., Meloidae). Deutsche Entomologische Zeitschrift 36(4-5): 401–407. https://doi.org/10.1002/mmnd.4810360436

Shapovalov AM (2012) A new species of the subgenus *Eurymeloe* Reitter, 1911 (Coleoptera, Meloidae: *Meloe*) from the steppe zone of Russia and Kazakhstan. Caucasian Entomological Bulletin 8(2): 205–210. https://doi.org/10.23885/1814-3326-2012-8-2-205-210

Vera JA (2004) Geología de España. Sociedad Geológica de España-Instituto Geológico y Minero de España, Madrid, 890 pp. [2 maps]

Wiley EO (1978) The evolutionary species concept reconsidered. Systematic Zoology 27(1): 17–26. https://doi.org/10.2307/2412809

Wiley EO, Mayden RL (2000) A defense of the evolutionary species concept. In: Wheeler QD, Meier R (Eds) Species concepts and phylogenetic theory: A debate. Columbia University Press, New York, 198–208.

ZooKeys 1109: 49–65 (2022)
doi: 10.3897/zookeys.1109.81125
https://zookeys.pensoft.net

RESEARCH ARTICLE

A peer-reviewed open-access journal
ZooKeys
Launched to accelerate biodiversity research

Comparative mitogenomics of the genus *Motacilla* (Aves, Passeriformes) and its phylogenetic implications

Chao Yang[1,2], Xiaojuan Du[1], Yuxin Liu[1], Hao Yuan[1,3], Qingxiong Wang[2], Xiang Hou[2], Huisheng Gong[2], Yan Wang[2], Yuan Huang[1], Xuejuan Li[1*], Haiyan Ye[1*]

1 *College of Life Sciences, Shaanxi Normal University, Xi'an 710062, China* **2** *Shaanxi Institute of Zoology, Xi'an 710032, China* **3** *School of Basic Medical Sciences, Xi'an Medical University, Xi'an, China*

Corresponding authors: Xuejuan Li (Xuejuan Li, lixuejuan456@163.com), Haiyan Ye (tiantian@snnu.edu.cn)

Academic editor: Grace P. Servat | Received 7 March 2022 | Accepted 21 May 2022 | Published 1 July 2022

https://zoobank.org/218293A5-8675-4FA3-8B2D-81119A03C300

Citation: Yang C, Du X, Liu Y, Yuan H, Wang Q, Hou X, Gong H, Wang Y, Huang Y, Li X, Ye H (2022) Comparative mitogenomics of the genus *Motacilla* (Aves, Passeriformes) and its phylogenetic implications. ZooKeys 1109: 49–65. https://doi.org/10.3897/zookeys.1109.81125

Abstract

The genus *Motacilla* belongs to Motacillidae (Passeriformes), where mitochondrial features are poorly understood and phylogeny is controversial. Whole mitochondrial genome (mitogenome) data and large taxon sampling are considered to be ideal strategies to obtain this information. We generated four complete mitogenomes of *M. flava*, *M. cinerea*, *M. alba* and *Dendronanthus indicus*, and made comparative analyses of *Motacilla* species combined with mitogenome data from GenBank, and then reconstructed phylogenetic trees based on 37 mitochondrial genes. The mitogenomes of four mitogenome sequences exhibited the same gene order observed in most Passeriformes species. Comparative analyses were performed among all six sampled *Motacilla* mitogenomes. The complete mitogenomes showed A-skew and C-skew. Most protein-coding genes (PCGs) start with an ATG codon and terminate with a TAA codon. The secondary structures of RNAs were similar among *Motacilla* and *Dendronanthus*. All tRNAs except for trnS(agy) could be folded into classic clover-leaf structures. Three domains and several conserved boxes were detected. Phylogenetic analysis of 90 mitogenomes of Passeriformes using maximum likelihood (ML) and Bayesian inference (BI) revealed that *Motacilla* was a monophyletic group. Among *Motacilla* species, *M. flava* and *M. tschutschensis* showed closer relationships, and *M. cinerea* was located in a basal position within *Motacilla*. These data provide important information for better understanding the mitogenomic characteristics and phylogeny of *Motacilla*.

* These authors contribute equally to this work.

Keywords
Comparative analysis, mitogenome, phylogeny

Introduction

In most animals, the mitochondrial genome (mitogenome) contains 13 protein-coding genes (PCGs), two rRNA genes (rRNAs), 22 tRNA genes (tRNAs), and one noncoding region (the control region, CR) (Wolstenholme 1992; Boore 1999). Mitochondrial sequences are commonly used for inferring phylogeny (Hassanin et al. 2005), and the mitogenome has been used as an effective marker for exploring the phylogenies of some avian taxa (Li et al. 2016a; Mackiewicz et al. 2019; Cai et al. 2019).

Passeriformes comprises 6533 currently described species (Gill et al. 2020). The genus *Motacilla* belongs to Motacillidae (Passeriformes) and contains 12 species (Alström et al. 2003; del Hoyo et al. 2004), which show striking plumage pattern variation (Harris et al. 2018). *Motacilla flava* Linnaeus, 1758 is a small, insectivorous oscine (Ödeen and Björklund 2003) and is closely related to *M. alba* Linnaeus, 1758, distributed in the Palearctic (Dong and Zhang 2011). Some mitochondrial fragments, such as nad2 and CR of *M. alba* (Li et al. 2016b), have been used to study the phylogeography and population history of *Motacilla*. Additionally, some mitochondrial genes, such as nad2 (Suppl. material 1: Fig. S1A; Dong et al. 2016) and cytb (Suppl. material 1: Fig. S1B; Zhang et al. 2016), have been used to study the phylogenetic relationships of *Motacilla*. However, the phylogenetic position of some *Motacilla* species is still controversial. For example, *M. alba* has been reported to form a sister group with *M. madaraspatensis* Gmelin, 1789 (Suppl. material 1: Fig. S1A, Dong et al. 2016), but it has also been grouped with *M. cinerea* Tunstall, 1771 (Suppl. material 1: Fig. S1B; Zhang et al. 2016). In addition, phylogenetic results reconstructed from genome-wide SNPs (Suppl. material 1: Fig. S1C, Harris et al. 2018) have some incongruence with those based on mitochondrial genes or mitogenomes (Suppl. material 1: Fig. S1A, B, D; Dong et al. 2016; Zhang et al. 2016; Gao et al. 2019).

An increasing number of avian mitogenome sequences are being generated with high-throughput sequencing technology (Morinha et al. 2016; Yang et al. 2018), facilitating the identification of mitogenomic characteristics such as gene order and base composition through the comparison of mitogenomes. However, the limited *Motacilla* mitogenomic sequences available from the GenBank database restricts the exploration of mitogenome features in this genus. For example, recent studies of *Motacilla* (Dong et al. 2016; Zhang et al. 2016; Harris et al. 2018; Gao et al. 2019) have focused on the phylogenetic relationships within this genus but have not conducted further comparative analyses among mitogenomes. In the present study, we obtained complete mitogenome sequences of *M. flava*, *M. cinerea*, *M. alba*, and *Dendronanthus indicus* Gmelin, 1789, performed comparative analyses and generated phylogenies (Subspecies differentiation was not discussed here). The new mitogenome data not only may help us understand the mitogenomic characteristics of *Motacilla* but also provide a basis for exploring phylogenetic relationships.

Methods

Specimen collection

Muscle samples were collected from the following species: *M. flava* (from China, Shaanxi Province, Hongjiannao in 2013); *M. cinerea* (from China, Shaanxi Province, Feng County in 2017); and *M. alba* and *D. indicus* (from China, Shaanxi Province, Lantian in 2018). All specimens of muscle samples were preserved in 100% ethanol and stored at -20 °C at the Shaanxi Institute of Zoology, Shaanxi Province, China.

Mitogenome sequencing, assembly and annotation

The mitogenome of *M. flava* was sequenced by Genesky Biotechnologies Inc., Shanghai, China, using the Illumina HiSeq2000 platform, while those of *M. cinerea*, *M. alba* and *D. indicus* were sequenced at Biomarker Technologies Inc., Beijing, China, using the Illumina Xten platform and a 150 bp paired-end strategy. Genomic DNA was extracted using a DNeasy kit and fragmented using ultrasonic methods to prepare a small-inserted-fragment library. The library data were obtained via Bridge PCR and Illumina paired-end sequencing.

There were 15,149,744 paired-end raw reads of *M. flava*, of which 47,390 reads were used for mitogenome assembly, with average coverage of 417.1X. There were 20,702,440 paired-end raw reads of *M. cinerea*, with clean data 6.92 G. A total of 261,229 reads were used for mitogenome assembly, with average coverage of 2256.2X. There were 7,868,047 raw reads in *M. alba*, with 7,860,296 reads with clean data, and 8,430,436 raw reads of *D. indicus*, with 8,420,710 reads with clean data.

The raw data from *M. flava*, *M. cinerea* and *M. alba* were quality trimmed with CLC Genomics Workbench 9.5.2 (CLC bio, Aarhus, Denmark) using the default parameters. Mitogenome assembly was performed in MITOBIM 1.8 (Hahn et al. 2013), with *M. alba* (GenBank: NC029229) as a reference. The mitogenomic sequences of *D. indicus* were assembled using MitoZ 2.4 (Meng et al. 2019). Mitochondrial PCGs were identified using Geneious 11.1.3 (Kearse et al. 2012) by searching for open reading frames and employing the *M. alba* mitogenome (GenBank: NC029229) as a reference. Most tRNAs were identified using tRNAscan-SE 1.21 (Lowe and Eddy 1997), with secondary structures used as references. The remaining tRNAs, rRNAs and CRs were identified by comparison with other *Motacilla* species. Each mitochondrial gene was confirmed by alignment with the corresponding homologous genes from other *Motacilla* species available in GenBank. The secondary structures of rrnS and rrnL were generated using the mitogenomic rRNAs of *Remiz consobrinus* as a reference (Gao et al. 2013).

Comparative analysis and phylogenetic reconstruction

The six mitogenomes (*M. flava*, *M. cinerea* and *M. alba* mitogenomes from collected specimens combined with *M. tschutschensis*, *M. alba* and *M. cinerea* genomes from GenBank) were used for comparative analysis. A mitogenome of *M. lugens*

(KU246035/NC_029703) was excluded because this has been shown to represent a chimera (Sangster and Luksenburg 2021). The nucleotide compositions of the mitogenomes and different datasets were calculated using Geneious 11.1.3 (Kearse et al. 2012). Nucleotide bias was calculated using the formulas AT-skew = (A–T)/(A+T) and GC-skew = (G–C)/(G+C) (Perna and Kocher 1995). Relative synonymous codon usage (RSCU) was calculated with MEGA 11 (Tamura et al. 2021).

A total of 90 mitogenomes of Passeriformes were used to reconstruct phylogenetic relationships; the included mitogenomes came from 12 taxonomic families with *Aethopyga gouldiae* (Nectariniidae) used as an outgroup (Suppl. material 7: Table S1). Each mitochondrial gene was aligned individually using MUSCLE in MEGA 11 (Tamura et al. 2021), starting with the alignment of PCGs to amino acid sequences. One mitogenomic dataset (mtDNA) was used for phylogenetic analysis, which included the nucleotide sequences of 13 PCGs, two rRNAs and 22 tRNAs, with a length of 15,722 bp. The best models of GTR+F+R5 for maximum likelihood (ML) analysis and GTR+F+I+G4 for Bayesian inference (BI) analysis were assessed in ModelFinder (Kalyaanamoorthy et al. 2017) using the Bayesian information criterion (BIC) in PhyloSuite 1.2.1 (Zhang et al. 2020). Phylogenetic relationships were analyzed using ML phylogenies with IQ-TREE 1.6.8 (Nguyen et al. 2015) with 1000 bootstrap replicates. The BI phylogeny was analysed with MrBayes 3.2.7 (Ronquist et al. 2012). Two independent runs with four simultaneous Markov chains were run for 5,000,000 generations and were sampled every 100 generations. The first 25% of generations were discarded as burn-in. The effective sample size (ESS) values were estimated in Tracer 1.7 (Rambaut et al. 2018), with ESS values > 200.

Results and discussion

Mitogenomic structure and organization

The obtained complete mitogenomes of *M. flava*, *M. cinerea*, *M. alba* and *D. indicus* ranged from 16,831 bp to 16,870 bp in length and each contained 37 genes and a noncoding region (CR) (Fig. 1). The complete mitogenome sequences were submitted to GenBank (MW929088–MW929091). Four gene arrangements have been identified among the Passeriformes mitogenomes sequenced to date (Caparroz et al. 2018; Mackiewicz et al. 2019). The gene order cytb-trnT-trnP-nad6-trnE-CR-trnF-rrnS is found in the mitogenomes of three *Motacilla* species and *D. indicus*, which is consistent with the order observed in most Passeriformes species (Mackiewicz et al. 2019). The major strand (J-strand) encodes 12 PCGs and two rRNAs as well as trnF, trnV, trnL(uur), trnI, trnM, trnW, trnD, trnK, trnG, trnR, the HSL cluster [trnH, trnS(agy), trnL(cun)] and trnT (Fig. 1). The lengths of the intergenic spacers range from 1–23 bp in the three *Motacilla* mitogenomes and 1–18 bp in *D. indicus*, with the longest intergenic spacer being located between the trnP and nad6 genes.

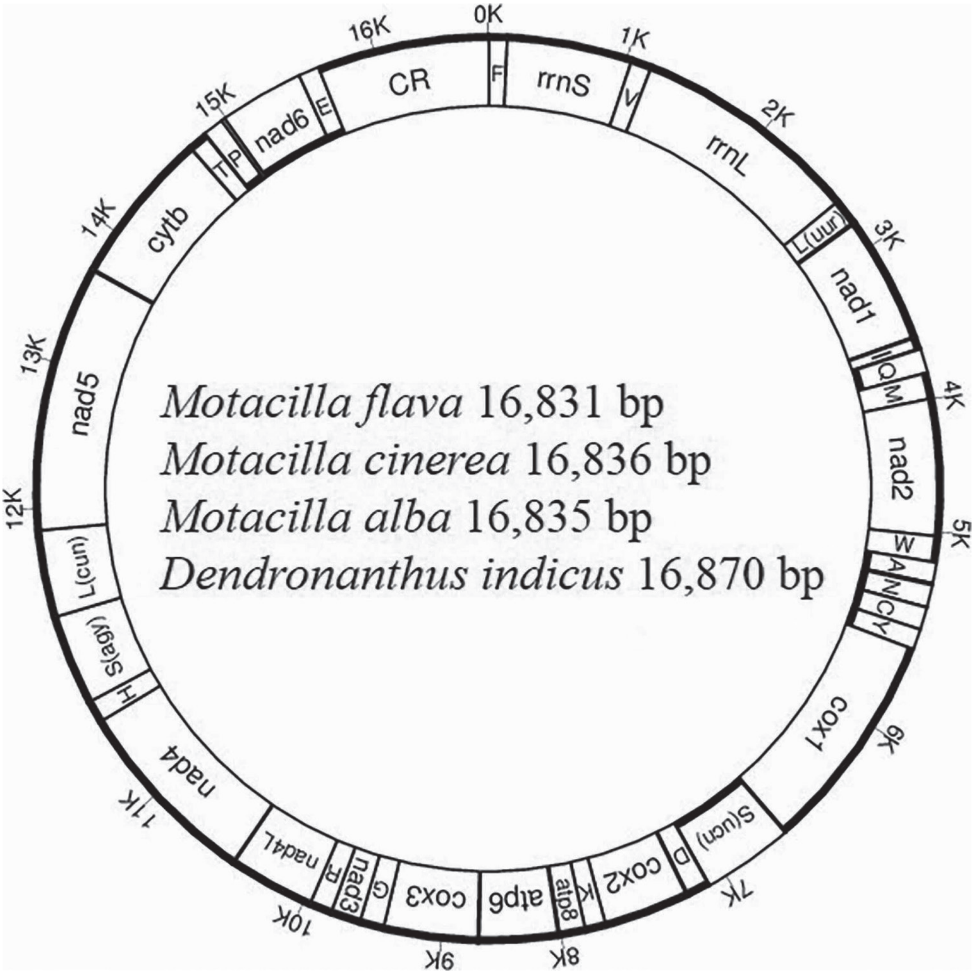

Figure 1. Gene map of four newly sequenced mitogenomes. Notes: tRNAs are abbreviated with a single letter; mitochondrial genes encoded by the J- and N-strands, indicated in bold, are located outside and inside of the circle, respectively.

Comparative analysis of *Motacilla* mitogenomes

The gene orders and nucleotide compositions of the six sampled *Motacilla* mitogenomes were generally similar. For instance, the A+T content ranges from 53.5% to 53.9%, which was slightly higher than the G+C contents. All mitogenomes showed a tendency toward A-skew and obvious C-skew (Suppl. material 8: Table S2), which was similar to findings in other birds (Kan et al. 2010; Eberhard and Wright 2016; Li et al. 2016a).

Protein-coding genes

The A+T contents of the 13 PCGs excluding stop codons ranged from 52.4% to 52.9% in sampled *Motacilla* mitogenomes (Suppl. material 8: Table S2). The highest

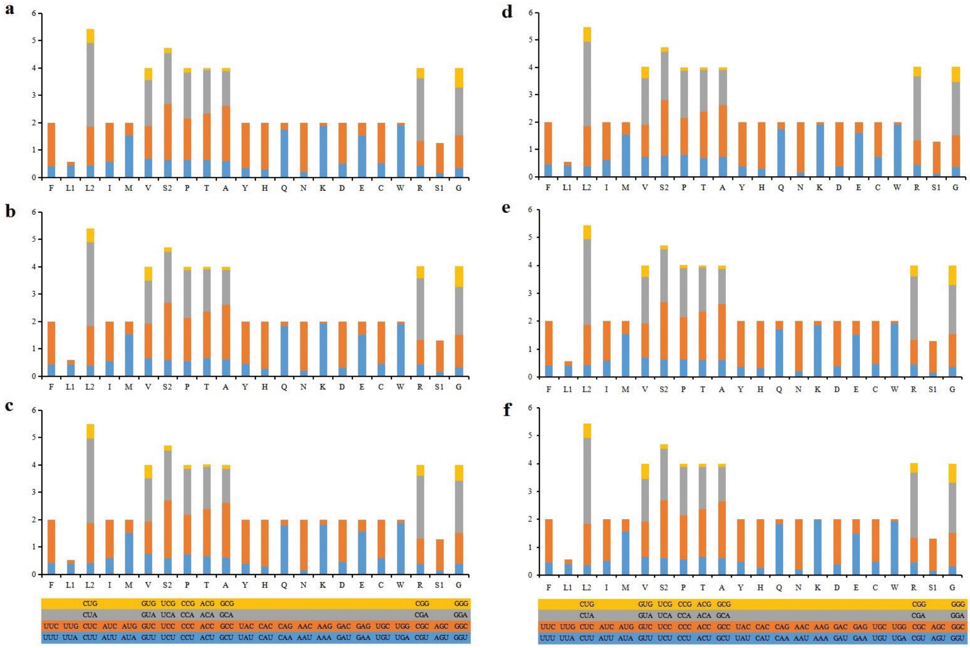

Figure 2. RSCU analysis of the PCGs of six mitogenomes from the genus *Motacilla*. Note **a** *M. alba* **b** *M. cinerea* **c** *M. flava* **d** *M. tschutschensis* **e** *M. alba* (MN356232) **f** *M. cinerea* (NC_027933).

A+T content was found at the second codon position in all *Motacilla* mitogenomes. Obvious T-skew was recovered at the second codon position, while the most significant A-skew was found at the third codon position. The three codon positions showed different degrees of C-skew, which was most obvious at the third codon position.

The first and last codons of the PCGs of *Motacilla* were compared (Suppl. material 9: Table S3). Twelve of the 13 PCGs started with an ATG codon, while nad3 started with ATT. The start codons were conserved in the six mitogenomes. The termination codons of the PCGs included TAA, TAG, AGG, AGA, TA and T, which are conserved among PCGs with the exception of cox2, cox3 and nad2. The incomplete T termination codons found in cox3 and nad4 have also been reported in other avian mitogenomes (Ma et al. 2014; Li et al. 2015; Eberhard and Wright 2016).

RSCU analysis indicated that among all PCGs, codons including A or C at the third position were frequently overused relative to other synonymous codons (Fig. 2). The codon usage among *Motacilla* species was found to be conserved, with CUA (L), CGA (R) and UCC(S) representing the most frequently used codons.

RNA genes

Similar to other avian mitogenomes, rrnS was found to be located between trnF and trnV, and rrnL was located between trnV and trnL(uur). The length of rrnS was 975 bp in *M. alba* (MN356232) and 973 bp in the other *Motacilla* mitogenomes, while the length of rrnL was 1595 bp in all *Motacilla* species. The A+T content was slightly greater than the G+C content in the rRNA genes, ranging from 52.2% to 52.3% in rrnS and 55.2% to 55.4% in rrnL, and both rRNA genes exhibited A-skew and C-skew (Suppl. material 8: Table S2).

The rrnS included three domains and 47 helices in *M. flava* (Suppl. material 2: Fig. S2), while rrnL included six domains and 60 helices (Suppl. material 3: Fig. S3). Most of the identified sequences and secondary structures were conserved compared with those of other *Motacilla* rRNAs. In addition, most of the stems of the rRNA secondary structures were similar to those found in other Passeriformes mitogenomes. For example, stems 21 and 47 of rrnS and 15 and 40 of rrnL were consistent with those found in *R. consobrinus* (Gao et al. 2013).

A total of eight tRNAs (trnQ, trnA, trnN, trnC, trnY, trnS(ucn), trnP and trnE) were located on the N-strand, while the remaining 14 tRNAs were located on the J-strand (Fig. 1). The lengths of the 22 tRNAs in each *Motacilla* species ranged from 66 to 75 bp. The A+T content ranged from 58.3% to 58.6% in the tRNAs, which exhibited A-skew and G-skew (Suppl. material 8: Table S2).

Twenty-one of the 22 tRNAs of *M. flava* were folded into a clover-leaf-like secondary structure, with the exception of trnS(agy), lacking a dihydrouridine (DHU) stem (Suppl. material 4: Fig. S4), which is considered to be a typical feature of metazoan mitogenomes (Wolstenholme 1992). Comparisons among *Motacilla* tRNAs showed that the most conserved tRNAs were trnL(UUR), trnM, trnW, trnA, trnC, trnH, trnL(CUN), trnT, trnP and trnE (Suppl. material 4: Fig. S4), which contained the same nucleotides. Some mismatched base pairs found in *Motacilla* were similar to those observed in some other Passeriformes species (*Pyrgilauda ruficollis*, Ma et al. 2014; *R. consobrinus*, Gao et al. 2013), such as the C-C pair located in the acceptor stem of trnL(uur) and the anticodon stem of trnG, A-A in the TφC stem of trnD, and U-U in the anticodon stem of trnG.

Control region

The CR was located between the trnE and trnF genes and were 1243–1250 bp in length. The average A+T content was 56.2% among all sampled *Motacilla* mitogenomes, which was slightly higher than that of G+C. The CRs showed a tendency toward T-skew and C-skew (Suppl. material 8: Table S2), with C-skew being more obvious. This C-skew was consistent with findings in other reported avian CRs (e.g., Huang et al. 2017).

The CR regulates the replication of the H strand and the transcription of all mitochondrial genes (Clayton 1992) and can be divided into three domains: extended termination-associated sequence (ETAS) domain I, central conserved domain II, and conserved sequence block (CSB) domain III (Sbisà et al. 1997; Randi and Lucchini 1998; Ruokonen and Kvist 2002). Among the three domains of the CR, domain I showed slight A-skew and obvious C-skew, domain II showed a tendency toward T-skew and C-skew, and domain III exhibited A-skew and a highly significant C-skew (Suppl. material 8: Table S2).

The proportions of variable sites among the three domains were 3.6%, 2.4% and 9.0%, respectively. Thus, most variation was found in domain III, similar to the findings of previous studies (Ruokonen and Kvist 2002; Huang et al. 2017). A poly-C sequence was found near the 5' end of CR domain I in *M. flava*, with a sequence of CCCCCCCCCCTTCCCCCCCC, and this sequence was relatively conserved in the sampled mitogenome CRs (Suppl. material 5: Fig. S5). Within the *M. flava* CR sequence, boxes F, E, D, C, B and a bird similarity box in domain II were identified. The F, E, D and C boxes were similar to those found in other avian mitogenomes (Suppl. material 5: Fig. S5; Huang et al. 2017). Among these boxes, the F-box, bird similarity box and B-box were fully conserved among sampled mitogenomic sequences. Domain III contained CSB1, whose sequence was similar to that found in other birds (Huang et al. 2017). However, it was difficult to identify sequences corresponding to O_H, CSB2, CSB3 and bidirectional LSP/HSP promoters found in other birds (Li et al. 2015), which might play important roles in mitogenome replication. Furthermore, tandem repeat sequences in CRs are found in many avian mitogenomes (Yang et al. 2018). However, none of the sampled *Motacilla* CRs contained tandem repeats.

Phylogenetic analysis

The ML and BI phylogenetic trees were reconstructed using the mtDNA dataset, showing consistent topological results among Motacillidae (Fig. 3 and Suppl. material 6: Fig. S6). The analyses supported the monophyly of Motacillidae with 100% bootstrap support and posterior probabilities of 1.0. Among the three sampled genera among Motacillidae (*Anthus*, *Dendronanthus* and *Motacilla*), *Anthus* was sister to *D. indicus* and *Motacilla*. The monophyly of *Motacilla* was also recovered, with *D. indicus* forming a sister group with *Motacilla*.

Within *Motacilla*, the following phylogenetic relationships were recovered: (((*M. flava*+*M. tschutschensis*)+*M. alba*)+*M. cinerea*), similar to previous studies (Suppl. material 1: Fig. S1A; Dong et al. 2016; Suppl. material 1: Fig. S1D; Gao et al. 2019). *Motacilla cinerea* was in the basal position within *Motacilla*, and *M. flava* showed a closer relationship with *M. tschutschensis*. However, *M. alba* showed a closer relationship with *M. cinerea* (Suppl. material 1: Fig. S1B; Zhang et al. 2016), while *M. cinerea* presented a closer phylogenetic relationship with *M. flava* (Suppl. material 1: Fig. S1C; Harris et al. 2018). These differences might be due to the different data types, dataset sizes and sampling strategies involved. For example, the phylogenetic tree topologies obtained from the complete mitogenome are not identical to those resulting from individual mitochondrial genes in some avian taxa (Campillo et al. 2019). In addition, the phylogenetic relationships recovered from nuclear segment datasets are inconsistent with those recovered from mitogenomes in some aves (Li et al. 2016a; Campillo et al. 2019). Therefore, our results indicate that further studies are needed to address the phylogenetic relationships within *Motacilla* by adding more sampling and some nuclear data.

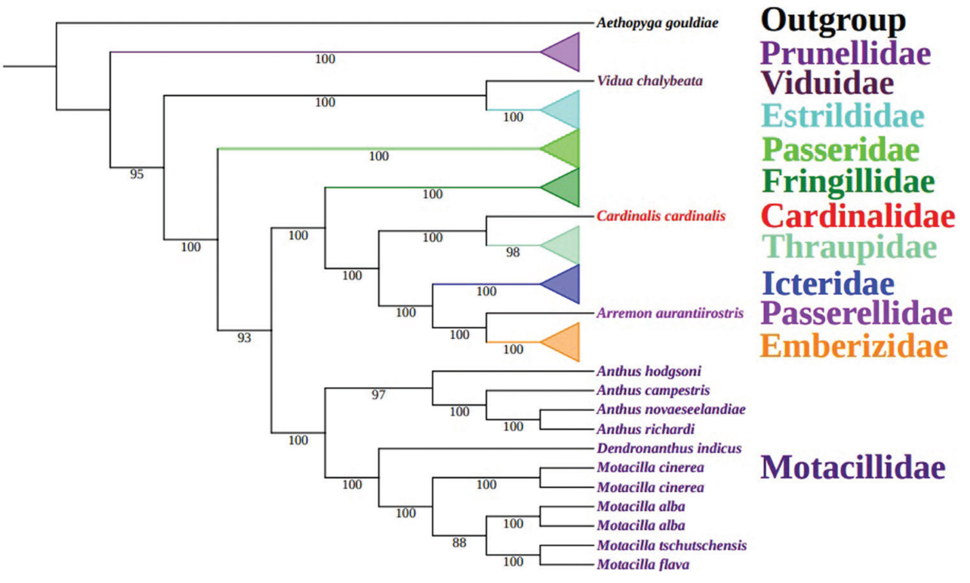

Figure 3. Phylogenetic results based on the maximum likelihood method using the mtDNA dataset.

Conclusions

The complete mitogenomes of *Motacilla flava*, *M. cinerea*, *M. alba* and *Dendronanthus indicus* were sequenced and were shown to present the typical genome organization and gene order found in other Passeriformes mitogenomes. We focused on comparative analyses of the six mitogenomes to identify the mitogenomic characteristics of the genus *Motacilla*, such as the base composition, codon usage and RNA secondary structures. The complete mitogenomes showed a tendency toward A-skew and C-skew. Most PCGs start with typical ATG codons and terminated with TAA codons. All tRNAs could be folded into classic clover-leaf structures except for trnS(agy), which lacked a DHU arm. In addition, 90 mitogenomes of Passeriformes were used to build the tree of phylogenetic relationships. The phylogenetic tree supported the monophyly of Motacillidae. Within *Motacilla*, the phylogenetic topology of (((*M. flava*+*M. tschutschensis*)+*M. alba*)+*M. cinerea*) was recovered.

Acknowledgements

We would like to thank Liliang Lin for kindly providing us with results of data analyses. This work was supported by the National Natural Science Foundation of China (Grant No. 31601846 and 31801993), Natural Science Foundation of Shaanxi Province, China (Grant No. 2017JQ3014 and 2020JM-270), China Postdoctoral Science Foundation (Grant No. 2016M602760), Fundamental Research Funds for the Central Universities, China (Grant No. GK202003052 and GK202103068), Projects of the Department of Science and Technology of Shaanxi Province, China (Grant No. 2019NY-089 and 2018ZDXM-NY-071), and the First Wildlife Resource Survey Project of Xi'an (Grant No. XCZX2015-0297-3). The complete mitogenomes of *Motacilla flava*, *M. cinerea*, *M. alba* and *Dendronanthus indicus* are openly available on GenBank at https://www.ncbi.nlm.nih.gov/nuccore, with accession No. MW929088-MW929091. CY, XD and XL analyzed the data and wrote the manuscript. CY, YH, XL and YH participated in the design of the experiments. XD, XD, YL, HY, QW, XH, HG and YW helped to improve the manuscript. All authors read and approved the final manuscript.

References

Alström P, Mild K, Zetterström B (2003) Pipits and Wagtails of Europe, Asia and North America: identification and systematics. Christopher Helm, London.

Boore JL (1999) Animal mitochondrial genomes. Nucleic Acids Research 27(8): 1767–1780. https://doi.org/10.1093/nar/27.8.1767

Cai T, Cibois A, Alström P, Moyle RG, Kennedy JD, Shao S, Zhang R, Irestedt M, Ericson PGP, Gelang M, Qu YH, Lei FM, Fjeldså J (2019) Near-complete phylogeny and taxonomic revision of the world's babblers (Aves: Passeriformes). Molecular Phylogenetics and Evolution 130: 346–356. https://doi.org/10.1016/j.ympev.2018.10.010

Campillo LC, Burns KJ, Moyle RG, Manthey JD (2019) Mitochondrial genomes of the bird genus *Piranga*: Rates of sequence evolution, and discordance between mitochondrial and nuclear markers. Mitochondrial DNA. Part B, Resources 4(2): 2566–2569. https://doi.org/10.1080/23802359.2019.1637286

Caparroz R, Rocha AV, Cabanne GS, Tubaro P, Aleixo A, Lemmon EM, Lemmon AR (2018) Mitogenomes of two neotropical bird species and the multiple independent origin of mitochondrial gene orders in Passriformes. Molecular Biology Reports 45(3): 279–285. https://doi.org/10.1007/s11033-018-4160-5

Clayton DA (1992) Transcription and replication of animal mitochondrial DNAs. International Review of Cytology 141: 217–232. https://doi.org/10.1016/S0074-7696(08)62067-7

del Hoyo J, Elliott A, Christie D (2004) Handbook of the Birds of the World (Volume 9): Cotingas to Pipits and Wagtails. Lynx Edicions, Barcelona.

Dong L, Zhang YY (2011) Theoretical backgrounds and recent advances in avian molecular phylogeography. Acta Ecologica Sinica 31(14): 4082–4093.

Dong XY, Pan T, Kang X, Zhang YN, Sun XN, Qian LF (2016) Complete mitochondrial genome of *Motacilla alba* and implications for Motacillidae taxonomy. Mitochondrial DNA. Part A, DNA Mapping, Sequencing, and Analysis 27(6): 4675–4676. https://doi.org/10.3109/19401736.2015.1106497

Eberhard JR, Wright TF (2016) Rearrangement and evolution of mitochondrial genomes in parrots. Molecular Phylogenetics and Evolution 94(Pt A): 34–46. https://doi.org/10.1016/j.ympev.2015.08.011

Gao RR, Huang Y, Lei FM (2013) Sequencing and analysis of the complete mitochondrial genome of *Remiz consobrinus*. Zoological Research 34(3): 228–237.

Gao XD, Xu DJ, Xia T, Dou HS, Sha WL, Zhang HH (2019) The complete mitochondrial genome of Eastern Yellow Wagtail (*Motacilla tschutschensis*). Mitochondrial DNA. Part B, Resources 4(2): 3486–3487. https://doi.org/10.1080/23802359.2019.1674737

Gill F, Donsker D, Rasmussen P (2020) IOC World Bird List (v 10.2). http://www.worldbirdnames.org/

Hahn C, Bachmann L, Chevreux B (2013) Reconstructing mitochondrial genomes directly from genomic next-generation sequencing reads-A baiting and iterative mapping approach. Nucleic Acids Research 41(13): e129. https://doi.org/10.1093/nar/gkt371

Harris RB, Alström P, Ödeen A, Leaché AD (2018) Discordance between genomic divergence and phenotypic variation in a rapidly evolving avian genus (*Motacilla*). Molecular Phylogenetics and Evolution 120: 183–195. https://doi.org/10.1016/j.ympev.2017.11.020

Hassanin A, Léger N, Deutsch J (2005) Evidence for multiple reversals of asymmetric mutational constraints during the evolution of the mitochondrial genome of Metazoa and consequences for phylogenetic inferences. Systematic Biology 54(2): 277–298. https://doi.org/10.1080/10635150590947843

Huang ZH, Shen YM, Ma YR (2017) Structure and variation of the Fringillidae (Aves: Passeriformes) mitochondrial DNA control region and their phylogenetic relationship. Mitochondrial DNA. Part A, DNA Mapping, Sequencing, and Analysis 28(6): 867–871. https://doi.org/10.1080/24701394.2016.1199023

Kalyaanamoorthy S, Minh BQ, Wong TKF, von Haeseler A, Jermiin LS (2017) ModelFinder: Fast model selection for accurate phylogenetic estimates. Nature Methods 14(6): 587–589. https://doi.org/10.1038/nmeth.4285

Kan XZ, Li XF, Zhang LQ, Chen L, Qian CJ, Zhang XW, Wang L (2010) Characterization of the complete mitochondrial genome of the Rock pigeon, *Columba livia* (Columbiformes: Columbidae). Genetics and Molecular Research 9(2): 1234–1249. https://doi.org/10.4238/vol9-2gmr853

Kearse M, Moir R, Wilson A, Stones-Havas S, Cheung M, Sturrock S, Buxton B, Cooper A, Markowitz S, Duran C, Thierer T, Ashton B, Meintjes P, Drummond A (2012) Geneious Basic: An integrated and extendable desktop software platform for the organization and analysis of sequence data. Bioinformatics (Oxford, England) 28(12): 1647–1649. https://doi.org/10.1093/bioinformatics/bts199

Li XJ, Huang Y, Lei FM (2015) Comparative mitochondrial genomics and phylogenetic relationships of the *Crossoptilon* species (Phasianidae, Galliformes). BMC Genomics 16(1): e42. https://doi.org/10.1186/s12864-015-1234-9

Li XJ, Lin LL, Cui AM, Bai J, Wang XY, Xin C, Zhang Z, Yang C, Gao RR, Huang Y, Lei FM (2016a) Taxonomic status and phylogenetic relationship of tits based on mitogenomes and nuclear segments. Molecular Phylogenetics and Evolution 104: 14–20. https://doi.org/10.1016/j.ympev.2016.07.022

Li XL, Dong F, Lei FM, Alström P, Zhang R, Ödeen A, Fjeldså J, Ericson PGP, Zou FS, Yang XJ (2016b) Shaped by uneven Pleistocene climate: mitochondrial phylogeographic pattern and population history of white wagtail *Motacilla alba* (Aves: Passeriformes). Journal of Avian Biology 47(2): 263–274. https://doi.org/10.1111/jav.00826

Lowe TM, Eddy SR (1997) tRNAscan-SE: A program for improved detection of transfer RNA genes in genomic sequence. Nucleic Acids Research 25(5): 955–964. https://doi.org/10.1093/nar/25.5.955

Ma YG, Huang Y, Lei FM (2014) Sequencing and phylogenetic analysis of the *Pyrgilauda ruficollis* (Aves, Passeridae) complete mitochondrial genome. Zoological Research 35(2): 81–91. https://doi.org/10.3109/19401736.2014.984179

Mackiewicz P, Urantówka AD, Kroczak A, Mackiewicz D (2019) Resolving phylogenetic relationships within Passeriformes based on mitochondrial genes and inferring the evolution of their mitogenomes in terms of duplications. Genome Biology and Evolution 11(10): 2824–2849. https://doi.org/10.1093/gbe/evz209

Meng GL, Li YY, Yang CT, Liu SL (2019) MitoZ: A toolkit for animal mitochondrial genome assembly, annotation and visualization. Nucleic Acids Research 47(11): e63. https://doi.org/10.1093/nar/gkz173

Morinha F, Clemente C, Cabral JA, Lewicka MM, Travassos P, Carvalho D, Dávila JA, Santos M, Blanco G, Bastos E (2016) Next-generation sequencing and comparative analysis of *Pyrrhocorax pyrrhocorax* and *Pyrrhocorax graculus* (Passeriformes: Corvidae) mitochondrial genomes. Mitochondrial DNA. Part A, DNA Mapping, Sequencing, and Analysis 27(3): 2278–2281.

Nguyen LT, Schmidt HA, von Haeseler A, Minh BQ (2015) IQ-TREE: A fast and effective stochastic algorithm for estimating maximum-likelihood phylogenies. Molecular Biology and Evolution 32(1): 268–274. https://doi.org/10.1093/molbev/msu300

Ödeen A, Björklund M (2003) Dynamics in the evolution of sexual traits: Losses and gains, radiation and convergence in yellow wagtails (*Motacilla flava*). Molecular Ecology 12(8): 2113–2130. https://doi.org/10.1046/j.1365-294X.2003.01883.x

Perna NT, Kocher TD (1995) Patterns of nucleotide composition at fourfold degenerate sites of animal mitochondrial genomes. Journal of Molecular Evolution 41(3): 353–358. https://doi.org/10.1007/BF01215182

Rambaut A, Drummond AJ, Xie D, Baele G, Suchard MA (2018) Posterior summarisation in Bayesian phylogenetics using Tracer 1.7. Systematic Biology 67(5): 901–904. https://doi.org/10.1093/sysbio/syy032

Randi E, Lucchini V (1998) Organization and evolution of the mitochondrial DNA control region in the avian genus *Alectoris*. Journal of Molecular Evolution 47(4): 449–462. https://doi.org/10.1007/PL00006402

Ronquist F, Teslenko M, van der Mark P, Ayres DL, Darling A, Höhna S, Larget B, Liu L, Suchard MA, Huelsenbeck JP (2012) MrBayes 3.2: Efficient Bayesian phylogenetic inference and model choice across a large model space. Systematic Biology 61(3): 539–542. https://doi.org/10.1093/sysbio/sys029

Ruokonen M, Kvist L (2002) Structure and evolution of the avian mitochondrial control region. Molecular Phylogenetics and Evolution 23(3): 422–432. https://doi.org/10.1016/S1055-7903(02)00021-0

Sangster G, Luksenburg JA (2021) Sharp increase of problematic mitogenomes of birds: causes, effects and remedies. Genome Biology Evolution 13(9): evab210. https://doi.org/10.1093/gbe/evab210

Sbisà E, Tanzariello F, Reyes A, Pesole G, Saccone C (1997) Mammalian mitochondrial D-loop region structural analysis: Identification of new conserved sequences and their functional and evolutionary implications. Gene 205(1–2): 125–140. https://doi.org/10.1016/S0378-1119(97)00404-6

Tamura K, Stecher G, Kumar S (2021) MEGA11: Molecular evolutionary genetics analysis version 11. Molecular Phylogenetics and Evolution 38(7): 3022–3027. https://doi.org/10.1093/molbev/msab120

Wolstenholme DR (1992) Animal Mitochondrial DNA: Structure and Evolution. International Review of Cytology 141: 173–216. https://doi.org/10.1016/S0074-7696(08)62066-5

Yang C, Yang MX, Wang QX, Lu YC, Li XJ (2018) The complete mitogenome of *Falco amurensis* (Falconiformes, Falconidae), and a comparative analysis of genus *Falco*. Zoological Science 35(4): 367–372. https://doi.org/10.2108/zs170182

Zhang Z, Qian LF, Wang YP, Zhang BW (2016) The complete mitochondrial genome of *Motacilla cinerea* (Passeriformes: Motacillidae). Mitochondrial DNA. Part A, DNA Mapping, Sequencing, and Analysis 27(5): 3680–3681. https://doi.org/10.3109/19401736.2015.1079853

Zhang D, Gao FL, Jakovlić I, Zou H, Zhang J, Li WX, Wang GT (2020) PhyloSuite: An integrated and scalable desktop platform for streamlined molecular sequence data management and evolutionary phylogenetics studies. Molecular Ecology Resources 20(1): 348–355. https://doi.org/10.1111/1755-0998.13096

Supplementary material 1

Figure S1

Authors: Chao Yang, Xiaojuan Du, Yuxin Liu, Hao Yuan, Qingxiong Wang, Xiang Hou, Huisheng Gong, Yan Wang, Yuan Huang, Xuejuan Li, Haiyan Ye

Data type: Image.

Explanation note: Phylogenetic hypotheses of previous studies. a: Dong et al. (2016); b: Zhang et al. (2016); c: Harris et al. (2018); d: Gao et al. (2019).

Link: https://doi.org/10.3897/zookeys.1109.81125.suppl1

Supplementary material 2

Figure S2

Authors: Chao Yang, Xiaojuan Du, Yuxin Liu, Hao Yuan, Qingxiong Wang, Xiang Hou, Huisheng Gong, Yan Wang, Yuan Huang, Xuejuan Li, Haiyan Ye

Data type: Image.

Explanation note: Secondary structures of rrnS of *M. flava*. Note: differences within the six mitogenomes from the genus *Motacilla* are indicated by filled grey circles.

Link: https://doi.org/10.3897/zookeys.1109.81125.suppl2

Supplementary material 3

Figure S3

Authors: Chao Yang, Xiaojuan Du, Yuxin Liu, Hao Yuan, Qingxiong Wang, Xiang Hou, Huisheng Gong, Yan Wang, Yuan Huang, Xuejuan Li, Haiyan Ye

Data type: Image.

Explanation note: Secondary structures of rrnL of *M. flava*. Note: differences within the six mitogenomes from the genus *Motacilla* are indicated by filled grey circles.

Link: https://doi.org/10.3897/zookeys.1109.81125.suppl3

Supplementary material 4

Figure S4

Authors: Chao Yang, Xiaojuan Du, Yuxin Liu, Hao Yuan, Qingxiong Wang, Xiang Hou, Huisheng Gong, Yan Wang, Yuan Huang, Xuejuan Li, Haiyan Ye

Data type: Image.

Explanation note: Secondary structures of tRNAs of *M. flava*. Note: differences within the six mitogenomes from the genus *Motacilla* are indicated by filled grey circles.

Link: https://doi.org/10.3897/zookeys.1109.81125.suppl4

Supplementary material 5

Figure S5

Authors: Chao Yang, Xiaojuan Du, Yuxin Liu, Hao Yuan, Qingxiong Wang, Xiang Hou, Huisheng Gong, Yan Wang, Yuan Huang, Xuejuan Li, Haiyan Ye

Data type: Image.

Explanation note: Control region structures of *M. flava*. Note: differences within the six mitogenomes from the genus *Motacilla* are indicated with filled circles.

Link: https://doi.org/10.3897/zookeys.1109.81125.suppl5

Supplementary material 6

Figure S6

Authors: Chao Yang, Xiaojuan Du, Yuxin Liu, Hao Yuan, Qingxiong Wang, Xiang Hou, Huisheng Gong, Yan Wang, Yuan Huang, Xuejuan Li, Haiyan Ye

Data type: Image.

Explanation note: Maximum likelihood and Bayesian inference phylogenetic results based on the mtDNA dataset, corresponding to Fig. 3. Note: a: ML tree, b: BI tree.

Link: https://doi.org/10.3897/zookeys.1109.81125.suppl6

Supplementary material 7

Table S1

Authors: Chao Yang, Xiaojuan Du, Yuxin Liu, Hao Yuan, Qingxiong Wang, Xiang Hou, Huisheng Gong, Yan Wang, Yuan Huang, Xuejuan Li, Haiyan Ye

Data type: Doc file.

Explanation note: Mitogenome sequences employed for reconstructing phylogenetic trees.

Link: https://doi.org/10.3897/zookeys.1109.81125.suppl7

Supplementary material 8

Table S2

Authors: Chao Yang, Xiaojuan Du, Yuxin Liu, Hao Yuan, Qingxiong Wang, Xiang Hou, Huisheng Gong, Yan Wang, Yuan Huang, Xuejuan Li, Haiyan Ye

Data type: Doc file.

Explanation note: Nucleotide composition and bias of six mitogenomes of the genus *Motacilla*. Notes: Stop codons of protein-coding genes were excluded; AT-skew=[A-T]/[A+T], GC-skew=[G-C]/[G+C]. The sequenced mitogenome species in this study are shown in the bold format.

Link: https://doi.org/10.3897/zookeys.1109.81125.suppl8

Supplementary material 9

Table S3

Authors: Chao Yang, Xiaojuan Du, Yuxin Liu, Hao Yuan, Qingxiong Wang, Xiang Hou, Huisheng Gong, Yan Wang, Yuan Huang, Xuejuan Li, Haiyan Ye

Data type: Doc file.

Explanation note: Initial and terminal codons of protein-coding genes in the six mitogenomes from the genus *Motacilla*. Notes: The sequenced mitogenome species in this study are shown in the bold format.

Link: https://doi.org/10.3897/zookeys.1109.81125.suppl9

ZooKeys 1109: 67–101 (2022)
doi: 10.3897/zookeys.1109.83807
https://zookeys.pensoft.net

RESEARCH ARTICLE

A peer-reviewed open-access journal
ZooKeys
Launched to accelerate biodiversity research

Two new species and a new genus of ray spiders (Araneae, Theridiosomatidae) from the Ryukyu Islands, southwest Japan, with notes on their natural history

Yuya Suzuki[1,2], Takehisa Hiramatsu[3], Haruki Tatsuta[2]

1 *The United Graduate School of Agricultural Sciences, Kagoshima University, 1-21-24, Korimoto, Kagoshima-shi, Kagoshima, 890-0065, Japan* **2** *Graduate School of Systems Life Sciences, Kyushu University, 744 Motooka, Nishi-ku, Fukuoka, 819-0395 Japan* **3** *Fregrance-Uwado 203, Uwado, Kawagoe-shi, Saitama, 350-0816, Japan*

Corresponding author: Yuya Suzuki (sasaganiya1206@gmail.com)

Academic editor: Miquel A. Arnedo | Received 15 March 2022 | Accepted 16 May 2022 | Published 1 July 2022

https://zoobank.org/9C8BF86D-194A-46EF-9D49-072D09BF9E48

Citation: Suzuki Y, Hiramatsu T, Tatsuta H (2022) Two new species and a new genus of ray spiders (Araneae, Theridiosomatidae) from the Ryukyu Islands, southwest Japan, with notes on their natural history. ZooKeys 1109: 67–101. https://doi.org/10.3897/zookeys.1109.83807

Abstract

This paper provides descriptions of two new theridiosomatid species, *Theridiosoma nigrivirgatum* **sp. nov.** and *Sennin tanikawai* **gen. nov.**, **sp. nov.** from the Ryukyu Islands, southwest Japan, with photographs and illustrations of both sexes. *Sennin* **gen. nov.** is a troglophilic genus composed of two species, *S. tanikawai* **sp. nov.** (Iriomote Island, Japan) and *S. coddingtoni* (Zhu, Zhang & Chen, 2001), **comb. nov.** (southern China). *Zoma dibaiyin* Miller, Griswold & Yin, 2009, which recently joined the Japanese fauna, was morphologically reexamined based on specimens from the Ryukyus, and taxonomic features of *Zoma* males were reassessed. A distributional map of theridiosomatid spiders in the Ryukyus is also provided, including *T. dissimulatum* Suzuki, Serita & Hiramatsu, 2020, and *T. alboannulatum* Suzuki, Serita & Hiramatsu, 2020 with their habitat types, web morphology, and web-building behavior in detail.

Keywords

Araneoidea, embolic apophysis, limestone cave, Iriomote Island, new combination, Okinawa Island, orb web, taxonomy

Introduction

The family Theridiosomatidae Simon, 1881 (Araneae: Araneoidea) is composed of small-sized (body length, ca. 0.5–3 mm) spiders that prefer dark and humid environments such as forest floors, mountainous streams, and caves (Coddington 1986a). The family is characterized by a sternal pit organ (Wunderlich 1980) that has a pair of pits on the anterior margin of the sternum, except in *Chthonos* Coddington, 1986 (Coddington 1986a), large globular palp of males, a pair of spermathecae fused or in contact with each other in females except in *Coddingtonia* Miller, Griswold & Yin, 2009 (Miller et al. 2009), and elongated trichobothria on the dorsum of the third and fourth legs (Coddington 1986a). All genera except *Chthonos* are known as web-builders (Coddington 1986a), and several genera build conventional orb webs (e.g., *Baalzebub* Coddington, 1986, *Epeirotypus* O. Pickard-Cambridge, 1894, and *Naatlo* Coddington, 1986), while others construct orb webs with radial anastomosis (e.g., *Theridiosoma* O. Pickard-Cambridge, 1879) or deformed webs, called sparse networks (e.g., *Ogulnius* O. Pickard-Cambridge, 1882, *Wendilgarda* Keyserling, 1886). Webs of some genera are characterized by a tension line, a non-sticky isolated radius that stretches from the center of the web and attaches to the substrates (e.g., *Epeirotypus*, *Naatlo*, and *Theridiosoma*). Spiders of these genera drag the tension line with forelegs and hold it into coiled conditions while holding the web with hindlegs. Therefore, the web acquires a distorted conical shape (Shinkai and Shinkai 1985; Coddington 1986a). When flying insects approach the web, the tension line is promptly released, and the launched web captures the prey. This latch-mediated spring actuation results in an ultrafast web shooting motion (Alexander and Bhamla 2020).

Currently, 19 genera and 133 species of Theridiosomatidae are recorded mainly in tropical and subtropical regions worldwide (World Spider Catalog 2022). After the revision by Coddington (1986a), new genera and new species were described mostly from China and Southeast Asia (Miller et al. 2009; Chen 2010; Wunderlich 2011; Zhao and Li 2012; Labarque and Griswold 2014; Zhao and Li 2014; Prete et al. 2018). Twelve genera, namely *Baalzebub*, *Chthonopes* Wunderlich, 2011, *Coddingtonia*, *Epeirotypus*, *Karstia* Chen, 2010, *Menglunia* Zhao & Li, 2012, *Ogulnius*, *Sinoalaria* Zhao & Li, 2014, *Tagalogonia* Labarque & Griswold, 2014, *Theridiosoma*, *Wendilgarda*, and *Zoma* Saaristo, 1996, were recorded from East to Southeast Asia. These genera are distributed in both neotropics and Asia, with several exceptions such as *Karstia* and *Menglunia*, which are endemic to China, and *Tagalogonia*, endemic to the Philippines (World Spider Catalog 2022).

The Ryukyu Islands, comprising hundreds of continental islands located between Kyushu and Taiwan, were formed by a complicated geological history of several land bridge connections with the Chinese continent. Consequently, the fauna constitutes continental components and consists of many endemic species that have been derived from the continental ancestry (e.g., Ota 1998, 2000). Spider fauna of the Ryukyu Islands has been surveyed by many arachnologists (e.g., Shimojana 1977), but small-sized spiders such as Theridiosomatidae have only recently been examined (e.g., Shinkai and Hiramatsu 2000). Our recent surveys on the islands revealed two new species of *Theridiosoma* from the Ryukyus, and two theridiosomatid species as new members of the spider fauna in the Ryukyus: *Theridiosoma dissimulatum* Suzuki, Serita & Hiramatsu, 2020, *T. alboannulatum* Suzuki, Serita & Hiramatsu, 2020, *Wendilgarda ruficeps* Suzuki, 2019 and *Zoma dibaiyin* Miller, Griswold & Yin, 2009 (Ono and Ogata 2018; Suzuki et al. 2020; Suzuki and Matsushima 2021; Suzuki and Serita 2021).

During our survey in the Ryukyu Islands conducted between 2020 and 2022, several unidentified specimens of theridiosomatid spiders were further discovered from secondary forests, grasslands, and bushes in Okinawa, Kume and Aka Islands, and limestone caves on Iriomote Island. Based on morphological examination, we concluded that these specimens belong to two new species. One species was determined to be an undescribed *Theridiosoma* species. We confirmed that the second undescribed species from caves on Iriomote Island possesses unique characteristics that do not correspond to the taxonomic characteristics of known theridiosomatid genera. We were also aware that *Karstia coddingtoni* (Zhu, Zhang & Chen, 2001), known from Southern China, shares common features with the undescribed species in Iriomote Island. Here, we suggest the establishment of a new genus named *Sennin* gen. nov., that comprises of these two species. Furthermore, several specimens of the Chinese species *Zoma dibaiyin* Miller, Griswold & Yin, 2009, which was recently recognized in the Japanese fauna (Ono and Ogata 2018; Suzuki and Serita 2021), were morphologically reexamined, and taxonomic characteristics of *Zoma* males were reassessed. We provide descriptions of these three theridiosomatid species, including two new species with illustrations and photographs of both sexes. Furthermore, geographical distributional data including other theridiosomatids in the Ryukyus are also provided with a comparison of their natural history, especially habitat types, web morphology, and web-building behavior.

Materials and methods

The specimens were preserved in 80% (v/v) ethanol solution. Morphological features of the specimens were observed, and photographs were taken using a stereoscopic microscope (Nikon AZ100M, Japan). Photographed images were stacked using microscope imaging software (Nikon NIS-Elements D 4.20.00 64-bit, Japan). Photographs of *Z. dibaiyin* were taken using a digital camera (Nikon CF Plan X20 objective lens + Olympus M. Zuiko 75–300 mm attached to Olympus OM-D E-M1) and stacked using imaging software (Zerene Stucker; Zerene Systems, Washington, USA). The vulvae were treated with Proteinase K before being photographed. Measurements of the legs are given in the following format: femur + patella + tibia + metatarsus + tarsus = total, in millimeters. The formula of macrosetae on the legs is as follows: **d**, dorsal; **p**, prolateral; **r**, retrolateral. All specimens used in this study were deposited in the collection of the Department of Zoology, National Museum of Nature and Science (**NSMT**; curator: Ken-ichi Okumura), Tsukuba, Japan. Specimens without registration numbers in the 'material examined' section were deposited in the personal collection of YS.

Observations of *Sennin tanikawai* sp. nov. were conducted in Yutsun-do cave and Ôtomi-daiichi-do cave on Iriomote Island in August 1998, and April and June 2021.

The measurements of webs and visual observations of web-building behavior were conducted using a 6V search light. The web size was measured for the horizontal and vertical diameters of the capture area. The number of sticky spirals was counted along a radius located at an angle of 45° in the upper right sector of the orb. Web-building behavior was observed in the adult females. Webs were photographed and behaviors on the webs were recorded as movie in the spiders' natural habitat using a digital camera (Laowa 50 mm Ultra Macro + Olympus OM-D-E-M1; Canon DS6041 + Canon Macro Lens EF 100 mm).

Abbreviations of morphological terminology are in accordance with Coddington (1986a), Zhu et al. (2001), Miller et al. (2009), Chen (2010), and Zhao and Li (2012). MAL, MAW, PCP, and RCP are defined herein for the first time; see below for all abbreviations for morphology:

AL abdomen length;
ALE anterior lateral eye;
AME anterior median eye;
AW abdomen width;
C conductor;
CA cymbial apophysis;
CaL carapace length;
CAW cymbial apophysis width;
CaW carapace width;
CB copulatory bursae;
CD copulatory duct;
CL cymbial lamella;
E embolus;
EA embolic apophysis;
ED embolic division;
ES epigynal scape;
ESL epigynal scape length;
FD fertilization duct;
MA median apophysis;
MAL length of dorsal protrusion on median apophysis;
MAW width of dorsal protrusion on median apophysis;
PC paracymbium;
PCP posterior conductor projection;
PLE posterior lateral eye;
PME posterior median eye;
PTL palpal tibia length;
RCP retrolateral conductor projection;
S spermatheca;
ST subtegulum;
T tegulum;
VW vulva width.

Abbreviations for web architecture:

HL hub loop;
OH open hub;
RA radial anastomosis;
RD radii;
SS sticky spirals;
TL tension line;
TS temporary spiral.

Key to the theridiosomatid species in the Ryukyu Islands

1	Male	**2**
–	Female	**6**
2	Cymbium with a long dorsal cymbial apophysis, embolic apophyses entirely covered with conductor	***Sennin tanikawai* sp. nov.**
–	Cymbium lacking cymbial apophysis	**3**

3 One embolic apophysis exposed from conductor .... ***Zoma dibaiyin***
– Two embolic apophyses exposed from conductor....................................... **4**
4 Conductor with a projection........................... ***Theridiosoma dissimulatum***
– Conductor lacking a projection... **5**
5 Two paralleled embolic apophyses of same length ....
.... ***Theridiosoma alboannulatum***
– One embolic apophysis longer than the other ....
.... ***Theridiosoma nigrivirgatum* sp. nov.**
6 Epigyne with a scape on posterior margin.......... ***Sennin tanikawai* sp. nov.**
– Epigyne lacking a scape... 7
7 Epigyne with a sclerotized median pit.................................. ***Zoma dibaiyin***
– Epigyne lacking a sclerotized median pit... **8**
8 Epigyne with an invagination on posterior margin...................................... **9**
– Epigyne lacking an invagination on posterior margin..................................
.... ***Theridiosoma alboannulatum***
9 Heart-shaped invagination with a pair of spurs ***Theridiosoma dissimulatum***
– Slit-like invagination......................... ***Theridiosoma nigrivirgatum* sp. nov.**

Taxonomy

Family Theridiosomatidae Simon, 1881

Genus *Theridiosoma* O. Pickard-Cambridge, 1879

Type species. *Theridiosoma gemmosum* (L. Koch, 1877), from Nuremberg, West Germany (not examined).

Remarks. Males of *Theridiosoma* species can be distinguished from other theridiosomatid genera by the morphology of the embolic division of the male palp: short and tubular embolus with embolic apophyses fragmented into several long bristle-like parts (Coddington 1986a: figs 131, 133). Embolic apophysis varies in number and shape among species and is regarded as an important taxonomic character (e.g., Zhao and Li 2012; Suzuki et al. 2020). Median apophysis is less sclerotized, curved and attenuates distally (Coddington 1986a: figs 132, 133), which is less useful for distinguishing species. A sclerotized projection ('conductor projection') is present on prolateral side of conductor in some species, while absent in others (Coddington 1986a; Suzuki et al. 2020). Distal margin of conductor beneath embolic apophyses ('posterior margin of embolic division' in Suzuki et al. 2020) is generally sclerotized and the shape is useful as a taxonomic character (e.g., Suzuki et al. 2020: figs 7E, 8E, 10E, 11E). Tegular surface beneath conductor is generally sclerotized with many folds (referred as 'ventral side of tegulum beneath posterior edge of embolic division' in Suzuki et al. 2020), of which shape and surface texture vary among species (Zhao and Li 2012; Suzuki et al. 2020).

Females of the genus can be distinguished from related genera (*Baalzebub*, *Epilineutes* and *Wendilgarda*) by having relatively sclerotized, robust copulatory ducts running from the bursa to the spermathecae (Coddington 1986a: figs 145, 152). Surface of epigynal plate is smooth and its posterior margin generally lacks scape-like structures. Shape of posterior margin of epigynal plate varies among *Theridiosoma* species: rounded or almost straight in some species, while having a pair of small, sclerotized processes (named as 'spurs' in Coddington 1986a) or a small slit-like invagination in others (Coddington 1986a; Miller et al. 2009; Suzuki et al. 2020). *Zoma* females possess a similar genitalia except in having a sclerotized median pit on the surface of the epigynal plate and lacking any processes nor invaginations on the posterior margin of the epigynal plate in known species (Saaristo 1996; Miller et al. 2009; Zhao and Li 2012; Ballarin et al. 2021).

Theridiosoma nigrivirgatum **sp. nov.**

https://zoobank.org/C1CB60C1-B782-4E34-9FAB-F44D3B12B4A0
[New Japanese name: Jyabara-karakara-gumo]
Figs 1–3, 11, 12C, 13A–C, 15A

Type material. ***Holotype*****: Japan, Okinawa Is. (Okinawa Prefecture):** ♂ (NSMT-Ar 21717), Urasoe City, Nakama, Urasoe-daikoen Park (26°14'50.2"N, 127°43'49.8"E, alt. 112 m), 8 Mar. 2021, Y. Suzuki leg. ***Paratypes*****:** 2 ♀, same data as the holotype; 1 ♂ 1 ♀ (NSMT-Ar 21718), Urasoe City, Nakama, Urasoe-daikoen Park (26°14'59.2"N, 127°43'54.6"E, alt. 64 m), 16 Apr. 2021, Y. Suzuki leg.; 1 ♂ 1 ♀ (NSMT-Ar 21719), Nakagami District, Nishihara Town, Senbaru (26°15'01.8"N, 127°45'57.8"E, alt. 104 m), 25 Apr. 2021, Y. Suzuki leg.

Other material examined. Japan, Okinawa Is. (Okinawa Prefecture): 10 ♀, Naha City, Shuri-sueyoshi Town, Sueyoshi-koen Park (26°13'45.0"N, 127°42'49.8"E, alt. 49 m), [7 Mar. 2021 (1 ♀), 8 Mar. 2021 (9 ♀)], Y. Suzuki leg.; 5 ♀, Nakagami District, Nishihara Town, Tanabaru, Tanabaru Gusuku (26°14'44.3"N, 127°45'16.4"E, alt. 141 m), 8 Apr. 2021, Y. Suzuki leg.; 2 ♂, Kunigami District, Kunigami Village, Yona (26°44'35.2"N, 128°14'55.1"E, alt. 195 m), 19 Sep. 2021, Y. Suzuki leg.; 1 ♀, Ôgusuku (26°17'09.5"N, 127°48'13.1"E, alt. 136 m), Nakagami Distirct, Kitanakagusuku Village, R. Serita leg. **Kume Is. (Okinawa Prefecture):** 1 ♀ 2 juv., Shimajiri District, Kumejima Town, Jyanado (26°20'46.2"N, 126°47'52.0"E, alt. 16 m), 10 Sep. 2021, Y. Suzuki leg. **Aka Is. (Okinawa Prefecture):** 1 ♀, Shimajiri District, Zamami Village, Aka, streamside at dim forest (26°11'47.11"N, 127°16'57.09"E, alt. 65 m), 16 Mar. 2022, Y. Suzuki leg.

Etymology. The specific name is a Latin adjective derived from the black striped pattern on the dorsal abdomen of the new species.

Diagnosis. Males of the new species resemble *T. alboannulatum* Suzuki, Serita & Hiramatsu, 2020 in having two parallel embolic apophyses exposed from conductor and lacking a conductor projection on the male palp. They can be distinguished by the presence of one embolic apophysis longer than another and the shape of the sclerotized distal margin of conductor beneath embolic apophyses: a ridge separates the two triangular surfaces and sharply cornered at the terminal of the ridge in *T. nigrivirgatum* sp. nov. (Figs 2C, 3C), while a ridge is lacking in

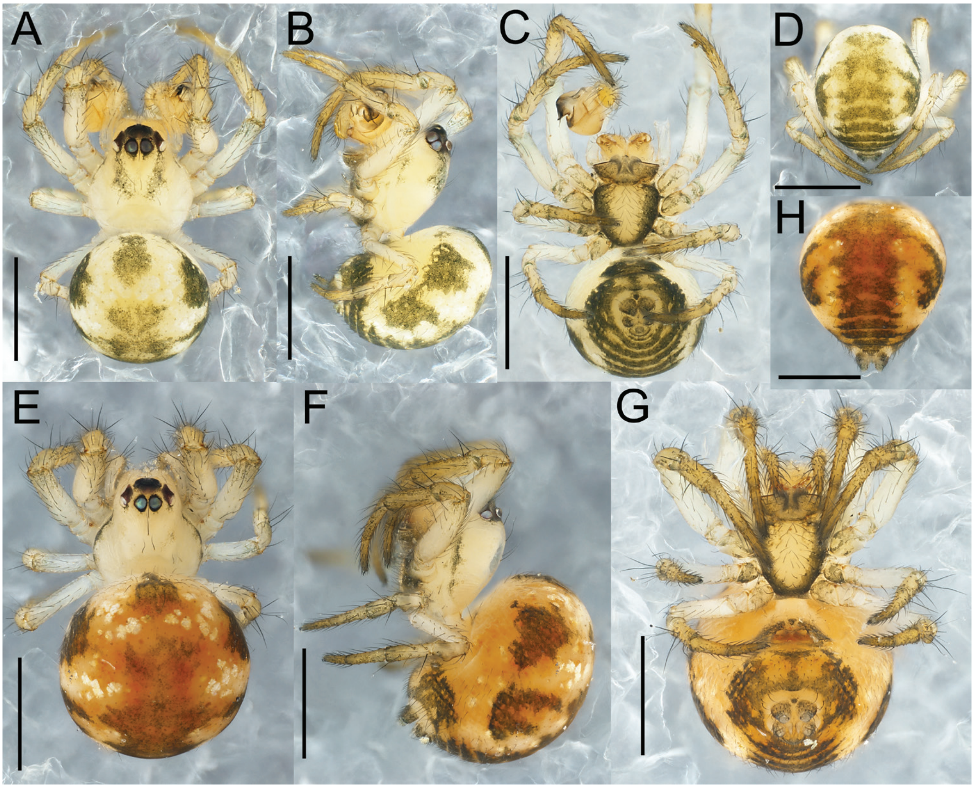

Figure 1. *Theridiosoma nigrivirgatum* sp. nov., male holotype (NSMT-Ar 21717 **A–D**) and female paratype (NSMT-Ar 21718 **E–H**) **A, E** habitus, dorsal view **B, F** habitus, lateral view **C, G** habitus, ventral view **D, H** abdomen, posterior view. Scale bars: 0.5 mm.

T. alboannulatum (Suzuki et al. 2020: fig. 12E, F). Females of the new species resemble those of *T. diwang* Miller, Griswold & Yin, 2009 in having a small and narrow slit on the posterior margin of the epigynal plate, but can be distinguished by the shape of the vulva: genital plate is bell-shaped and longer than wide; spermathecae are positioned at the anterior part of the vulva in *T. nigrivirgatum* sp. nov. (Figs 2G, 3G), while the vulva is wider than long, copulatory ducts extend anteriorly, and the position of spermatheca is lower than the anterior margin of the copulatory ducts in *T. diwang* (Miller et al. 2009: fig. 3G). Both sexes can be distinguished from congeners by their abdominal color and patterns: a dark marking on the anterior dorsum, two pairs of dark markings on the dorsolateral side, and dark striped markings on the posterior dorsum (Fig. 1).

Description. Male (holotype, NSMT-Ar 21717). Measurements. Body 1.02 long. Carapace 0.45 long, 0.46 wide, and 0.36 high. Eye size and interdistances, AME 0.054, ALE 0.047, PME 0.050, PLE 0.042, AME-AME 0.022, AME-ALE 0.017, PME-PME 0.012, PLE-PLE 0.030. Leg length: leg I 0.47 + 0.17 + 0.31 + 0.29 + 0.20 = 1.44; leg II 0.38 + 0.15 + 0.26 + 0.24 + 0.18 = 1.21; leg III 0.23 + 0.13 + 0.14 + 0.18 + 0.13 = 0.81; leg IV 0.30 + 0.13 + 0.20 + 0.20 + 0.15 = 0.98. Abdomen 0.58 long, 0.60 wide, 0.80 high.

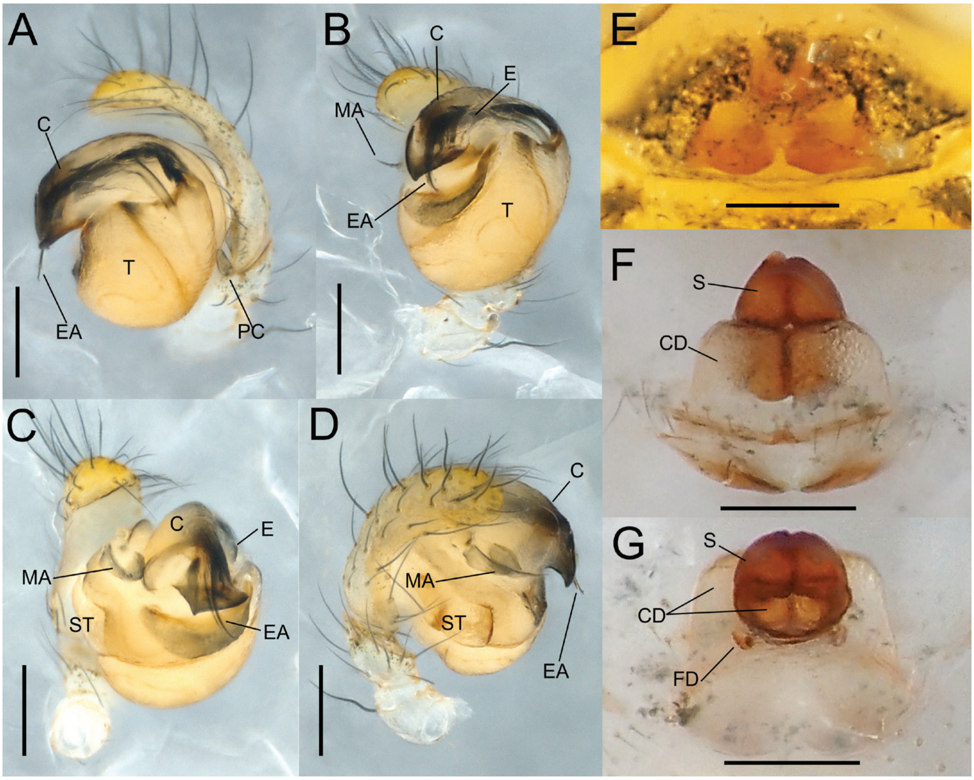

Figure 2. *Theridiosoma nigrivirgatum* sp. nov., male holotype genitalia (NSMT-Ar 21717 **A–D**) and female paratype genitalia (NSMT-Ar 21718 **E–G**) **A** retrolateral view **B** ventral view **C** posterior-ventral view **D** prolateral view **E** ventral view **F** ventral view **G** dorsal view. Abbreviations: **C** conductor **CD** copulatory ducts **E** embolus **EA** embolic apophysis **FD** fertilization ducts **MA** median apophysis **PC** paracymbium **S** spermatheca **ST** subtegulum **T** tegulum. Scale bars: 0.1 mm.

Carapace oval, wider than long (CaL/CaW 0.98). Chelicerae with three teeth on promargin. Abdomen oval and wider than long (AL/AW 0.97).

Coloration and markings (Fig. 1A–D). Carapace, chelicerae, and legs dark yellowish brown (turning to yellowish brown in ethanol). Cephalic groove stained with dark spots. Anterolateral margin of carapace dark grey. Mouthparts dark yellowish brown. Sternum pale yellowish brown with black lateral margins. Eyes on the dark bases. Legs yellowish brown with femora pale and lacking annulations. Abdomen pale yellowish brown with a dark greyish marking on anterior dorsum, two pairs of dark greyish spots on dorsolateral sides, and dark-colored longitudinal stripes on posterior dorsum. Spinnerets and ventral side of abdomen dark grey.

Palp (Figs 2A–D, 3A–D). Palpal patella with a strong retrolateral macroseta. Paracymbium hook-like with a blunt tip. Tegulum bulbous. Embolic division covered with a semitransparent conductor and composed of several apophyses. Conductor lacking conductor projection. Two long and parallel bristle-like embolic apophyses exposed from the conductor. Posterior margin of the embolic division strongly sclerotized

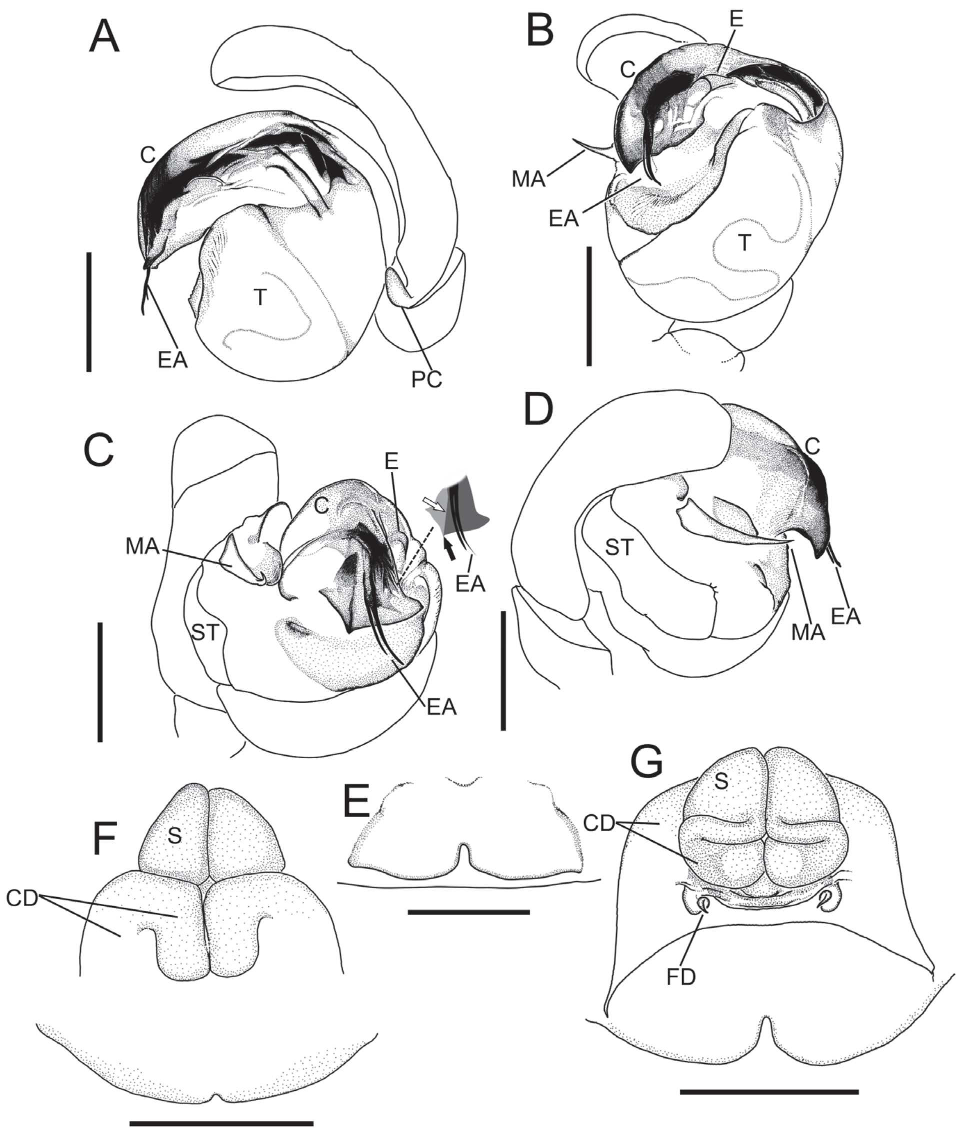

Figure 3. *Theridiosoma nigrivirgatum* sp. nov., male holotype genitalia (NSMT-Ar 21717 **A–D**) and female paratype genitalia (NSMT-Ar 21718 **E–G**) **A** retrolateral view **B** ventral view **C** posterior-ventral view **D** prolateral view **E** ventral view **F** ventral view **G** dorsal view. Abbreviations: **C** conductor **CD** copulatory ducts **E** embolus **EA** embolic apophysis **FD** fertilization ducts **MA** median apophysis **PC** paracymbium **S** spermatheca **ST** subtegulum **T** tegulum. White and black arrows indicate a ridge that separate the two triangular surfaces and a sharply cornered terminal of the ridge, respectively. Scale bars: 0.1 mm.

with angular corners, the middle one pointed, the retrolateral one blunt, a ridge separates two triangular surfaces: one is covered by embolic division and the other is not (Fig. 3C). Tegular surface beneath conductor weakly sclerotized with denticles. Median apophysis narrower toward the pointed tip.

Female (paratype: NSMT-Ar 21718). Measurements. Body 1.31 long. Carapace 0.51 long, 0.50 wide, 0.41 high. Eye size and interdistances: AME 0.057, ALE 0.058, PME 0.060, PLE 0.053, AME-AME 0.019, AME-ALE 0.032, PME-PME 0.009, PLE-PLE 0.043. Leg length: leg I 0.61 + 0.20 + 0.29 + 0.26 + 0.19 = 1.55; leg II 0.40 + 0.16 + 0.24 + 0.19 + 0.16 = 1.15; leg III 0.24 + 0.15 + 0.14 + 0.17 + 0.13 = 0.83; leg IV 0.40 + 0.17 + 0.23 + 0.20 + 0.14 = 1.97. Abdomen 0.86 long, 0.87 wide, 0.90 high.

Carapace oval and almost as long as wide (CaL/CaW 1.02). Chelicerae with three teeth on promargin. Abdomen oval and as long as wide (CaL/CaW 0.99).

Coloration and markings (Fig. 1E–H). Carapace and chelicerae pale yellowish brown. Lateral margin of carapace dark grey. Eyes on the dark bases. Eyes, mouthparts, sternum, and legs as in male. Abdomen yellowish brown with dark greyish markings similar to the male, and dark orange markings on the dorsum and sides.

Genitalia (Figs 2E–G, 3E–G). Epigyne a wide plate with a short and narrow slit in the middle of the posterior margin. Vulva. Copulatory ducts moderately complicated. Spermathecae rounded triangular and juxtaposed. Fertilization ducts with curved tips.

Variations. The color and patterns of the abdomen vary: male specimens collected from Northern Okinawa lack longitudinal stripes on the posterior dorsum of the abdomen.

Taxonomic justification. *Theridiosoma nigrivirgatum* sp. nov. can safely be assigned to the genus according to the male palpal morphology: embolus short and tubular, and embolus apophyses fragmented into several long bristle-like parts.

Remarks. The males and females are considered to be the same species because of the similarity of body color and patterns and their sympatric occurrences. Although this species sympatrically occurred with *T. dissimulatum* on southern Okinawa Island (Fig. 11), no other undescribed candidates were collected.

Distribution. Japan (Okinawa, Kume and Aka Islands; Fig. 11).

Habitat. The new species inhabits forest floors of secondary forests, bushes, and grasslands. The species is frequently collected from an open environment covered by Poaceae grasses, where *T. dissimulatum* is never found (Fig. 12C). The habitat of this species resembles that of *T. alboannulatum* (Fig. 12D).

Web morphology. This species weaves a concave orb web with radial anastomosis and a tension line connected to substrates (Fig. 13A–C). A spider drags a tension line with a strong force so that the web is deformed to a conical shape. The web is similar to that of the congeners.

Egg sac. pale whitish brown and spherical with a long horizontal line and a short stalk (Fig. 15A).

Theridiosoma dissimulatum Suzuki, Serita & Hiramatsu, 2020

Figs 11, 12A, 15B

Theridiosoma dissimulatum Suzuki, Serita & Hiramatsu, 2020: 137, figs 1E–H, 3D–F, 5C, D, 8A–J, 9A–P, 13E–H (holotype male and paratypes from Amami Island, Japan; not examined).

Material examined. Japan, Amami Is. (Kagoshima Prefecture): 1 ♀, Amami City, Nase-uragami Town (28°23'55.6"N, 129°32'27.5"E, alt. 139 m), 1 Jul. 2021, Y. Suzuki leg.; 4 ♀, Amami City, Sumiyo Town, Nishinakama, Santaro-toge Pass (28°15'48.7"N, 129°25'09.0"E, alt. 141 m), 6 May 2021, Y. Suzuki leg.; 1 ♀, Ôshima District, Yamato Village, Ôganeku, Materiya-no-taki Waterfall (28°19'04.4"N, 129°21'08.2"E, alt. 176 m), 4 Jul. 2021, Y. Suzuki leg. **Okinoerabu Is. (Kagoshima Prefecture):** 2 ♂ 4 ♀, Ôshima District, China Town, Tokudoki (27°21'34.5"N, 128°33'02.8"E, alt. 134 m), 8 Dec. 2021, Y. Suzuki leg. **Okinawa Is. (Okinawa Prefecture):** 2 ♂ 3 ♀, Naha City, Shuri-sueyoshi Town, Sueyoshi-koen Park (26°13'39.6"N, 127°42'55.3"E, alt. 25 m), 7 Mar. 2021, Y. Suzuki leg.; 2 ♀, Kunigami District, Ôgimi Village, Nerome (26°40'49.7"N, 128°08'01.1"E, alt. 128 m), 14 Apr. 2021, Y. Suzuki leg.; 1 ♀, Kunigami District, Ôgimi Village, Ôgimi (26°40'57.9"N, 128°08'21.6"E, alt. 311 m), 15 May 2021, Y. Suzuki leg. **Iriomote Is. (Okinawa Prefecture):** 1 ♂ 3 ♀, Yaeyama District, Taketomi Town, Haiminaka, Ôtomi-rindo Path (24°17'52.6"N, 123°52'47.3"E, alt. 18 m), 30 Apr. 2021, Y. Suzuki leg.; 1 ♂ 3 ♀, Ôtomi-daiichi-do Cave (24°17'31.0"N, 123°52'45.7"E, alt. 30 m), 1 May 2021, Y. Suzuki leg.

Remarks. This species can easily be distinguished from *T. nigrivirgatum* sp. nov. by the presence of a conductor projection on the male palp and a heart-shaped invagination with a pair of spurs on the posterior margin of the female epigynal plate (Suzuki et al. 2020). Refer to the description in Suzuki et al. (2020) for further morphological information.

Distribution. Japan (Amami, Okinoerabu, Okinawa, Ishigaki, and Iriomote Islands; Fig. 11).

Habitat. This species was collected from dim moist forests, especially from locations beside streams (Fig. 12A).

Web morphology. *Theridiosoma dissimulatum* weaves a concave orb web and drags a tension line with the forelegs.

Egg sac. pale reddish brown and spherical with a long horizontal line and a short stalk (Fig. 15B).

Theridiosoma alboannulatum Suzuki, Serita & Hiramatsu, 2020

Figs 12D, 13D–E, 15C

Theridiosoma alboannulatum Suzuki, Serita & Hiramatsu, 2020: 149, figs 2I–L, 4G–I, 6E–F, 12A–J, 13P (holotype male and paratypes from Iriomote Island, Japan; not examined).

Material examined. Japan, Kurima Is. (Okinawa Prefecture): 2 ♂, Miyakojima City, Shimojikuruma (24°43'29.2"N, 125°15'09.2"E, alt. 41 m),, 17 Nov. 2021, Y. Suzuki leg. **Miyako Is. (Okinawa Prefecture):** 3♂ 3 ♀, Miyakojima City, Hiraranishihara, grassland at roadside (24°49'53.5"N, 125°18'55.0"E, alt. 46 m), 24 Apr. 2022, Y. Suzuki leg. **Kuroshima Is. (Okinawa Prefecture):** 2 ♂ 1♀, Yaeyama District, Taketomi

Town, edge of coastal forest besides Hokei beach (24°14'26.2"N, 123°59'32.7"E, alt. 0 m), 2 Nov. 2021, Y. Suzuki leg. **Yonaguni Is. (Okinawa Prefecture):** 1 ♀, Yaeyama District, Yonaguni Town, Yonaguni (24°27'58.8"N, 123°01'20.1"E, alt. 49 m), 12 Oct. 2021, Y. Suzuki leg.; 2 ♂ 2♀, Yaeyama District, Yonaguni Town, Sonai Village (24°28'10.5"N, 123°00'31.7"E, alt. 19 m), 12 Oct. 2021, Y. Suzuki leg.; 1 ♂ 1♀, Yaeyama District, Yonaguni Town, wetland beside secondary forest (24°27'16.3"N, 122°59'24.3"E, alt. 38m), 14 Oct. 2021, Y. Suzuki leg.

Note. See diagnosis section for comparison with *T. nigrivirgatum* sp. nov.

Habitat. This species inhabits grasslands, bushes, and secondary forests. Spiders were collected from the basal parts of grasses.

Web morphology. The spider weaves a concave web between the grasses (Fig. 13D, E).

Egg sac. similar to that of *T. nigrivirgatum* sp. nov. (Fig. 15C).

Distribution. Japan (Miyako, Kurima, Iriomote, Kuroshima, and Yonaguni Islands; Fig. 11).

Genus *Zoma* Saaristo, 1996

Type species. *Zoma zoma* Saaristo, 1996, from Seychelles (not examined).

Composition. *Zoma zoma* Saaristo, 1996, *Z. dibaiyin* Miller, Griswold & Yin, 2009, *Z. fascia* Zhao & Li, 2012, *Z. taiwanica* (Zhan, Zhu & Tso, 2006).

Remarks. Females of the genus can be distinguished by the flat and bluntly triangular genital plate with a sclerotized median pit and a pair of smaller, generally less recognizable, lateral pits (Fig. 4J; see also Saaristo 1996). Males of the type species *Z. zoma* have not yet been described. Therefore, the taxonomic characteristics of *Zoma* males are poorly defined. Males of three *Zoma* species, *Z. dibaiyin*, *Z. fascia*, and *Z. taiwanica* have relatively simpler palps with a filiform embolic apophysis emerging beneath from the conductor, while two or more apophyses in *Theridiosoma* (Fig. 3B, C vs. Fig. 5A, B). *Zoma* species have wider and straight median apophysis, while curved and sharp tip in *Theridiosoma* (Fig. 3B–D vs. Fig. 5A–C). *Zoma* species can be distinguished from congeners by the presence of a transverse whitish silver band on the dorsum abdomen (Saaristo 1996; Miller et al. 2009).

Zoma dibaiyin Miller, Griswold & Yin, 2009

Figs 4–5, 11, 12B, 13F–H

Zoma dibaiyin Miller, Griswold & Yin, 2009: 27, figs 10A–F, 11A–B, 13A–D (holotype male and paratypes from China; not examined); Ono and Ogata 2018: 120, 504, 505; Suzuki and Serita 2021a: 231, figs 1–3.

Material examined. **Japan, Amami Is. (Kagoshima Prefecture):** 1♂ 1 ♀ (NSMT-Ar. 21720, 21721), Ôshima District, Setouchi Town, Katsuura (28°12'33.7"N, 129°19'54.0"E, alt. 354 m), 4 Jul. 2021, Y. Suzuki leg.; 1 ♂ 1 ♀, Amurogama (28°13'15.4"N, 129°18'59.3"E, alt. 111 m), 4 Jul. 2021, Y. Suzuki leg.; 1 ♂, Amami City, Sumiyo Town, Nishinakama, Santarou-toge Pass (28°15'48.7"N, 129°25'09.0"E, alt. 141 m), 6 May 2021, Y. Suzuki leg.; **Okinawa Is. (Okinawa Prefecture):** 1 ♂ 1 ♀, Kunigami District, Ôgimi Village, Nerome (26°40'49.7"N, 128°08'01.1"E, alt. 128 m), 14 Apr. 2021, Y. Suzuki leg.; **Kume Is. (Okinawa Prefecture):** 1 ♂ 1 ♀, Shimajiri District, Kumejima Town, Uezu, Mt. Daruma-yama (26°21'42.9"N, 126°45'34.9"E, alt. 149 m), 10 Sep. 2021, Y. Suzuki leg.

Diagnosis. Males of this species can be distinguished from congeners by the embolic apophysis with a curved tip running along the sclerotized surface of the ventral tegulum, and females by a nearly transverse posterior margin of the epigynal plate (more convex in *Z. zoma* and rounded in *Z. taiwanica*) and lower position of the spermathecae (higher in *Z. taiwanica*) (Miller et al. 2009; Ballarin et al. 2021).

Description. Male (NSMT-Ar 21720). Measurements. Body 1.62 long. Carapace 0.74 long, 0.68 wide, 0.60 high. Eye size and interdistances: AME 0.090, ALE 0.076, PME 0.093, PLE 0.065, AME-AME 0.015, AME-ALE 0.032, PME-PME 0.008, PLE-PLE 0.070. Leg length: leg I 0.80 + 0.23 + 0.57 + 0.47 + 0.28 = 2.35; leg II 0.50 + 0.21 + 0.46 + 0.31 + 0.28 = 1.76; leg III 0.40 + 0.19 + 0.23 + 0.24 + 0.24 = 1.30; leg IV 0.44 + 0.14 + 0.34 + 0.27 + 0.27 = 1.46. Abdomen 0.88 long, 0.95 wide, 1.01 high.

Carapace oval, longer than wide (CaL/CaW 1.34). Chelicerae with three teeth on promargin. Abdomen oval, wider than long (AL/AW 0.93).

Coloration and markings (Fig. 4A, B). Carapace, chelicerae, maxillae, labium, sternum, and legs yellowish brown. Eyes on the dark bases. Cephalic groove stained with dark spots. Legs lacking annulation. Abdomen dark brown encircled dorsolaterally with a whitish silver band.

Palp (Figs 4C–H, 5). Paracymbium with sharp tip. Tegulum bulbous. Median apophysis weakly sclerotized, wider than long. Embolic division branched into a few bristle-like apophyses, embolus short and tubular, and a long and filiform embolic apophysis emerging beneath from a translucent conductor. Tip of embolic apophysis curved and running along sclerotized surface of the tegulum beneath the conductor. Conductor having two projections: posterior conductor projection strongly sclerotized and triangular with a blunt tip; retrolateral conductor projection strongly sclerotized and weakly curved anteriorly with a triangular posterior tip. Posterior margin of conductor with a sharp tip.

Female (NSMT-Ar 21721). Measurements. Body 2.04 long. Carapace 0.82 long, 0.76 wide, 0.67 high. Eye size and interdistances: AME 0.089, ALE 0.082, PME 084, PLE 0.076, AME-AME 0.023, AME-ALE 0.034, PME-PME 0.009, PLE-PLE 0.076. Leg length: leg I 0.66 + 0.32 + 0.42 + 0.33 + 0.22 = 1.95; leg II 0.64 + 0.30 + 0.4 1 + 0.33 + 0.21 = 1.89; leg III 0.36 + 0.18 + 0.20 + 0.25 + 0.18 = 1.17; leg IV 0.53 + 0.21 + 0.34 + 0.27 + 0.22 = 1.57. Abdomen 1.21 long, 1.32 wide, 1.16 high.

Carapace, mouthparts, and abdomen as in male (CaL/CaW 1.08; AL/AW 0.92).

Coloration and markings (Fig. 4I) similar to male.

Genitalia (Fig. 4J, K). Epigynal plate flat and wider than long with a sclerotized posterior margin and a median pit. Spermathecae touching each other, copulatory

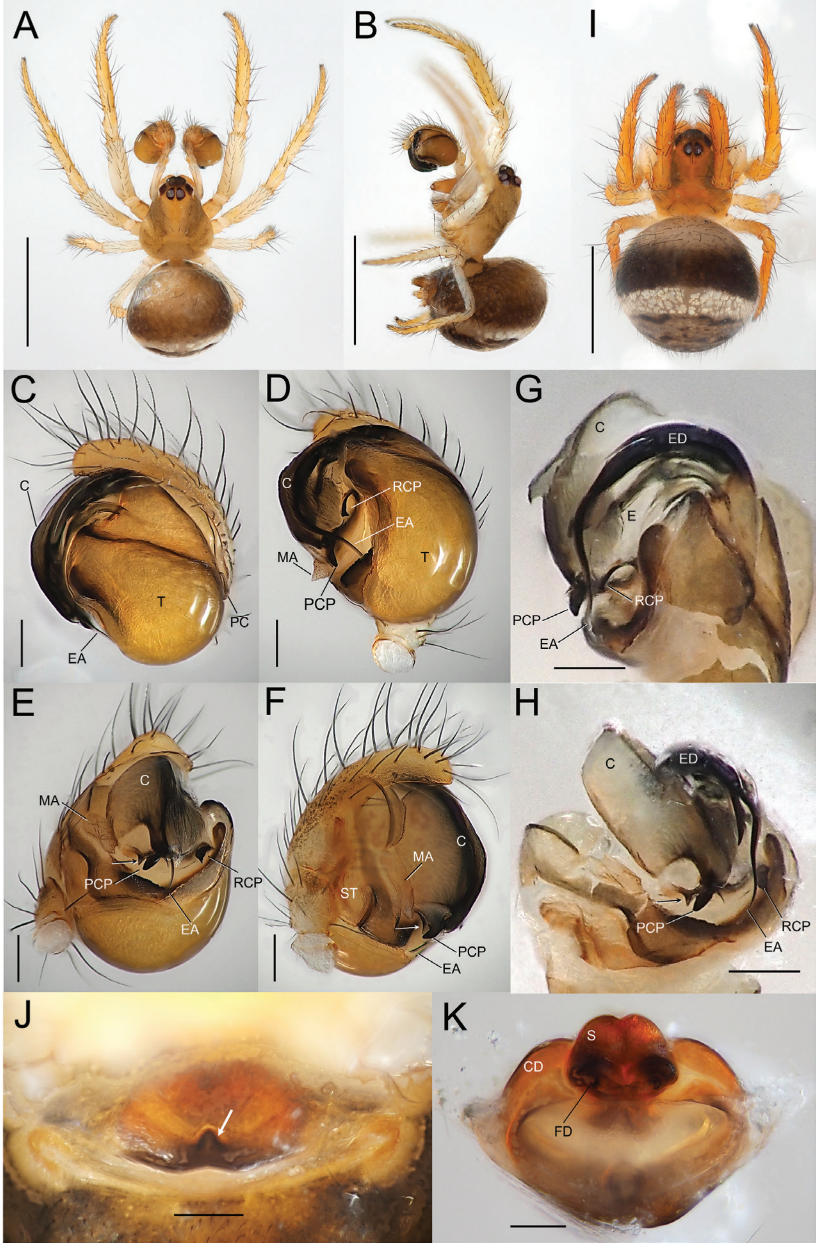

Figure 4. *Zoma dibaiyin* Miller, Griswold & Yin, 2009, male habitus and genitalia (NSMT-Ar 21720 **A–H**) and female habitus and genitalia (NSMT-Ar 21721 **I–K**) **A** habitus, dorsal view **B** habitus, lateral view **C** palp, retrolateral view **D** palp, ventral view **E** palp, posterior-ventral view **F** palp, prolateral view **G** embolic division, prolateral view **H** embolic division, posterior-ventral view **I** habitus, dorsal view **J** epigyne, ventral view **K** vulva, dorsal view. Abbreviations: **C** conductor **CD** copulatory ducts **E** embolus **EA** embolic apophysis **FD** fertilization ducts **MA** median apophysis **PC** paracymbium **PCP** posterior conductor projection **RCP** retrolateral conductor projection **S** spermatheca **ST** subtegulum **T** tegulum. Arrows in **E, F, H** indicate a cornered margin of posterior membrane of conductor. Arrow in **J** indicates a sclerotized median pit. Scale bars: 1.0 mm (**A, B, I**); 0.1 mm (**C–H, J, K**).

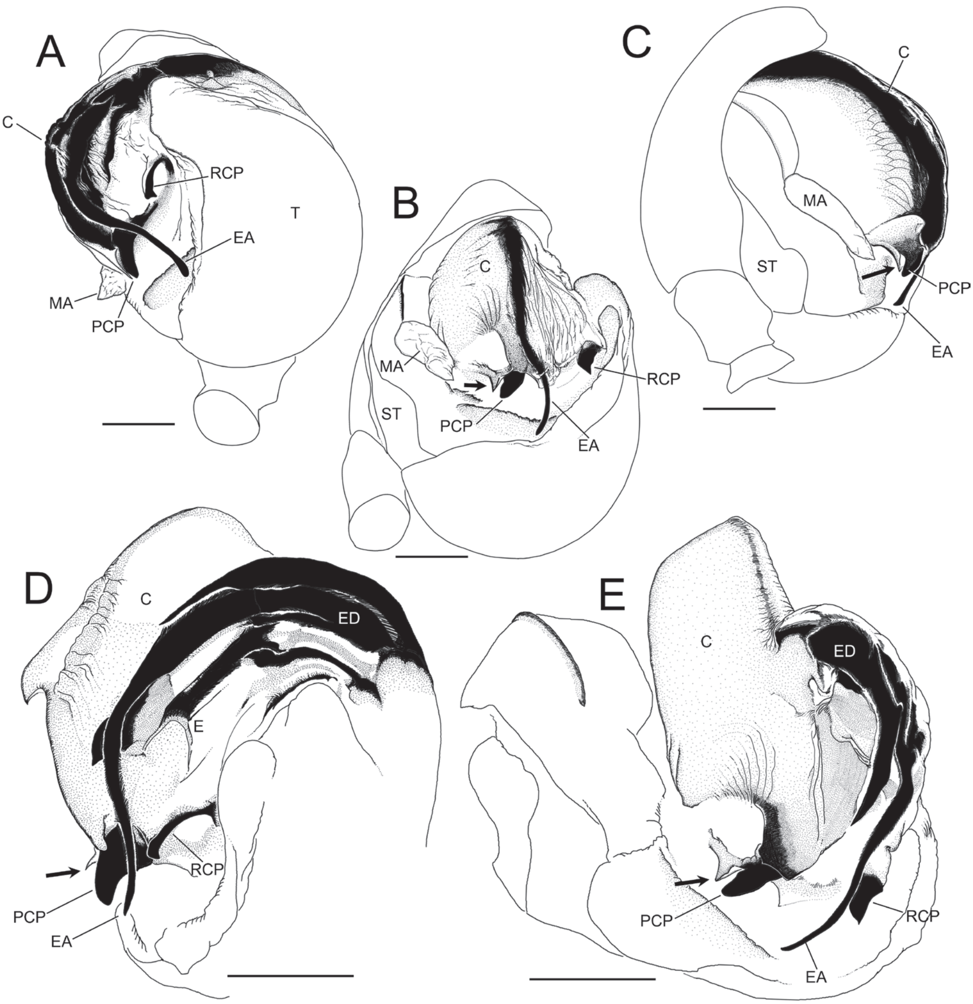

Figure 5. *Zoma dibaiyin* Miller, Griswold & Yin, 2009, male genitalia (NSMT-Ar 21720) **A** ventral view **B** posterior-ventral view **C** prolateral view **D** conductor and embolic division, retrolateral view **E** conductor and embolic division, posterior-ventral view. Abbreviations: **C** conductor **CD** copulatory ducts **E** embolus **EA** embolic apophysis **MA** median apophysis **PC** paracymbium **PCP** posterior conductor projection **RCP** retrolateral conductor projection **ST** subtegulum **T** tegulum. Arrows in **B–E** indicate a cornered margin of posterior membrane of conductor. Scale bars: 0.1 mm.

ducts wide at their openings, and the course of the ducts simple. See Miller et al. (2009) for further details.

Remarks. A strongly sclerotized triangular projection with a rounded tip (Figs 4E, 5B) and a cornered margin of the posterior membrane of the conductor (Figs 4E, 5B, arrowed) were visible in the ventro-posterior view of the male palp. The triangular projection does not seem to be homologous to conductor projection in *Theridiosoma*, as the former protrudes from the posterior margin of the conductor, while the latter was positioned on the surface of the conductor. Herein, we define it as posterior conductor projection (PCP).

The embolus on the male palp was not determined in *Z. dibaiyin* and *Z. fascia* (Miller et al. 2009; Zhao and Li 2012). In *Z. taiwanica*, the embolus is described as a 'short and tubular structure' but lacks explanations in illustrations (Zhang et al. 2006). Ballarin et al. (2021) determined the embolus as a strongly sclerotized, thin, stick-like apophysis located on the retrolateral side of the embolic division (Ballarin et al. 2021). Considering the shape of *Theridiosoma*'s embolus, which is short, tubular, and hidden under conductor (see Coddington 1986a: fig. 131), we suppose the 'embolus' of *Zoma* species determined in Ballarin et al. (2021) is not an embolus. The true embolus of *Z. dibaiyin* is found beneath basal part of embolic apophyses (Fig. 5D). Hereafter we defined the sclerotized stick-like structure as a retrolateral conductor projection (RCP), and distinguishable from an embolus. The shape of RCP is useful as a taxonomic character for differentiating species within the genus *Zoma*: S-shaped with pointed tip in *Z. fascia*, claviform with rounded tip in *Z. taiwanica* (Zhao and Li 2012: figs 28, 30; Zhang et al. 2006: figs 4–6; Ballarin et al. 2021: fig. 5B, C), and weakly curved anteriorly with a triangular posterior tip in *Z. dibaiyin* (Figs 4D, 5D).

Distribution. China (Yunnan), Japan (Honshu to the Ryukyu Islands; Fig. 11).

Habitat. This species inhabits the forest floor and streamside in dim and wet forests (Fig. 12B).

Web morphology. This species weaves a concave orb web with radial anastomosis above the ground (Fig. 13F–H). The orb web is almost horizontal. A tension line stretched from the center of the web and attached to substrates such as rocks and dead leaves. The mesh of sticky spirals tends to be fine (occasionally, the number of sticky lines is > 30). For details of the web morphology, see Hiramatsu (2021).

Egg sac. light brown with a distinct circular suture at the upper end. The sac was suspended from a long horizontal line with a short stalk (see Hiramatsu 2021).

Genus *Sennin* gen. nov.

https://zoobank.org/AAA86579-ABA5-4385-B0D7-68D7676BD871

[New Japanese name: Hora-ana-karakara-gumo-zoku]

Type species. *Sennin tanikawai* sp. nov.

Etymology. The generic name *Sennin* is noun in apposition, masculine, and derived from the Japanese word meaning mountain hermits, a person who acquires a spiritual power after living a secluded life deep in the mountains. Iriomote Island, where the new species inhabits, is famous for a man called Sennin, who was self-sufficient, lived in the coastal caves, and single-handedly built a wooden hut.

Diagnosis. This genus can be distinguished from other theridiosomatid genera by the following characteristics: a large, oblong cymbial outgrowth (cymbial apophysis) protruding from the basal and dorsal part of cymbium of male palp (Figs 7A–C, 9 A–C); an embolic division with three elongated bristle-like embolic apophyses with the longest one coiled (Figs 7F–J, 9F–J); the anterior margin of the epigynal plate with a pair of sclerotized, triangular extensions protruding anteriorly from the anterolateral side (Figs 8A, D; 10A, D; arrowed; Zhu et al. 2001: fig. 4; Chen 2010: figs 19, 20); the vulva with long copulatory ducts coiling at the lateral side of the spermatheca (Figs 8C, D, 10C, D).

Composition. *Sennin tanikawai* sp. nov., *S. coddingtoni* (Zhu, Zhang & Chen, 2001), comb. nov.

Remarks. This genus is related to *Baalzebub* Coddington, 1986, based on the shape of the median apophysis on the male palp, the embolic apophyses that are not exposed from the conductor, and the general morphology of the epigyne. The elongated and oblong dorsal cymbial apophysis, one of the most conspicuous characters of *Sennin* gen. nov. (Figs 7A–C, 9A–C), differentiates the new genus from *Baalzebub*. Although some species of *Baalzebub* have a small protrusion on the retrolateral-dorsal side of basal part of cymbium (e.g., paracymbium in *B. acutum*; Prete et al. 2016: figs 2D, 3C; named 'Höcker' (= lump) in *B. brauni*; Wunderlich 1976: figs 17, 18), it is not as prominent as that of *Sennin* gen. nov. The embolic apophyses of *Baalzebub* are short, blunt, and spatulate, but those of *Sennin* are longer, bristle-like, and strongly curved or coiled (Figs 7F–J, 9F–J). As for the female genitalia of species of *Baalzebub*, the epigynal plate is upside-down triangular with sclerotized central epigynal pit, the spermathecae elliptical, and longer laterally with connate tips, and the course of copulatory ducts is simple (Coddington 1986a). *Sennin* gen. nov. has similar spermathecae, but the course of the copulatory duct is more complex, with a coiled trajectory at the basal side of the spermathecae (Figs 8C, D, 10C, D).

Sennin coddingtoni comb. nov. was formerly placed in *Karstia* Chen, 2010, but it shares conspicuous characteristics with *S. tanikawai* sp. nov. and can clearly be differentiated from *K. upperyangtzica* Chen, 2010, the type species of the genus. Therefore, we transferred it from *Karstia* to *Sennin* gen. nov. *Karstia upperyangtzica* and *K. cordata* Dou & Li (2012) females have an upside-down triangular epigynal plate with a sclerotized epigynal pit, and a simple course of copulatory ducts; males have cymbial apophysis as a very small protrusion, and embolic division with short, spatulate embolic apophyses (Chen 2010; Dou and Lin 2012; Zhang and Wang 2017). Based on these morphological characteristics, it is difficult to differentiate *K. upperyangtzica* and *K. cordata* from *Baalzebub*; therefore, taxonomic revision of *Karstia* is needed. In this study, we defer revision of *Karstia*, which may require direct examination of the type specimens and further molecular analysis.

As mentioned above, taxonomic relationship between *Sennin* gen. nov. and its potentially closest-related genera (*Baalzebub* and probably *Karstia*) is not yet well defined. This also indicated that the establishment of *Sennin* gen. nov. could render these related genera polyphyletic. To revise taxonomic status of these taxa in terms of monophyly, further integrative phylogenetic approach covering large number of species and genera is required.

According to the morphology and a potential close-relatedness to *Baalzebub*, *Sennin* gen. nov. is here suggested to be assigned to the subfamily Theridiosomatinae.

Sennin tanikawai **sp. nov.**
https://zoobank.org/2FB64512-C697-4195-AE82-62C4563508DD
[New Japanese name: Iriomote-hora-ana-karakara-gumo]
Figs 6–10, 11, 12E, 14A–G, 15D–E

Type material. ***Holotype*****: Japan, Iriomote Is. (Okinawa Prefecture)**: ♂ (NSMT-Ar 21722), Yaeyama District, Taketomi Town, Haiminaka, Ôtomi-Daini-Do Cave, 31 Mar. 1985, A. Tanikawa leg. ***Paratypes*****:** 2 ♀ (NSMT-Ar 21723), 27 Mar. 1995, A. Tanikawa leg.; 9 ♂ (NSMT-Ar 21724–21725), 31 Mar. 1985, A. Tanikawa leg.; 1 ♀ (NSMT-Ar 21726), 1 Aug. 1970, Y. Shirota leg.; 2 ♀ (NSMT-Ar 21727), 27 Oct. 1977, N. Tsurusaki leg.; above paratypes are collected at same locality as the holotype; 1 ♂ (NSMT-Ar 21728), a small opening of Ôtomi-Daini-Do Cave (24°17'09.4"N, 123°53'24.9"E, alt. 10 m), 24 Jun. 2021, Y. Suzuki leg.

Additional material examined. Japan, Iriomote Is. (Okinawa Prefecture): 1 ♀, Yaeyama District, Taketomi Town, Haemi, Ôtomi-daiichi-do Caves (24°17'31.0"N, 123°52'45.7"E, alt. 30 m), 3 May 2021, Y. Suzuki leg.; 1 ♀, Yaeyama District, Taketomi Town, Takana, Yutsun-Do Caves, a small cave on coastal cliff (24°23'08.90"N, 123°53'27.89"E, alt. 10 m), 21 Mar. 2019, Y. Suzuki leg.; 1 ♀, Takana, Yutsun-Do Caves, a large cave opening on coastal cliff (24°23'05.88"N, 123°53'25.00"E, alt. 7 m), 28 Mar. 2008, T. Hiramatsu leg.; 6 ♂ 7 ♀, Takana, Yutsun-Do Caves, a large cave opening on coastal cliff (24°23'05.88"N, 123°53'25.00"E, alt. 7 m), 1 May 2021, Y. Suzuki leg.; 2 ♀, Takana, Yutsun-Do Caves, cavities of rocks on coastal cliff (24°23'04.96"N, 123°53'23.82"E, alt. 10m), 22 Jun. 2021, Y. Suzuki leg.; 3 ♀, Takana, Yutsun-Do Caves, a cave beside Shirahama-haemi-sen road (24°23'06.5"N, 123°53'31.2"E, alt. 27 m), 24 Jun. 2021, Y. Suzuki leg.; 1 ♂ 1♀, Haemi, limestone rocky walls in a secondary forest (24°16'08.48"N, 123°52'01.52"E, alt. 16 m), 24 Jun. 2021, Y. Suzuki leg.

Etymology. The specific name is patronym dedicated to Dr. Akio Tanikawa, a Japanese arachnologist who has contributed remarkably to the elucidation of the spider fauna in Iriomote Island and offered us many specimens including type specimens.

Diagnosis. Males of this species can be distinguished from the allied *Sennin coddingtoni* comb. nov. by the following characteristics: cymbial apophysis is wider in relation to palpal tibia length while it is almost the same length as *S. coddingtoni* comb. nov. (CAW/PTL = 2.41 in *S. tanikawai* sp. nov., also see Fig. 9A, B; 1.00 in *S. coddingtoni* comb. nov.; also see Zhu et al. 2001: fig. 7); median apophysis of *S. tanikawai* sp. nov. is longer and narrower dorsally (MAL/MAW 1.63; Fig. 9E) compared to that of the latter (MAL/MAW 0.85, based on Chen 2010: fig. 24); the less-sclerotized distal part of median apophysis is lanceolate with pointed tip on ventral terminal in *S. tanikawai* sp. nov. (arrows in Figs 7E, 9E), while that of *S. coddingtoni* comb. nov. is falcate (Chen 2010: fig. 24). Females of *S. tanikawai* sp. nov. can be distinguished from *S. coddingtoni* comb. nov. by the following characteristics: longer epigynal scape (ESL/VW 0.46 in *S. tanikawai* sp. nov., Fig. 10; 0.16 in *S. coddingtoni* comb. nov., based on Chen 2010: fig. 19); tip of spermatheca is strongly curved anteriorly in

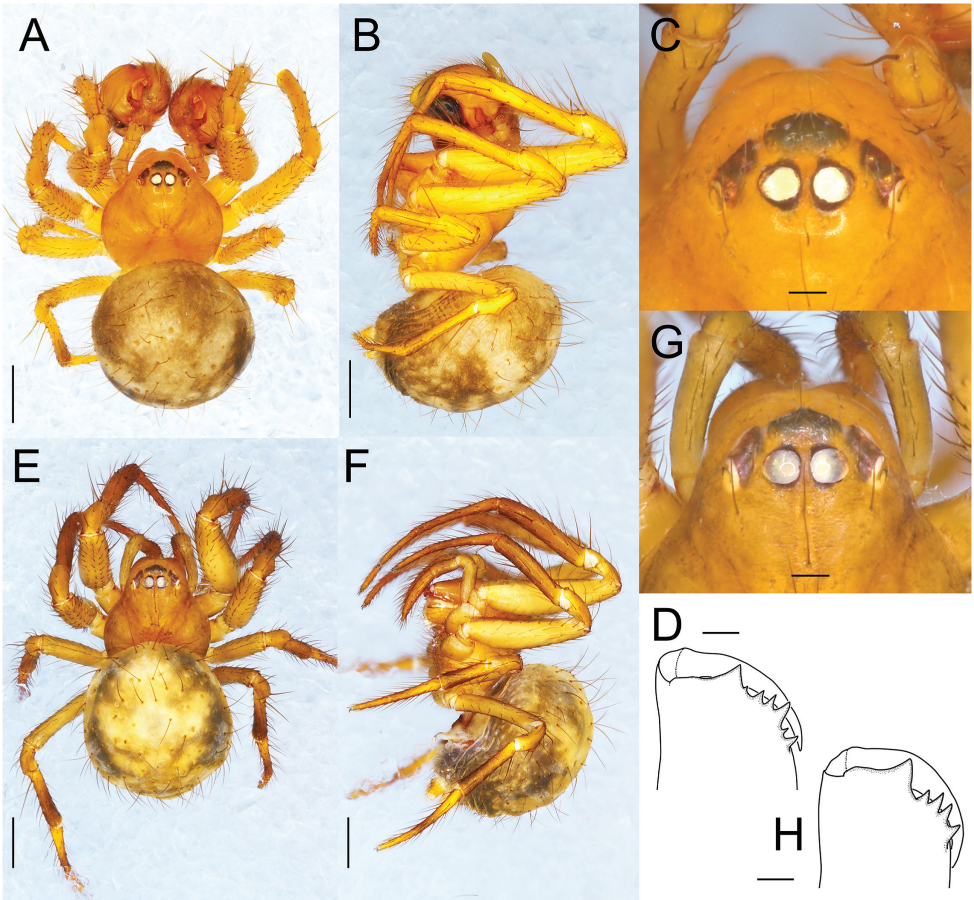

Figure 6. *Sennin tanikawai* sp. nov., male holotype (NSMT-Ar 21722 **A–D**) and female paratype (NSMT-Ar 21723 **E–H**) **A, E** habitus, dorsal view **B, F** habitus, lateral view **C, G** eye region, dorsal view **D, H** chelicera, anterior view. Scale bars: 0.5 mm (**A, B, E, F**); 0.1 mm (**C, G, D, H**).

S. tanikawai sp. nov., whereas it is almost straight in *S. coddingtoni* comb. nov.; the course of copulatory ducts: ducts from both sides juxtaposed at the middle of vulva ventral to spermathecae and continue posteriorly straight toward epigynal scape, then make a right-angle turn and apart laterally (arrows in Figs 8C, 10C), while in *S. coddingtoni* comb. nov. the ducts apart to each other ventrally to the spermatheca and curved laterally (Zhu et al. 2001: fig. 5).

Description. Male (NSMT-Ar 21722). Measurements. Body 2.30 long. Carapace 1.07 long, 1.10 wide, 0.72 high. Eye size and interdistances: AME 0.09, ALE 0.09, PME 0.10, PLE 0.08, AME-AME 0.02, AME-ALE 0.03, PME-PME 0.03, PLE-PLE 0.08, Leg length: leg I 1.62 + 0.53 + 1.30 + 1.08 + 0.50 = 5.03; leg II 1.30 + 0.49 + 1.03 + 0.91 + 0.49 = 4.22; leg III 0.70 + 0.39 + 0.56 + 0.63 + 0.38 = 2.66; leg IV 0.93 + 0.40 + 0.73 + 0.69 + 0.38 = 3.14. Abdomen 1.32 long, 1.44 wide, 1.61 high.

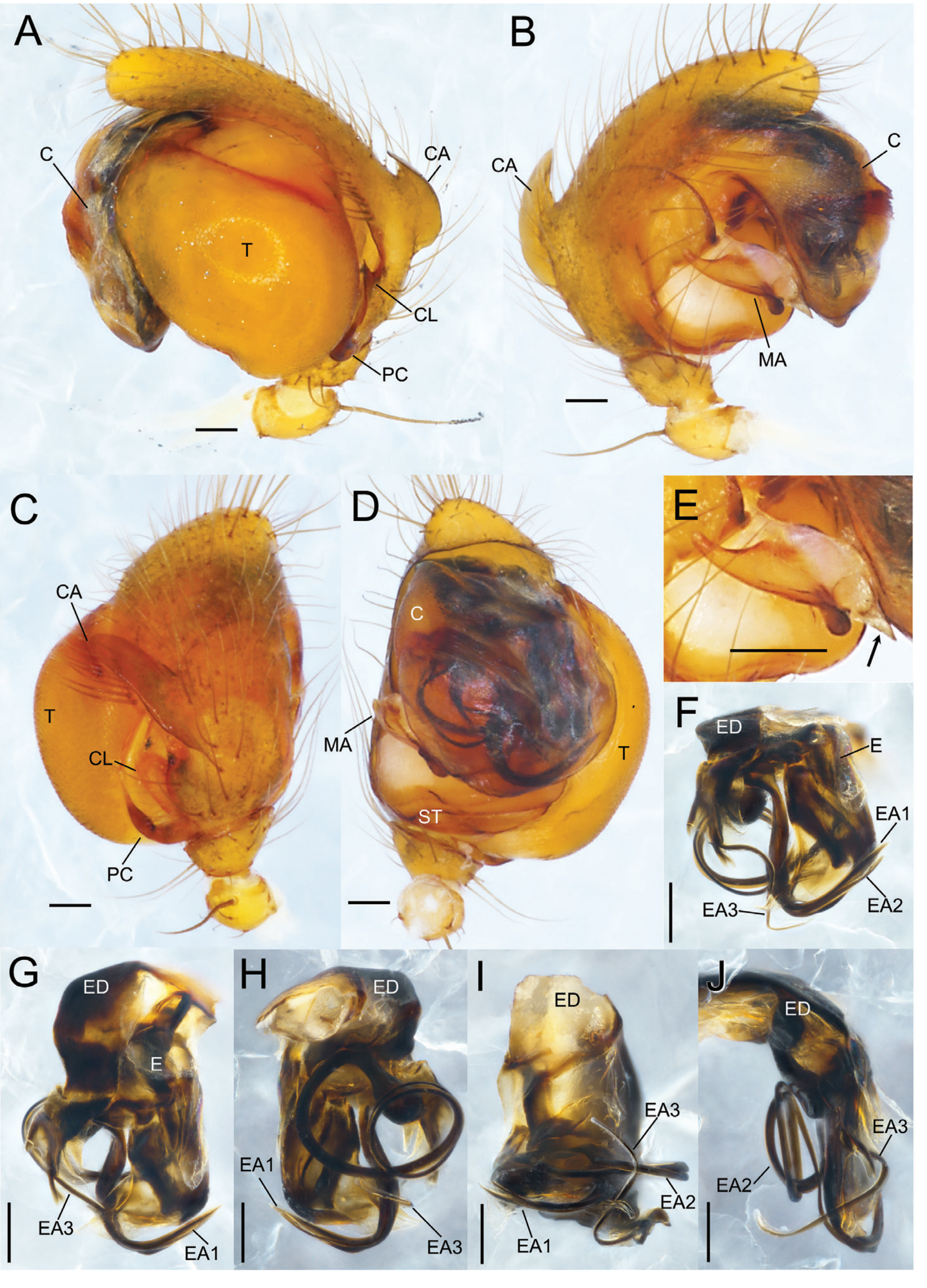

Figure 7. *Sennin tanikawai* sp. nov., male holotype genitalia (NSMT-Ar 21722) **A–D** male palp **F–J** embolic division **A** retrolateral view **B** prolateral view **C** dorsal view **D** ventral view **E** median apophysis, ventral view **F** posterior-ventral view **G** ventral view **H** anterior-dorsal view **I** posterior-dorsal view **J** prolateral view. Abbreviations: **C** conductor **CA** cymbial apophysis **CL** cymbial lamella **E** embolus **EA** embolic apophysis **ED** embolic division **EM** embolus **MA** median apophysis **PC** paracymbium **ST** subtegulum **T** tegulum. Arrow in **E** indicates the tip of less-sclerotized region of median apophysis. Scale bars: 0.1 mm.

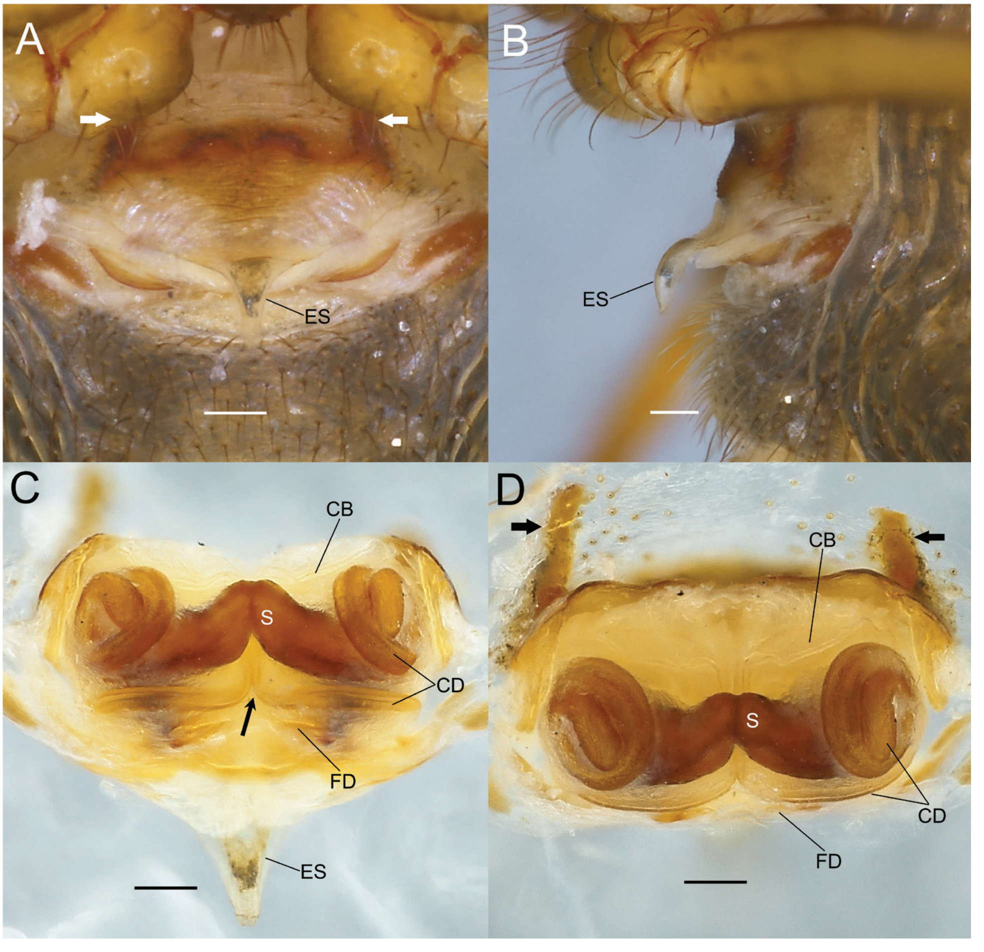

Figure 8. *Sennin tanikawai* sp. nov., female paratype genitalia (NSMT-Ar 21723) **A** epigyne, ventral view **B** epigyne, lateral view **C** vulva, dorsal view **D** vulva, anterior view. Abbreviations: **CB** copulatory bursae **CD** copulatory ducts **ES** epigynal scape **FD** fertilization ducts **S** spermatheca. Arrows in **A, D** indicate a pair of sclerotized extensions on the anterior margin of epigynal plate. Arrow in **C** indicates a pair of copulatory ducts juxtaposed. Scale bars: 0. 1 mm.

Carapace oval, wider than long (CaL/CaW 0.97). Chelicerae with six teeth on promargin with the largest one positioned close to the fang base, no teeth on retromargin (Fig. 6D). Anterior eye row recurved, posterior eye row straight. Cymbial apophysis of palp 0.297 long, 0.111 wide. Macrosetae: leg I: femur r1-p1, patella d1, tibia d2-r1-p1; leg II: femur r1, patella d1, tibia d2-r1; leg III: patella d1, tibia d1; leg IV: patella d1, tibia d1. Abdomen oval, wider than long (AL/AW 0.92). Abdomen covered with long and thin setae.

Coloration and markings (Fig. 6). Carapace, mouthparts, sternum, and legs dark yellowish brown (turning to yellowish brown in ethanol). Eyes on dark bases. Legs lacking annulation. Abdomen pale yellowish grey, dorsum of abdomen with two pairs of sigilla.

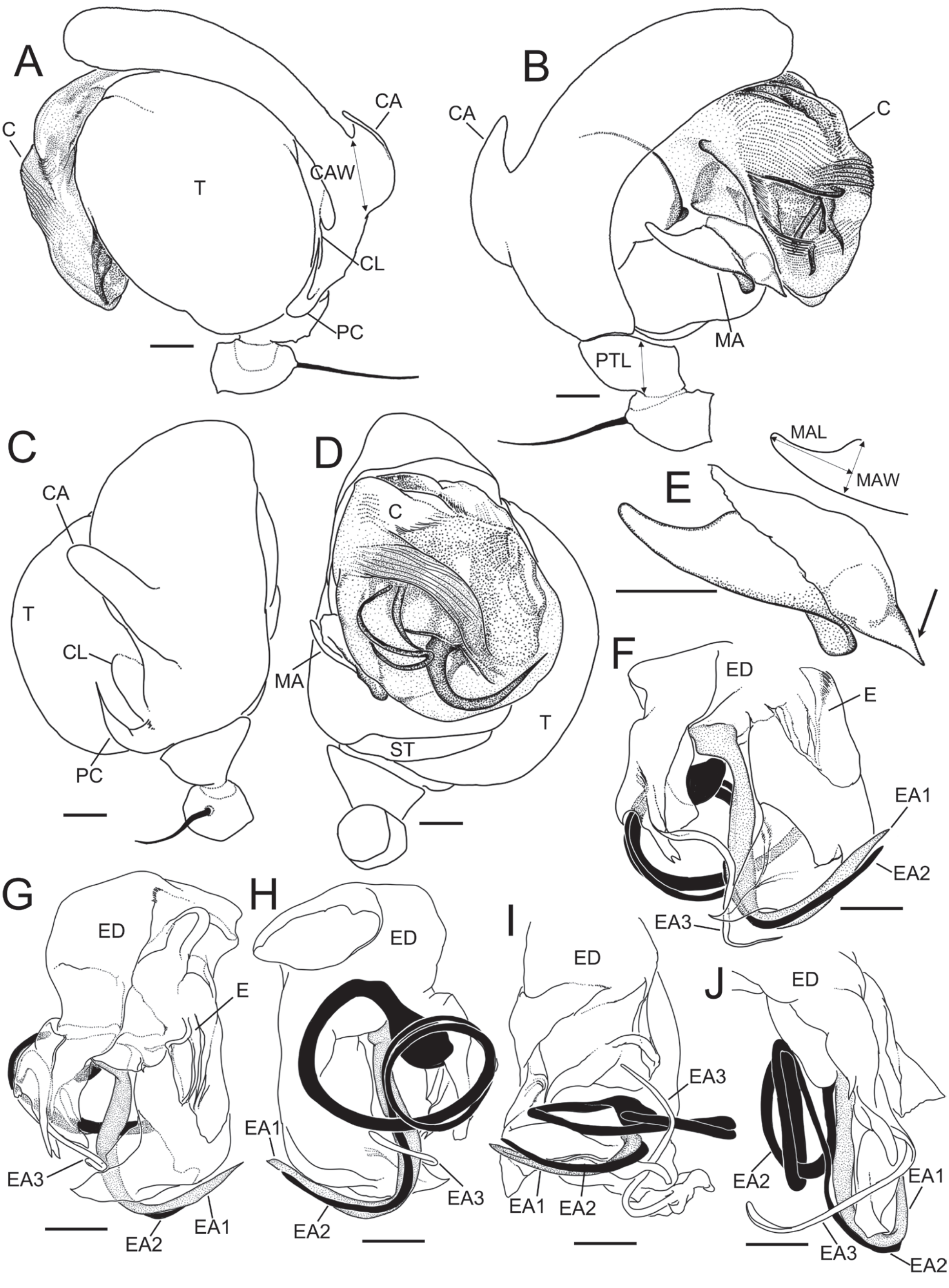

Figure 9. *Sennin tanikawai* sp. nov., male holotype genitalia (NSMT-Ar 21722) **A–D** male palp **F–J** embolic division **A** retrolateral view **B** prolateral view **C** dorsal view **D** ventral view **E** median apophysis, ventral view **F** posterior-ventral view **G** ventral view **H** anterior-dorsal view **I** posterior-dorsal view **J** prolateral view. Abbreviations: **C** conductor **CA** cymbial apophysis **CL** cymbial lamella **E** embolus **EA** embolic apophysis **ED** embolic division **EM** embolus **MA** median apophysis **PC** paracymbium **ST** subtegulum **T** tegulum. Arrow in **E** indicates the tip of less-sclerotized region of median apophysis. Scale bars: 0.1 mm.

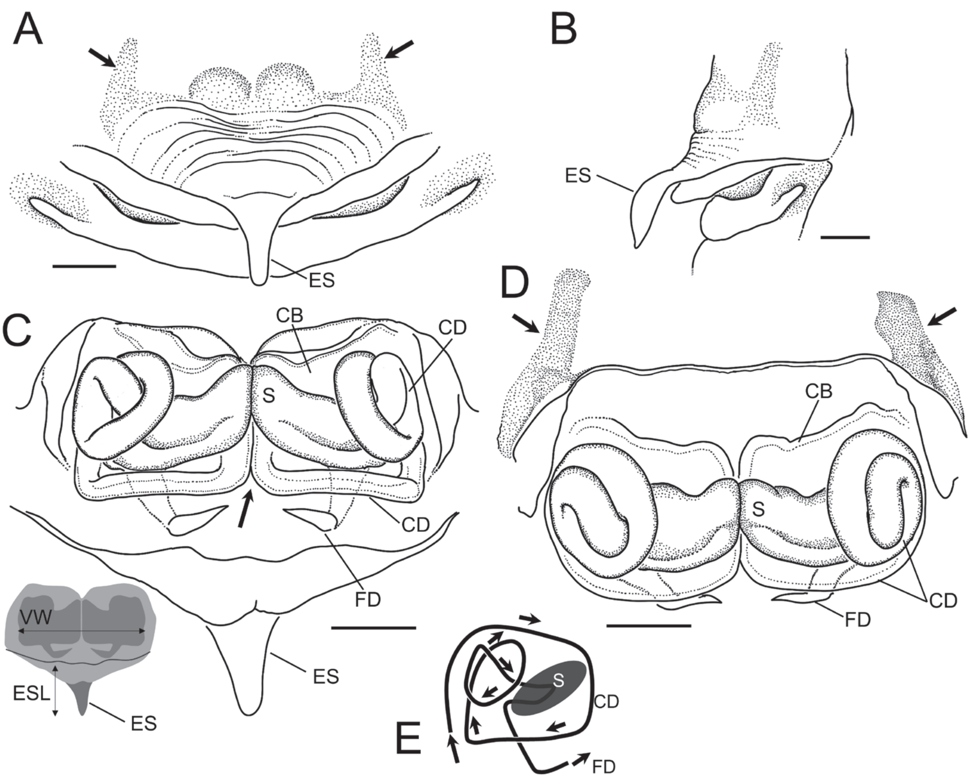

Figure 10. *Sennin tanikawai* sp. nov., female paratype (NSMT-Ar 21723) **A** epigyne, ventral view **B** epigyne, lateral view **C** vulva, dorsal view **D** vulva, anterior view **E** course of copulatory duct. Abbreviations: **CB** copulatory bursae **CD** copulatory ducts **ES** epigynal scape **ESL** epigynal scape length **FD** fertilization ducts **S** spermatheca **VW** vulva width. Arrows in **A, D** indicate a pair of sclerotized extensions on the anterior margin of epigynal plate. Arrow in **C** indicates the pair of copulatory ducts juxtaposed. Scale bars: 0.1 mm.

Palp (Figs 7, 9). Palpal patella with a strong dorsal macroseta. Paracymbium hook-like with a sharp tip. Cymbial lamella robust. Dorsal cymbial apophysis oblong, plate-like with blunt tip, extending anterior-retrolaterally. Tegulum large, bulbous, and occupying a large part of the palpal organ. Embolic division is a complex of long bristle-like apophyses, entirely covered with translucent conductor, and none of the embolic apophyses are exposed. Embolus short, blunt, and covered with a membrane. Three embolic apophyses conspicuous, EA 1 thickest, protruding middle of embolic division, S-shaped and sharper distally; EA 2 longest among them, bristle-like, basal part swelled, forming a loop at the ventro-prolateral side, distal part along with EA 1; EA 3 thinnest, protruding from prolateral side of embolic division. Median apophysis with a deep groove dividing it into two parts, distal translucent, weakly sclerotized and sharper ventrally, basal triangular, strongly sclerotized with narrower dorsally and spatula-like at ventral tip, MAL 1.07, MAW 0.66.

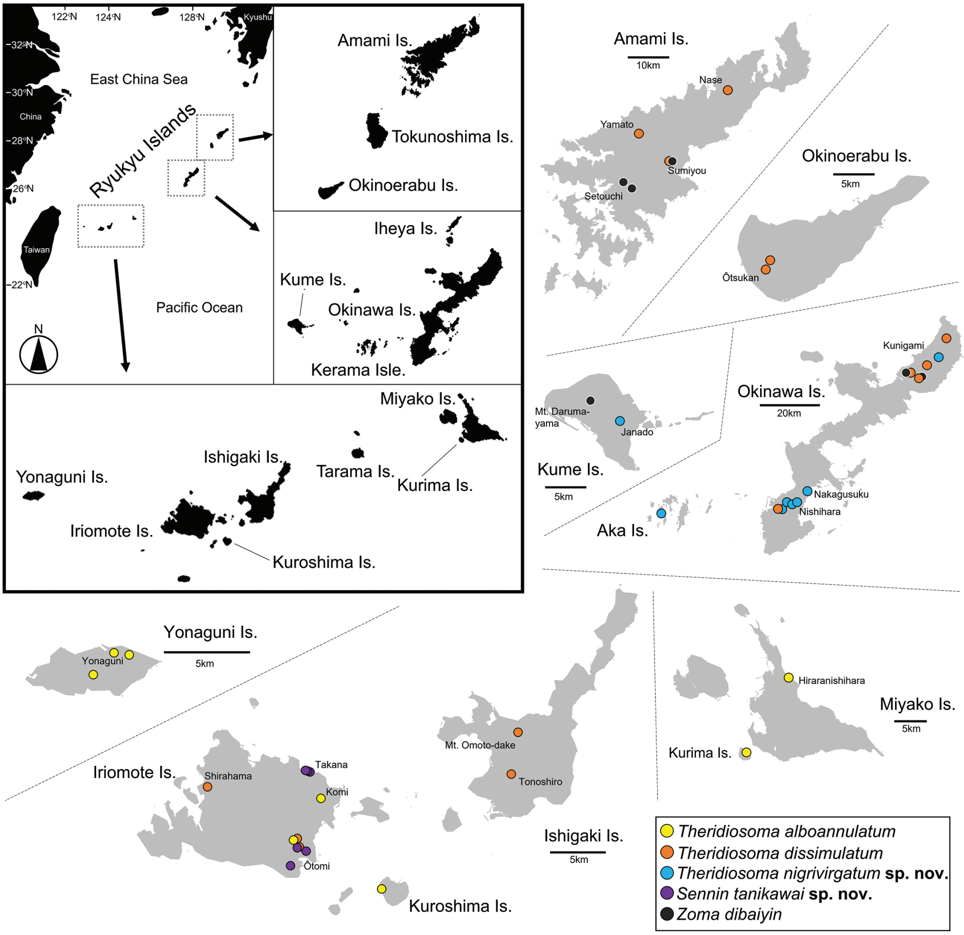

Figure 11. Distribution of theridiosomatid species in the Ryukyu Islands, Japan.

Female (paratype, NSMT-Ar 21723). Measurements. Body 2.37 long. Carapace 1.05 long, 1.06 wide, 0.65 high. Eye size and interdistances: AME 0.10, ALE 0.10, PME 0.12, PLE 0.09, AME-AME 0.02, AME-ALE 0.04, PME-PME 0.03, PLE-PLE 0.08. Leg length: leg I: 1.43 + 0.49 + 1.01 + 0.87 + 0.48 = 4.28; leg II: 1.22 + 0.45 + 0.85 + 0.70 + 0.40 = 3.62; leg III: 0.77 + 0.40 + 0.52 + 0.56 + 0.37 = 2.62; leg IV: 0.90 + 0.36 + 0.71 + 0.59 + 0.38 = 2.94. Abdomen 1.58 long, 1.45 wide, 1.49 high.

Carapace oval, as long as wide (CaL/CaW 0.99). Chelicerae with five teeth on promargin with the largest one positioned close to fang base, no teeth on posterior margin (Fig. 6H). Anterior eye row recurved, posterior eye row straight. Macrosetae: leg I: femur p1, patella d1, tibia d2-r1-p1; leg II: patella d1, tibia d2-r1; leg III: patella d1, tibia d1; leg IV: patella d1, tibia d1. Abdomen as in male (AL/AW 1.09).

Coloration and markings (Fig. 6). As in male.

Genitalia (Figs 8, 10). Epigyne a wide plate with an epigynal scape protruding from the posterior margin, epigynal scape spoon-like, and convex ventrally. Anterior

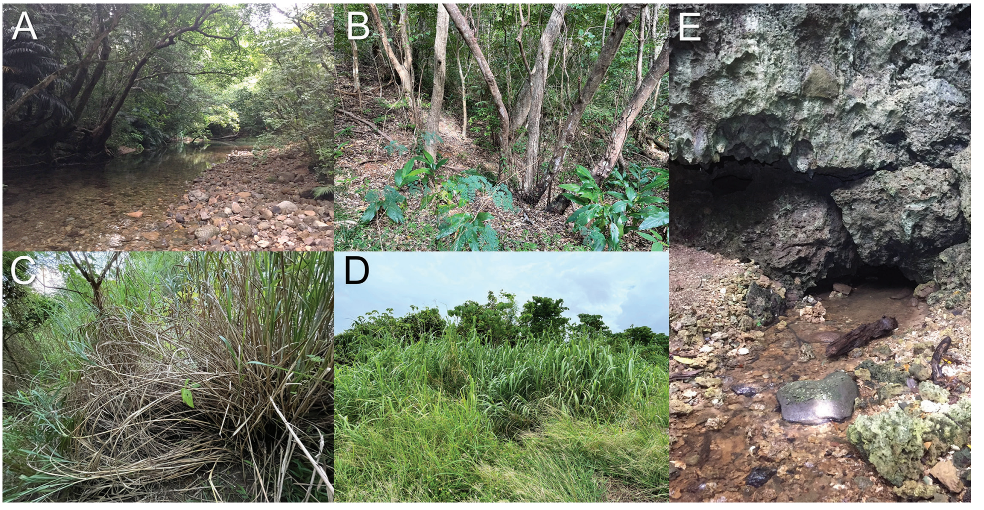

Figure 12. Habitats of theridiosomatid species in Ryukyu Islands **A** streamside in dim forest at Iriomote Island **B** forest floor of secondary forest at Kume Island **C** grassland at Kume Island **D** grassland at Yonaguni Island **E** crevices on limestone rocky wall at Iriomote Island.

margin of epigynal plate with a pair of dark-colored, sclerotized extensions protruding anteriorly from anterolateral side. Vulva. Spermatheca elliptical, longer laterally juxtaposed at the tip. Copulatory bursae developed. Course of copulatory ducts complicated: originating from copulatory bursae at ventral side, touching each other along the mesial line of the vulva, running posterior-dorsally under spermathecae, bend at a right angle toward laterally, curving anterior-dorsally at lateral side of vulva, forming a coil at lateral side of spermathecae, and then connecting to spermathecae. Fertilization ducts running under copulatory ducts and tip dorsally.

Variations. There is a variation in the color of the abdomen: some individuals with dark grey abdomen, while others with pale yellowish grey abdomen. Course of embolic apophyses also varies among individuals: EA 2 tightly coiled with distal part along with EA 1 and EA 3 running below EA 1 in some individuals including the type specimens, while EA 2 loosely coiled with distal part apart from EA 1 and EA 2 running above EA 1.

Remarks. Males and females are considered the same species because no other candidates were sympatric.

Distribution. Japan (Iriomote Island; Fig. 11).

Habitat. The new species inhabits entrance or insides of limestone caves and crevices of limestone rocky walls (Fig. 12E). Spiders are found in high density at the entrance and twilight zones of humid caves, while sparsely deep inside the dark zone. Its general morphology (pigmented body, eight developed eyes, etc.) and habitat suggest that the species is troglophilic rather than obligate troglobite.

Web morphology. The newly reported species built a conventional orb web with an open hub and two hub loops (Fig. 14A–C). The web was almost vertical, and the tension line extended upward obliquely from the upper side of the hub to the surface of

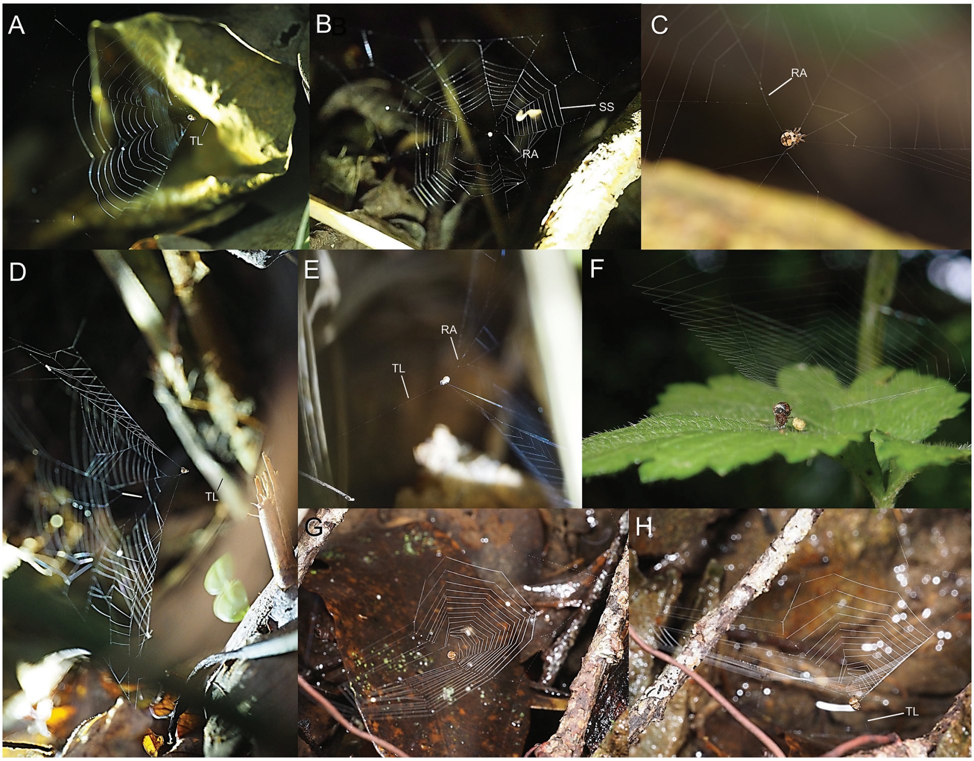

Figure 13. Web of *Theridiosoma* and *Zoma* spiders at Ryukyu Islands, Japan **A–C** web of *Theridiosoma nigrivirgatum* sp. nov. **D–E** web of *Theridiosoma alboannulatum* **F–H** web of *Zoma dibaiyin*. Abbreviations: **RA** radial anastomosis **SS** sticky spirals **TL** tension line.

the rock (Fig. 14D). The angle of the trapline was approximately 60° to the horizontal plane. The spider sat upward and held a trapline by both forelegs and grasped radii by legs III, and put legs IV on the hub (Fig. 14E). The web turned conical shape (Fig. 14D), but it seemed to be less distorted than that of *Theridiosoma* spp. The mean web diameter was 11.6 × 10.1 (cm vertical × horizontal) (n = 9), number of radii: 17 ± 2.3 (SD), and number of sticky spirals: 14.5 ± 2.5 (SD) (n = 8). As a result of observation of 209 webs in June 2021, it was found that some individuals do not make tension lines. The percentage of webs with a tension line was as follows: female adult, 77% and juvenile, 33% in Yutsun-do Cave; female adult, 67% and juvenile, 45% in Ôtomi-Daiichi-Do Cave. Juveniles were more likely to build ordinary webs lacking tension lines than adults at both sites. When a web is disturbed by wind, the spider immediately escapes from the web running along the tension line (n = 22, see Suppl. material 1). After the escape, some spiders try to hide themselves into limestone rock crevices.

Web-building behavior. (n = 5). (1) Frames and radii were laid. (2) The spider returned to the hub and made a temporary spiral as a circle. (3) The spider pulled out a sticky line by using only the outer leg IV several times while touching the temporary spiral by the inner leg IV (in *T. epeiroides* Bösenberg & Strand, 1906, it draws out a

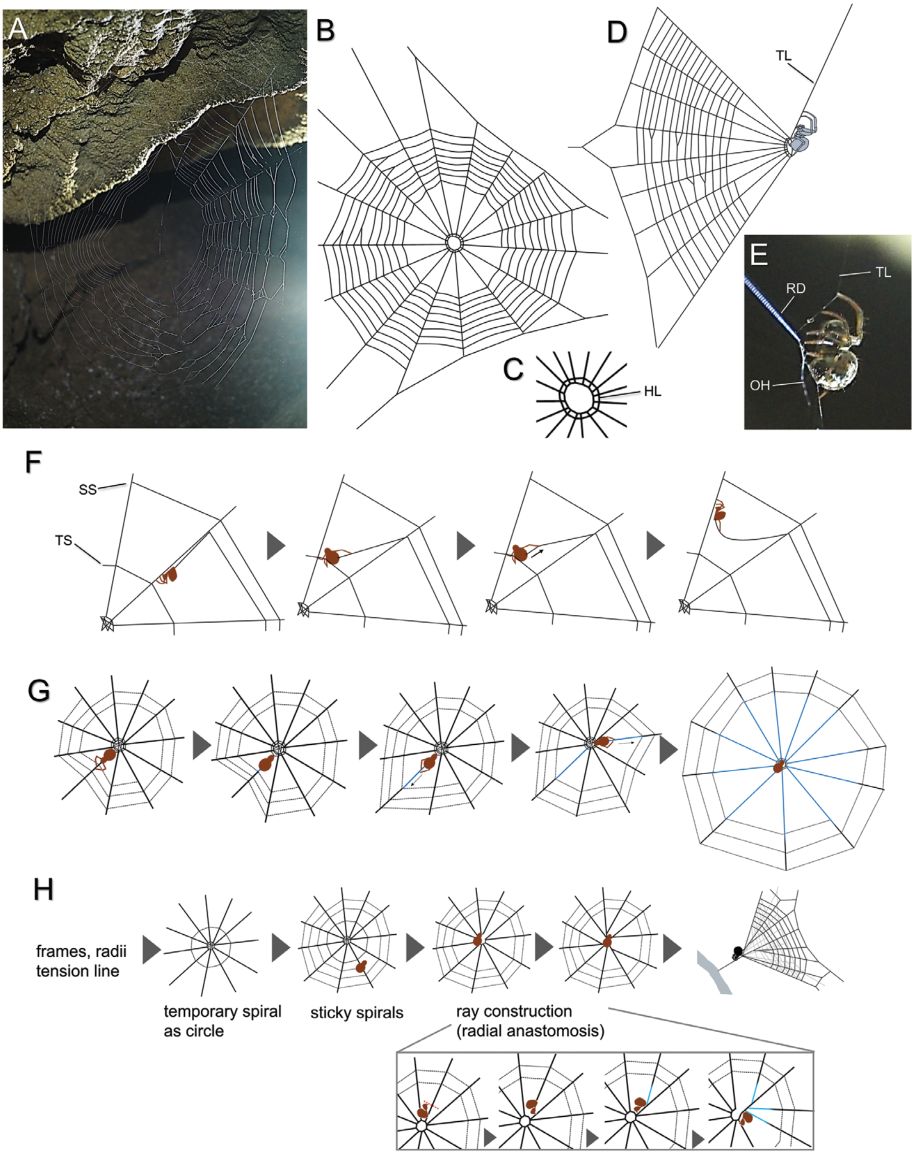

Figure 14. Web structure and building behavior in *Sennin tanikawai* sp. nov. (**A–G**) and *Theridiosoma epeiroides* (**H**) **A** orb web, frontal view **B** orb web, illustrated **C** open hub, frontal view **D** orb web, lateral view **E** spider holding tension line with forelegs **F** process of weaving sticky spirals by *S. tanikawai* sp. nov. **G** radial elongation behavior in *S. tanikawai* sp. nov. **H** web building processes of *Theridiosoma epeiroides*. Blue lines indicate elongated portion of radii. Abbreviations: **HL** hub loops **OH** open hub **RD** radii **SS** sticky spiral **TL** tension line **TS** temporary spiral.

sticky line using both legs IV alternately [Shinkai and Shinkai 1985]). (4) After drawing a sticky line, the spider walked to the frame along a radius holding it by the outer leg IV, shifted it inward, and then attached it to the radius (Fig. 14F; see Suppl. material 2). (5) The spider turned to the hub by drawing a new sticky line by the outer leg IV and moved the next radius along the temporary spiral (Fig. 14F). (6) The spider repeated sequences (3) to (5) and laid sticky spirals from outside to inside. (7) After finishing laying the sticky spirals, the temporary spiral was removed. (8) The spider moved near the hub and bit off the radius. (9) After biting off the radius, it changed the direction and attached its spinnerets to the radius and drew out a radius. The elongated radius was attached to the hub (Suppl. material 3). Thus, all radii were elongated (Fig. 14G). (10) The spider returned to the hub, laid two hub loops, and bit out its center. It ingested the ball of threads using both forelegs and digested it. (11) The spider held a tension line, and the web formed a cone. It took approximately one hour to complete the web.

Egg sac. Spherical and dark brown. The size was approximately 3 × 2 (mm, height × width), which was suspended with a long vertical line on the roof of a cave (Fig. 15D, E). This vertical line (pendant line) ranged from 2.5 to 5.3 cm, and the mean was 4.1 cm (n = 4). There was a single attachment point of the egg sac. The junction of the upper end of the egg sac and the lower end of the pendant line resembled a hatch, similar to a cap like structure in *Theridiosoma*. The lower end of the pendant line was thickened. The egg sac is cleaved at the joint. The egg sac of *K. upperyangtzica* resembles that of *S. tanikawai* sp. nov. but can be distinguished by the shape of 'cap' (thickened end of the pendant line): almost as long as wide in the former while clearly longer than wide in the latter (Chen 2010: fig. 29 vs. Fig. 15E).

Sennin coddingtoni (Zhu, Zhang & Chen, 2001), comb. nov.

Wendilgarda coddingtoni Zhu, Zhang & Chen, 2001: 2, figs 1–7 (holotype female and paratypes from Liangxi Cave, Dongtang Village, Libo Country, Guizhou Prov., China; not examined).
Karstia coddingtoni: Chen 2010: 4, figs 15–28 (transferred from *Wendilgarda*).

Remarks. See diagnosis section in *S. tanikawai* sp. nov.

Distribution. China (Yunnan).

Discussion

Habitat and distribution

Although theridiosomatid species prefer dim and moist habitats, microhabitat preferences seem to differ among species. For example, among the Japanese *Theridiosoma* species, *T. epeiroides* prefers dim forests, while *T. fulvum* Suzuki, Serita & Hiramatsu, 2020 and *T. paludicola* Suzuki, Serita & Hiramatsu, 2020 mainly inhabit open and semi-aquatic environments such as wetlands, riverbeds, and pondside (Suzuki et al.

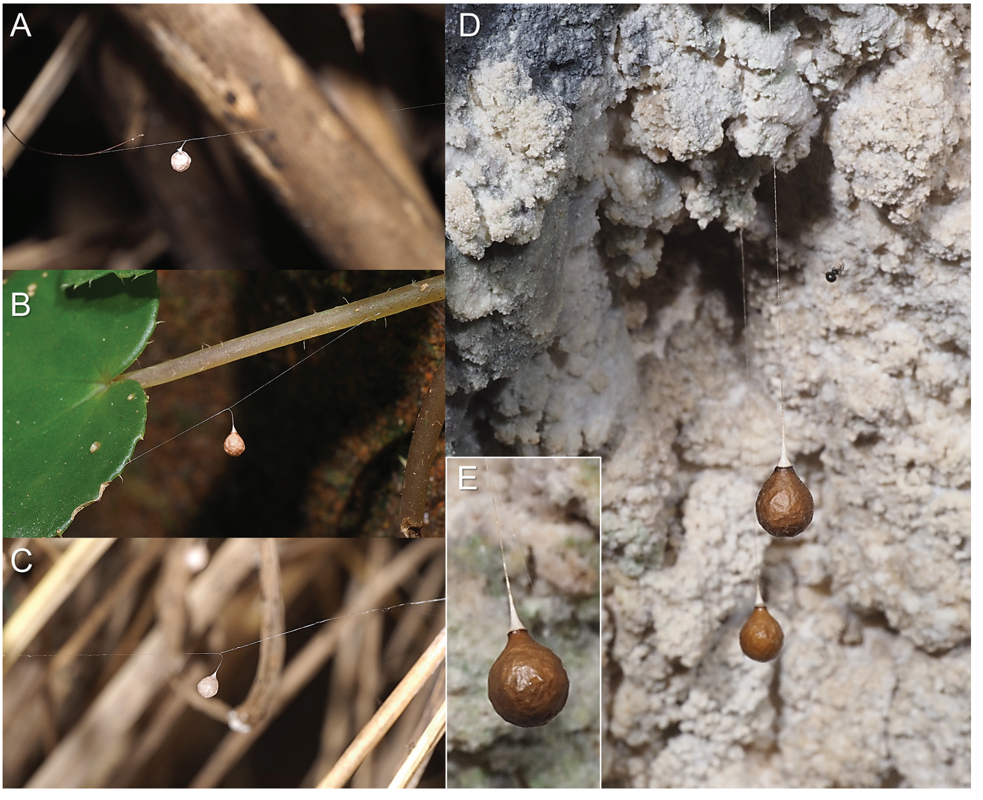

Figure 15. Egg sacs of theridiosomatid species **A** egg sac of *Theridiosoma nigrivirgatum* sp. nov. (cap opened) **B** egg sac of *Theridiosoma dissimulatum* **C** egg sac of *Theridiosoma alboannulatum* **D–E** egg sac of *Sennin tanikawai* sp. nov.

2020). In the Ryukyu Islands, both *T. dissimulatum* and *Z. dibaiyin* are predominantly collected from dim forests, whereas *T. nigrivirgatum* sp. nov. and *T. alboannulatum* were frequently found in open habitats such as grasslands (Fig. 12C, D), where the former two species are rarely found. Our survey revealed that *T. nigrivirgatum* sp. nov. is distributed on the Okinawa Islands, while *T. alboannulatum* is found on Miyako and Yaeyama Islands (Fig. 11), indicating that the distributional boundary of the two species can be found along the Tokara gap.

Sennin tanikawai sp. nov. showed habitat preferences for limestone caves. Although troglophilic theridiosomatid species have never been reported in other regions of Japan, the congener *S. coddingtoni* comb. nov. is also known to inhabit the insides of limestone caves (Zhu et al. 2001; Chen 2010). Troglophilic species are more common in the neotropical and Chinese genera, for example, *Baalzebub* in China and Central America, *Alaria*, *Cuacuba*, *Karstia*, and *Sinoalaria* (Coddington 1986a; Chen 2010; Zhao and Li 2012, 2014; Prete et al. 2018; Prete and Brescovit 2020). Congeners of *Sennin* gen. nov. are expected to be found in the region between southern China and Iriomote Island, especially Taiwan.

Web architecture and construction behavior of *S. tanikawai* sp. nov.

Sennin tanikawai sp. nov. built a conventional orb with an open hub, resembling that of *Meta* (Araneae: Tetragnathidae). However, modification of the hub after the construction of sticky spirals, temporary spirals as circle, and elongation of radii clearly differentiate the new species from ordinary orb weavers (Tetragnathidae and Araneidae). Elongation of radii after spinning spirals is observed among tiny Araneoids of the families Anapidae, Symphytognathidae, and Mysmenidae (Shinkai and Shinkai 1985; Coddington 1986a,b; Eberhard 1987; Shinkai and Hiramatsu 2000), and is also seen in *Theridiosoma epeiroides* during the construction of radial anastomosis (as 'ray', Fig. 14H; also see Shinkai and Shinkai 1985). *Sennin tanikawai* sp. nov. elongates all the radii without anastomosing, and it finally bites the hub as a hole and adds two hub loops (Fig. 14G). A series of radial elongation and hub construction behaviors has never been described in other theridiosomatids. The use of legs during the spinning of sticky spirals also differs between *S. tanikawai* sp. nov. and *T. epeiroides*. *Theridiosoma epeiroides* reels a sticky line out using both forth legs alternately, but *S. tanikawai* sp. nov. pulls out it by only outer leg IV while touching a temporary spiral as circle by inner leg IV (Fig. 14F). The significance of this difference in behavior of both species in web building is uncertain because details of the behavior are largely unknown in other theridiosomatid spiders. *Sennin tanikawai* sp. nov. holds the radius away from its body with one leg IV after attaching a sticky line (Fig. 14F, also see Suppl. material 1). This behavior has also been reported in theridiosomatids (e.g., *Theridiosoma*, *Epeirotypus*, *Ogulnius*), and some anapids (*Anapis*, *Anapisona*) (Eberhard 1981). The function of this behavior is probably to avoid adhering sticky lines to the radius (Eberhard 1981).

Coddington (1986a) revised Theridiosomatidae mainly from neotropical and neosubtropical regions and discussed their natural histories, especially web morphology and web-building behaviors. The webs of *Epeirotypus* and *Naatlo* (Epeirotypinae) are typical orbs with tension lines, lack radial anastomosis, and hubs with two or more persistent hub loops (Table 1; also see Coddington, 1986a: figs 67, 69; Coddington 1986b: fig. 12.7), resembling the web of *S. tanikawai* sp. nov. Unlike *S. tanikawai* sp. nov., *Epeirotypus* species lacks radial elongation (Coddington 1986a). The web of *Baalzebub* also resembles that of *S. tanikawai* sp. nov. in appearance, but the former has a single hub loop without a tension line (Coddington 1986a: figs 165, 167), while the latter has two hub loops with a tension line. *Baalzebub* species adds a single hub loop after spinning sticky spirals, but the process of web building is unknown in detail. In appearance, the web of *S. tanikawai* sp. nov. is closer to those of *Epeirotypus* and *Naatlo* than that of *Baalzebub*. Based on the morphology of genitalia, *S. tanikawai* sp. nov. is closely related to *Baalzebub*. The subfamily Theridiosomatinae, to which *Baalzebub* belongs, is not closely related to Epeirotypinae in the cladistic analysis (Coddington 1986a). Therefore, the similarity in webs of two subfamilies might be the result of convergence. The multiple hub loops may contribute to the reinforcement of the central region of the web to defuse the tension by the 'slingshot' behavior. There are several differences in the webs and related behaviors of *S. tanikawai* sp. nov. and

Epeirotypinae: the upward running of the tension line (downward in Epeirotypinae), upward posture of the spider on the hub (dorsal side up position in Epeirotypinae), quick escape behavior along the tension line (not observed in Epeirotypinae), and a 'halfway' slingshot posture (the web is more strongly distorted in Epeirotypinae). These characteristics suggest that the principal function of the tension line in this species may be to escape from any predator, and the function of prey-capture may be secondary. The main predator of *S. tanikawai* sp. nov. is unknown. Bat (Chiroptera) is one of the major predators inhabiting caves, but they are less likely to forage for this species, as all cave-dwelling bats reported on Iriomote Island forage insects outside caves (Okinawa Prefectural Board of Education 1985). *Plato* is confirmed to have no tension line (Coddington 1986a; Eberhard 2020), while the presence or absence of tension lines has not been examined in most cave-dwelling theridiosomatids: *Cuacuba*, *Karstia*, and *Sinoalaria* (Chen 2010; Zhao and Li 2014; Prete et al. 2018). If these cave-living theridiosomatids also lack a tension line, it would be interesting to know whether or how they perform escape behavior.

Table 1. Comparison of habitat and web morphology of theridiosomatid genera of which web morphology were described in published papers. Data source: [a] Coddington (1986a), [b] Eberhard (1986), [c] Eberhard (2020), [d] Chen (2010), [e] Shinkai and Shinkai (1985), [f] Hiramatsu (2021). + = present; -= absent, ? = unknown.

Subfamily	Genus	Habitat	Orb web	Web shape	Web angle	Tension line	Angle of tension line	Radial anasto-mosis	Open hub	Hub loops
Platoninae	*Chthonos*[a]	leaf litter[1]	-	no web	-	-	-	-	-	-
	Plato[a]	caves, dark places	+	loose orb web	vertical or diagonal	-	?	+	-	-
Epeiroty-pinae	*Epeirotypus*[a, b, c]	shrubs, shaded wet forest	+	concave orb web	vertical or diagonal	+	almost horizontal or downward	-	+	2–5
	Naatlo[a]	humid shaded forest	+	concave orb web	vertical or diagonal	+	?	-	+	2
Ogulniinae	*Ogulnius*[a, b]	wet, shaded forest	-	sparse network	-	-	-	-	-	-
Theridio-somatinae	*Baalzebub*[a]	interior of hollow logs, under fallen tree, caves	+	ordinary orb web	vertical or diagonal	-	-	-	+	1
	Epilineutes[a]	over stream water	+	conventional orb web	vertical or diagonal	+ (rare)	?	+	-	-
	Karstia[d]	limestone caves	+	?	vertical?	?	?	?	?	?
	Sennin gen. nov.	limestone caves	+	conventional orb web	vertical or diagonal	+	almost upward, sometimes horizontal	-	+	2
	Theridiosoma[a, c, e]	wet, shaded forest, etc.	+	concave orb	vertical or diagonal	+	almost horizontal or downward	+	-	-
	Wendilgarda[c]	over stream water or ponds	-	Naruko web	-	-	-	-	-	-
	Zoma[f]	wet, shaded forest	+	concave orb	horizontal	+	vertical to the ground	+	-	-

As the tension line is sporadic throughout theridiosomatids (Coddington 1986a), the origin and function of the tension line can vary (for example, Eberhard 2020: fig. 9.4.(d)(e)). Further morphological and molecular analyses of theridiosomatids, including *Sennin* gen. nov. species, are expected to elucidate the evolutionary process of the tension line.

Acknowledgements

We wish to express our heartfelt thanks to Akio Tanikawa, Nobuo Tsurusaki, Tatsumi Suguro, and Ryohei Serita for offering invaluable specimens; Kyushu Regional Forest Office, Okinawa Forest Management Office (Okinawa, Japan) and World Heritage Site Promotion Office, Taketomi Town (Okinawa, Japan) for permitting our survey in national forests; Paulo Pantoja and Lara Lopardo for their helpful comments and suggestions on earlier versions of this manuscript; Tadashi Miyashita for his insightful comments on the discussion section; Ethan Yeoman for providing information on the morphology of *Baalzebub* species; Ren-Chung Cheng and Wen-Chun Huang for offering information about theridiosomatid spiders in Taiwan, and Ken-ichi Okumura for his support on deposition of the type specimens to NSMT. We would like to thank Motoaki Iwata, Kotaro Okazaki, Azumi Kudaka, Nobuyuki Nakama, Kohei Yoshida, Tomohiro Suzuki, Mitsuho Kato, Akitoshi Takano, and Koichiro Tonomura for their support in the field survey. Part of this research was supported by the Sasakawa Research Foundation (ID: 2021-5010).

References

Alexander SLM, Bhamla MS (2020) Ultrafast launch of slingshot spiders using conical silk webs. Current Biology 30(16): PR928–R929. https://doi.org/10.1016/j.cub.2020.06.076

Ballarin F, Yamasaki T, Su YC (2021) A survey on poorly known rainforest litter-dwelling spiders of Orchid Island (Lanyu, Taiwan) with the description of a new species (Araneae: Linyphiidae, Tetrablemmidae, and Theridiosomatidae). Zootaxa 4927(2): 197–208. https://doi.org/10.11646/zootaxa.4927.2.2

Chen HM (2010) *Karstia*, a new genus of troglophilous theridiosomatid (Araneae, Theridiosomatidae) from southwestern China. Guizhou Science 28(4): 1–10.

Coddington JA (1986a) The genera of the spider family Theridiosomatidae. Smithsonian Contributions to Zoology 422(422): 1–96. https://doi.org/10.5479/si.00810282.422

Coddington JA (1986b) The monophyletic origin of the orb web. In: Shear WA (Ed.) Spiders. Webs, behavior, and evolution. Stanford University Press, Stanford, CA, USA, 319–336.

Dou LA, Lin YC (2012) Description of *Karstia cordata* sp. nov. (Araneae, Theridiosomatidae) from caves in Chongqing, China. Dong Wu Fen Lei Xue Bao 37: 734–739.

Eberhard WG (1981) Construction behavior and the distribution of tension in orb webs. Bulletin - British Arachnological Society 5: 189–204.

Eberhard WG (1986) Ontogenetic changes in the web of *Epeirotypus* sp. (Araneae, Theridiosomatidae). The Journal of Arachnology 14: 125–128.

Eberhard WG (1987) Web-building behavior of anapids, symphytognathids, and mysmenid spiders (Araneae). The Journal of Arachnology 14: 339–356.

Eberhard WG (2020) Spider Webs: Behavior, Function, and Evolution. The University of Chicago Press, Chicago, USA, 658 pp. https://doi.org/10.7208/chicago/9780226534749.001.0001

Hiramatsu T (2021) Kishidaia 118: 14–23. [Note on the natural history of *Zoma dibaiyin* (Araneae: Theridiosomatidae)] [In Japanese]

Labarque FM, Griswold CE (2014) New ray spiders from Southeast Asia: the new Philippine genus *Tagalogonia* gen. nov. and continental genus *Coddingtonia* Miller, Griswold and Yin, 2009 (Araneae: Theridiosomatidae), with comments on their intergeneric relationships. In: Williams GC, Gosliner TM (Eds) The Coral Triangle: The 2011 Hearst Philippine Biodiversity Expedition. California Academy of Sciences, San Francisco, 407–425.

Miller JA, Griswold CE, Yin CM (2009) The symphytognathoid spiders of the Gaoligongshan, Yunnan, China (Araneae, Araneoidea): Systematics and diversity of micro-orbweavers. ZooKeys 11: 9–195. https://doi.org/10.3897/zookeys.11.160

Okinawa Prefectural Board of Education (1985) [Emergency survey reports on national treasure in Iriomote Island III: Animals]. Okinawa Prefectural Board of Education, Naha, 88 pp. [In Japanese]

Ono H, Ogata K (2018) Spiders of Japan: their natural history and diversity. Tokai University Press, Kanagawa, 713 pp. [In Japanese with English title]

Ota H (1998) Geographic patterns of endemism and speciation in amphibians and reptiles of the Ryukyu Archipelago, Japan, with special reference to their paleogeographical implications. Researches on Population Ecology 40(2): 189–204. https://doi.org/10.1007/BF02763404

Ota H (2000) The Current geographic faunal pattern of reptiles and amphibians of the Ryukyu Archipelago and adjacent regions. Tropics 10(1): 51–62. https://doi.org/10.3759/tropics.10.51

Prete PH, Brescovit AD (2020) A new species of *Cuacuba* (Araneae, Theridiosomatidae) from Brazilian caves. Studies on Neotropical Fauna and Environment 55(2): 109–115. https://doi.org/10.1080/01650521.2019.1704386

Prete PH, Cizauskas I, Brescovit AD (2016) A new species of the spider genus *Baalzebub* (Araneae, Theridiosomatidae) from Brazilian caves. Studies on Neotropical Fauna and Environment 51(2): 97–103. https://doi.org/10.1080/01650521.2016.1183965

Prete PH, Cizauskas I, Brescovit AD (2018) Three new species of the spider genus *Plato* and the new genus *Cuacuba* from caves of the states Pará and Minas Gerais, Brazil (Araneae, Theridiosomatidae). ZooKeys 753: 107–162. https://doi.org/10.3897/zookeys.753.20805

Saaristo MI (1996) Theridiosomatid spiders of the granitic islands of Seychelles (Araneae, Theridiosomatidae). Phelsuma 4: 48–52.

Shimojana M (1977) Preliminary report on the cave spider fauna of the Ryukyu Archipelago. Acta Arachnologica 27(Specialnumber): 337–365. https://doi.org/10.2476/asjaa.27.Specialnumber_337

Shinkai A, Hiramatsu T (2000). Kishidaia 79: 13–19. [Observations of spiders in Iriomote Island (I)] [In Japanese]

Shinkai A, Shinkai E (1985) The web-building behavior and predatory behavior of *Theridiosoma epeiroides* Bösenberg et Strand (Araneae, Theridiosomatidae) and the origin of the ray-formed web. Acta Arachnologica 42(1): 181–185. https://doi.org/10.2476/asjaa.33.9 [In Japanese with English synopsis]

Suzuki Y (2019) A new species of the genus *Wendilgarda* (Araneae: Theridiosomatidae) from Japan. Acta Arachnologica 68(2): 59–62. https://doi.org/10.2476/asjaa.68.59

Suzuki Y, Matsushima R (2021). Kishidaia 118: 33–37. [Find this spider No. 08. *Wendilgarda ruficeps*] [In Japanese]

Suzuki Y, Serita R (2021). Kishidaia 118: 230–236. [Spiders collected on Okinawa Island] [In Japanese]

Suzuki Y, Serita R, Hiramatsu T (2020) Japanese spiders of the genus *Theridiosoma* (Araneae: Theridiosomatidae) with the description of four new species. Acta Arachnologica 69(2): 133–150. https://doi.org/10.2476/asjaa.69.133

World Spider Catalog (2022) World Spider Catalog. Version 23.0. Natural History Museum Bern. https://doi.org/10.24436/2 [accessed on 29 April 2022]

Wunderlich J (1976) Spinnen aus Australien. 1. Uloboridae, Theridiosomatidae und Symphytognathidae (Arachnida: Araneida). Senckenbergiana Biologica 57: 113–124.

Wunderlich J (1980) Sternal-organe der Theridiosomatidae-eine bisher übersehene Autapomorphie (Arachnida: Araneae). Verhandlungen Naturwissenschaftlichen Vereins, Hamburg 23: 255–257.

Wunderlich J (2011) Extant and fossil spiders (Araneae). Beiträge zur Araneologie 6: 1–640.

Zhang ZS, Wang LY (2017) Chinese spiders illustrated. Chongqing University Press, China, 954 pp.

Zhang JX, Zhu MS, Tso IM (2006) First record of the family Theridiosomatidae from Taiwan, with description of a new species (Arachnida: Araneae). Bulletin - British Arachnological Society 13: 265–266.

Zhao QY, Li SQ (2012) Eleven new species of theridiosomatid spiders from southern China (Araneae, Theridiosomatidae). ZooKeys 255: 1–48. https://doi.org/10.3897/zookeys.255.3272

Zhao QY, Li SQ (2014) *Sinoalaria*, a name to replace *Alaria* (Araneae, Theridiosomatidae). Acta Arachnologica Sinica 23: e41. https://doi.org/10.3969/j.issn.1005-9628.2014.01.009

Zhu MS, Zhang JX, Chen HM (2001) A new species of the genus *Wendilgarda* from China (Araneae: Theridiosomatidae). Acta Zoologica Taiwanica 12: 1–7.

Supplementary material 1

Video S1

Authors: Yuya Suzuki, Takehisa Hiramatsu, Haruki Tatsuta

Data type: Video (mp4. file).

Explanation note: *Sennin tanikawai* sp. nov. escaping from the web via a tension line.

Link: https://doi.org/10.3897/zookeys.1109.83807.suppl1

Supplementary material 2

Video S2

Authors: Yuya Suzuki, Takehisa Hiramatsu, Haruki Tatsuta

Data type: Video (mp4. file).

Explanation note: SS weaving behavior in *Sennin tanikawai* sp. nov.

Link: https://doi.org/10.3897/zookeys.1109.83807.suppl2

Supplementary material 3

Video S3

Authors: Yuya Suzuki, Takehisa Hiramatsu, Haruki Tatsuta

Data type: Video (mp4. file).

Explanation note: Radial elongation behavior in *Sennin tanikawai* sp. nov.

Link: https://doi.org/10.3897/zookeys.1109.83807.suppl3

ZooKeys 1109: 103–114 (2022)
doi: 10.3897/zookeys.1109.81544
https://zookeys.pensoft.net

RESEARCH ARTICLE

A peer-reviewed open-access journal
ZooKeys
Launched to accelerate biodiversity research

The complete mitochondrial genome of *Meloe proscarabaeus* (Coleoptera, Meloidae): genome descriptions and phylogenetic inferences

Song Chen[1], Changhua Liu[1], Yuanmin Hao[1], Yueyue Liu[2], Xu Liu[1], Chao Du[3]

1 *Key Laboratory of Integrated Crop Pest Management in Southwest China (Ministry of Agriculture), Institute of Plant Protection, Sichuan Academy of Agricultural Sciences, Chengdu, China* **2** *Institute of Quality Standard and Testing Technology Research, Sichuan Academy of Agricultural Sciences, Chengdu, China* **3** *Baotou Teachers College, Baotou, China*

Corresponding authors: Xu Liu (liuxu6186@126.com), Chao Du (ductub@163.com)

Academic editor: Warren Steiner | Received 1 February 2022 | Accepted 13 June 2022 | Published 1 July 2022

https://zoobank.org/FA25FBFF-F670-47F2-88A4-CB84D8277F75

Citation: Chen S, Liu C, Hao Y, Liu Y, Liu X, Du C (2022) The complete mitochondrial genome of *Meloe proscarabaeus* (Coleoptera, Meloidae): genome descriptions and phylogenetic inferences. ZooKeys 1109: 103–114. https://doi.org/10.3897/zookeys.1109.81544

Abstract

Oil beetles are meloids, which are characterised for their cleptoparasitic habits in bee nests and oily fluid of cantharidin that causes blistering and swelling of the skin. The complete mitochondrial genome of *Meloe proscarabaeus* is determined using the next-generation sequencing technology and its genomic characteristics are described. The 15,653-bp long genome is a circular molecule consisting of 13 protein-coding genes (PCG), 22 transport RNA, two ribosomal RNA, and a control region. The A + T bias of the mitochondrial genome is manifested in the complete sequence and the codon usage of protein-coding genes. The genetic distance within and between genera is calculated to confirm the taxonomic status of *M. proscarabaeus*. The phylogenetic relationships among 15 available meloid taxa are inferred by the maximum likelihood (ML) method based on 13 mitochondrial PCGs. The ML trees resulting from nucleotide and amino acid datasets recover both the monophyly of *Meloe* and *Epicauta* and the polyphyly comprising *Hycleus* and *Mylabris*. This study provides the first description of a mitochondrial genome belonging to the genus *Meloe*. The mitochondrial genome sequence and its characteristics are expected to be conducive to future studies on taxonomy, systematics, and molecular phylogenetics of the family Meloidae.

Keywords

Genome feature, meloid, mitogenome, oil beetle, phylogenetic relationship

Introduction

The oil beetle *Meloe proscarabaeus* Linnaeus, 1758 is a characteristic species of the meloid genus *Meloe* Linnaeus, 1758, which comprises about 155 species in 16 subgenera and is mainly distributed in the Holarctic region (Sánchez-Vialas et al. 2021; Pan and Bologna 2021). Oil beetles are well known for the oily fluid of hemolymph released from their leg joints, which contains the poison cantharidin that causes blistering and swelling of the skin (Muzzi et al. 2020; Du et al. 2021). Additionally, oil beetles are distinguished by their hypermetamorphic development and cleptoparasitic habits in bee nests (Saul-Gershenz and Millar 2006; Saul-Gershenz et al. 2018).

The taxonomy and phylogeny of the genus *Meloe* are based on morphological characteristics and molecular data (Di Giulio et al. 2002, 2014; Muzzi et al. 2020; Pan and Bologna 2021; Sánchez-Vialas et al. 2021). The genus is considered monophyletic, but more detailed molecular phylogenetic studies are necessary to solve the phylogenetic relationships within the genus. With the simple genetic structure, the high rate of evolution, and the advantage in acquiring methods, the mitochondrial genome has been used widely in many phylogenetic studies of animals (Avise 1994; Cameron 2014; Du et al. 2020). There are 15 meloid species in five genera that have had their complete mitochondrial genomes published in the GenBank database. Previous studies have utilised mitochondrial genome sequences to infer the phylogeny of Meloidae, but without data on the genus *Meloe* due to the absence of mitochondrial genomes for the genus (Du et al. 2017; Liu et al. 2020).

In this study, we determine the complete mitochondrial genome of *M. proscarabaeus* using next-generation sequencing, and we describe its genomic characteristics. Furthermore, we reconstruct the phylogenetic trees based on the nucleotide and amino acid sequences from all available mitochondrial genomes to analyse the phylogenetic relationships among the family Meloidae. The sequence and phylogenetic inferences of *M. proscarabaeus* mitochondrial genome will be a significant increase in furthering the study on coleopteran mitochondrial genome architecture and phylogenetics.

Materials and methods

Sample and genomic DNA extraction

The adults of *Meloe proscarabaeus* were collected from a hill slope in Dongsheng, Inner Mongolia, China (39°45.33'N, 110°01.83'E). The fresh samples were immediately preserved in 100% ethanol and stored in a –20 °C refrigerator. We identified the specimens according to the morphological characters that descried by Pan and Bologna (2021). Total genomic DNA was extracted from a frozen adult using Tianamp Genomic DNA kit following the manufacturer's protocol. The quality of DNA was determined using 1% agarose gel electrophoresis.

Next-generation sequencing and genomic assembly

The library was constructed using an Illumina TruSeq Library Preparation kit with an insert size of 250 bp and sequenced using the paired-end strategy on an Illumina HiSeq 2500 platform. A total of 4.4 Gb raw data was yielded with an average read length of 150 bp. The raw data were trimmed and filtered using fastp with parameters of phred quality ≥ 30 and unqualified percent < 20 to remove adapters and low-quality reads (Chen et al. 2018). Then the clean data were used to assemble the mitochondrial genome of *M. proscarabaeus* by MITObim v. 1.9.1 with the default settings (Hahn et al. 2013). The mitochondrial genome of *Lytta caraganae* (GenBank accession number NC_033339.1; Du et al. 2017) was employed as a reference sequence. The assembled sequence was aligned with other meloid mitochondrial genomes described by Du et al. (2017) to ensure the assembling quality.

Gene annotation and sequence analysis

The complete mitochondrial genome of *M. proscarabaeus* was automatically annotated by the software MitoZ (Meng et al. 2019) and manually compared with other meloid mitochondrial genomes. Of these, PCGs were checked by the identification of open reading frames and aligning with mitochondrial PCGs of other meloids. The annotated mitochondrial genome was analysed its genome characteristics, including nucleotide composition, the composition of skewness, codon usages, and relative synonymous codon usage (RSCU), using MEGA6 (Tamura et al. 2013). All available mitochondrial genomes of 15 meloid species were used to calculate the genetic distances within and between genera in Meloidae. *P*-distances were calculated using MEGA6 with the bootstrap method of 1,000 replications for the variance estimation.

Phylogenetic analysis

To infer the phylogenetic relationships among the family Meloidae, all available mitochondrial genomes of 15 meloid species, including the *M. proscarabaeus*, were employed to reconstruct the maximum-likelihood (ML) trees with the *Tribolium castaneum* (GenBank accession number NC_003081.2; Friedrich and Muqim 2003) as the outgroup. According to GenBank annotations, the nucleotide and amino acid sequences of 13 mitochondrial PCGs from each species were extracted and stop codons removed. Orderly combined sequences were aligned using MAFFT with the default settings (Katoh and Standley 2013) and the gaps and ambiguous sites removed to concatenate into consensus sequences including a 10,934 bp nucleotide and a 3,633 amino acid dataset, respectively. IQ-Tree was employed to estimate the best-fit models of partitioning schemes (Nguyen et al. 2015). The nucleotide and the corresponding amino acid datasets were partitioned for 13 genes individually. The best-fitting models of partitioning schemes were selected with the greedy search algorithm, under the Bayesian information criterion. The ML trees of both datasets were also reconstructed using IQ-Tree with 1000 bootstraps to assess the node support.

Results

Genome structure and composition

The 5.4 Gb raw data was yielded by the next-generation sequencing with 36,048,728 reads, and the 4.9 Gb (95.06%) clean data was obtained after filtering. The complete mitochondrial genome of *M. proscarabaeus* was assembled using 1,160,002 reads, and the average depth of coverage was assessed at 7,635.95 X. The mitochondrial genome was annotated and then submitted to the GenBank under the accession number OL840851. The complete mitochondrial genome of *M. proscarabaeus is* 15,653 bp in length, which is of moderate length among mitochondrial genomes within Meloidae (Du et al. 2016, 2017; Zhou et al. 2021).

The complete mitochondrial genome of *M. proscarabaeus* is a circular DNA molecule consisting of 13 protein-coding genes, 22 transport RNAs, two ribosomal RNAs, and a control region (Fig. 1). The length of *rrnL* and *rrnS* were determined to be 1,329 bp and 816 bp, respectively, and the control region was 1,013 bp in length. The nucleotide base composition of the mitochondrial genome was 37.5% A, 31.6% T, 19.1% C, and 11.9% G. The total A + T content was 69.1%, and the AT skew was 0.0854.

Protein-coding gene and codon usage

The total length of the 13 mitochondrial protein-coding genes in *M. proscarabaeus* is 11,127 bp, accounting for 71.10% of the total length of the genome, encoding 3,711 codons in total. All 13 protein-coding genes start using regular initiation codons, including ATT and ATG, and ATA (Table 1), which were commonly used as start codons in insect mitochondrial genomes. Most protein-coding genes terminated with conventional stop codons (such as TAA or TAG), except *cox3*, *nad5*, and *nad4* stopped with T (Table 1).

The A + T bias is also manifested in the codon usage of protein-coding genes (Fig. 2). Relatively synonymous codon usages, excluding stop codons, showed that the third position of synonymous codons always has more frequency with A or T than G or C. Additionally, the first three frequently used codons UUA (Leu2), UCU (Ser2), GUU (Val), and some other frequently used codons, including AUU (Ile), UUU (Phe) AAU (Asn), etc. are comprised of two or three A and/or T nucleotides.

RNAs and control regions

All 22 transfer RNAs were annotated in the mitochondrial genome of *M. proscarabaeus*. Their length ranged from the shortest *trnS* with 59 bp to the longest *trnK* with 71 bp (Table 1). The maldistribution of transfer RNAs was also found in the mitochondrial genome. For example, there are two clusters comprising six transfer RNAs (*trnA-trnR-trnN-trnS-trnE-trnF*) between *nad3* and *nad5*

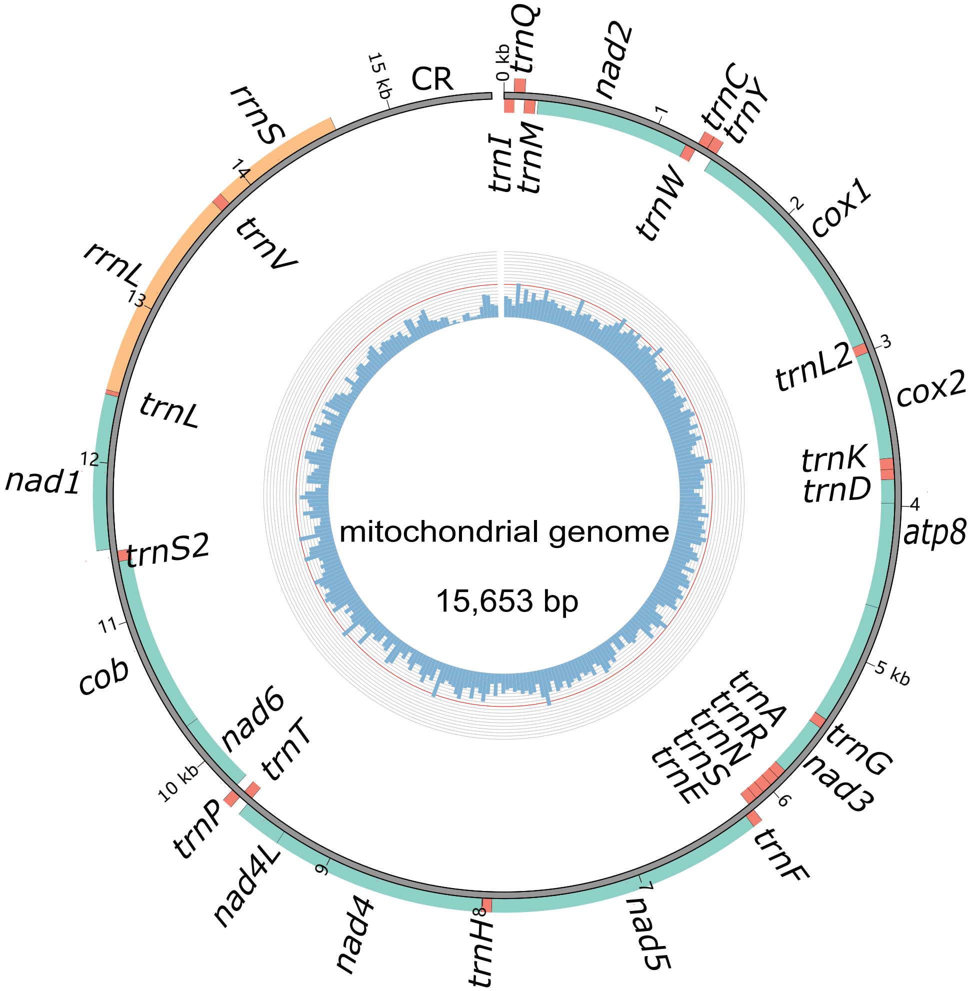

Figure 1. The circular structure of the mitochondrial genome of *Meloe proscarabaeus*. The inner circle represents GC content (the ratio of guanine to cytosine), the outer circle represents genetic characteristics, orange represents ribosomal RNA, red represents transport RNA, and green represents protein-coding regions. Genes in the inner circle (on the J chain) are transcribed clockwise, while those outside the circle (on the N chain) are transcribed counter-clockwise.

genes and three transfer RNAs (*trnW-trnC-trnY*) between *nad2* and *cox1*. The remaining RNAs are dispersed among other genes in a single or double way (Fig. 1). Two ribosomal RNAs mitochondrial genome of *M. proscarabaeus* were aligned with these of other meloid and assigned to the blanks between neighbouring genes. The *rrnL* gene was located between *trnL* and *trnV* with a length of 1,328 bp, the *rrnS* was located between *tnrV* and the control region with a length of 815 bp (Table 1). The control region was located between *rrnS* and *trnI* with 1,015 bp in length (Table 1; Fig. 1).

Table 1. Annotation of the *Meloe proscarabaeus* mitogenome.

Gene	Location	Inc	Size	Strand	Anticodon	Start codon	Stop codon
trnI	1–66		66	J	GAU		
trnQ	64–132	-3	69	N	UUG		
trnM	132–201	-1	70	J	CAU		
nad2	220–1215	18	996	J		ATT	TAA
trnW	1214–1279	-2	66	J	UCA		
trnC	1279–1341	-1	63	N	GCA		
trnY	1344–1408	2	65	N	GUA		
cox1	1401–2948	-8	1548	J		ATT	TAA
trnL2	2944–3007	-5	64	J	UAA		
cox2	3008–3695	0	688	J		ATA	T*
trnK	3696–3766	0	71	J	CUU		
trnD	3767–3831	0	65	J	GUC		
atp8	3832–3993	0	171	J		ATT	TAA
atp6	3984–4655	-10	672	J		ATG	TAA
cox3	4655–5437	-1	783	J		ATG	TAA
trnG	5441–5503	3	63	J	UCC		
nad3	5504–5857	0	354	J		ATA	TAG
trnA	5856–5918	-2	64	J	UGC		
trnR	5919–5982	0	64	J	UCG		
trnN	5983–6049	0	67	J	GUU		
trnS	6050–6108	0	59	J	UCU		
trnE	6109–6169	0	61	J	UUC		
trnF	6168–6231	-2	64	N	GAA		
nad5	6232–7942	0	1711	N		ATT	T*
trnH	7943–8006	0	64	N	GUG		
nad4	8007–9339	0	1333	N		ATG	T*
nad4l	9333–9620	-7	288	N		ATG	TAA
trnT	9623–9685	2	63	J	UGU		
trnP	9686–9748	0	63	N	UGG		
nad6	9751–10242	2	492	J		ATT	TAA
cob	10242–11381	-1	1140	J		ATG	TAA
trnS2	11380–11447	-2	68	J	UGA		
nad1	11465–12415	17	951	N		ATT	TAG
trnL	12416–12479	0	65	N	UAG		
rrnL	12442–13769	-38	1328	N			
trnV	13757–13825	-13	69	N	UAC		
rrnS	13824–14638	-2	815	N			
CR	14639–15653	0	1015	J			

Inc: intergenic nucleotides, negative values refer to overlapping nucleotides.
trnL2 and *trnS2* refer to *trnL* (UAA) and *trnS* (UGA), respectively.
*TAA stop codon is completed by the addition of 3' A residues to the mRNA.

Genetic distances

The genetic distances within and between genera were calculated using the nucleotide and amino acid data of 13 mitochondrial PCGs among 15 meloid taxa. The result from the nucleotide data showed that the *p*-distances within genera for *Hycleus*, *Epicanta*, and *Mylabris* are 0.167, 0.173, and 0.232, respectively, with an average of 0.191, while the *p*-distances between genera ranged from 0.234 to 0.281 with an average of 0.258 (Fig. 3). The result from the amino acid data showed that the *p*-distances within

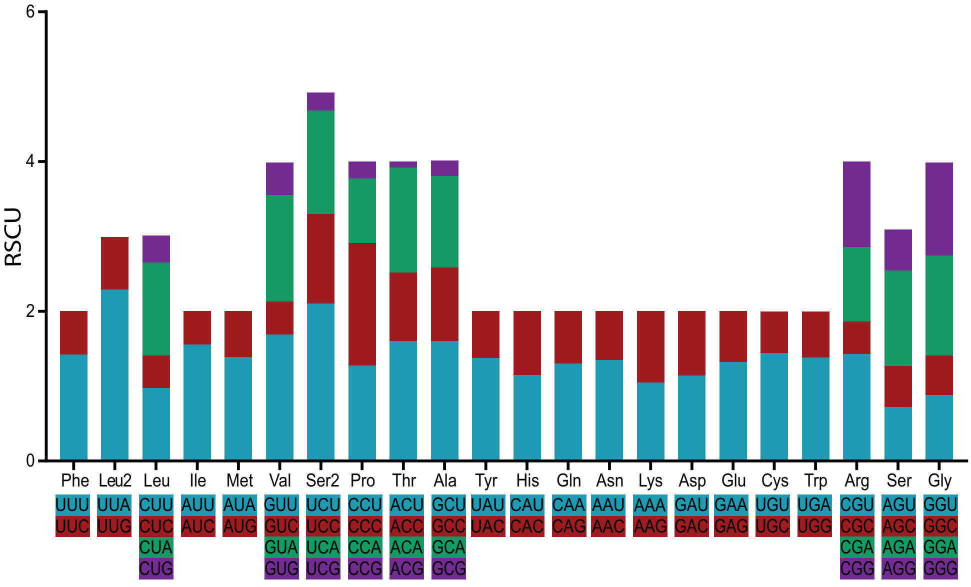

Figure 2. Relative synonymous codon usage (RSCU) in the *Meloe proscarabaeus* mitochondrial genome. An average of 3,711 codons were analysed, excluding stop codons. Codon families are provided on the x-axis. Leu, Leu2, Ser, and Ser2 indicate *trnL1* (CUN), *trnL2* (UUR), *trnS1* (AGN), and *trnS2* (UCN), respectively.

genus of these three genera are 0.124, 0.107, and 0.163, respectively, with the mean of 0.115, and the *p*-distance between genera ranging from 0.173 to 0.226 with the mean of 0.187 (Fig. 3). The *p*-distances within genus are significantly lower than between genera from both datasets ($p < 0.01$). The *p*-distance between *M. proscarabaeus* and *M. poggii* was 0.116 and 0.064 from the nucleotide and the amino acid data, and far less than the corresponding distances between genera.

Phylogenic relationship

The phylogenetic relationships within the family Meloidae were inferred by using maximum likelihood methods, based on the nucleotide and amino acid data from mitogenomes of 15 meloid taxa. The best-fit partitioning schemes and corresponding substitution models are shown in Table 2. Log likelihoods of consensus trees constructed from 1000 bootstrap trees are –88,585.1106 and –32,785.8864 for the nucleotide and amino acid data, respectively.

The ML trees resulting from both datasets strongly support the monophyly of *Meloe* and *Epicauta*, whereas the genera *Hycleus* and *Mylabris* are not monophyletic (Fig. 4). The monophyletic *Meloe*, including *M. proscarabaeus* and *M. poggii*, sisters with *Lytta* into a branch in both phylogenetic trees, but the branch clusters with *Epicauta* or *Hycleus* in the ML tree from nucleotide or amino acid data, respectively (Fig. 4).

Table 2. The best-fit schemes and evolutionary models for two datasets from mitochondrial genomes.

Dataset	Subset	Best model	Partition names
nucleotide	1	TIM+F+I+G4	*nad2*
	2	GTR+F+I+G4	*cox1*
	3	HKY+F+I+G4	*cox2*, *apt6*, *nad3*, *nad4*, *nad4l*, *nad6*
	4	TPM3+F+G4	*apt8*
	5	TIM2+F+I+G4	*cox3*, *cob*
	6	TPM3+F+I+G4	*nad5*
	7	K3Pu+F+I+G4	*nad1*
Amino acid	1	mtMet+G4	*nad2*, *cox2*, *apt8*, *nad3*, *nad6*
	2	mtZOA+G4	*cox1*
	3	mtVer+G4	*apt6*
	4	mtMAM+G4	*cox3*
	5	mtInv+I+G4	*nad5*
	6	mtInv+G4	*nad4*, *nad4l*
	7	mtMAM+I+G4	*cob*
	8	mtART+G4	*nad1*

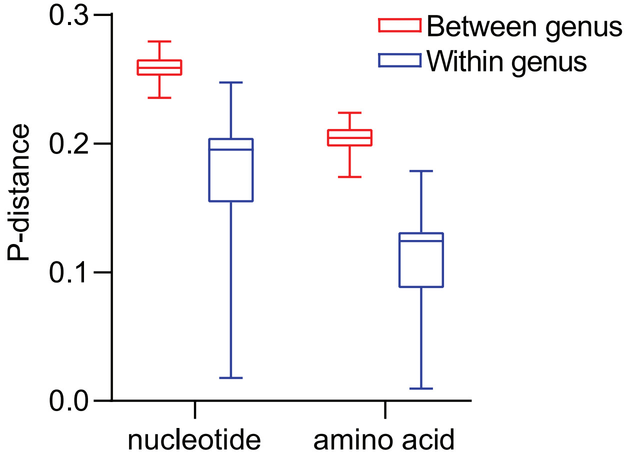

Figure 3. Genetic distance within and between genera. Each boxplot represents the *p*-distance based on the nucleotide and the amino acid datasets from 13 mitochondrial PCGs. The lower horizontal bar represents the smallest observation, the lower edge of the rectangle represents the 25 percentile, the central bar within the rectangle represents the median, the upper edge of the rectangle represents 75 percentile, and the upper horizontal bar represents the largest observation.

Discussion

The first mitochondrial genome of an oil beetle *Meloe proscarabaeus* was sequenced and annotated in this study. The gene arrangement and orientation were the same as the common ancestor for the Insecta (Boore et al. 1998; Taanman 1999). The A + T content and AT skew of *M. proscarabaeus* is the moderate level within Meloidae, and the biased usage of A and T nucleotides is also exhibited in mitochondrial PCGs, because

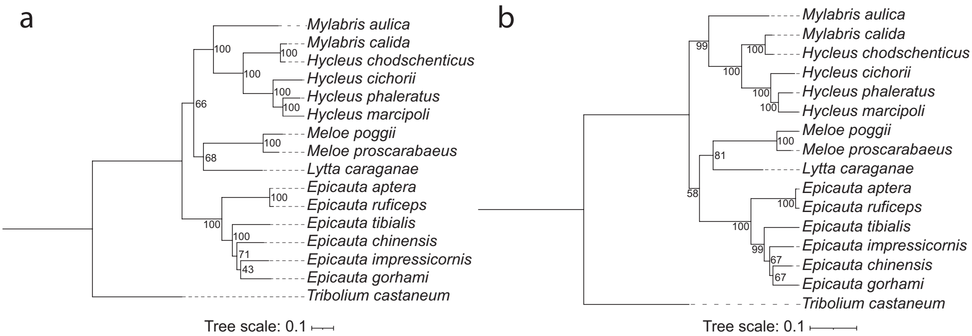

Figure 4. Phylogenetic trees of 14 meloid species based on the nucleotide (a) and amino acid (b) dataset inferred from the maximum likelihood. The numbers abutting branches refer to the bootstrap supports. *Tribolium castaneum* (Tenebrionidae) was used to root the trees as an outgroup.

the A + T bias is a common phenomenon in insect mitochondrial genomes (Du et al. 2017). Incomplete stop codons commonly exist in mitochondrial genomes of insects (Du et al. 2016; 2017). It is usual that the single T was employed as the stop codon in many insect mitochondrial genomes, and the incomplete stop codon could be functional in polycistronic transcription cleavage and polyadenylation processes (Ojala et al. 1981). The control region was located between *rrnS* and *trnI* with 1,015 bp in length, which is similar to that of other meloid mitochondrial genomes (Du et al. 2017). It is a noncoding region and a functional region that controls the replication and transcription of the mitochondrial genome and is the biggest region in which variations occurred to affect both sequence and the length of the entire mitochondrial genome (Andrews et al. 1999).

The genetic distance within and between genera was calculated to confirm the taxonomic status of *M. proscarabaeus*. The *p*-distances within genus are significantly lower than between genera from both datasets ($p < 0.01$), but the *p*-distance within *Mylabris* was a little higher than that between *Hycleus* and *Mylabris* (Fig. 3), which may be because of too a few *Mylabris* taxa and also discussed in some fishes and birds (Ma et al. 2020; Du et al. 2020). The *p*-distances resulting from the nucleotide and the amino acid data between *M. proscarabaeus* and *M. poggii* were both far less than the corresponding distances between genera. This indicates there exist a significant distinction in genetic distance within and between genera, and subsequently confirm the taxonomic status of *M. proscarabaeus*.

Phylogenetic analysis within Meloidae recover the monophyly of *Meloe* and *Epicauta*, and a polyphyly comprising *Hycleus* and *Mylabris*. Within the polyphyly, both trees based on the nucleotide and the amino acid datasets show that *M. calida* Pallas, 1782 clustered with *H. chodschenticus* Ballion, 1878 rather than *M. aulica* Menetries, 1832 (Fig. 4). The polyphyly of Mylabrini was also recovered by other studies utilising partial genes (mitochondrial 16S and nuclear ITS2 sequences) and complete mitochondrial PCGs (Bologna et al. 2008; Du et al. 2017). It may be caused by the high similarity between *Hycleus* and *Mylabris* and the inadequate number of taxa available for molecular phylogenetic studies. Previous studies also recovered the different topology (Bologna et al. 2008; Du et al. 2017), which might be limited by the lack of enough taxon sampling. To date, no phylogeny has definitively inferred the phylogenetic relationships within the families. In consideration of the diverse meloid species, the increasingly published information would help achieve more convincing conclusions for the phylogeny of the family.

Conclusion

The mitochondrial genome of *M. proscarabaeus* was assembled and described. The genome descriptions provide an informative reference for mitochondrial genomes of *Meloe* beetles. The mitochondrial genome sequence and its characteristics would be beneficial for future studies on taxonomy, molecular phylogenetics, and systematics of meloid insects.

Acknowledgements

This study was supported by the Technology Innovation and Entrepreneurship Seedling Project (2020JDRC0128), the Natural Science Foundation of Inner Mongolia (2021ms03023), and the Research Program of Science and Technology at Universities of Inner Mongolia Autonomous Region (NJZY22018).

References

Andrews RM, Kubacka I, Chinnery PF, Lightowlers RN, Turnbull DM, Howell N (1999) Reanalysis and revision of the Cambridge reference sequence for human mitochondrial DNA. Nature Genetics 23(2): 147–147. https://doi.org/10.1038/13779

Avise JC (1994) Molecular Markers, Natural History and Evolution. Springer Science & Business Media, New York/Philadelphia, 511 pp. https://doi.org/10.1007/978-1-4615-2381-9

Bologna MA, Oliverio M, Pitzalis M, Mariottini P (2008) Phylogeny and evolutionary history of the blister beetles (Coleoptera, Meloidae). Molecular Phylogenetics and Evolution 48(2): 679–693. https://doi.org/10.1016/j.ympev.2008.04.019

Boore JL, Lavrov DV, Brown WM (1998) Gene translocation links insects and crustaceans. Nature 392(6677): 667–668. https://doi.org/10.1038/33577

Cameron S (2014) How to sequence and annotate insect mitochondrial genomes for systematic and comparative genomics research. Systematic Entomology 39(3): 400–411. https://doi.org/10.1111/syen.12071

Chen S, Zhou Y, Chen Y, Gu J (2018) fastp: An ultra-fast all-in-one FASTQ preprocessor. Bioinformatics (Oxford, England) 34(17): i884–i890. https://doi.org/10.1093/bioinformatics/bty560

Di Giulio A, Bologna MA, Pinto JD (2002) Larval morphology of the *Meloe* subgenus *Mesomeloe*: Inferences on its phylogenetic position and a first instar larval key to the *Meloe* subgenera (Coleoptera, Meloidae). The Italian Journal of Zoology 69(4): 339–344. https://doi.org/10.1080/11250000209356479

Di Giulio A, Carosi M, Khodaparast R, Bologna MA (2014) Morphology of a new blister beetle (Coleoptera, Meloidae) larval type challenges the evolutionary trends of phoresy-related characters in the genus *Meloe*. Entomologia 2: 164. https://doi.org/10.4081/entomologia.2014.164

Du C, He S, Song X, Liao Q, Zhang X, Yue B (2016) The complete mitochondrial genome of *Epicauta chinensis* (Coleoptera: Meloidae) and phylogenetic analysis among coleopteran insects. Gene 578(2): 274–280. https://doi.org/10.1016/j.gene.2015.12.036

Du C, Zhang L, Lu T, Ma J, Zeng C, Yue B, Zhang X (2017) Mitochondrial genomes of blister beetles (Coleoptera, Meloidae) and two large intergenic spacers in *Hycleus* genera. BMC Genomics 18(1): e698. https://doi.org/10.1186/s12864-017-4102-y

Du C, Liu L, Liu Y, Fu Z (2020) The complete mitochondrial genome of the Eurasian wryneck *Jynx torquilla* (Aves: Piciformes: Picidae) and its phylogenetic inference. Zootaxa 4810(2): 351–360. https://doi.org/10.11646/zootaxa.4810.2.8

Du C, Li W, Fu Z, Yi C, Liu X, Yue B (2021) De novo transcriptome assemblies of *Epicauta tibialis* provide insights into the sexual dimorphism in the production of cantharidin. Archives of Insect Biochemistry and Physiology 106(4): e21784. https://doi.org/10.1002/arch.21784

Friedrich M, Muqim N (2003) Sequence and phylogenetic analysis of the complete mitochondrial genome of the flour beetle *Tribolium castanaeum*. Molecular Phylogenetics and Evolution 26(3): 502–512. https://doi.org/10.1016/S1055-7903(02)00335-4

Hahn C, Bachmann L, Chevreux B (2013) Reconstructing mitochondrial genomes directly from genomic next-generation sequencing reads – A baiting and iterative mapping approach. Nucleic Acids Research 41(13): e129. https://doi.org/10.1093/nar/gkt371

Katoh K, Standley DM (2013) MAFFT multiple sequence alignment software version 7: Improvements in performance and usability. Molecular Biology and Evolution 30(4): 772–780. https://doi.org/10.1093/molbev/mst010

Liu YY, Zhou ZC, Chen XS (2020) Characterization of the complete mitochondrial genome of *Epicauta impressicornis* (Coleoptera: Meloidae) and its phylogenetic implications for the Infraorder Cucujiformia. Journal of Insect Science 20(2): 16. https://doi.org/10.1093/jisesa/ieaa021

Ma Q, He K, Wang X, Jiang J, Zhang X, Song Z (2020) Better resolution for Cytochrome b than Cytochrome c Oxidase subunit I to identify *Schizothorax* species (Teleostei: Cyprinidae) from the Tibetan Plateau and its adjacent area. DNA and Cell Biology 39(4): 579–598. https://doi.org/10.1089/dna.2019.5031

Meng G, Li Y, Yang C, Liu S (2019) MitoZ: A toolkit for animal mitochondrial genome assembly, annotation and visualization. Nucleic Acids Research 47(11): e63–e63. https://doi.org/10.1093/nar/gkz173

Muzzi M, Di Giulio A, Mancini E, Fratini E, Cervelli M, Gasperi T, Mariottini P, Persichini T, Bologna MA (2020) The male reproductive accessory glands of the blister beetle *Meloe proscarabaeus* Linnaeus, 1758 (Coleoptera: Meloidae): Anatomy and ultrastructure of the cantharidin-storing organs. Arthropod Structure & Development 59: e100980. https://doi.org/10.1016/j.asd.2020.100980

Nguyen LT, Schmidt HA, Von Haeseler A, Minh BQ (2015) IQ-TREE: A fast and effective stochastic algorithm for estimating maximum-likelihood phylogenies. Molecular Biology and Evolution 32(1): 268–274. https://doi.org/10.1093/molbev/msu300

Ojala D, Montoya J, Attardi G (1981) tRNA punctuation model of RNA procession in human mitochondria. Nature 290(5806): 470–474. https://doi.org/10.1038/290470a0

Pan Z, Bologna MA (2021) Morphological revision of the Palaearctic species of the nominate subgenus *Meloe* Linnaeus, 1758 (Coleoptera, Meloidae), with description of ten new species. Zootaxa 5007(1): 1–74. https://doi.org/10.11646/zootaxa.5007.1.1

Sánchez-Vialas A, Recuero E, Jiménez-Ruiz Y, Ruiz JL, Marí-Mena N, García-París M (2021) Phylogeny of Meloini blister beetles (Coleoptera, Meloidae) and patterns of island colonization in the Western Palaearctic. Zoologica Scripta 50(3): 358–375. https://doi.org/10.1111/zsc.12474

Saul-Gershenz LS, Millar JG (2006) Phoretic nest parasites use sexual deception to obtain transport to their host's nest. Proceedings of the National Academy of Sciences of the United States of America 103(38): 14039–14044. https://doi.org/10.1073/pnas.0603901103

Saul-Gershenz L, Millar JG, McElfresh JS, Williams NM (2018) Deceptive signals and behaviors of a cleptoparasitic beetle show local adaptation to different host bee species. Proceedings of the National Academy of Sciences of the United States of America 115(39): 9756–9760. https://doi.org/10.1073/pnas.1718682115

Taanman JW (1999) The mitochondrial genome: Structure, transcription, translation and replication. Biochimica et Biophysica Acta 1410(2): 103–123. https://doi.org/10.1016/S0005-2728(98)00161-3

Tamura K, Stecher G, Peterson D, Filipski A, Kumar S (2013) MEGA6: Molecular Evolutionary Genetics Analysis version 6.0. Molecular Biology and Evolution 30(12): 2725–2729. https://doi.org/10.1093/molbev/mst197

Zhou Z, Liu Y, Chen X (2021) Structural features and phylogenetic implications of three new mitochondrial genomes of blister beetles (Coleoptera: Meloidae). Journal of Insect Science 21(6): e19. https://doi.org/10.1093/jisesa/ieab100

ZooKeys 1109: 115–140 (2022)
doi: 10.3897/zookeys.1109.73937
https://zookeys.pensoft.net

RESEARCH ARTICLE

A peer-reviewed open-access journal
ZooKeys
Launched to accelerate biodiversity research

Ten new species of genus *Tachycines* (Orthoptera, Rhaphidophoridae, Aemodogryllinae) from karst caves in Guizhou, China

Xulin Zhou[1,2,3*], Weicheng Yang[1,3*]

1 *School of Life Sciences, Guizhou Normal University; Guiyang, Guizhou 550031, China* **2** *Guizhou Institute of Mountain Resources, Guiyang, 550001, China* **3** *Institute of Karst Caves, Guizhou Normal University, Guiyang, Guizhou 550031, China*

Corresponding author: Weicheng Yang (yangweicheng0908@sina.com))

Academic editor: Tony Robillard | Received 4 September 2021 | Accepted 31 March 2022 | Published 1 July 2022

http://zoobank.org/52B4B123-9343-4F85-A279-36717B1F8DFD

Citation: Zhou X, Yang W (2022) Ten new species of genus *Tachycines* (Orthoptera, Rhaphidophoridae, Aemodogryllinae) from karst caves in Guizhou, China. ZooKeys 1109: 115–140. https://doi.org/10.3897/zookeys.1109.73937

Abstract

Ten new karst cave-dwelling rhaphidophorids species of the subgenus *Gymnaeta* of the genus *Tachycines* are described from Guizhou Province, southern China; i.e., *Tachycines* (*Gymnaeta*) *zhongi* **sp. nov.**, *Tachycines* (*Gymnaeta*) *jinniui* **sp. nov.**, *Tachycines* (*Gymnaeta*) *shibenzhangi* **sp. nov.**, *Tachycines* (*Gymnaeta*) *lahaidensis* **sp. nov.**, *Tachycines* (*Gymnaeta*) *pinglangus* **sp. nov.**, *Tachycines* (*Gymnaeta*) *shanduensis* **sp. nov.**, *Tachycines* (*Gymnaeta*) *buyii* **sp. nov.**, *Tachycines* (*Gymnaeta*) *portae* **sp. nov.**, *Tachycines* (*Gymnaeta*) *ziyunensis* **sp.nov.,** and *Tachycines* (*Gymnaeta*) *jialiangensis* **sp. nov.** All specimens were collected from Guizhou Plateau.

Keywords

Aemodogryllini, caves, Guizhou, *Gymnaeta*, new species, rhaphidophorids

Introduction

The subgenus *Gymnaeta* Adelung, 1902 belongs to the tribe Aemodogryllini that is comprised of 67 species predominantly distributed in China, with eight species extending southwards to Southeast Asia: six in Vietnam, one in Myanmar, and one

* The authors contributed equally to this work.

in the Philippines (Adelung 1902; Karny 1926, 1929, 1934a, b; Gorochov 1994, 1998, 2001, 2010, 2012; Zhang and Liu 2009; Qin et al. 2019; Cigliano et al. 2021). In addition to the surface species, several species of the subgenus *Tachycines* (*Gymnaeta*) inhabit cave habitats (Gorochov 2001; Gorochov et al. 2006; Jiao et al. 2008; Rampini et al. 2008; Feng et al. 2019, 2020; Qin et al. 2019; Zhou and Yang 2020; Zhu et al. 2020).

In recent years, the interest in cave organisms research has increased, and many cave beetles, spiders, cave crickets, ant-loving beetles, cave millipedes, and cave Gesneriaceae species have been reported (Figs 11–13; Gorochov et al. 2006; Lin and Li 2014; Yin et al. 2015; Tian et al. 2016, 2017, 2019; Song et al. 2017; Wang et al. 2017; Liu and Golovatch 2018; Deuve et al. 2020), but there are still many cave species remaining undiscovered, for example, the cave-dwelling rhaphidophorids covered in this study. Twenty-nine species of cave-dwelling rhaphidophorids have been reported in China. Guizhou province is the central area of karst distributions in southern China, where 18 cave-dwelling rhaphidophorids have been found (Gorochov et al. 2006; Rampini et al. 2008; Wen 2018; Feng et al. 2019, 2020; Qin et al. 2019; Zhou and Yang 2020; Zhu et al. 2020; Li et al. 2021; Zhu and Shi 2021). In this work, another ten new species are added to the Chinese fauna based on newly acquired material from Guizhou. This study further reveals the high degree of morphological similarity and cryptic diversity of species in the subgenus *Gymnaeta*, making it more challenging to delimitate these species using morphological characteristics. Furthermore, we agree with the views presented by Zhu et al. (2020) and confirm that *Tachycines* (*Gymnaeta*) *aspes* (Rampini & Di Russo, 2008) is a valid species and not a synonym of *Tachycines* (*Gymnaeta*) *proximus* (Gorochov, Rampini & Di Russo, 2006) according to the varying degrees of reduction of the fastigium vertices and eyes, the higher number of spines on the hind tibia, and the shape of male genitalia. Moreover, we consider that *Eutachycines crenatus* (Gorochov, Rampini & Di Russo, 2006) should be transferred to the subgenus *Gymnaeta*, due to the following genitalic characteristics: median lobe that is shorter than lateral lobe and four lateral lobes that are not sclerotized.

Materials and methods

All specimens in this article were collected in karst caves by hand, sometimes assisted with a swipe net, and preserved in 75% ethanol. Morphological characteristics were examined using an Olympus SZ61 stereomicroscope. The male genitalia was preserved in a solution of ethanol and glycerin. Photographs were taken by an Olympus DP22 digital camera and processed with Adobe Photoshop CS6. All specimens are deposited in the Institute of Karst Caves, Guizhou Normal University, Guizhou Province, China (**IKCGZNU**).

The morphological terms and classification follow Gorochov et al. (2006) and Qin et al. (2019).

Taxonomy

Genus *Tachycines*

Subgenus *Gymnaeta* Adelung, 1902

Gymnaeta Adelung, 1902. *Annuaire du Musée Zoologique de l'Académie Impériale des Sciences de St. Petersburg* 7: 62; Kirby 1906. *A Synonymic Catalogue of Orthoptera* 2: 125.

Diestrammena (*Gymnaeta*): Jacobson, 1905[1902–1905]. In: Jacobson and Bianchi, *Orthopteroid and Pseudoneuropteroid Insects of Russian Empire and adjacent countries*, 329, 352, 434; Gorochov 1994. In: Gorochov and Kireichuk [Eds.], *Proceedings of the Zoological Institute of the Russian Academy of Sciences*, 257: 49; Otte 2000. *Orthoptera Species File* 8: 55; Jiao et al. 2008. *Zootaxa* 1917: 55; Zhang and Liu 2009. *Zootaxa* 2272: 21.

Tachycines (*Gymnaeta*): Karny, 1934. *Konowia* 13 (1–3): 218; Karny 1937. *Genera Insectorum* 206: 248; Storozhenko 1990. *Entomologicheskoe Obozrenie* 69(4): 845, 847; Qin et al. 2018. *Zootaxa* 4374(4): 452; Qin et al. 2019. *Zootaxa* 4560(2): 274; Feng et al. 2019. *Zootaxa* 4674(4): 492; Zhou and Yang 2020. *ZooKeys* 937: 21–29; Zhu et al. 2020. *Zootaxa* 4809(1): 72.

Type species. *Gymnaeta berezovskii* Adelung, by subsequent designation; authority: Kirby, W.F. 1906. A Synonymic Catalogue of Orthoptera (Orthoptera Saltatoria, Locustidae vel Acridiidae) 2: i–viii, 1–562.

Tachycines (*Gymnaeta*) *zhongi* sp. nov.

http://zoobank.org/705C74CA-5D8A-46E1-8223-FDA318E27D72
Figs 1A–D, 15

Specimens examined. ***Holotype***, 1♂, Daxiao Dong, Xinchang township, Liuzhi Special District, 900 m, 2019-VII-28, collected by Jinhua Zhong, Xulin Zhou, Lingzhi Ou, Guang Wang, Benzhang Shi, Juan Liao and Liangfeng An; ***paratypes***, 5♂, 2♀, same collection data as for holotype.

Diagnosis. This new species is similar to *T*. (*G.*) *caudatus* (Gorochov et al., 2006) regarding the shape of the female subgenital plate, but the female subgenital plate of the new species has a small triangle on both sides, while the latter is without. Also similar to *T*. (*G.*) *chenhui* (Rampini & Di Russo, 2008) regarding the shape of the male epiphallus, but the new species is smaller, with its body length not exceeding 13 mm, vertex conical tubercles extremely reduced, scarce (Fig. 1D), ventral conical projections of 3rd–8th abdominal sternites less developed, forming smaller and shorter projections, hind tarsus keeled ventrally; *T*. (*G.*) *chenhui* has a larger body exceeding 13 mm, vertex conical tubercles of intermediate development, ventral conical projections of 3rd–8th abdominal sternites developed, forming larger and longer projections, hind tarsus with bristles ventrally.

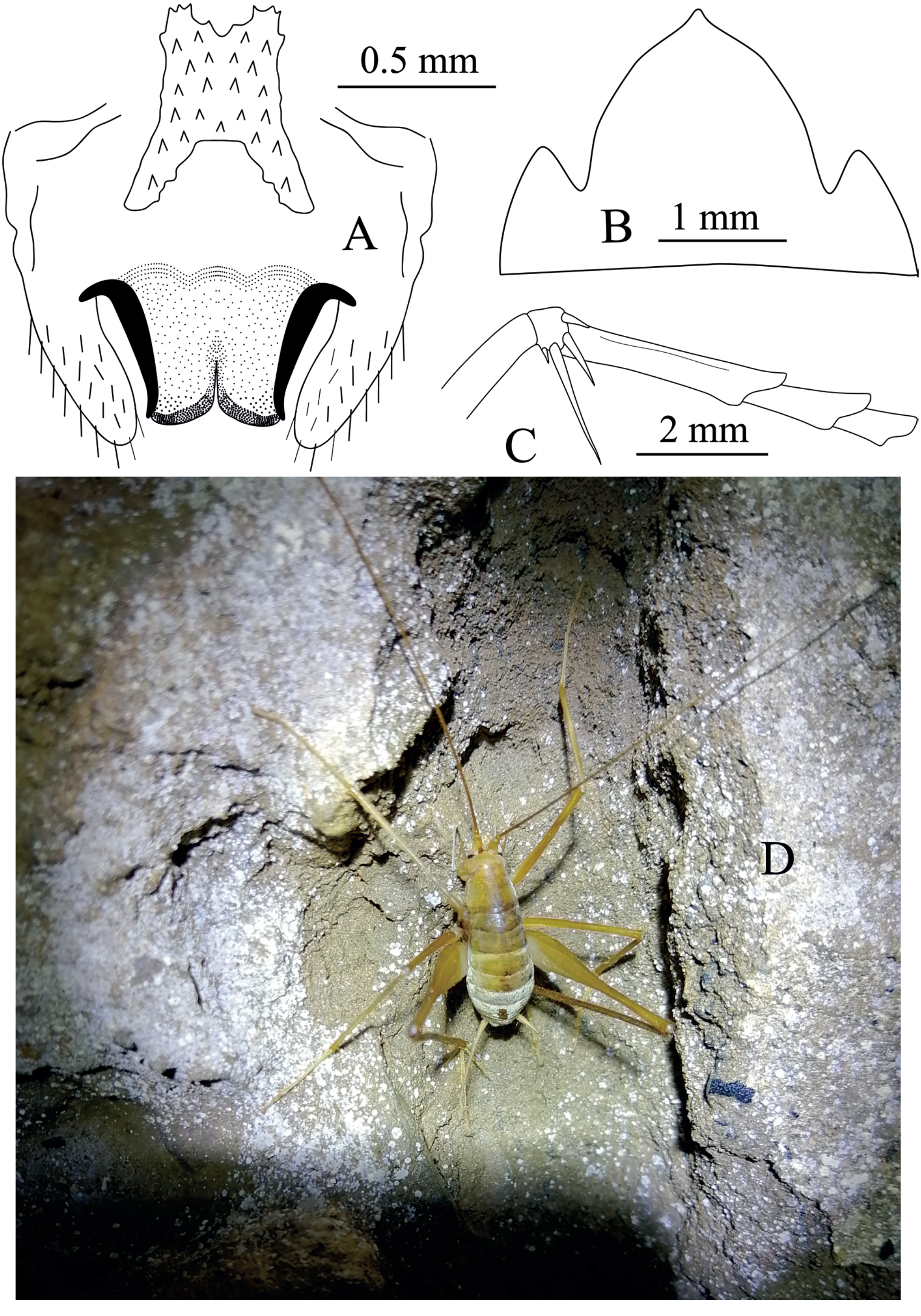

Figure 1. *Tachycines* (*Gymnaeta*) *zhongi* sp. nov., **A** male genitalia, dorsal view **B** female subgenital plate in ventral view **C** hind tarsus in lateral view **D** male live habitus dorsal view.

Description. Male. Body medium and small-sized (Fig. 1D). Eyes slightly reduced, ocelli absent; conical tubercles of vertex reduced. Legs elongate and slender; fore femur approx. 3.1–3.2 times longer than the pronotum, ventrally unarmed, the internal genicular lobe with single small spine, external genicular lobe with single elongate movable spur; ventral side of fore tibiae with one internal spur and two external spurs. Mid femur with an elongate movable spur on the inner and outer genicular lobes, ventrally unarmed; mid tibiae beneath with one internal spur and one external spur. Hind femur without ventral spine, internal genicular lobe with one small spine; hind tibiae dorsally on both sides with 23–25 spines, sparsely arranged. Supra-internal spur of hind tibiae not exceeding ventral apex of hind tarsus. Hind tarsus keeled ventrally and with one dorsal apical spine (Fig. 1C). Small and short ventral conical projections of 3rd–8th abdominal sternites developed, but distal ones obtuse and densely ciliated. Cerci extremely long. Male genitalia with H-shaped epiphallus, middle lobe and lateral sclerites of genitalia almost at the same level at the bottom (Fig. 1A).

Female. Other characteristics are similar to the male. Subgenital plate with three lobes, median lobe large and nearly triangular (Fig. 1B). Ovipositor is slightly longer than half the length of hind femur.

Coloration. Body uniformly yellowish brown.

Measurements (mm). Body ♂11.2–11.6, ♀10.8–12.1; pronotum ♂3.5, ♀3.8; fore femur ♂11.1–11.5, ♀10.8–12.3; hind femur ♂18.5–19.3, ♀18.4–20.0, ovipositor 10.0–11.2.

Distribution of light zone. Weak light and dark light zones.

Cave adaptation type. Troglobite.

Etymology. The specific epithet refers to the person's last name who led us to collect the specimens.

***Tachycines* (*Gymnaeta*) *jinniui* sp. nov.**

http://zoobank.org/144C1AF3-1041-4D1C-A340-C9C6832F74CC

Figs 2A, 14, 15

Specimens examined. ***Holotype***, 1♀, Jinniu Cave (Fig. 14), Libo County, 2017-X-23, collected by Xulin Zhou, Dongshan Xu, Weicheng Yang; ***paratype***, 1♀, same collection data as for holotype.

Diagnosis. The new species is very similar to *Tachycines* (*Gymnaeta*) *trapezialis* Zhou & Yang, 2020 but differs from the latter by having slightly reduced eyes and the conical tubercles of the vertex intermediately reduce, the hind tibia dorsally on each side has 78–85 spines instead of 54–60 spines.

Description. Female. Body medium sized. Vertex conical tubercles slightly reduced, apex obtuse, ommateum black and well developed. Legs elongate and slender; fore femur approx. 2.5–2.7 times longer than the pronotum, ventrally unarmed, the internal genicular lobe with a small spine, external genicular lobe with one elongate movable spur; ventral side of fore tibiae with one internal spur and two external spurs. Mid femur with an elongate movable spur on internal and external genicular lobes, ventrally unarmed; mid tibiae beneath with two internal spurs and two external spurs. Hind femur without ventral spine, internal genicular lobe without spine; hind tibiae dorsally on both sides with 79–86 spines, arranged in groups. Supra-internal spur of hind tibiae not exceeding ventral apex of hind tarsus. Hind tarsus keeled ventrally, with one dorsal apical spine. Cerci long and slender. Ovipositor shorter than half length of hind femur.

Male. Unknown.

Coloration. Body color uniform, yellowish brown, eyes black.

Measurements (mm). Body ♀ 13.7–16.7; pronotum ♀ 5.1–5.3; fore femur ♀ 13.6–14.1; hind femur ♀ 25.2–26.0; ovipositor 8.4–8.5.

Distribution of light zone. Dark light zone.

Cave adaptation type. Troglophile.

Etymology. The new species is named after the collection locality of the specimens (Jinniu cave).

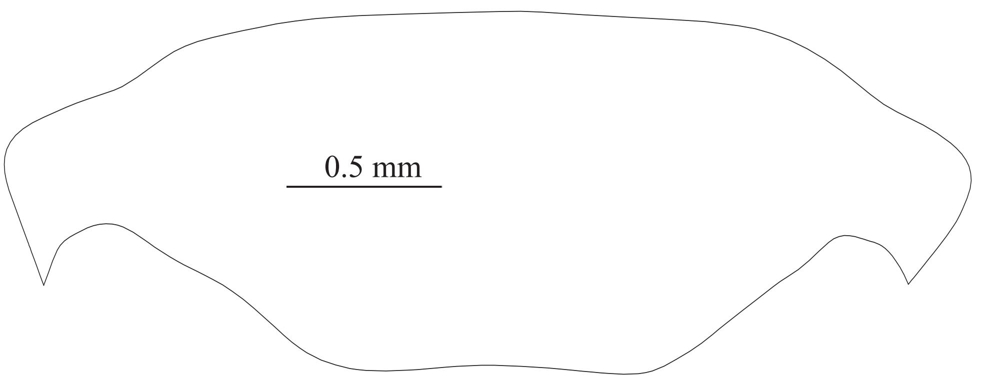

Figure 2. *Tachycines* (*Gymnaeta*) *jinniui* sp. nov., female, subgenital plate in ventral view.

***Tachycines* (*Gymnaeta*) *shibenzhangi* sp. nov.**

http://zoobank.org/84644FCC-1440-4FF1-B00E-3D1A70F9450A

Figs 3A–D, 15

Specimens examined. ***Holotype***, 1♂, Xuehua Cave, Zhonghe Town, Sandu County, 2019-VII-28, collected by Xulin Zhou, Benchang Shi, Changzhen Zheng, Haixia Luo, Gui Liang, Hailian Lan, Panpan Ren and Juan Liao; ***paratypes***, 16♂, 15♀, same data as the holotype.

Diagnosis. The characteristic of the male genitalia of the new species is distinct from that of other groups: the epiphallus of the male genitalia is semi-circular, and the lateral sclerites sub-elliptical. In addition, the conical tubercles of the vertex are absent, the ommateum are extremely degenerated, the mid tibiae ventrally without spur or spine, the ventral conical projections of 3rd–8th abdominal sternites developed, and the distal ones are obtuse and densely ciliated.

Description. Male. Body smaller than the average for the subgenus. Vertex conical tubercles absent, ommateum extremely degenerated, present by narrow stripes with several black facets (some individuals have no black facets and are completely blind). Legs elongate

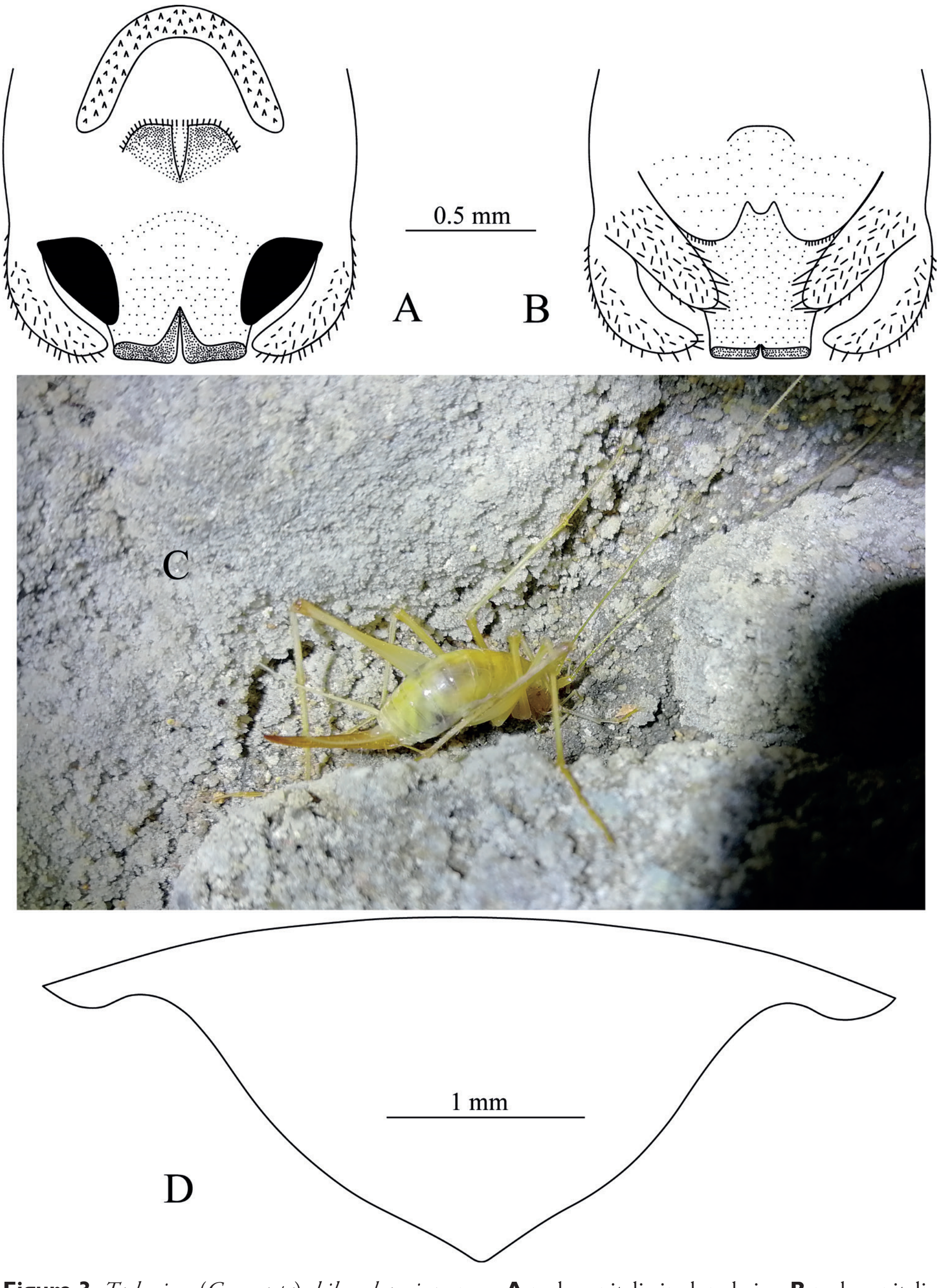

Figure 3. *Tachycines* (*Gymnaeta*) *shibenzhangi* sp. nov., **A** male genitalia in dorsal view **B** male genitalia in ventral view **C** female live habitus in dorsal view **D** female subgenital plate in ventral view.

and slender, fore femur approx. 2.6–3.0 times longer than the pronotum, ventrally unarmed, external genicular lobe with one elongate movable spur, internal knee lobe without spine; fore tibiae beneath with one external spur (sometimes with two external spurs), but without internal spur. Mid femur with an elongate movable spur on both internal and external genicular lobes, ventrally unarmed; mid tibiae ventrally without internal or external spur. Hind femur without spines ventrally; hind tibiae dorsally with 11–18 inner spines and 13–18 outer spines, sparsely arranged. Supra-internal spur of hind tibiae not exceeding ventral apex of hind tarsus. Hind tarsus ventrally with bristles. Ventral conical projections of 3rd–8th abdominal sternites developed, but distal ones obtuse and densely ciliated. Epiphallus of male genitalia nearly semi-circular, lateral sclerites sub-elliptical (Fig. 3A, B).

Female. Appearance is similar to the male. Subgenital plate nearly triangular, apical area slightly blunt. Ovipositor is longer than half length of hind femur, dorsal margin smooth, and apical area of ventral margin denticulate.

Coloration. Body color uniform, pale yellow, abdomen slightly transparent and the internal organs are visible.

Measurements (mm). Body ♂9.4–12.1, ♀11.2–12.5; pronotum ♂2.9–3.3, ♀ 3.0–3.2; fore femur ♂ 8.1–8.8, ♀ 8.2–9.6; hind femur ♂ 13.6–14.6, ♀ 13.6–14.8; ovipositor 9.1–10.0.

Distribution of light zone. Dark light zone.

Cave adaptation type. Troglobite.

Etymology. The specific epithet refers to the name of the person who provided crucial help in collecting the specimens.

***Tachycines* (*Gymnaeta*) *lahaidensis* sp. nov.**

http://zoobank.org/365EE275-1199-4EC4-A0BA-0CD676277EEE
Figs 4A–D, 15

Specimens examined. ***Holotype***, 1♂, Lahaide Dong, Pinglang Town, Duyun City, 2015-VII-24, collected by Qing Wen, Dongshan Xu, Yuanchan Yu, Yi Luo, Guang Zhang; ***paratypes***, 6♂, 8♀, same data as the holotype.

Diagnosis. The new species is very similar to *Tachycines* (*Gymnaeta*) *shibenzhangi* sp. nov., as both species have an arc-shaped epiphallus. The difference is that the ventral surface of the hind tarsus keeled in the new species, but differs from the latter in that: lower notch of the epiphallus is rather small, hind tarsus keeled beneath, epiphallus of male nearly n-shaped; ventral conical projections of 3rd–8th abdominal sternites developed, apex mucronate without dense cilia.

Description. Male. Body medium sized. Vertex conical tubercles inconspicuous, eyes moderately reduced, approx. 1/2 the size of the normal eye. Legs elongate, slender; fore femur approx. 2.1–2.5 times longer than the pronotum, ventrally unarmed, external genicular lobe with one elongated movable spur, internal knee lobe without spine; fore tibiae ventrally with two external spurs and one internal spur. Mid femur with an elongate movable spur on the internal and external genicular lobes, ventrally unarmed; mid tibiae beneath with one external spur and one internal spur. Hind femur without

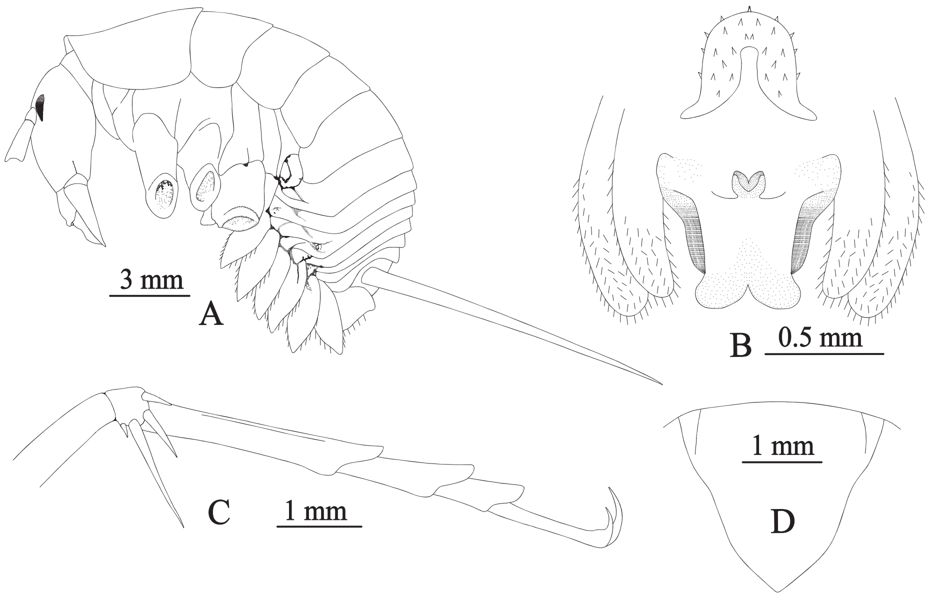

Figure 4. *Tachycines* (*Gymnaeta*) *lahaidensis* sp. nov., **A** male body in lateral view **B** male genitalia in dorsal view **C** hind tarsus in lateral view **D** female subgenital plate in ventral view.

spine ventrally; hind tibiae dorsally with 27–30 internal spines and 22–26 external spines, sparsely arranged. Supra-internal spur of hind tibiae not exceeding the ventral apex of hind tarsus. Hind tarsus keeled ventrally. Ventral conical projections of 3rd–8th abdominal sternites developed, distally mucronate without cilia. Epiphallus of male genitalia nearly n-shaped, lateral sclerites distinctly long and narrow.

Female. Appearance is similar to the male. The subgenital plate is nearly triangular, its apical area slight obtuse (Fig. 4D). Ovipositor is longer than half length of the hind femur, dorsal margin smooth, apical area of ventral margin denticulate, bent slightly upwards.

Coloration. Body brown, ovipositor wheat.

Measurements (mm). Body ♂ 10.5–12.3, ♀ 11.2–12.6; pronotum ♂ 4.0–4.8, ♀ 3.8–3.9; fore femur ♂ 10.2–10.30, ♀ 10.1–10.3; hind femur ♂ 18.9–19.0, ♀ 18.0–18.1; ovipositor 10.0–11.0.

Distribution of light zone. Dark light zone.

Cave adaptation type. Troglobite.

Etymology. The specific epithet refers to the Lahaide cave.

***Tachycines* (*Gymnaeta*) *pinglangus* sp. nov.**

http://zoobank.org/C2D9C063-9A83-464F-8EE2-EDDD561C4745

Figs 5A–D, 15

Specimens examined. ***Holotype*** 1♂, Lagaobieran Dong, Pinglang Town, Duyun City, 2015-VII-25, collected by Qing Wen; ***paratypes***, 11♂, 16♀, 2015-VII-25, collected by Qing Wen, Dongshan Xu, Yi Luo, Yuanchan Yu, Guang Zhang.

Diagnosis. The new species is very similar to *Tachycines* (*Gymnaeta*) *ferecaecus* (Gorochov, Rampini & Di Russo, 2006): both species have a nearly quadrate-shaped epiphallus, but the new species can be distinguished from the latter by the absence of an ommateum (without any black facets), only the base of the ommateum was faintly visible.

Description. Male. Body medium sized in the subgenus (Fig. 5A). Vertex conical tubercles almost absent, ommateum completely reduced (appears to be without any black facets, only ommateum base); Legs elongate and slender; fore femur approx. 2.8–3.2 times longer than the pronotum, ventrally unarmed, external genicular lobe with one elongate movable spur, internal knee lobe without spine; fore tibiae beneath with one external spur (sometimes with two external spurs), but without internal spur. Mid femur with an elongate movable spur on the internal and external genicular lobes, ventrally unarmed; mid tibiae ventrally with one external spur and one internal spur. Hind femur without spines ventrally; hind tibiae dorsally with 12–15 internal spines and 12 or 13 external spines, sparsely arranged. Supra-internal spur of hind tibiae shorter than the ventral apex of hind tarsus. Hind tarsus with bristles ventrally. Ventral conical projections of 3rd–8th abdominal sternites developed, distally obtuse, and densely ciliated. Epiphallus of male genitalia nearly quadrate, median lobe of genitalia with a pair of wide apical lobules, but without distinct lateral sclerites (Fig. 5B).

Female. Appearance is similar to the male. The subgenital plate is nearly triangular, and the apical area slightly obtuse. Ovipositor is longer than half of the hind femur length, brown, dorsal margin smooth, apical area of ventral margin denticulate, bent slightly upwards.

Coloration. Body yellowish brown, ovipositor wheat.

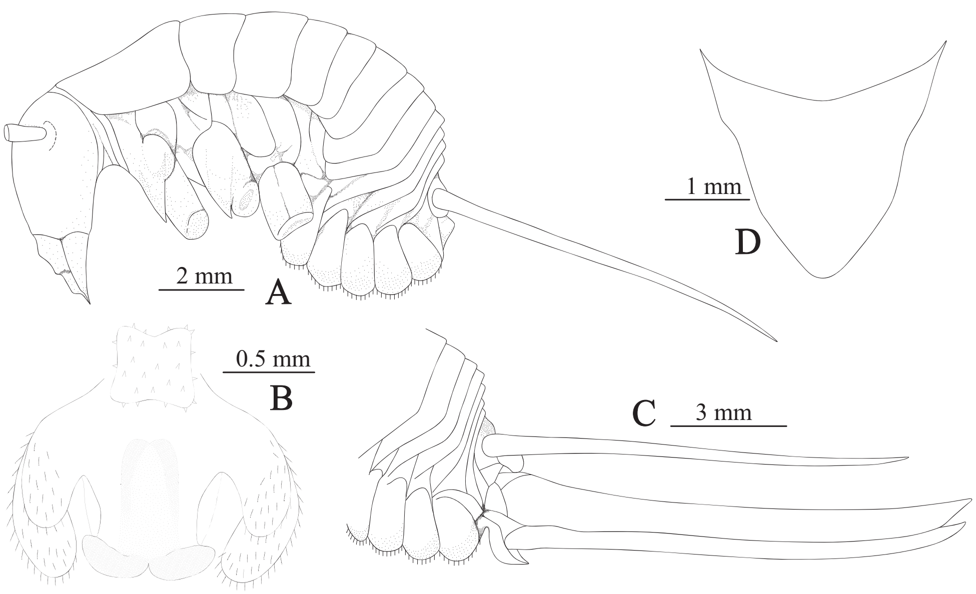

Figure 5. *Tachycines* (*Gymnaeta*) *pinglangus* sp. nov., **A** male body in lateral view **B** male genitalia in dorsal view **C** female terminal in lateral view **D** female subgenital plate in ventral view.

Measurements (mm). Body ♂ 9.5–13.0, ♀ 8.2–12.0; pronotum ♂ 3.2–3.8,♀ 3.2–3.4; fore femur ♂ 10.2–10.50, ♀ 10.2–10.4; hind femur ♂ 13.2–14.7, ♀ 13.2–14.6; ovipositor 8.0–10.4.

Distribution of light zone. Dark light zone.

Cave adaptation type. Troglobite.

Etymology. The specific epithet refers to the locality where the type specimens were collected.

***Tachycines* (*Gymnaeta*) *shanduensis* sp. nov.**
http://zoobank.org/ED670C87-E4D5-48C1-A93C-83949F4F8FC3
Figs 6A–D, 15

Specimens examined. ***Holotype*** 1♂, Shuilong Cave, Sandu County, 2019-VII-22, collected by Xulin Zhou, Benchang Shi, Changzhen Zheng, Gui Liang, Haixia Luo, Hailian Lan, Juan Liao; ***paratypes***, 6♂, 8♀, same data as holotype.

Diagnosis. This species is rather similar to *Tachycines* (*Gymnaeta*) *solida* (Gorochov, Rampini & Di Russso, 2006) and *Tachycines* (*Gymnaeta*) *tongrenus* Feng, Huang & Luo, 2020, but the male epiphallus of the new species has a distal shallow notch clearly wider than the upper notch, the median process of the male genitalia is significantly longer than the lateral sclerites, hind tibiae dorsally on both sides with 34–46 spines, hind tarsus keeled beneath; however, in *Tachycines* (*Gymnaeta*) *solida*, the male epiphallus has the upper and lower notches almost the same size, hind tibiae dorsally on both sides with 62–69 spines; in *Tachycines* (*Gymnaeta*) *tongrenus*, the hind tibia dorsally with 48–49 inner spines and 54–56 outer spines, hind tarsus with bristles ventrally.

Description. Male. Body rather large for this subgenus. Vertex conical tubercles are well developed, bisected from the base; ommateum is black and well developed (Fig. 6A). Legs elongate and slender; fore femur approx. 1.9–2.1 times longer than the pronotum, ventrally unarmed, external genicular lobe with one elongate movable spur, internal knee lobe with a small spine; fore tibiae beneath with two external spurs and one internal spur. Mid femur with an elongate movable spur on both internal and external genicular lobes, ventrally unarmed; mid tibiae beneath with one external spur and one internal spur. Hind femur without spines ventrally; hind tibiae dorsally with 34–43 internal spines and 38–46 external spines, arranged in groups. Supra-internal spur of hind tibiae shorter than the dorsal apex of hind tarsus. Hind tarsus keeled ventrally, with one dorsal apical spine. Epiphallus of male genitalia nearly H-shaped, lateral sclerites distinctly long and narrow, upper notch rather smaller than lower notch.

Female. Appearance is similar to male (Fig. 6B). Subgenital plate with three lobes, median lobe large, triangular, and apical area sharp (Fig. 6C). Ovipositor is shorter than half of the hind femur length, dorsal margin smooth, apical area of ventral margin denticulate.

Coloration. Body dark brown, mixed with tawny stripes, hind femur with brown diagonal stripe.

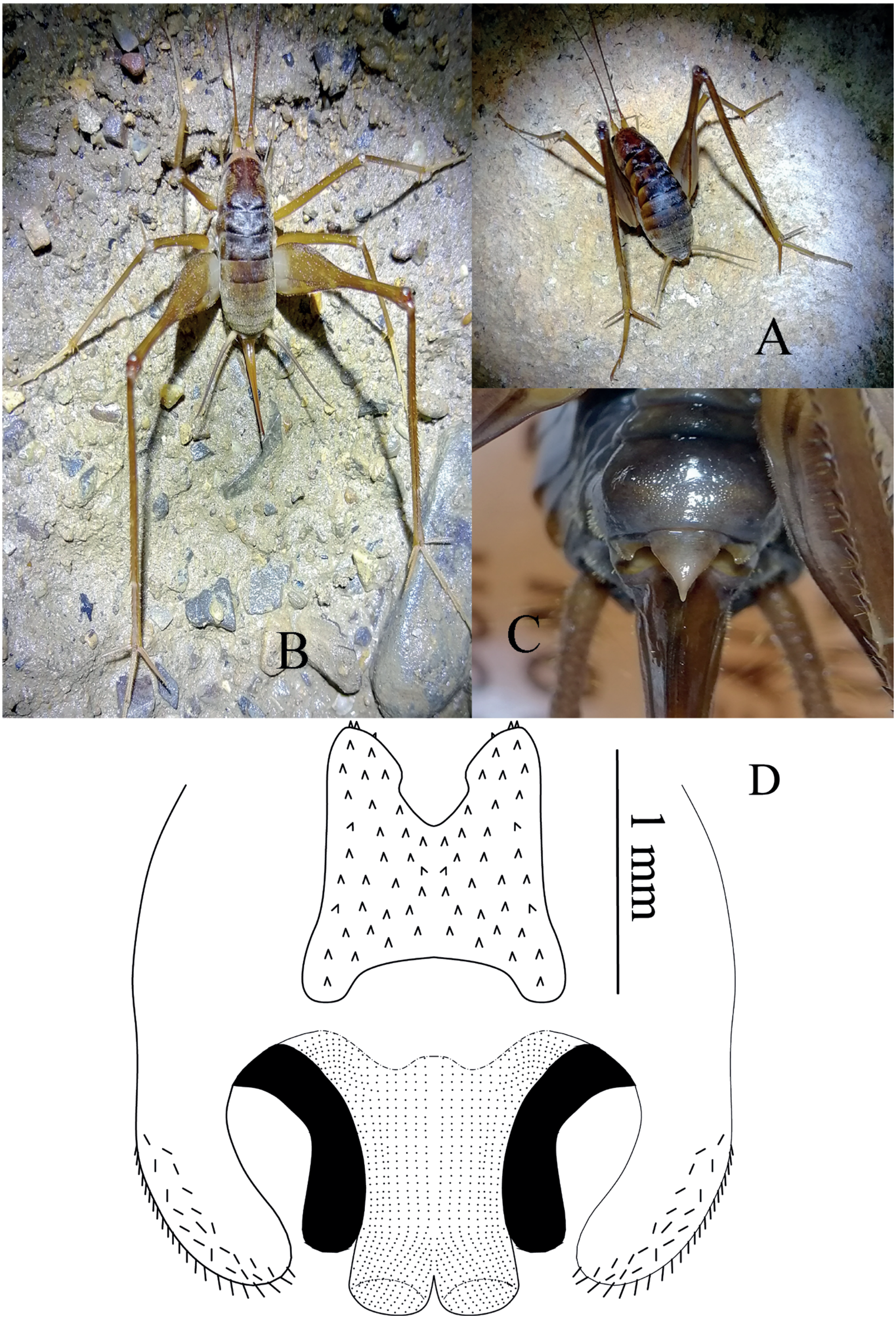

Figure 6. *Tachycines* (*Gymnaeta*) *shanduensis* sp. nov., **A** male live habitus in dorsal view **B** female live habitus in dorsal view **C** female subgenital plate in ventral view **D** male genitalia in dorsal view.

Measurements (mm). Body ♂ 17.3–19.5, ♀17.3.0–19.6; pronotum ♂ 6.8–7.6, ♀ 66–7.3; fore femur ♂ 13.3–15.1, ♀ 13.8–14.6; hind femur ♂ 28.5–31.9, ♀ 28.4–30.7; ovipositor 12.8–13.5.

Distribution of light zone. Light zone, weak light zone, and dark light zone.

Cave adaptation type. Troglophile.

Etymology. The name of the new species refers to the type locality.

Tachycines (*Gymnaeta*) *buyii* sp. nov.

http://zoobank.org/935DF22A-FD7C-4C2C-80FF-04743039FDE2
Figs 7A–C, 15

Specimens examined. ***Holotype*** 1♂, Sanjiaoshan Cave, Ziyun County, 2019-X-2, collected by Xulin Zhou, Haixia Luo, Panpan Ren, Meizhen Deng and Suqin Zhao; ***paratypes***, ♂15, ♀18, same data as holotype.

Diagnosis. This new species is rather similar to *Tachycines* (*Gymnaeta*) *solida* (Gorochov, Rampini & Di Russo, 2006), but differs as follows: the new species epiphallus of male genitalia with upper notch smaller and shallower than lower notch, hind tarsus ventrally with bristles; in *T.* (*G.*) *solida* the epiphallus of the male genitalia with upper notch and lower notch almost the same size, hind tarsus keeled ventrally.

Description. **Male.** Body rather small for this subgenus. Vertex conical tubercles well-developed, bisected from the base; ommateum black and well developed. Legs elongate and slender; fore femur 2.0–2.1 times longer than the pronotum, ventrally unarmed, external genicular lobe with one elongate movable spur, internal knee lobe without spine; fore tibiae beneath with two external spurs and one internal spur. Mid femur with an elongate movable spur on both internal and external genicular lobes, ventrally unarmed; mid tibiae beneath with one external spur and one internal spur. Hind femur without spines ventrally; hind tibiae dorsally with 35–44 internal spines and 36–46 external spines, arranged in groups. Supra-internal spur of hind tibiae not exceeding the ventral apex of hind tarsus. Hind tarsus ventrally with bristles. Epiphallus of male genitalia nearly H-shaped, lower notch rather deeper than upper notch (Fig. 7A, B).

Female. Appearance is similar to the male. Subgenital plate with three lobes, median lobe large and triangular. Ovipositor is slightly shorter than half of the hind femur length, dorsal margin smooth, apical area of ventral margin denticulate.

Coloration. Body brown, mixed with dark brown patches. Hind femur with brown stripe, and dark brown rings located at 2/3 of the length.

Measurements (mm). Body ♂10.5–11.3, ♀10.8–11.5; pronotum ♂3.9–4.5, ♀4.1–4.6; fore femur ♂ 8.3–8.9, ♀ 8.4–9.3; hind femur ♂ 14.7–16.5, ♀ 15.3–17.8; ovipositor 7.2–8.6.

Distribution of light zone. Light zone, weak light zone, and dark light zone.

Cave adaptation type. Troglophiles.

Etymology. The specific epithet refers to the native BuYi people who have lived in southern Guizhou for generations.

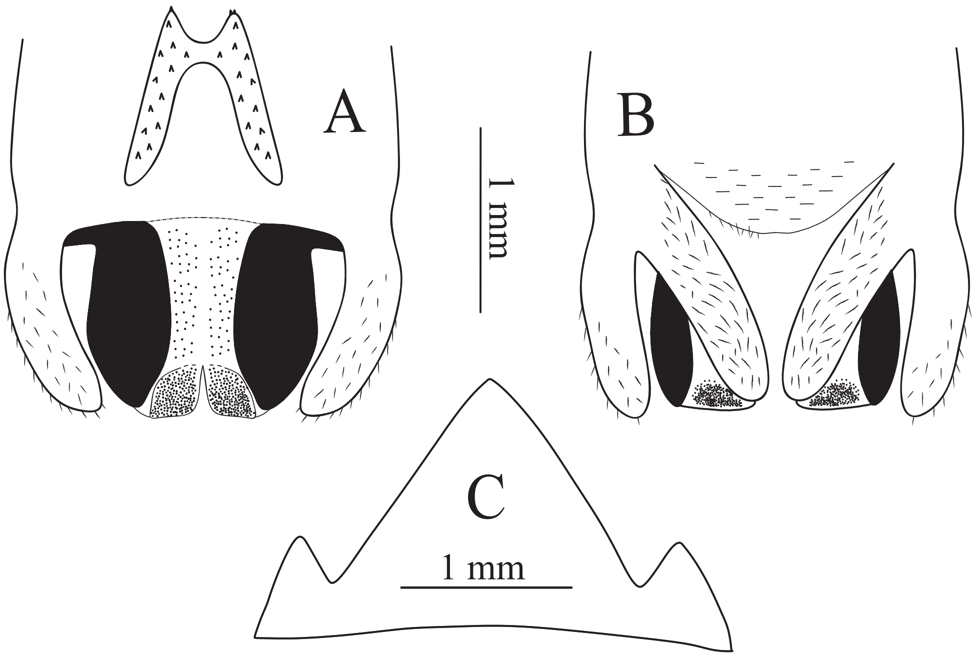

Figure 7. *Tachycines* (*Gymnaeta*) *buyii* sp. nov., **A** male genitalia in dorsal view **B** male genitalia in ventral view **C** female subgenital plate in ventral view.

Tachycines (*Gymnaeta*) *portae* sp. nov.

http://zoobank.org/6A1D6FF0-A4CC-4921-9E0B-0E6EDFC09E7E

Figs 8A–C, 15

Specimens examined. ***Holotype*** 1♂, Niujingchongzi Dong Weining County, 2019-VII-17, collected by Xulin Zhou, Lingzhi Ou, Guang Wang, Rongxiang Su Benzhang Shi, Juan Liao and Liangfeng An. ***paratypes***, 4♂, 2♀, same data as holotype.

Diagnosis. The new species is most closely related to *Tachycines* (*Gymnaeta*) *buyii* sp. nov., but it can be distinguished from the latter by the structure of epiphallus, and hind tarsus keeled ventrally.

Description. Male. Body rather small for this subgenus. Vertex conical tubercles well developed, bisected from the base; ommateum black and well developed. Legs elongate and slender; fore femur 1.8–1.9 times longer than the pronotum, ventrally unarmed, external genicular lobe with one elongate movable spur, internal knee lobe with a small spine; fore tibiae beneath with two external spurs and one internal spur. Mid femur with an elongate movable spur on both internal and external genicular lobes, ventrally unarmed; mid tibiae beneath with one external spur and one internal spur. Hind femur without spines ventrally; hind tibiae dorsally with 65–81 internal spines and 63–81 external spines, arranged in groups. Supra-internal spur of hind tibiae not exceeding the ventral apex of hind tarsus. Hind tarsus keeled ventrally. Epiphallus of male genitalia nearly door-shaped, lower notch rather deeper than upper notch (Fig. 8A, B).

Female. Appearance is similar to the male. Subgenital plate with three lobes, median lobe large triangular (Fig. 8C); ovipositor is slightly longer than half of the hind femur length, dorsal margin smooth, apical area of ventral margin denticulate.

Coloration. Body brown, mixed with brown patches; hind femur with brown stripe.

Measurements (mm). Body ♂6.0–7.0, ♀6.3–7.0; pronotum ♂4.0–4.5, ♀3.8–4.5; fore femur ♂6.8–8.0, ♀6.5–7.5; hind femur ♂10.0–11.5, ♀10.5–11.5; ovipositor 5.5–6.0.

Distribution of light zone. Light and weak light zone.

Cave adaptation type. Troglophile.

Etymology. The specific epithet refers to the shape of epiphallus, the Latin word *porta* meaning door.

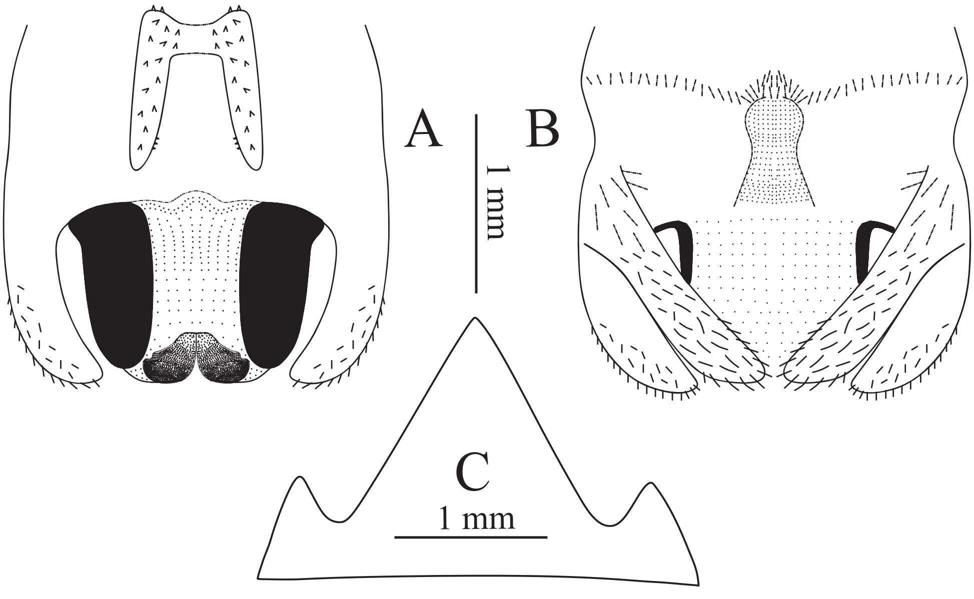

Figure 8. *Tachycines* (*Gymnaeta*) *portae* sp. nov., **A** male genitalia in dorsal view **B** male genitalia in ventral view **C** female subgenital plate in ventral view.

***Tachycines* (*Gymnaeta*) *ziyunensis* sp. nov.**

http://zoobank.org/53F85BED-D0B8-46F5-AC23-0DE66CF2C3F1

Figs 9A–E, 15

Specimens examined. ***Holotype*** 1♂, Sanjiaoshan cave, Ziyun County, 2019-X-2, collected by Xulin Zhou, Haixia Luo, Panpan Ren, Meizhen Deng and Suqin Zhao, ***paratypes*** 15♂, 38♀, same data as holotype.

Diagnosis. The new species is rather similar to *Tachycines* (*Gymnaeta*) *shibenzhangi* sp. nov., it can easily be distinguished by the eyes moderately reduced, ventral conical projections of 3rd–8th abdominal sternites developed, distal mucronate without ciliated;

but the latter of eyes extremely reduce, ventral conical projections of 3rd–8th abdominal sternites developed, distal obtuse and densely ciliated.

Description. Male. Body medium size (Fig. 9D, E). Vertex conical tubercles almost absent, ommateum moderately reduced. Legs elongate and slender; fore femur approx. 2.5–3.1 times longer than the pronotum, ventrally unarmed, external genicular lobe with one elongate movable spur, internal knee lobe with a small spine; fore tibiae beneath with one external spur and one internal spur. Mid femur with an elongate movable spur on both internal and external genicular lobe, ventrally unarmed; mid tibiae beneath without internal and external spur. Hind femur without spines ventrally; hind tibiae dorsally with 9–15 internal spines and 9–13 external spines, sparsely arranged, supra-internal spur of hind tibiae not exceeding the ventral apex of hind tarsus. Hind tarsus ventrally with bristles (Fig.9C). ventral conical projections of 3rd–8th abdominal sternites developed, distal mucronate without cilia. Epiphallus of male genitalia nearly semi-circular, lateral sclerites sub-elliptical; median process of male genitalia with semi-sclerotized lobules at apical part and divided into two lobes, significantly longer than lateral sclerites (Fig. 9A, B).

Female. Appearance is similar to the male. Subgenital plate with three lobes, median lobe large, triangular; ovipositor is slightly longer than half of the hind femur length.

Coloration. The body color is yellowish, face without dark brown stripes, uniformly pale yellow, ventral conical projections of abdominal sternites shiny white. Ovipositor is brownish yellow.

Measurements (mm). Body ♂11.4–12.8, ♀12.2–13.2, pronotum ♂ 3.5–4.3, ♀ 3.9–4.3, fore femur ♂ 11.0–12.1, ♀ 10.2–10.8, hind femur ♂ 17.9–19.2, ♀ 16.9–17.9; ovipositor 8.9–10.3.

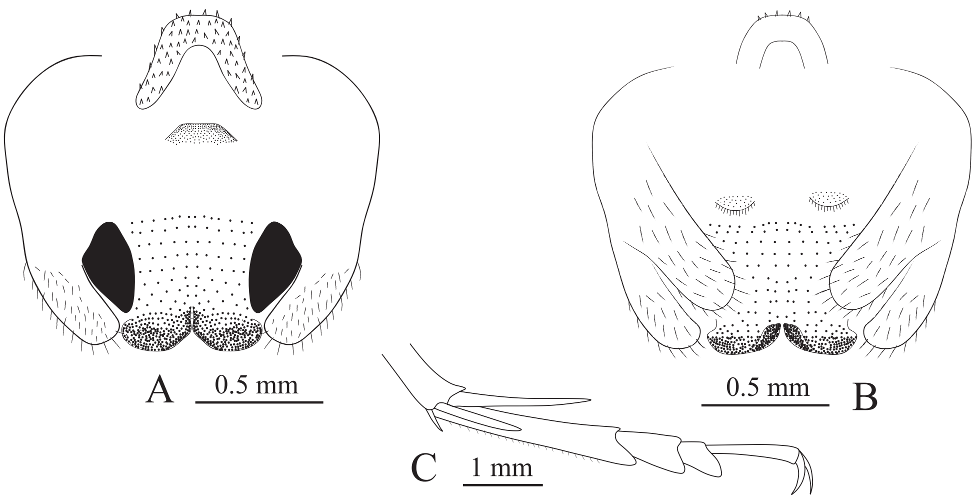

Figure 9. *Tachycines* (*Gymnaeta*) *ziyunensis* sp. nov., **A** male genitalia in dorsal view **B** male genitalia in ventral view **C** hind tarsus in lateral view **D** male live habitus in dorsal view **E** nymph of male, living habitus in dorsal view.

Distribution of light zone. Dark light zone.
Cave adaptation type. Troglobite.
Etymology. The name of the new species refers to the type locality.

Tachycines (*Gymnaeta*) *jialiangensis* sp. nov.

http://zoobank.org/68C1DDDD-C8AD-432B-9BBD-85D4610A79A5
Figs 10A–C, 15

Specimens examined. ***Holotype*** 1♂, Lajilou Cave, Jialiang Town, Libo County, 2017-X-23, collected by Xulin Zhou, Dongshan Xu, Weicheng Yang; ***paratypes***, 4♂, 2♀, same data as holotype.

Diagnosis. This species is similar to *T.* (*G.*) *ziyunensis* sp. nov. but differs in that the hind tarsus ventrally bears bristles in *T.* (*G.*) *ziyunensis* sp. nov., and by the hind tibiae armed with 9–15 spines on both sides; however, the hind tarsus is keeled ventrally in *T.* (*G.*) *jialiangensis* sp. nov., and the hind tibiae are provided with 17–25 spines on both sides.

Description. Male. Body medium in size. Vertex conical tubercles almost absent, ommateum moderately reduced. Legs elongate and slender; fore femur 2.9–3.0 times longer than the pronotum, ventrally unarmed, external genicular lobe with single elongate movable spur, internal knee lobe without spine; fore tibiae beneath with two external spurs and one internal spur. Mid femur with an elongate movable spur on both internal and external genicular lobes, ventrally unarmed; mid tibiae beneath with an external spur and without internal spur. Hind femur without spines ventrally; hind tibiae dorsally with 18–25 internal spines and 17 or 18 external spines, sparsely arranged. Supra-internal spur of hind tibiae

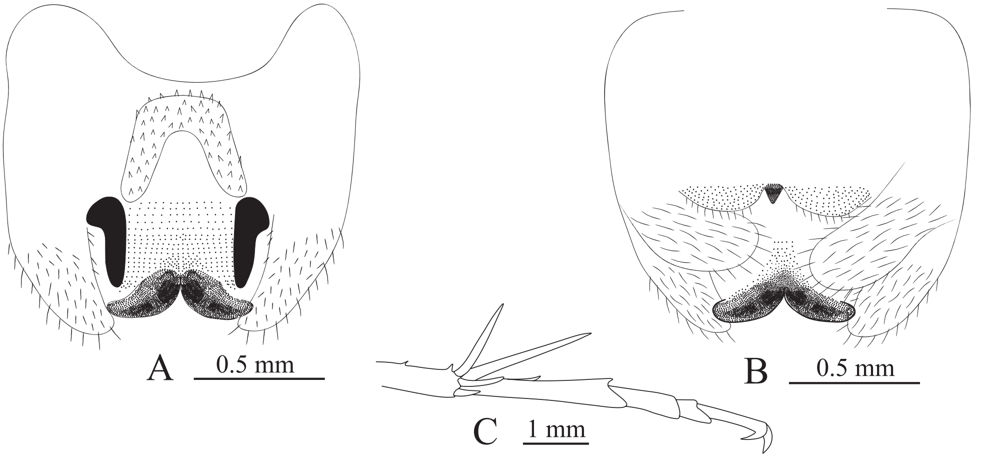

Figure 10. *Tachycines* (*Gymnaeta*) *jialiangensis* sp. nov., **A** male genitalia in dorsal view **B** male genitalia in ventral view **C** hind tarsus in lateral view.

not exceeding ventral apex of hind tarsus. Hind tarsus keeled ventrally (Fig. 10C). ventral conical projections of 3rd–8th abdominal sternites developed, distally mucronate without cilia. Epiphallus of male genitalia nearly semi-circular, lateral sclerites sub-elliptical, median process of male genitalia with semi-sclerotized lobules at apical part and divided into two lobes, significantly longer than lateral sclerites (Fig. 10A, B).

Female. Appearance is similar to the male. Subgenital plate with three lobes, median lobe large, triangular; ovipositor slightly shorter than half of the hind femur length, dorsal margin smooth, apical area of ventral margin denticulate.

Coloration. Body color uniform, pale yellow; face without dark brown stripes; ventral conical projections of 3rd–8th abdominal sternites shiny white.

Measurements (mm). Body ♂ 11.8–12.0, ♀ 11.2–13.0; pronotum ♂ 3.5–3.6, ♀ 3.4–4.2; fore femur ♂ 10.3–10.6, ♀10.4–13.2; hind femur ♂17.5–18.4, ♀17.1–21.66, ovipositor 8.3–9.9.

Distribution of light zone. Dark light zone.

Cave adaptation type. Troglobite.

Etymology. The name of the new species refers to the type locality.

Discussion

Environmental conditions typical of the habitat deep within caves include the complete absence of light, a stable and usually very high humidity (> 95%), relatively low levels of available nutrients, and a nearly constant temperature (Taylor 2004). Cave organisms have been evolving in unusual and fascinating habitats, and the nature of these seems to be the loss of some structures (generally of eyes and pigment), such as in cavefish, cave-dwelling rhaphidophorids, and cave-adapted ground beetles. These organisms successfully navigate within such environments, find and capture food, identify and reproduce with conspecifics, and compete with one another for resources, all in the absence of visual cues. During the adaptive evolution in a cave environment, these cave-dwellers have evolved morphological, physiological, and behavioral modifications, many of which could promote their success lives in constant darkness (William et al. 2019).

There are two subfamilies of Rhaphidophoridae, Aemodogryllinae and Rhaphidophorinae, occurring in East Asia. Among them, species of the subgenus *Gymnaeta* are widely adapted to cave ecosystems, and belong to the Aemodogryllinae. The distribution of cave species of *Gymnaeta* is consistent with that of karst landforms, while the surface species are widely distributed in East Asia, ranging from forests to swamps, deserts, and the Tibet Plateau. According to our observation of many years, the surface-dwelling species of *Gymnaeta* usually demonstrate the following characteristics: a larger body size, darker body coloration, the ommateum and conical tubercles on the vertex well-developed, abdominal sternites without ventral projections, ventral spurs of the fore tibiae and mid tibiae well developed, the dorsal spines of hind tibiae dark and arranged in dense clusters, and the hind femur muscles well-developed, and hence these species are physically agile and good jumpers. Surface-dwelling species of *Gymnaeta* are widely distributed throughout China.

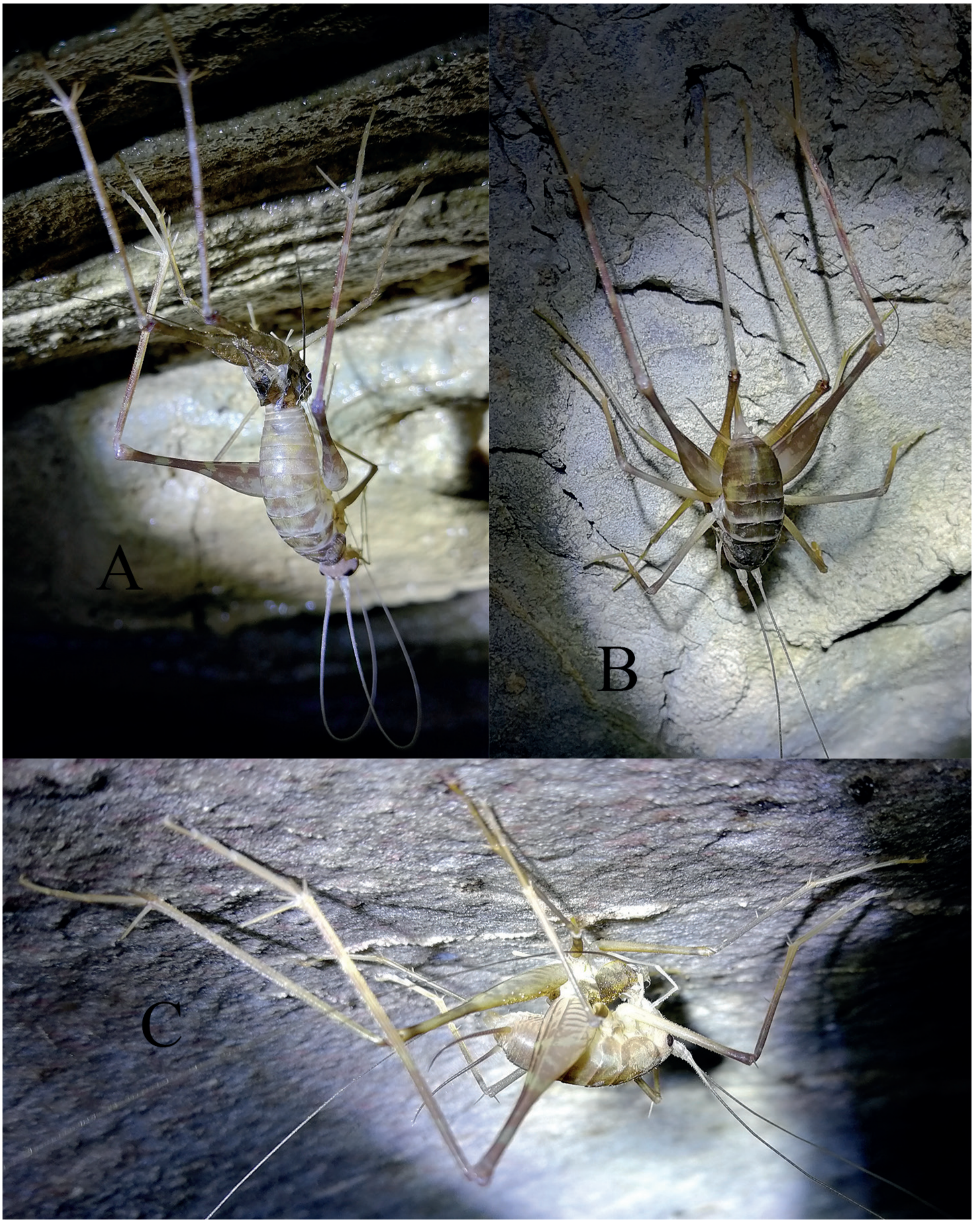

Figure 11. The ecdysial *Tachycines* (*Gymnaeta*) *solida* (Gorochov, Rampini & Di Russo, 2006). **A** in cave Donggou Dong **B, C** in cave Yu Dong.

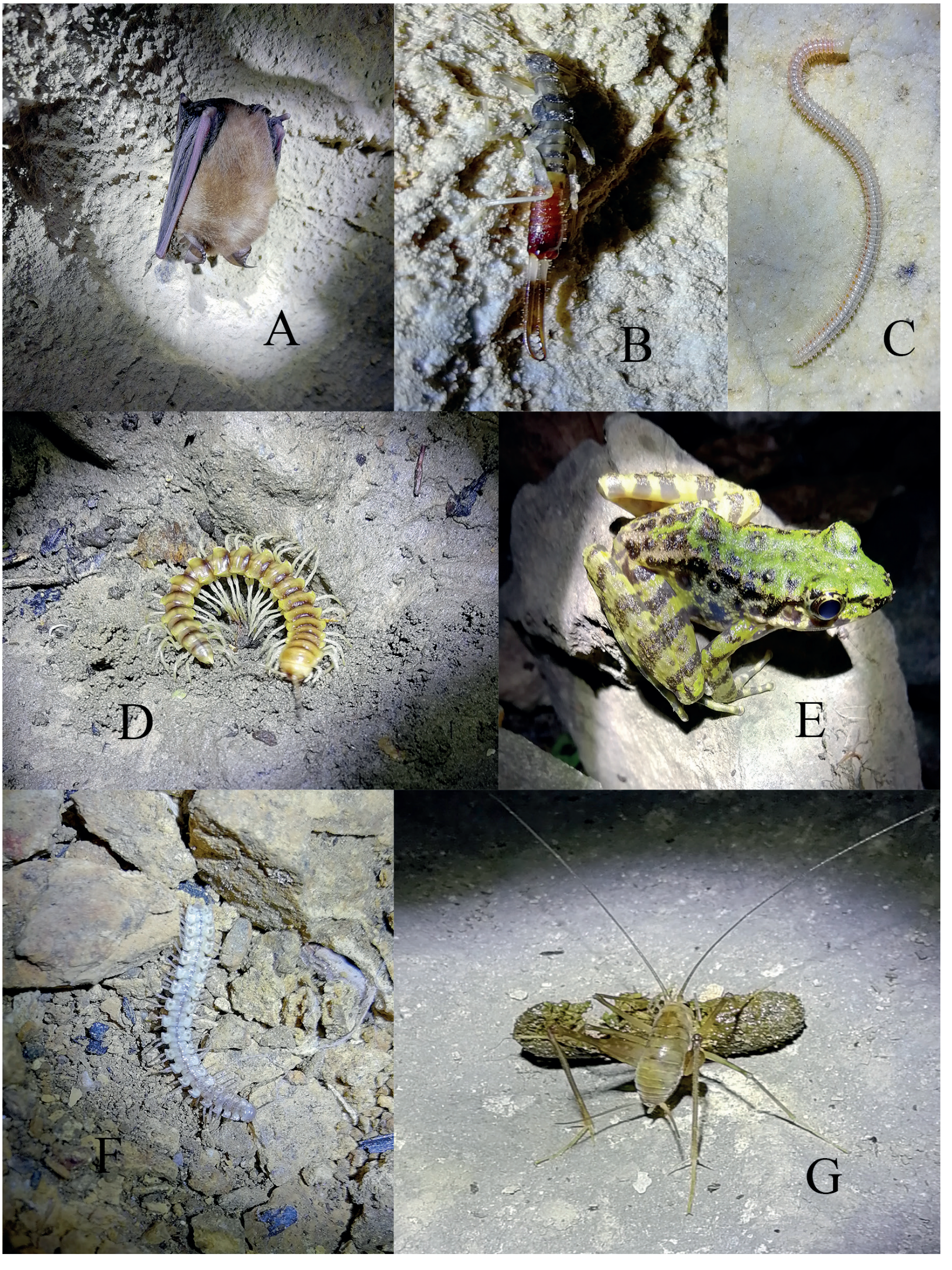

Figure 12. Other species found in the caves **A** *Rhinolophus* sp. (Chiroptera, Rhinolophidae) in cave Donggou Dong **B** a running earwig in cave Xuehua Dong **C** *Glyphiulus* sp. in cave Xuehua Dong **D** a Polydesmida in cave Da Dong **E** an *Odorrana* sp. in cave Wuming Dong near Banzhu town **F** an *Epanerchodus* millipede in cave Sanjiaoshan Dong **G** a *Tachycines* (*Gymnaeta*) sp. nymph feeding on rat droppings from Donggou Dong.

Figure 13. A Entrance of Ban Dong **B** entrance of Mawan Dong from Fuyan town **C** Entrance of Mawan Dong from Lengjiagou **D** entrance of Donggou Dong **E** *Primulina eburnea* in entrance of Ban Dong **F** two collectors in a small humid passageway in cave Sanjiaoshan Dong, showing the habitat where *Tachycines* (*Gymnaeta*) *ziyunensis* sp. nov. was collected.

In contrast, the cave-adapted species of the subgenus have the ommateum and conical tubercles of the vertex reduced, the body appears thinner and smaller, the legs appear more slender, the ventral spurs of fore tibiae and mid tibiae are reduced and sometimes absent, the dorsal spines of hind tibiae are not pigmented and are sparse, the hind femur muscles are not obvious, and the ventral projections of abdominal sternites are developed. The cave-dwelling *Gymnaeta* are not good at jumping, as they have less developed legs muscles, leading them to almost walking on the ground like cave beetles when in danger. They are mainly distributed in karst areas of south China. We think that these morphological changes have occurred through adaptive evolution to cave environments. In addition, we consider the presence or absence of cilia on the distal of abdominal sternites projections in cave-adapted species of the subgenus *Gymnaeta* an important taxonomic characteristic. While these species in Chinese karst caves may be morphologically similar to surface-dwelling species, we suggest they may be genetically distinct, potentially representing different subspecies or lineages and we expect our future work to expand on these theories.

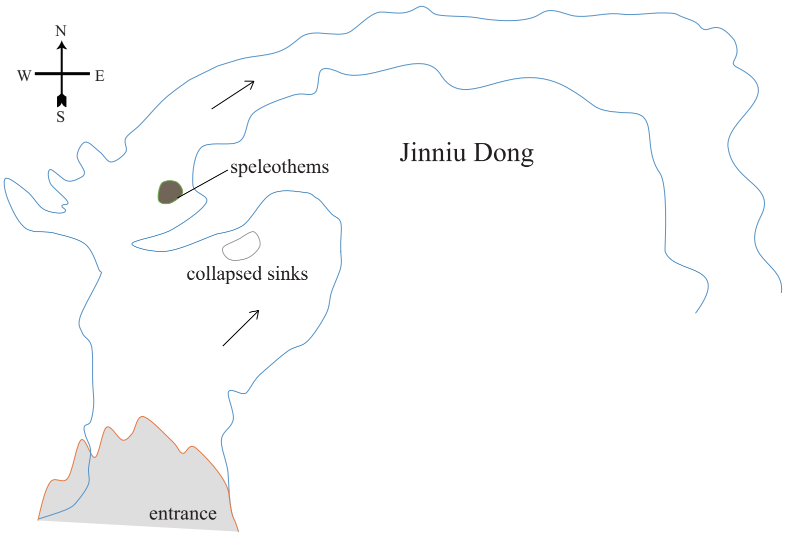

Figure 14. Map of Cave Jinniu Dong, type locality of *Tachycines* (*Gymnaeta*) *jinniui* sp. nov. The arrowhead indicates where in the cave system the rhaphidophorids were found.

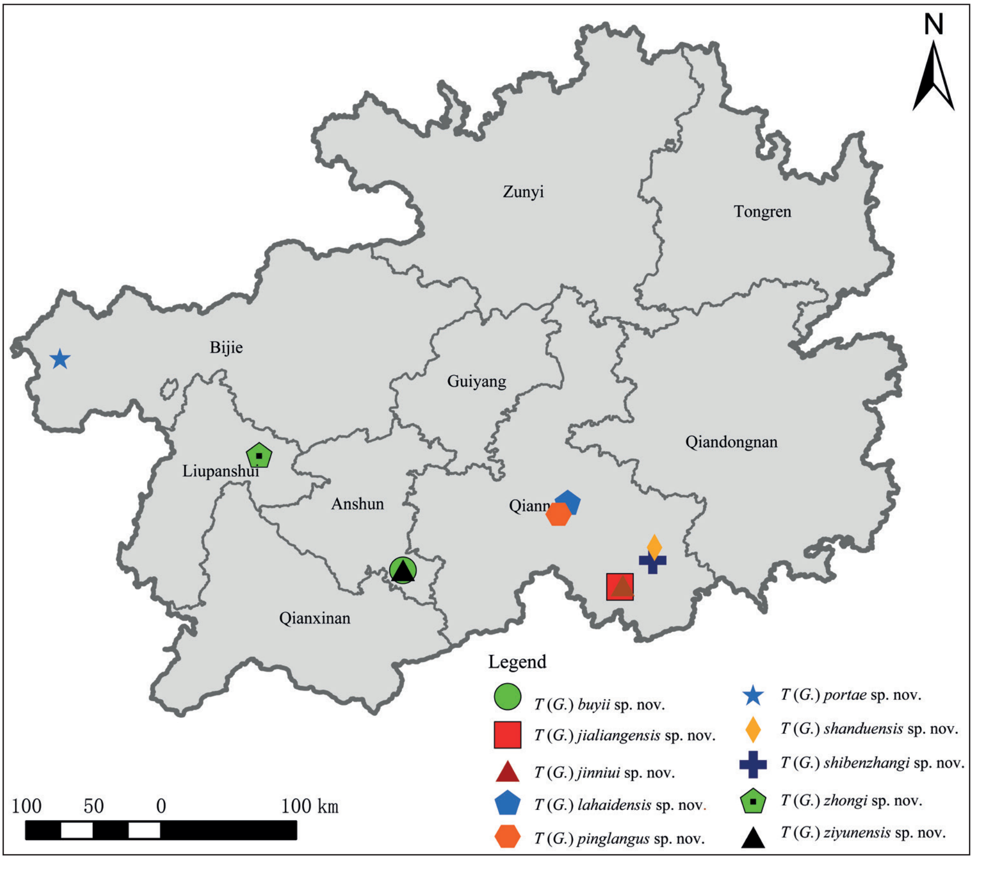

Figure 15. Distribution map for new species of subgenus *Gymnaeta* from Guizhou mentioned in this study.

Conservation suggestions for China's karst cave habitats and species

Caves and their associated ecosystems (mostly karst) represent resources of great value. These values can be grouped into three general clusters: ecological-scientific, economic, and cultural. Cave habitats and species are attracting increasing interest and concern among conservationists, cavers, and speleobiologists, and for good reason. Most troglobionts are highly restricted geographically and often are numerically rare, making them vulnerable to even relatively minor disturbances. As cave organisms are an essential part of biodiversity, it is hoped that we can raise public awareness and take adequate measures to protect karst cave ecosystems.

In China, we have a rich diversity of troglobionts, but the biodiversity of Karst caves in China is under serious threat. We should choose high value and high priority caves, which need emergency attention in relation to protection, management, and conservation actions in the karst region of China. Such a fact does not exclude the need for the conservation of the other caves that should require attention, management, and/or conservation plans coordinated by the environmental supervisory agencies.

Acknowledgments

We are grateful to all collectors of the specimens cited in this paper, especially Qing Wen, Hongmei Tao, Xu Zhang, Dongshan Xu, Yi Luo, Yuanchan Yu, Sheng Chen, Yi Du, Lingzhi Ou, Xiaojing Yang, Shenglou Long, Guang Wang, Benzhang Shi, Lu Rao, Liya Zhang, Dong Jia, Changzhen Zheng, Gui Liang, Haixia Luo, Hailian Lan, Meizheng Deng, Suqing Zhao, Ran Wang, Juan Liao. In addition, uncle Jian and his family (Furong Jiang Town), uncle Bo Zhou and his family, aunt Xiaoxin Zhou and Qin Zhou, uncle Yong Wang, cousin Laixing Wang, teacher Yanfeng Wu, Zhian Wang, Longfei Zhu, Qianqian Xie, Guichang Zhou, Bin Liu, Xing Xiong, Lu Yu, Jin Dai and Junfei An, all of them kindly helped in fieldwork. Thanks to my family for their continued support, and my cousin Tengjiang Zhou for his careful guidance in line illustration. Thanks to Guo Zhong, Xian Hu, Yuchun Lan, Yan Wang, and other friends for their help in image processing. We appreciate Dr. Shulin Yang, Dr. Zhiteng Chen, Xiaolan Wu, Dr. Hao Yu for their help with the manuscript, and we appreciate Zulun Zhao and Shian Ye for their help on preparing the distribution map. This research was supported by the National Natural Science Foundation of China (grant no. 30560024), Science-technology Foundation projects of Guizhou Province (黔科合LH字LKS[2016]7207号，黔科合支撑 [2017]2811号，黔科合重大专项字[2016]3022号，黔科合J字[2011]2181号,黔科合支撑[2019]2858号), Doctoral Fund of Guizhou Normal University, and the fourth high-level innovative talents "thousand level" program of Guizhou Province of 2017, the National Key Research and Development Program of the Thirteenth in China (2016YFC0502606), High-Level Innovative Talents Project of Guizhou Province in 2016 ([2016]21), Innovation Talent Team Capability Improvement Project of Guizhou Academy of Sciences ([2019]08).

References

Adelung N (1902) Beitrag zur Kenntnis der palaarktischen Stenopelmatiden (Orthoptera, Locustodea). Extrait L Annuaire Musee Zoologique L Academie Imperiale Science St. Petersbourg 7: 55–75.

Cigliano MM, Braun H, Eades DC, Otte D (2021) Orthoptera Species File. Version 5.0/5.0. http://Orthoptera.SpeciesFile.org [accessed 22 March 2021]

Deuve T, Li H, Tian MY (2020) Descriptions of the first semi-aphenopsian troglobiotic Patrobini and of a new anophthalmic cave-dwelling Trechini from central Sichuan, China (Coleoptera: Caraboidea), Annales de la Société entomologique de France (N.S.) 56 (2): 93–105. https://doi.org/10.1080/00379271.2020.1722748

Feng XL, Huang SH, Luo CQ (2019) A new species of the subgenus *Tachycines* (*Gymnaeta*) (Orthoptera: Rhaphidophoridae) from karst caves of southern Guizhou, China. Zootaxa 4674(4): 491–495. https://doi.org/10.11646/zootaxa.4674.4.8

Feng XL, Huang SH, Luo CQ (2020) Three new cave species of the subgenus *Tachycines* (*Gymnaeta*) (Orthoptera: Rhaphidophoridae: Aemodogryllinae) from northern Guizhou, China. Zootaxa 4820(3): 563–571. https://doi.org/10.11646/zootaxa.4820.3.9

Gorochov AV (1994) News of systematics and faunistics of Vietnam insects Part 4. Proceedings of the Zoological Institute of the Russian Academy of Sciences 257: 37–50.

Gorochov AV (1998) Material on the fauna and systematics of the Stenopelmatoidea (Orthoptera) of Indochina and someother territories. I. Entomologicheskoe Obozrenie 77(1): 81–105.

Gorochov AV (2001) The higher classification, phylogeny and evolution of the superfamily Stenopelmatoidea. In: Field LH (Ed.), The Biology of Wetas, King Crickets and Their Allies. CABI, Wallingford, 3–33. https://doi.org/10.1079/9780851994086.0003

Gorochov AV (2010) New data on the Chinese representatives of the Genus *Diestrammena* (Orthoptera: Rhaphidophoridae: Aemodogryllinae). Far Eastern Entomologist = Dal'nevostochnyi Entomolog 212: 12–15.

Gorochov AV (2012) Contribution to the knowledge of the fauna and systematics of the Stenopelmatoidea (Orthoptera) of Indochina and some other territories. X. Entomological Review 92(7): 747–772. https://doi.org/10.1134/S0013873812070032

Gorochov AV, Rampini M, Di Russo C (2006) New species of the genus *Diestrammena* (Orthoptera: Rhaphidophoridae: Aemodogryllinae) from caves of China. Russian Entomological Journal 15(4): 355–360.

Jiao ZJ, Niu CY, Liu XW, Lei CL, Bi WX (2008) Descriptions of Chinese species of the subgenus *Diestrammena* (*Gymnaeta*) Adelung (Orthoptera: Rhaphidophoridae). Zootaxa 1917(1): 55–60. https://doi.org/10.11646/zootaxa.1917.1.4

Karny HH (1926) Gryllacridae (China–Ausbeute von R. Mell). Mitteilungen aus dem Zoologischen Museum in Berlin 12: 363.

Karny HH (1929) On the cricket–Locusts (Gryllacrids) of China. Lingnan Science Journal 7: 749–753.

Karny HH (1934a) Schwedisch–chinesische wissenschaftliche Expedition nach den nordwestlichen Provinzen Chinas, unter Leitung von Dr. Sven Hedin und Prof. Sü Ping–chang. Insekten gesammelt vom schwedischen Arzt der Expedition Dr. David Hummel 1927–1930. 6. Rhaphidophorinae. Arkiv för Zoologi, A, 26(2): 1–8.

Karny HH (1934b) Zur Kenntnis der ostasiatischen Rhaphidophorinen (Orth. Salt. Gryllacrididae). Konowia, Zeitschrift fürSystematische Insektenkunde 13(3): 216–218.

Li B, Feng X, Luo C (2021) Four new species of the subgenus *Tachycines* (*Gymnaeta*) (Rhaphidophoridae: Aemodogryllinae: Aemodogryllini) from caves in northern Guizhou, China. Zootaxa 4991(1): 150–160. https://doi.org/10.11646/zootaxa.4991.1.7

Lin YC, Li SQ (2014) New cave-dwelling armored spiders (Araneae, Tetrablemmidae) from Southwest China. ZooKeys 388: 35–67. https://doi.org/10.3897/zookeys.388.5735

Liu WX, Golovatch S (2018) The millipede genus *Epanerchodus* Attems, 1901 in continental China, with descriptions of seven new cavernicolous species (Diplopoda, Polydesmida, Polydesmidae). Zootaxa 4459(1): 53–84. https://doi.org/10.11646/zootaxa.4459.1.2

Qin YY, Liu XW, Li K (2019) Review of the subgenus *Tachycines* (*Gymnaeta*) Adelung, 1902 (Orthoptera, Rhaphidophoridae, Aemodogryllinae, Aemodogryllini). Zootaxa 4560(2): 273–310. https://doi.org/10.11646/zootaxa.4560.2.3

Rampini M, Di Russo C, Cobolli M (2008) The Aemodogryllinae cave crickets from Guizhou, Southern China (Orthoptera, Rhaphidophoridae). Monografie Naturalistiche 3: 129–141.

Song Y, Zhao HF, Luo YF, Li SQ (2017) Three new species of *Pinelema* from caves in Guangxi, China (Araneae, Telemidae). ZooKeys 692: 83–101. https://doi.org/10.3897/zookeys.692.11677

Taylor SJ (2004) Cave Adapted Insects[M]. Springer Netherlands.

Tian MY, Huang SB, Wang XH, Tang MR (2016) Contributions to the knowledge of subterranean trechine beetles in southern China's karsts: five new genera (Insecta: Coleoptera: Carabidae: Trechini). ZooKeys 564: 121–156. https://doi.org/10.3897/zookeys.564.6819

Tian MY, Huang SB, Wang DM (2017) Discovery of a most remarkable cave-specialized trechine beetle from southern China (Coleoptera: Carabidae: Trechinae). ZooKeys 725: 37–47. https://doi.org/10.3897/zookeys.725.21040

Tian MY, Huang SB, Chen MZ, Ding KJ (2019) Remarkable cave-adapted ground beetles of the tribe Pterostichini from China: a new subgenus and three new species (Coleoptera: Carabidae), Annales de la Société entomologique de France (N.S.) 55(1): 1–16. https://doi.org/10.1080/00379271.2018.1546554

Wang CX, Xu X, Li SQ (2017) Integrative taxonomy of *Leptonetela* spiders (Araneae, Leptonetidae), with descriptions of 46 new species. Zoological Research 38(06): 321–448. https://doi.org/10.24272/j.issn.2095-8137.2017.076 [J]

Wen Q (2018) A Preliminary Study on Insect Taxonomy of Karst Cave in Guizhou Province. Guizhou Normal University, Guiyang, Guizhou, 104 pp.

William B. W, David C. C, Tanja P (2019) Encyclopedia of Caves [3rd edn.], Academic Press, Chapter 16 – Biodiversity: China, Pages 127–135. https://doi.org/10.1016/B978-0-12-814124-3.00016-9

Yin ZW, Nomura S, Li LZ (2015) Ten new species of cavernicolous Tribasodites from China and Thailand, and a list of East Asian cave-inhabiting Pselaphinae (Coleoptera, Staphylinidae). Acta Entomologica Musei Nationalis Pragae 55(1): 105–127.

Zhang F, Liu XW (2009) A review of the subgenus *Diestrammena* (*Gymnaeta*) from China (Orthoptera: Rhaphidophoridae Aemodogryllinae). Zootaxa 2272(1): 21–36. https://doi.org/10.11646/zootaxa.2272.1.2

Zhou XL, Yang WC (2020) A new species of *Tachycines* Adelung, 1902 (Orthoptera, Rhaphidophoridae, Aemodogryllinae, Aemodogryllini) from karst caves in Guizhou, China. ZooKeys 937: 21–29. https://doi.org/10.3897/zookeys.937.49173

Zhu QD, Shi FM (2021) Description of four new species of the subgenus *Tachycines* (*Gymnaeta*) Adelung, 1902 (Orthoptera: Rhaphidophoridae) from caves in China and additional notes on some previously known species. European Journal of Taxonomy 764: 1–17. https://doi.org/10.5852/ejt.2021.764.1465

Zhu QD, Chen HM, Shi FM (2020) Remarks on the genus *Tachycines* Adelung, 1902 (Orthoptera: Rhaphidophoridae: Aemodogryllinae) with description of eight new species from caves in southern China. Zootaxa 4809(1): 71–94. https://doi.org/10.11646/zootaxa.4809.1.4

ZooKeys 1109: 141–191 (2022)
doi: 10.3897/zookeys.1109.80775
https://zookeys.pensoft.net

RESEARCH ARTICLE

A peer-reviewed open-access journal
ZooKeys
Launched to accelerate biodiversity research

Revision of the water scavenger beetle genus *Notionotus* Spangler, 1972 in the Neotropical Region (Coleoptera, Hydrophilidae, Enochrinae)

Liza M. González-Rodríguez[1], Andrew Edward Z. Short[1]

1 *Department of Ecology & Evolutionary Biology, and Division of Entomology, Biodiversity Institute, University of Kansas, Lawrence, KS 66045, USA*

Corresponding author: Liza M. González-Rodríguez (lizmgr287@gmail.com)

Academic editor: Mariano Michat | Received 19 January 2022 | Accepted 9 March 2022 | Published 1 July 2022

http://zoobank.org/A418DA2C-02DD-4023-A9F8-41FA0AEAAC83

Citation: González-Rodríguez LM, Short AEZ (2022) Revision of the water scavenger beetle genus *Notionotus* Spangler, 1972 in the Neotropical Region (Coleoptera, Hydrophilidae, Enochrinae). ZooKeys 1109: 141–191. https://doi.org/10.3897/zookeys.1109.80775

Abstract

The Neotropical species of the water scavenger beetle genus *Notionotus* Spangler, 1972 are revised using an integrative taxonomic approach combining morphology with DNA sequence data from two genes. Support exists for four putative species groups into which 18 species are placed, including twelve that are described here as new: *N. bicolor* **sp. nov.** (Suriname), *N. bifidus* **sp. nov.** (Venezuela), *N. brunbadius* **sp. nov.** (Brazil), *N. garciae* **sp. nov.** (Brazil), *N. giraldoi* **sp. nov.** (Brazil), *N. insignitus* **sp. nov.** (Venezuela), *N. juma* **sp. nov.** (Brazil), *N. parvus* **sp. nov.** (Suriname), *N. patamona* **sp. nov.** (Guyana), *N. peruensis* **sp. nov.** (Peru), *N. retusus* **sp. nov.** (Guyana), and *N. vatius* **sp. nov.** (Brazil). Four new synonymies are created: *N. shorti* Queney **syn. nov.** is found to be conspecific with *N. dilucidus* Queney; *N. edibethae* García **syn. nov.**, *N. nucleus* Perkins **syn. nov.**, and *N. perijanus* García **syn. nov.** are found to be conspecific with *N. tricarinatus* Perkins. New records are provided for all previously described species except *N. mexicanus* Perkins. Within the Neotropical region, the range of the genus is greatly expanded and now known from as far south as Bolivia and the Brazilian state of Mato Grosso do Sul. While a few species are found in hygropetric habitats, most are associated with the margins of forested streams. Genitalia and habitus images are provided for nearly all species, as well as a key to the four species groups.

Resumen

Las especies de escarabajos acuáticos detritívoros neotropicales del género *Notionotus* Spangler, 1972 son revisadas usando taxonomía integrativa, combinando morfología con datos de secuencias de ADN para dos genes. Se encontró soporte para cuatro grupos de especies conformados por 18 especies, incluyendo 12 que son aquí descritas como nuevas: *N. bicolor* **sp. nov.** (Suriname), *N. bifidus* **sp. nov.** (Venezuela), *N. brunbadius* **sp. nov.** (Brazil), *N. garciae* **sp. nov.** (Brazil), *N. giraldoi* **sp. nov.** (Brazil), *N. insignitus* **sp. nov**. (Venezuela), *N. juma* **sp. nov.** (Brazil), *N. parvus* **sp. nov.** (Suriname), *N. patamona* **sp. nov.** (Guyana), *N. peruensis* **sp. nov.** (Peru), *N. retusus* **sp. nov.** (Guyana), *N. vatius* **sp. nov.** (Brazil). Se sinonimizan cuatro especies: *N. shorti* Queney **syn. nov.** se considera conespecífico con *N. dilucidus* Queney; *N. edibethae* García **syn. nov.**, *N. nucleus* Perkins **syn. nov.**, y *N. perijanus* García **syn. nov.** son conespecíficos con *N. tricarinatus* Perkins. Nuevos registros son provistos para todas las especies previamente descritas excepto para *N. mexicanus* Perkins. Hasta el momento, en la región neotropical, el rango de distribución del género es ampliamente expandido, se conoce desde el Sur de Bolivia hasta el estado brasileño de Mato Grosso do Sul. Si bien algunas especies son encontradas en hábitats higropétricos, la mayoría de ellas están asociadas a las orillas de arroyos boscosos. Se proveen imágenes del hábito dorsal y genitalia para la mayoría de las especies, al igual que la clave para los cuatro grupos de especies.

Keywords

aquatic insects, integrative taxonomy, new species, South America

Introduction

The genus *Notionotus* Spangler, 1972 is a group of small to minute water scavenger beetles that occur in streams and seepages in the tropics of the New World and Southeast Asia. The original concept of *Notionotus* was based on two new species from the Venezuelan Andes (Spangler 1972). In the Neotropics, its range was soon expanded north to Mexico, with three species described by Perkins (1979) from Guatemala, Mexico and Panama, and subsequent additional species from Venezuela (García 2000). Most recently, three species were described from French Guiana and Guyana (Queney 2010) with additional new records being provided in a series of biotic surveys in Suriname and Guyana (Short and Kadosoe 2011; Short 2013; Short et al. 2017, 2018). *Notionotus* has also been reported from the Old World tropics, with seven species described from southeast India and Southeast Asia (Hebauer 2001, 2003) and southern China (Jia and Short 2011). Currently there are 17 described species, including ten from the Neotropics and seven from tropical Asia.

During the last two decades, extensive fieldwork for aquatic beetles in the Neotropics has resulted in the collection of many new specimens of *Notionotus*, including some that represent new species. We here use an integrative approach, combining adult morphological data with DNA sequences from two gene loci, to revise the Neotropical species of the genus. This revision provides a taxonomic foundation not only for future descriptive work on the genus, but also for evolutionary studies on the diversity and biogeography of the Neotropical region.

Materials and methods

Molecular methods

We amplified and sequenced the mitochondrial gene COI and the nuclear ribosomal gene 28S for 56 specimens of *Notionotus*, including 55 specimens from the Neotropical region and one unidentified specimen from India which we used as an outgroup to root the tree. We sampled specimens from most localities for which we had appropriate material, including a broad geographic sampling of *N. tricarinatus* and *N. dilucidus* as these two species had large ranges with some observed variation in the aedeagus. All specimens were preserved as frozen tissue samples since collection with the exception of the specimen from Costa Rica (SLE2381) which was pinned. Molecular extraction and sequencing methods follow those of Kohlenberg and Short (2017). Resulting DNA sequences were assembled and edited in Geneious R 8.0.5 (Biomatters, http://www.geneious.com/). All sequences are deposited in GenBank (see Table 1 for accession numbers). We used IQ-TREE 1.4.4 (Nguyen et al. 2015) to infer phylogenetic relationships. Each gene was placed in its own partition. The optimal models of substitution for each partition were selected using the Auto function in IQ-TREE 1.4.4. In order to assess nodal support, we performed 1000 ultrafast bootstrap replicates (Minh et al. 2013).

Table 1. List of DNA voucher specimens and GenBank accession numbers used in this study. "N/A" indicates the gene fragment was not successfully amplified or sequenced.

Taxon	Extraction	Locality	COI Accession	28S Accession
N. bicolor	SLE1810	Suriname: Sipaliwini: Kabalebo Nature Resort	ON239446	ON243733
N. bicolor	SLE2120	Suriname: Sipaliwini: Kabalebo Nature Resort	ON239447	N/A
N. bifidus	SLE1113	Venezuela: Amazonas: Tobogán de la Selva	ON239437	ON243725
N. bifidus	SLE2369	Venezuela: Amazonas: Tobogán de la Selva	ON239438	ON243726
N. brunbadius	SLE1553	Brazil: Amazonas: Ducke Reserve	ON239441	ON243731
N. brunbadius	SLE2102	Brazil: Amazonas: Ducke Reserve	ON239442	ON243732
N. dilucidus	SLE0505	Suriname: Brokopondo: Brownsberg Nature Park	ON239422	N/A
N. dilucidus	SLE0506	Suriname: Brokopondo: Brownsberg Nature Park	ON239420	ON243688
N. dilucidus	SLE1799	Suriname: Sipaliwini: Kabalebo Nature Resort	ON239418	ON243695
N. dilucidus	SLE1811	Suriname: Sipaliwini: Kabalebo Nature Resort	ON239419	ON243696
N. dilucidus	SLE2107	Guyana: Region IX: Kusad Mountain	ON239411	ON243702
N. dilucidus	SLE2108	Guyana: Region VI: Upper Berbice	ON239417	ON243692
N. dilucidus	SLE2113	French Guiana: Crique Eau Chire	ON239406	ON243693
N. dilucidus	SLE2114	Suriname: Sipaliwini: Sipaliwini Savanna Reserve	ON239413	ON243703
N. dilucidus	SLE2121	Suriname: Brokopondo: Brownsberg Nature Park	ON239421	ON243694
N. dilucidus	SLE2330	Brazil: Roraima: ca. 13 km NE of Caroebe	N/A	ON243704
N. dilucidus	SLE2335	Guyana: Region 9: Kusad Mountain	ON239412	ON243705
N. dilucidus	SLE2339	French Guiana: St. Laurent du Maroni (ca. 15 km SW)	ON239415	ON243690
N. dilucidus	SLE2366	Venezuela: Amazonas: Tobogán de la Selva	ON239404	ON243687
N. dilucidus	SLE2368	Guyana: Region 8: 7 km NW Chenapau	ON239409	ON243699
N. dilucidus	SLE2374	Brazil: Roraima: Rio Cocal, near Tepequem	ON239408	ON243698
N. dilucidus	SLE2375	Suriname: Sipaliwini: Wehepai	ON239416	ON243706

Taxon	Extraction	Locality	COI Accession	28S Accession
N. dilucidus	SLE2377	Brazil: Roraima: Serra do Tepequém	ON239410	ON243700
N. dilucidus	SLE2378	Venezuela: Bolívar: Piedra de la Virgen	ON239405	ON243701
N. dilucidus	SLE2380	Guyana: Region IX: Parabara	ON239414	ON243707
N. dilucidus	SLE2383	French Guiana: Carbet ONF Grillon	ON239407	ON243697
N. dilucidus	SLE2389	Suriname: Sipaliwini: Raleighvallen	ON239423	ON243689
N. dilucidus	SLE2394	Suriname: Sipaliwini: Raleighvallen	N/A	ON243691
N. garciae	SLE1900	Brazil: Amazonas: Pres. Fig. (ca. 57 km E)	ON239440	ON243730
N. giraldoi	SLE2088	Brazil: Rondonia: Vale do Cachoeiras	ON239428	ON243718
N. giraldoi	SLE2332	Brazil: Rondonia: Ji-Parana (27 km SW)	ON239427	ON243719
N. giraldoi	SLE2334	Brazil: Rondonia: Ji-Parana (27 km SW)	ON239429	ON243720
N. insignitus	SLE1115	Venezuela: Bolívar: La Escalera	ON239443	ON243734
N. juma	SLE1269	Brazil: Amazonas: Novo Airão	ON239435	ON243727
N. juma	SLE2100	Brazil: Amazonas: Ducke Reserve	ON239436	ON243728
N. liparus	SLE2111	Venezuela: Aragua: Henri Pittier National Park	ON239403	ON243714
N. liparus	SLE2123	Venezuela: Barinas: Barinitas (ca. 13 km NW)	ON239401	ON243715
N. liparus	SLE2124	Venezuela: Mérida: Santo Domingo (ca. 2 km SE)	ON239400	ON243716
N. liparus	MSC1820	Venezuela: Aragua: Henri Pittier National Park	ON239402	KC992598
N. lohezi	SLE2337	French Guiana: Savane Roche Virginie	ON239444	ON243737
N. lohezi	SLE2387	French Guiana: Savane Roche Virginie	ON239445	ON243738
N. parvus	SLE2388	Suriname: Sipaliwini: Grensgeberte Moutains	ON239434	ON243729
N. retusus	SLE2110	Guyana: Region 8: ca. 7 km NW Chenapau	N/A	ON243735
N. retusus	SLE2372	Guyana: Region 8: Ayanganna Airstrip	ON239439	ON243736
N. tricarinatus	SLE1112	Venezuela: Zulia: Tukuko	ON239425	ON243710
N. tricarinatus	SLE2371	Venezuela: Zulia: Tukuko	ON239426	ON243711
N. tricarinatus	SLE2381	Venezuela: Aragua: Henri Pittier National Park	ON239424	ON243712
N. tricarinatus	SLE2391	Venezuela: Portuguesa: Biscucuy	N/A	ON243713
N. tricarinatus	SLE2392	Venezuela: Portuguesa: Biscucuy	N/A	ON243708
N. tricarinatus	SLE2397	Costa Rica: Cartago: Tapanti National Park	N/A	ON243709
N. vatius	SLE2104	Brazil: Bahia: Cachoeira Domingos Lopes	ON239430	ON243722
N. vatius	SLE2324	Brazil: Mato Grosso do Sul: Aquidauana (ca. 27 km S)	ON239432	ON243724
N. vatius	SLE2327	Brazil: Mato Grosso do Sul: Aquidauana (ca. 15 km E)	ON239433	ON243723
N. vatius	SLE2385	Brazil: Bahia: Livramento de Nossa Senhora	ON239431	ON243721
N. sp.	SLE0092	India: Tamil Nadu: Bodi Hills, Western Ghats	ON239399	KC992599
N. sp.	SLE2140	Peru: Cusco: 1 km N. Quince Mil	ON239398	ON243717

Morphological methods

We examined more than 900 specimens for this work, including the holotypes of most previously described Neotropical species. The specimens were examined using Olympus SZ61 and SZX7 microscopes and preparation of the specimens and dissection of the genitalia were carried out following the methodology of Girón and Short (2017). There was a modification in the time of exposure to heat of the genitalia during the clearing process depending on the level of sclerotization of the structure, which we reduced the time from 60 min to 30–40 min. Morphological terminology mainly followed Hansen (1991) and terminology adapted from Lawrence and Ślipiński (2013) regarding the use of meso- and metaventrite. Cleared genitalia photos were taken with Olympus BX51 microscope to 400× magnification (except for *N. rosalesi* genitalia to 100×), ~ 7–15 photos were taken per genitalia and stacked using CombineZP software. We generated the species distribution maps using the software SimpleMappr (Shorthouse 2010). The data on the holotype labels are provided verbatim and cited in quotation marks.

Depositories of examined material

CBDG Center for Biological Diversity, University of Guyana, Georgetown (G. Maharaj);
INPA Instituto Nacional de Pesquisas da Amazônia, Manaus, Brazil (M. Oliveira);
NMW Naturhistorisches Museum, Vienna, Austria (M. Jäch);
MALUZ Museo de Artrópodos de la Universidad del Zulia, Maracaibo, Venezuela (J. Camacho, M. García);
MNHN Muséum national d'Histoire naturelle, Paris, France;
MIZA Museo del Instituto de Zoología Agrícola, Maracay, Venezuela (L. Joly);
NZCS National Zoological Collection of Suriname, Paramaribo (P. Ouboter, V. Kadosoe);
SCC Private collection of Simon Clavier, Kourou, French Guiana;
SEMC Snow Entomological Collection, University of Kansas, Lawrence, KS (A. Short);
UMSP University of Minnesota Insect Collection, St. Paul, MN (R. Holzenthal, R.Thomson);
USNM U.S. National Museum of Natural History, Smithsonian Institution, Washington, DC (C. Micheli).

Results

From our integrated approach of combining morphological data with DNA sequence data from two genes, we found support for 18 species in the Neotropical region, including twelve new species. At the same time, we found that two of the most widespread species have been described multiple times, resulting in four new synonymies. For the 14 species that we had molecular data, the maximum likelihood analysis (Fig. 1) recovered two well-supported species groups. We found morphological characters that can be used to diagnose these two clades, which we here define as the *lohezi* and *liparus* species groups. In addition, two species that were not included in our molecular analysis are assigned to their own monotypic species groups as they present unique character combinations that were not consistent with either of the other species groups.

Among the 14 species for which we had molecular data, the minimum uncorrected pairwise distances in COI between any two species was 5.0% (between *N. giraldoi* and *N. vatius*) with the exception of *N. dilucidus*, in which the two specimens from Venezuela (SLE2366 and SLE2378) were 6% divergent from the remaining populations further to the east (Guyana, Brazil, Suriname, French Guiana). We sequenced one specimen from Peru that is known only from a single female, and we were unable to associate it with confidence to any of the described species for which we did not have DNA; however, due to the importance of the male genitalia in identifications, we refrain from describing this species here.

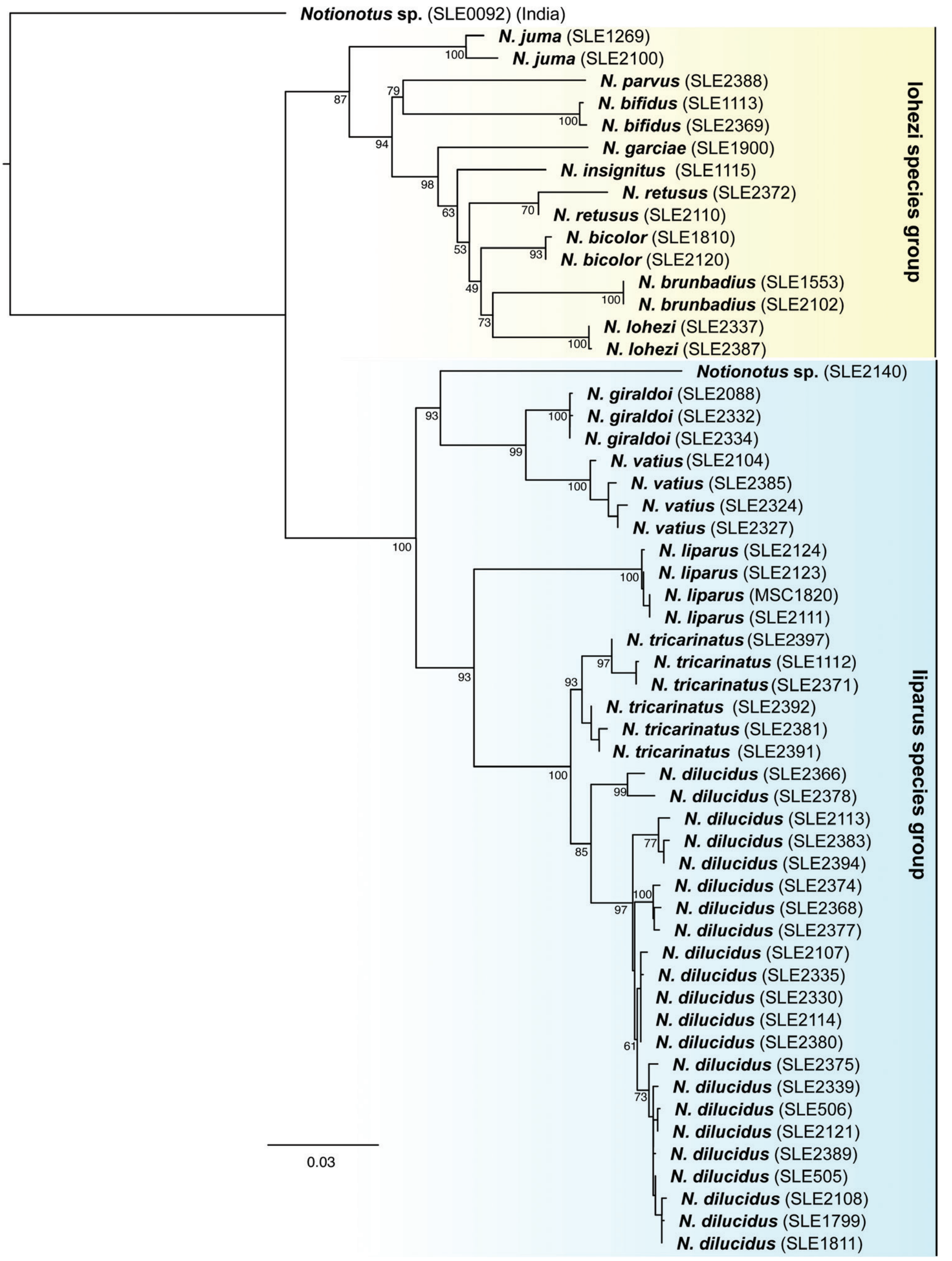

Figure 1. Maximum likelihood phylogeny of *Notionotus* spp. inferred from COI and 28S sequence data. Extraction numbers are given next to each terminal name (see Table 1).

List of species

Notionotus liparus species group

1. *Notionotus dilucidus* Queney, 2010: Brazil (Roraima), French Guiana, Guyana, Suriname, Venezuela
   Notionotus shorti Queney, 2010, syn. nov.
2. *Notionotus giraldoi* sp. nov.: Brazil (Rondonia)
3. *Notionotus liparus* Spangler, 1972: Venezuela
4. *Notionotus mexicanus* Perkins, 1979: Mexico
5. *Notionotus tricarinatus* Perkins, 1979: Costa Rica, Guatemala, Panama, Venezuela
   Notionotus edibethae García, 2000, syn. nov.
   Notionotus nucleus Perkins, 1979, syn. nov.
   Notionotus perijanus García, 2000, syn. nov.
6. *Notionotus vatius* sp. nov. :Brazil (Bahia, Mato Grosso do Sul)

Notionotus lohezi species group

7. *Notionotus bicolor* sp. nov.: Suriname
8. *Notionotus bifidus* sp. nov.: Venezuela
9. *Notionotus brunbadius* sp. nov.: Brazil (Amazonas)
10. *Notionotus garciae* sp. nov.: Brazil (Amazonas)
11. *Notionotus insignitus* sp. nov.: Venezuela
12. *Notionotus juma* sp. nov.: Brazil (Amazonas)
13. *Notionotus lohezi* Queney, 2010: Guyana
14. *Notionotus parvus* sp. nov.: Suriname
15. *Notionotus patamona* sp. nov.: Guyana
16. *Notionotus retusus* sp. nov.: Guyana

Notionotus peruensis species group

17. *Notionotus peruensis* sp. nov.: Peru

Notionotus rosalesi species group

18. *Notionotus rosalesi* Spangler, 1972: Trinidad, Venezuela

Taxonomy

Genus *Notionotus* Spangler, 1972

Notionotus Spangler, 1972: 139.

Type species. *Notionotus rosalesi* Spangler, 1972: 141; by original designation.

Differential diagnosis for Neotropical species. Small to very small beetles, total body length 1.5–2.0 mm. Color yellow, reddish brown, dark and pale brown to black. Body shape oval in dorsal view; moderately convex to convex in lateral view. Antennae with eight antennomeres. Maxillary palps short, nearly half the width of the head, second segment bending outwards, apical segment ~ 2 × as long as the penultimate segment (Fig. 4J; e.g., *N. bifidus* sp. nov.). Eyes reniform in dorsal view. Clypeus and labrum shallowly emarginate anteromedially, lateral margins of the labrum bearing setae. Head, pronotum and elytra with ground and systematic punctures; systematic punctures of the head very sparse. The elytral ground punctation is more evident in some species (Fig. 2A; e.g., *N. liparus*) than in others (Fig. 4G; e.g., *N. garciae* sp. nov.); systematic punctures extremely reduce and sparse detectable for short seta, forming very sparse rows (Fig. 4B; e.g., *N. patamona* sp. nov.); elytra without sutural stria. Prosternum carinate medially, strongly raised, and projected anteromedially. Elevation of mesoventrite strongly raised forming an anteromedial carina consisting of one (Fig. 10A, B) or two longitudinal ridges and one transverse (Fig. 10C, D), extending between procoxae on the same plane as metaventrite. Metaventrite densely pubescent, slightly elevated, with elevation broad posteromedially and convex medially forming a glabrous patch drop-shaped; and two posterolateral glabrous patches in a half-circle shape. Pro- and mesofemora mostly covered with pubescence on basal three-quarters (Fig. 3B; e.g., *N. tricarinatus*); metafemora with pubescence, sometimes on basal three-quarters, or along basal three-quarters of the anterior margin with some setae on the posterior basal margin (Fig. 2H; e.g., *N. rosalesi*). Abdominal ventrites densely pubescent, with fifth ventrite bearing an apical emargination to shallowly truncate. Aedeagus trilobed, size and form variable.

Remarks. As this revision only treats the New World species, we did not comprehensively examine the Old World species to generate a global genus description. Therefore, the diagnosis above should be considered for Neotropical species only. The Old World species of *Notionotus* are generally similar to the New World species, but some species do differ in significant characters: for example, *N. suturalis* Hebaeur, 2003 has a sutural stria and antennae with 9 antennomeres.

Remarks of diagnostic features of *Notionotus* Spangler, 1972. *Body shape and coloration.* The degree of convexity between species is variable; some are moderately convex, others weakly convex. The general dorsal coloration of the body among species ranges from yellow (e.g., *N. tricarinatus*, Fig. 3A) to nearly black (e.g., *N. liparus*, Fig. 2A), however color alone is usually not sufficient on its own to definitively identify most *Notionotus* species. This is due both to the fact that some species share the same coloration, as well as some species have a slight variation in dorsal coloration. Species with unique (so far as currently known) color patterns include *N. liparus* (entirely dark brown to black, Fig. 2A), *N. rosalesi* (tricolored, Fig. 2G) and *N. insignitus* sp. nov. (with pale spot on the elytral disc Fig. 4D). The coloration of the head in some species is uniform, but in others is bicolorous (with typically the frons being darker than the clypeus).

Mesoventrite. In *Notionotus* the elevation of the mesoventrite is composed of two or three laminae: one transverse ridge and one longitudinal (Fig. 10A, B) or two transverse ridges and one longitudinal ridge (Fig. 10C, D), which generally converge and fuse

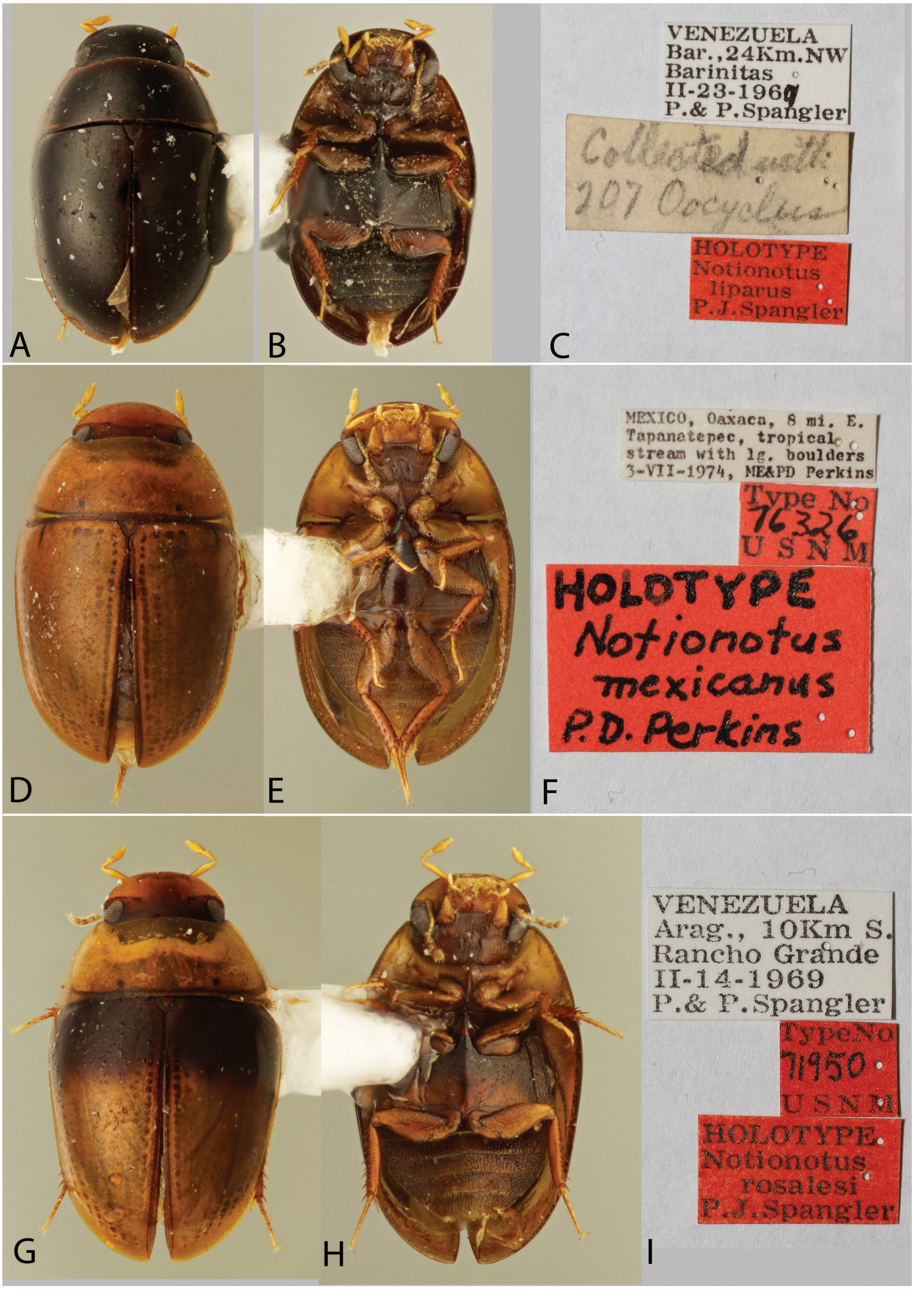

Figure 2. Habitus and labels of *Notionotus* spp.: *N. liparus* (holotype): **A** dorsal view **B** ventral view **C** labels; *N. mexicanus* (holotype): **D** dorsal view **E** ventral view **F** labels; *N. rosalesi* (holotype): **G** dorsal view **H** ventral view **I** labels.

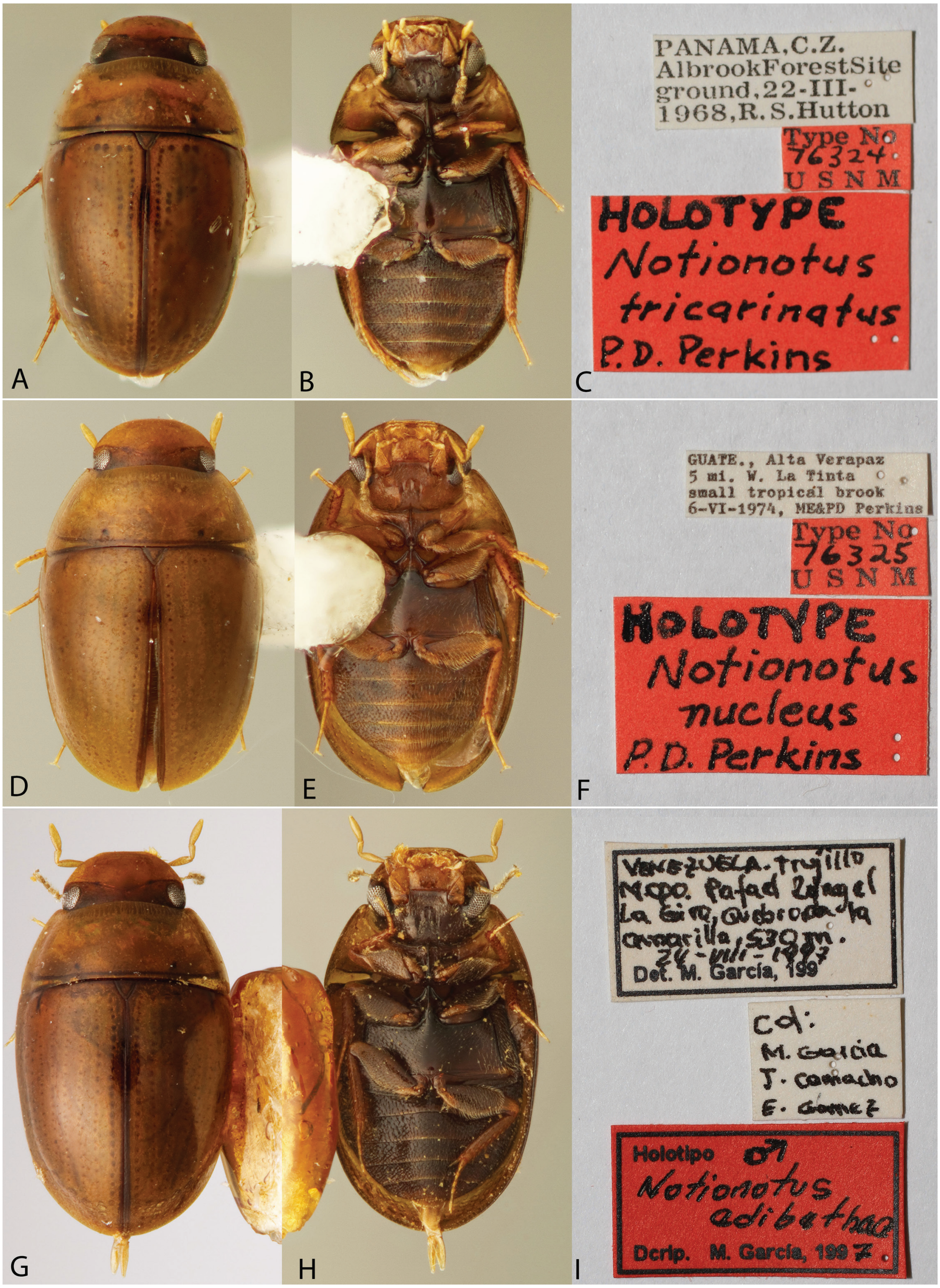

Figure 3. Habitus and labels of *Notionotus* spp.: *N. tricarinatus* (holotype): **A** dorsal view **B** ventral view **C** labels; *N. nucleus* (holotype): **D** dorsal view **E** ventral view **F** labels; *N. edibethae* (holotype): **G** dorsal view **H** ventral view **I** labels.

medially; the shape of the longitudinal ridge shows high variation among species. In general, the transverse ridges are medially elevated and laterally concave. The apex of the transverse ridge can be nearly acute (Fig. 10B), or blunt (Fig. 10C), and lateral sides vary from very to slightly concave or straight. The longitudinal ridge varies, it can be completely sharp or sharp anteriorly and broadening posteriorly reaching the end of the elevation, but it can also be broad anteriorly and sharp posteriorly. The point where the two or three ridges merged can be rounded and obtuse or wide and blunt respectively.

Elytral punctation. The density of the ground punctation is typically sparse, and the degree of impression is variable between species within the genus. In some species, the ground punctation is very weakly impressed and may almost appear absent and low magnification (Fig. 4H; e.g., *N. vatius* sp. nov.); in other cases, it is more coarse and moderately impressed (Fig. 4E; e.g., *N. juma* sp. nov.).

Aedeagus. The shape of the aedeagus is the most important and often crucial feature to identify species of *Notionotus*. Most species in the Neotropics exhibit two different generalized aedeagal forms: in some species, the median lobe and basal piece have the same length, or the median lobe is slightly longer than the parameres (e.g., *N. tricarinatus*, Fig. 6A). However, some species present the median lobe and basal lobe that are shorter than the parameres (e.g., *N. bicolor* sp. nov. (Fig. 8A), *N. retusus* sp. nov. (Fig. 8E), *N. parvus* sp. nov. (Fig. 9E)). In terms of shape, some species present variation in the apex of the median lobe, this is usually rounded (e.g., *N. patamona* sp. nov., Fig. 8D), but it varies from acute (e.g., *N. liparus*, Fig. 7A), emarginated (e.g., *N. juma*, Fig. 8G), and bifurcated (e.g., *N. bifidus* sp. nov., Fig. 9D). Additionally, the width of the median lobe varies from very slender (e.g., *N. giraldoi*, Fig. 7D) to very wide (e.g., *N. bifidus*, Fig. 9D). Nevertheless, in most of the species, the median lobe is wide at the base and slightly narrowing towards the apex.

***Notionotus liparus* species group**

Diagnosis. The species of this group can be diagnosed by the following combination of characters: (1) the shape of the elevation mesoventrite, having one transverse ridge and one longitudinal ridge (Fig. 10A, B); (2) parameres nearly as long as the basal piece; the length of the median lobe and the length of the parameres is approximately subequal. (e.g., *Notionotus liparus*, Fig. 7A).

***Notionotus dilucidus* Queney, 2010**

Figs 5A–J, 10A, 15

Notionotus dilucidus Queney, 2010: 130.

Type material examined. ***Paratype*** **(male):** "♂ ", "*Notionotus*/ *dilucidus* n. sp./ PARATYPE/ P. QUENEY descr. 2010", "Guyane [= French Guiana]: Roura,/ Cacao, Chemin/ Molokoi, crique,/ 16-IX-2009/ leg. P. Queney" (SEMC). ***Paratypes*** **(8 exs.):** same data as the dissected paratype (8 exs., SEMC).

Notionotus shorti **Queney, 2010: 133. syn. nov.**

Type material examined. ***Holotype*** **(male):** "♂ ", "*Notionotus shorti*/n. sp. HOLOTYPE/P. QUENEY descr.2010", "Guyana: Mazaruni-Potaro/District, Takutu Mountains,/ stream debris berlesed, 18-/XII-1983, leg. P.J. Spangler,/ W.E. Steiner & M. Levine" (USNM). ***Paratypes*** **(8 exs.):** same data as the holotype (8 exs., SEMC).

Additional material examined (362 exs.). Brazil: Roraima State: Serra do Tepequém, 3°47.334'N, 61°42.570'W, 14.i.2018, leg. Short, Benetti, & Santana, small forested stream, BR18-0114-02A (1 ex., SEMC, DNA voucher SLE2377); Caroebe, Rio Caroebe, ca. 13 km NE of Caroebe, 00°54.786'N, 59°34.397'W, 150 m, 17.i.2018, leg. Short and Benetti, margins of sandy river, BR18-0117-04A (26 exs., INPA, SEMC, including DNA voucher SLE2330); Rio Jatapú nr. Usina de Jatapú, 00°50.939'N, 59°18.262'W, 145 m, 17.i.2018, leg. A. Short, marginal pools of river, BR18-0117-02A (1 ex., SEMC); Amajari, Rio Cocal, 3°44.135'N, 61°43.542'W, 237 m, 15.i.2018, leg. A. Short, clearwater creek, BR18-0115-01A (6 exs., SEMC, including DNA voucher SLE2374). **French Guiana:** St. Laurent du Maroni ca. 15 km SW, Crique des cascades, 5.34662, -54.10539, 17 m, 4.iii.2020; leg. Short and Neff, stream margin, FG20-0304-02A (1 ex., SEMC); same data except leg. Short, leaf packs on rock, FG20-0304-02B (2 exs., SEMC, including DNA voucher SLE2339); same data except small rock pools in granite FG20-0304-02C (1 ex., SEMC); Carbet ONF Grillon, Piste Bélizon, Crique Grillon, 4.28219, -52.45163, 65 m, 11.iii.2020; leg. Short, rock pools by waterfall, FG20-0311-01C (2 exs., SEMC, including DNA voucher SLE2383); Crique à l'Est above Crique Eau Chire, 3.66383, -53.22193, 156 m, 10.xi.2016, leg. D. Post (1 ex., SEMC, DNA voucher SLE2113). **Guyana: Region 6:** Upper Berbice, ca. 1 km, W basecamp, 4°09.143'N, 58°11.207'W, 170 m, 22.ix.2014, leg. Short, Salisbury, La Cruz, margins of creek, GY14-0921-03H (6 exs., SEMC); Upper Berbice, Basecamp 1, creek next to basecamp (upstream), 4.154817, -58.178616, 24.ix.2014, leg. Short, creek margins, GY14-0924-01A (1 ex., SEMC, DNA voucher SLE2108); Upper Berbice, Basecamp 1, 4°09.289'N, 58°10.717'W, 96 m, 22.ix.2014, leg. Short, Salisbury, La Cruz, GY14-0924-01A (2 ex., SEMC). **Region 8:** Upper Potaro Camp I (ca. 7 km NW Chenapau), 5°0.673'N, 59°38.358'W, 500 m, 14.iii.2014, leg. Short, Salisbury, La Cruz, clear water creek rapids, GY14-0314-01A (7 exs., SEMC); same data except 5°0.660'N, 59°38.283'W, 484 m, 11.iii.2014, leg. Short, Baca, Salisbury, La Cruz, clear water creek rapids, GY14-0311-04A (6 exs., SEMC, including DNA voucher SLE2368); same data except Potaro margin trail, 5°0.571'N, 59°38.202'W, 524 m, 11.iii.2014, leg. Short and Baca, leaf packs in rocky stream, GY14-0311-05A (1 ex., SEMC). **Region 9:** Kusad, Mts., Mokoro Creek, 2°48.531'N, 59°51.900'W, 170 m, 27.x.2013, leg. Short, Isaacs and Salisbury, main seepage area, GY13-1027-03B (2 exs., SEMC); same data except basecamp, leg. A. Short and Washington, on wet rocks, GY13-1024-03C (4 exs., SEMC); same data except 24.x.2013, leg. Salisbury, small rock pool with detritus, GY13-1024-03A (1 ex., SEMC); Kusad, Mts., basecamp area, 2°48.588'N, 59°51.931'W, 194 m, 23.x.2013, leg. A. Short, leaf packs in flow of creek, GY13-1023-02B (9 exs., CDBG, SEMC, including DNA voucher SLE2335); Kusad, Mts., Taraara Wao, 2°47.417'N, 59°53.986'W, 113 m, 28.x.2013, leg. Short, Isaacs and Salisbury, margin and isolated side pools, GY13-1028-01A (5 exs., SEMC, including DNA voucher SLE2107); N. Parabara, creek by basecamp (Bototo wau creek), 2°10.908'N, 59°20.306'W, leg. Short, 31.x.2013, stream margins, GY13-1031-01A (1 ex., SEMC, DNA voucher SLE2380). **Region Mazaruni-Potaro:** Takutu Mountains, 6°15'N, 59°5'W, 2–14. xii.1983, leg. P.D. Perkins, stream ex. leaf packs and twigs (8 exs., SEMC) **Suriname: Brokopondo District:** Brownsberg Nature Park, near Capaci House, 4°56.934'N, 55°10.825'W, 460 m, 17.iii.2017, leg. A. Short, small stream, SR17-0317-01A (1 ex., SEMC); Leo Val/lrene Val return loop trail, 4.95069'N, -55.18599'W, 470 m, 18. iii.2017, leg. Baca and Johnson, stream, SR17-0318-01B (1 ex., SEMC); Leo Val, 4°57'16.08"N, -55°11'26.82"W, 317 m, 19.iii.2017, leg. Short, leaf packs/detritus from behind waterfall, SR17-0319-01C (5 exs., SEMC); same data except SR17-0323-01C (6 exs., SEMC); same data except 23.iii.2017, leg. Baca, submerged woody debris, SR17-0323-01A (1 ex., SEMC); same data except side pools in creek, SR17-0323-01D (1 ex., SEMC); Witti Kreek, 4°55.674'N, 55°09.874'W, 84 m, 21.iii.2017, leg. Short and Baca, small side stream, SR17-0321-01D (2 exs., SEMC, including DNA voucher SLE2121); Brownsberg Nature Park, Mazaroni Val, 04°56.351'N, 55°12.108'W, 394 m, 5.viii.2012, leg. Short, Maier, Mcintosh, forested waterfall and stream, SR12-0805-01A (22 exs., NZCS, SEMC); Brownsberg Nature Park, 04°57.268'N, 55°11.447'W, 317 m, 4.viii.2012, leg. Short, Maier, Mcintosh, forested waterfall and stream, SR12-0804-02A (21 exs., SEMC); Brownsberg Nature Park, 04°56.871'N, 55°10.911'W, 462 m, 4.viii.2012, leg. Short, Maier, McIntosh, SR12-0804-01A (2 exs., SEMC including SLE505 and SLE506). **Sipaliwini District:** Kabalebo Nature Resort: Bwkw rapids, 4.40041°N, 57.24658°W, 90 m, 9–10.9iii.2019, leg. Short and class, large isolated muddy pool by river, SR19-0309-02A (1 ex., SEMC); Moi Moi creek, 4.42313°N, 57.19198°W, 104 m, 10–14.iii.2019, leg. Short and class, rock and detrital pools along creek, SR19-0310-01A (3 exs., SEMC); same data except leg. Short and Baca, small seeps, SR19-0310-01F (10 exs., SEMC); same data except leg. Short, margin of detrital pool in drying creekbed, SR19-0310-01G (5 exs., SEMC); same data except leg. Short, Baca and class, SR19-0310-01J (1 ex., SEMC); same data except leg. Baca, margin of stream pool with root mats, SR19-0310-01L (5 exs., SEMC); same data except leg. Short and class, SR19-0310-01M (10 exs., SEMC, including DNA voucher SLE1799); same data except Leg. S. Baca, upstream riparian habitats, SR19-0310-01N (2 exs., SEMC); Sand Crk, 4.38476°N, 57.24636°W, 72 m, 13–15.iii.2019, leg. Short and Baca, upper marginal pool along river, SR19-0313-01D (2 exs., SEMC); Charlie Falls, 4.38302°N, 57.21161°W, 174 m, 11.iii.2019, leg. Short and class, rock pools in creekbed, SR19-0311-01A (39 exs., NZCS, SEMC, including DNA voucher SLE1811); same data except leg. Short, seepage, SR19-0311-01B (7 exs., SEMC); Sipaliwini Savanna Nature Res. 4-Brothers Mts, 2°00.342'N, 55°58.149'W, 337 m, 31.iii.2017, leg. Short and Baca, clear water stream sandy with detritus, SR17-0331-01B (31 exs., SEMC, including DNA Voucher SLE2114); same data except leg. Baca, small rocky creek, SR17-0331-01A (1 ex., SEMC); Raleighvallen Nature Reserve, Fungu Island, 4°43.459'N, 56°12.658'W, 30 m, 14.iii.2016, leg. A. Short, isolated river margin pools, rocky bottom, SR16-0314-01E (1 ex., SEMC); Coppename Rvr-Voltzberg trail, 15.iii.2016, leg. A. Short, small sandy stream, SR16-0315-02A (1 ex., SEMC); Lolopaise Area, 4°42.48'N, 56°13.15908'W, 24 m, 18.iii.2016, leg. Short et al., intermittent stream margins, flotation, SR16-0318-01D (1 ex., SEMC); Brownsberg Nature Park, 04°56.871'N, 55°10.911'W, 462 m, 4.viii.2012, leg. Short, Maier, Mcintosh, forested stream with lots of detritus, SR12-0804-01A (8 exs., SEMC); Raleighfallen Nature Reserve, trail to Raleighfallen, 04°42.480'N, 56°13.159'W, 24 m, 27.vii.2012, leg. Short, Mcintosh and Kadosoe, creek margins, SR12-0727-03A (22 exs., SEMC, including DNA voucher SLE2394); same data except leg. C. Mcintosh, detrital pools near creek in forest, SR12-0727-03D (1 ex., SEMC); Raleighvallen Nature Reserve Voltzberg Station, 04°40.910'N, 56°11.138'W, 78 m, 9.vii.2012, leg. Short, Maier, McIntosh, and Kadosoe, stream margins, SR12-0729-02A (1 ex., SEMC, DNA voucher SLE2389); Raleighfallen Nature Reserve, Voltzberg trail, 04°40.910'N, 56°11.138'W, 78 m, 30.vii.2012, leg. C. Maier and V. Kadosoe, margin of stream, SR12-0730-01A (1 ex., SEMC); Raleighfallen Nature Reserve, Fungu island, 04°43.459'N, 56°12.658'W, 30 m, 1.viii.2012, leg. Short, Maier, Mcintosh and Kadosoe, small creek, SR12-0801-01B (2 exs., SEMC); Camp 2, on Sipaliwini District, CI-RAP Survey, 2°10.973'N, 56°47.235'W, 210 m, 29–30.viii.2010, leg. Short and Kadosoe, Inselberg, SR10-0829-01A (2 exs., SEMC); Camp 1, Upper Palumeu, CI-RAP Survey, 2.47700°N, 55.62941°W, 275 m, 11.iii.2012, leg. Short and Kadosoe, around waterfall, SR12-0311-03A (2 exs., SEMC); Camp 3, Wehepai, 2°21.776'N, 56°41.861'W, 237 m, 4–6.ix.2010, leg. Short and Kadosoe, sandy forest creek, SR10-0904-01A (36 exs., SEMC, including DNA voucher SLE2375). **Venezuela: Bolívar State:** Piedra de la Virgen, 6°5'14.1"N, 61°23'55.8"W, 400 m, 31.vii.2008, leg. A. Short M. García, L. Joly, small forest stream, AS-08-056 (7 exs., SEMC, including DNA voucher SLE2378). **Amazonas State:** Tobogán de la Selva, 5°23.207'N, 67°36.922'W, 125 m, 14.i.2009, leg. A. Short, clumps of wet leaves on rock, VZ09-0114-01D (6 exs., MIZA, SEMC, including DNA voucher SLE2366).

Differential diagnosis. The general coloration of *Notionotus dilucidu*s is similar to *N. giraldoi*, *N. mexicanus*, and *N. tricarinatus* and these species are very difficult to differentiate with external characters alone. However, the shape of the aedeagus in *N. dilucidus* is quite distinct: the outer and inner margins of the parameres are sinuate, the apex of the parameres presents an indentation in which the depth can vary from very deep, slightly deep, or almost not distinguishable and pointing outwards (Fig. 5A–J).

Description. ***Size and form*:** Body length 1.6–1.8 mm. Body form elongate oval, moderately convex in lateral view (e.g., Fig. 2D). ***Color and punctation*:** Dorsally yellow to pale brown, head mostly yellow and frons pale brown; pronotum paler than elytra, with two small black round spots along posterior margin (e.g., Fig. 2D). Ventrally brown; maxillary palps and antennae yellow (antennal club slightly darker), mouth parts and legs pale brown. Clypeus and labrum with dense, fine, and weakly impressed ground punctation (punctures separated by 1–2 × their width); pronotum and elytra with ground punctation fine, weakly impressed and sparser than on head (punctures separated by 3 × their width). ***Head*:** Clypeus and labrum shallowly emarginate anteromedially, lateral margins of the labrum bearing setae. ***Thorax*:** Prosternum carinate medially, strongly raised, pointing anteriorly and acute. Elevation of mesoventrite with one transversal ridge, elevated medially, lateral sides concave; longitudinal ridge sharp, the point where the two ridges merged rounded and obtuse (Fig. 10A); elevation flat in lateral view; mesoventrite with triangular shape in ventral view. Metaventrite convex in the median region, pubescent with narrow glabrous patch on the medial and posterolateral area, medial region patch drop-shaped; anterior margin extending to mesoventrite elevation. Metafemora densely covered with hydrofuge pubescence on basal three-quarters (e.g., Fig. 2E). ***Abdomen*:** Abdominal ventrites very densely pubescent. Aedeagus (Fig. 5A) basal piece nearly the same length of a paramere. Base of the parameres slightly narrower than the base of the median lobe; outer margins sinuate, tapering almost reaching the apex, inner margins sinuate, apex of the parameres slightly bending outwards, rounded in the outer margin with an indentation in the inner margin (the depth of the indentation varies, Fig. 5A–J). Median lobe nearly as long as the parameres or a bit longer, broad at the base and gradually narrowing to the apex, apex of the median lobe rounded.

Variation. There is significant variation in the apex of the parameres of the aedeagus. The paramere tip is weakly sclerotized, as evidenced by its very pale to white appearance in cleared specimens (e.g., Fig. 5A–J). This tip varies from nearly evenly rounded (e.g., Fig. 5D, G) to possessing some level of indentation on the inner margin (e.g., Fig. 5A, H). Although this variation seems in part to be real, it also seems to be partly caused by artificial distortions; for example, the weakly sclerotized apex may become indented or inflated depending on the state of the genitalia during preparation. This would explain why there is a large variation in form as well as why the tip appears to be exhibit subtly asymmetry between parameres (e.g., Fig. 5C, F).

Distribution. This species is widely distributed throughout the Guiana Shield region, from Tobogán de la Selva in Venezuela east to the coast of French Guiana (Fig. 15). Reported from Suriname in Short and Kadosoe (2011) and Short (2013; as *N. shorti*) and from Guyana as *Notionotus* sp. B in Short et al. (2018).

Life history. This species is the most common and abundant species of the genus in the Guiana Shield region and is frequently collected in leaf packs or along the margins of forested streams. They are typically found in streams that are lined with detritus and have rocky or sandy substrates. Although some specimens have been collected in seepage-like habitats or adjacent to seepages, this does not seem to be a primary or favored habitat for this species.

Remarks. Queney (2010) described *N. dilucidus* based on specimens from several closely situated localities in French Guiana, and *N. shorti* based on a long series of specimens from a single collecting event in Guyana. The primary feature used to separate the two taxa was the apex of the parameters, which was given as “parameres apically shortly curved outwards” in *N. dilucidus* and “parameres apically almost straight” in *N. shorti*. We examined material from the type series of both species and confirmed there are notable differences in the paramere shape. If we only had access to the specimens that Queney (2010) examined and no other data, we also would have very likely concluded they were different species and described them as such. However, as we examined recently collected specimens from numerous other localities in the eastern Guiana Shield, we observed quite a bit of variation in the shape of the parameres that encompassed the forms present in *N. dilucidus* and *N. shorti*. In some cases, we noticed variation in this feature even among specimens from the same series. Additionally, the apex of the paramere even occasionally appears slightly asymmetrical in some dissections (e.g., Fig. 5F, J).

To help interpret these morphological observations, we sequenced 22 specimens that span the entire width of the Guiana Shield, including specimens from Venezuela, Brazil, Guyana, Suriname, and French Guiana. These specimens also represented a range of paramere form diversity. In general, we found little meaningful molecular divergence among these populations (Fig. 1) and these differences were not correlated to observed variations in the paramere apex. Therefore, we here consider *N. shorti* as a junior subjective synonym of *N. dilucidus*.

Among all sequenced specimens, the maximum pairwise divergence in the gene COI was 6.0%. Although this is on the higher end of intraspecific divergence observed in hydrophilids, it is seen in some taxa (see Short and Girón 2018; Smith and Short 2020). Additionally, given that its geographic range spans 1500 kilometers, it is not surprising to see such divergences. The two Venezuelan populations (from Tobogán de Selva in Amazonas State and the Escalera region of Bolívar State) were the most genetically distinct and sister to the more eastern populations. Indeed, with these samples removed, the maximum intraspecific divergence among remaining specimens drops to just 3.8%. However, we did not observe any significant morphological differences from these Venezuelan populations and therefore consider them to be part of a broader definition of *N. dilucidus*.

As both *N. dilucidus* and *N. shorti* were proposed in the same work (Queney 2010), we use our authority as first revisors (ICZN article 24.2.2) to give precedence to *N. dilucidus* as the valid name for this species.

Notionotus giraldoi **sp. nov.**

http://zoobank.org/05F6195D-EB81-47FB-B7FD-2256F49D877F
Figs 4I, 7D, 13A, 14

Type material. ***Holotype*** **(male):** "BRAZIL: Rondonia: Novo [*sic*: Nova] Uniao/ -10.91764°, -62.377°, 359 m/ Vale do Cachoeiras; 10.vii.2018/ leg. Short; Margin of rocky/ stream; BR18-0710-02B" (INPA). ***Paratypes*** **(56 exs.): Brazil: Mato Grosso do Sul State:** Rio Bento Gomes (Pantanal), Campo Allegre I, 15°45'S, 56°33'W, 1993–1994, leg. E. Stuhr, spring-fed brook, (9 exs., NMW, SEMC). **Rondonia State:** Same data as holotype (13 exs., SEMC, including DNA Voucher SLE2334); same data except margin of rocky stream with waterfall (12 exs., SEMC); same data except small sandy-bottom stream margin BR18-0710-02A (20 exs., INPA, SEMC, including DNA voucher SLE2088); same data except flotation of marginal root mats, BR18-0711-01C (1 ex., SEMC); Ji-Parana (27 km SW), Rio Urupa, rock pools along

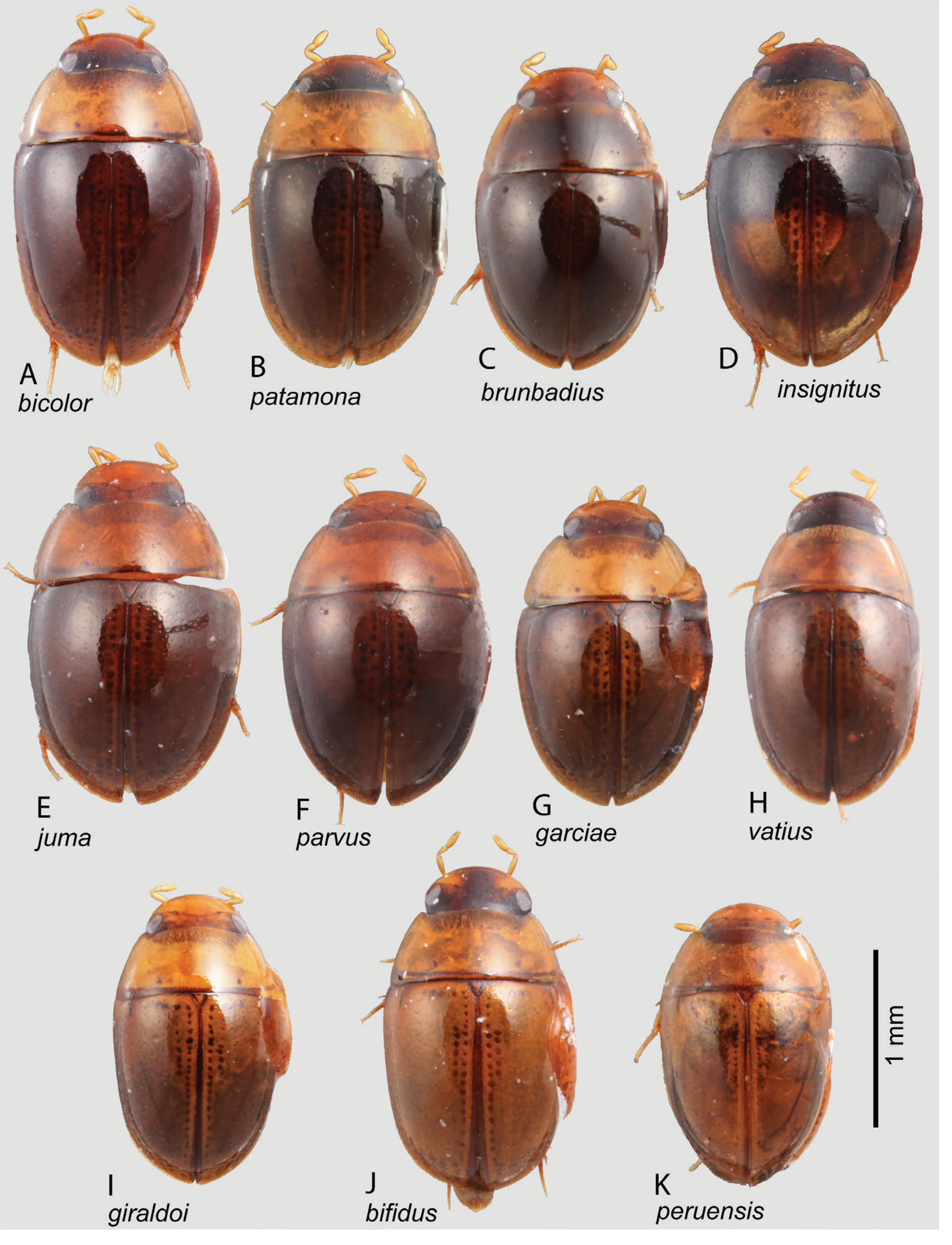

Figure 4. Habitus of *Notionotus* spp.: **A** *N. bicolor* (paratype) **B** *N. patamona* (holotype) **C** *N. brunbadius* (holotype) **D** *N. insignitus* (paratype) **E** *N. juma* (paratype) **F** *N. parvus* (holotype) **G** *N. garciae* (paratype) **H** *N. vatius* (holotype) **I** *N. giraldoi* (paratype) **J** *N. bifidus* (paratype) **K** *N. peruensis* (holotype).

margins of river, -11.03618, -62.14465, 135 m, leg. Short, 10.vii.2018, rock pools along margins of river, BR18-0710-01A (1 ex., SEMC, DNA voucher SLE2332).

Differential diagnosis. The dorsal coloration, shape of the elevation of the mesoventrite, area of pubescence on the metafemur and degree of impression of the ground punctation of *Notionotus giraldoi* are very similar to *N. dilucidus*, *N. mexicanus*, *N. tricarinatus*. It can be distinguished only by its aedeagus, including the unique shape of the parameres with a depression of the inner margin, as well as by the abrupt narrowing in the midlength of the median lobe (Fig. 7D).

Description. ***Size and form*:** Body length 1.7–1.9 mm. Body form elongate oval, convex in lateral view (Fig. 4I). ***Color and punctation*:** Dorsally yellow, head yellow; pronotum paler than elytra, with two small black round spots along posterior margin (Fig. 4I). Ventrally brown; maxillary palps, mouthparts, antennae (antennal club slightly darker) and legs yellow. Clypeus and labrum with dense, fine, and weakly impressed ground punctation (punctures separated by 2 × their width); pronotum and elytra with ground punctation fine, weakly impressed and sparser than on head (punctures separated by 3 × their width). ***Head*:** Clypeus and labrum shallowly emarginate anteromedially, lateral margins of the labrum bearing setae. ***Thorax*:** Prosternum carinate medially, strongly raised, pointing anteriorly and acute. Elevation of mesoventrite with one transversal ridge, elevated medially, lateral sides concave; longitudinal ridge sharp, the point where the two ridges merged rounded and obtuse (e.g., Fig. 10A, B); elevation flat in lateral view; mesoventrite with triangular shape in ventral view. Metaventrite convex in the median region, pubescent with narrow glabrous patch on the medial and posterolateral area, medial region patch drop-shaped; anterior margin extending to mesoventrite elevation. Metafemora densely covered with hydrofuge pubescence on basal three-quarters. ***Abdomen*:** Abdominal ventrites very densely pubescent. Aedeagus (Fig. 7D) with basal piece nearly the same length of a paramere. Base of the parameres slightly narrower than the base of the median lobe; outer margins sinuate, inner margins depressed in the midlength, depression extending to apex without reaching it; apex of parameres wide and blunt. Median lobe length almost equal to the parameres, wide at basal region, narrowing abruptly in the midlength, apical third slender, narrow, and rounded.

Etymology. L. M. González-Rodríguez names this species in honor of Juan José Giraldo Gutiérrez in gratitude for the encouragement and support in her career.

Distribution. Known from several localities in the Brazilian States of Rondonia and Mato Grosso do Sul (Fig. 14).

Life history. This species was collected along the margins of two adjacent streams, one with a sandy bottom and one with a rocky bottom (Fig. 13A). Specimens were collected by agitating the sand and detritus along the stream margin as well as washing root mats in tubs of water.

Notionotus liparus Spangler, 1972
Figs 2A–C, 7A, 11A, B, 14

Notionotus liparus Spangler, 1972: 144.

Type material examined. ***Holotype*** **(male):** “VENEZUELA/ Bar., 24 Km. NW/ Barinitas/II-23-1969/P.&P. Spangler”, “Collected with/ 207 Oocyclus”, “HOLOTYPE/ Notionotus/liparus/P.J. Spangler” (USNM).

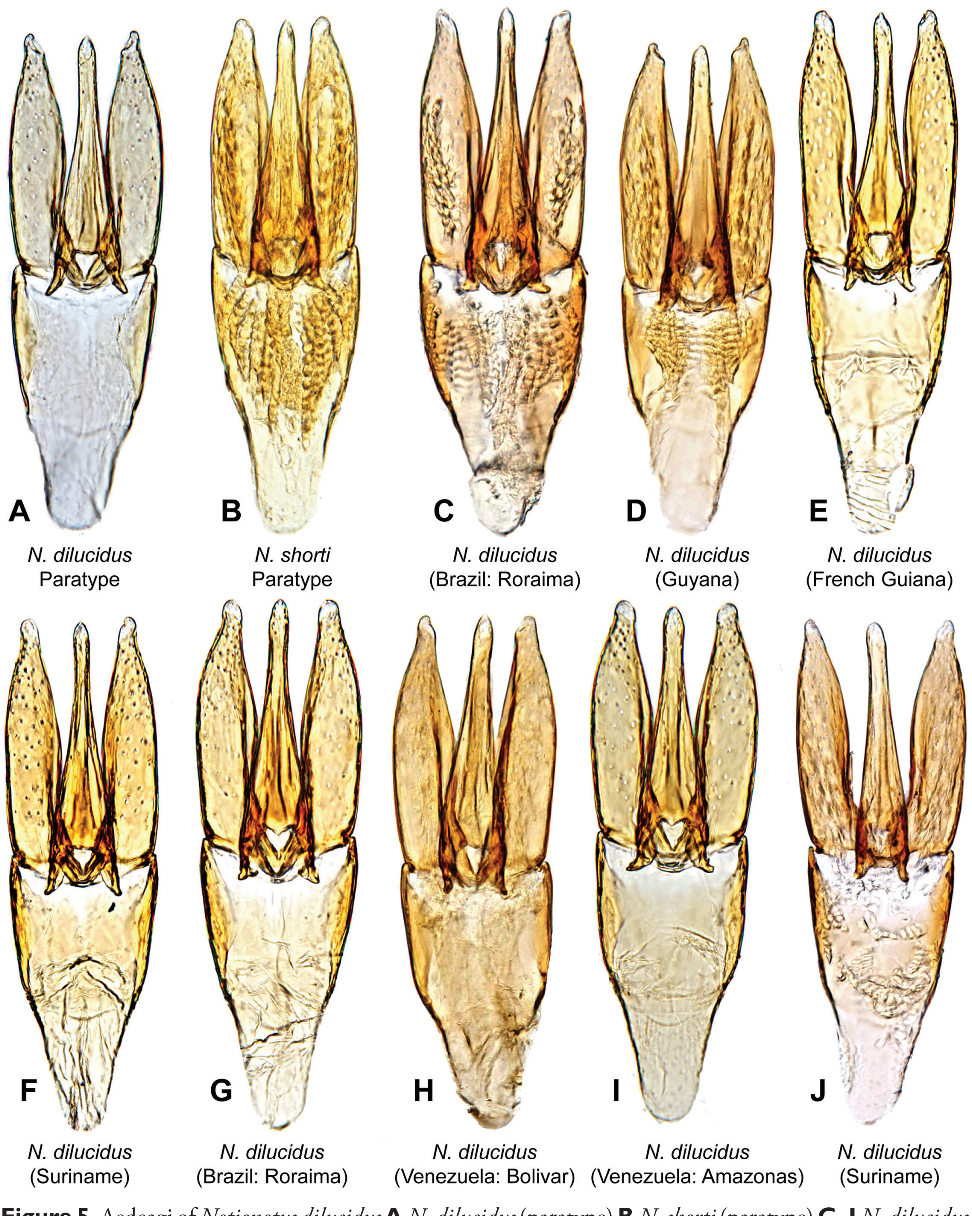

Figure 5. Aedeagi of *Notionotus dilucidus* **A** *N. dilucidus* (paratype) **B** *N. shorti* (paratype) **C–J** *N. dilucidus* **C** specimen from Roraima, Brazil **D** specimen from Guyana **E** specimen from French Guiana **F** specimen from Suriname **G** specimen from Roraima, Brazil **H** specimen from Bolívar State, Venezuela **I** specimen from Amazonas State, Venezuela **J** specimen from Suriname.

Additional material examined (139 exs.). Venezuela: Aragua State: Henri Pittier National Park, Río Curucuruma, 10°21.070'N, 67°34.920'W, 11.i.2006, leg. A.E.Z. Short, waterfall/seep, AS-06-023 (75 exs., MIZA, SEMC, including DNA Voucher MSC1820); Henri Pittier National Park, Río Castaño Regresiva del Diablo, 10.35669°N, 67.60645°W, 6.i.2009, leg. A.E.Z. Short, log in stream, VZ09-0106-01A (5 exs., SEMC); same data except seeps/wet rock, VZ09-0106-01B (19 exs., SEMC); Henri Pittier National Park, Ranch Grande, 10.i.2006, leg. Short, stream and seep at Toma, AS-06-021, (8 exs., SEMC), same data except 2.vii.2020, VZ10-0702-01A (1 ex., SEMC, DNA voucher SLE2111). **Barinas State:** 13 km NW Barinitas, 8°48.424'N, 70°31.139'W, 992 m, 24.i.2012, leg. A. Short & Gustafson, seepage by road, VZ12-0124-02A (22 exs., SEMC, including DNA voucher SLE2123); same data except small stream pool, VZ12-0124-02B (1 ex., SEMC). **Mérida State:** ca. 2.5 km S. La Azulita, 8°44.335'N, 70°37.131'W, 842 m, 28.i.2012, leg. G.T. Gustafson, stream pools, VZ12-0128-02B (1 ex., SEMC); ca. 12 km, SE of Santo Domingo, 8°51.933'N, 70°37.131'W, 1682 m, 22.i.2012, leg. Short & Arias, wall seep 1, VZ12-0122-03A (7 exs., SEMC, including DNA voucher SLE2124). **Trujillo State:** ca. 3 km NE Laguna Agua Negro, 9°19.371'N, 70°9.303'W, 1770 m, 21.i.2009, leg. Short, García & Camacho, small mountain stream w/ detritus, VZ09-0121-03x (1 ex., SEMC).

Differential diagnosis. *Notionotus liparus* can be recognized by the distinct black coloration among the other dark (reddish brown) species such as *N. brunbadius*, *N. parvus* and *N. retusus*, also for being the only dark species in the *liparus* group (Fig. 2A). It can also be differentiated by sharply marked punctation of the pronotum and elytra. Moreover, the outer margin of the parameres is sinuate and the apical third is slim and tapered. It is the only species in the *liparus* group with the apex of the median lobe acute.

Description. ***Size and form*:** Body length 1.6–1.8 mm. Body form elongate oval, convex in lateral view (Fig. 2A). ***Color and punctation*:** Dorsally black, with lateral margins of the pronotum and elytra reddish brown (Fig. 2A). Ventrally reddish brown, except for black abdominal ventrites; maxillary palps and antennae yellow (antennal club slightly darker) (Fig. 2B). Clypeus and labrum with dense, coarse, and moderately impressed ground punctation (punctures separated by 2 × their width); pronotum and elytra ground punctation dense, coarse, and moderately impressed and sparser than on head (punctures separated by 3 × their width). ***Head*:** Clypeus and labrum shallowly emarginate anteromedially, lateral margins of the labrum bearing setae. ***Thorax*:** Prosternum carinate medially, strongly raised, pointing anteriorly and acute. Elevation of mesoventrite with one transversal ridge, elevated medially, lateral sides concave; longitudinal ridge narrowed anteriorly and broadening posteriorly, the point where the two ridges merged blunt (e.g., Fig. 10A, B); elevation concave in lateral view; mesoventrite with triangular shape in ventral view. Metaventrite convex in the median region, pubescent with narrow glabrous patch on the medial and posterolateral area; anterior margin extending to mesoventrite elevation. Metafemora with dense hydrofuge pubescence along basal three-quarters of the anterior margin and along basal one-quarter of posterior margin, then apical half of the posterior margin with sparse setae (Fig. 2B). ***Abdomen*:** Abdominal ventrites very densely pubescent. Aedeagus (Fig. 7A) with basal piece 1.3 × the length of a paramere. Base of the parameres slightly narrower than the base of the median lobe; outer margin sinuate, inner margin nearly straight, tapering along apical third, parameres thin and rounded at apex. Median lobe shorter than the parameres, broad at the base and gradually widening to the apex, with the apex acute.

Distribution. This species is widespread in the Mérida Andes and Coastal Mountains of Venezuela (Fig. 14). Originally described from localities in the Venezuelan states of Barinas and Mérida (Spangler 1972, it was later recorded from the state of Aragua (García 2000). Here, we report additional localities in these three states as well as report it from the state of Trujillo for the first time.

Life history. This species is found in rock seepage habitats and wet rocks adjacent to waterfalls (Fig. 11A, B). Occasionally it is found in the pools that form at the best of these habitats.

Remarks. We sequenced four specimens from three Venezuelan states across the range of this species (Aragua, Barinas, and Mérida). The sequences are nearly identical (Fig. 1), supporting the concept of a widespread species in the Mérida Andes and Coastal mountains.

Notionotus mexicanus **Perkins, 1979**

Figs 2D–F, 7B, 14

Notionotus mexicanus Perkins, 1979: 306.

Type material examined. ***Holotype*** **(male):** "MEXICO, Oaxaca, 8 mi. E./Tapanatepec, tropical/stream with lg. boulders/3-VII-1974/ME&PD Perkins", "Type No/76326/U S N M", "HOLOTYPE/Notionotus/mexicanus/P.D.Perkins" (USNM).

Differential diagnosis. *Notionotus mexicanus* is very similar morphologically to *N. tricarinatus* sharing characters such as body length, yellow dorsal coloration, pronotum and elytra with fine ground punctation, and elevation of the mesoventrite with a transversal and a longitudinal ridge. It can be distinguished by the shape of the aedeagus, specifically the shape of the parameres: inner margins straight and sinuate reaching the apex, parameres narrowing along apical third, and narrower than *N. tricarinatus*.

Description. ***Size and form*****:** Body length 1.8 mm. Body form elongate oval, convex in lateral view (Fig. 2D). ***Color and punctation*****:** Dorsally yellow, head mostly yellow, frons pale brown; pronotum with two small black round spots along posterior margin (Fig. 2D). Ventrally brown; maxillary palps, mouthparts, antennae, pro and meso legs yellow, meta legs pale brown (Fig. 2E). Clypeus and labrum with dense, fine, and weakly impressed ground punctation (punctures separated by 2 × their width); pronotum and elytra ground punctation fine, weakly impressed and sparser than on head (punctures separated by 3 × their width). ***Head*****:** Clypeus and labrum shallowly emarginate anteromedially, lateral margins of the labrum bearing setae. ***Thorax*****:** Prosternum carinate medially, strongly raised, pointing anteriorly and acute. Elevation of mesoventrite with one transversal ridge, elevated medially, lateral sides concave; longitudinal ridge sharp, the point where the two ridges merged rounded and obtuse (e.g., Fig. 10A, B); elevation concave in lateral view; mesoventrite with triangular shape in ventral view. Metaventrite convex in the median region, pubescent with narrow glabrous patch on the medial and posterolateral area; anterior margin extending to mesoventrite elevation. Metafemora densely covered with hydrofuge pubescence on basal three-quarters (Fig. 2E). ***Abdomen*:** Abdominal ventrites very densely pubescent. Aedeagus (Fig. 7B) with basal piece 1.1 × the length of a paramere. Base of the parameres broader than the base of the median lobe; outer margin slightly convex along basal two-thirds, then slightly sinuate apically, inner margins nearly straight along basal two-thirds and then sinuate apically; apex of parameres rounded. Median lobe shorter than the parameres, approximately triangular, with acute apex.

Distribution. Only known from the type locality in Mexico (Fig. 14).

Life history. The type series was collected "from plant debris which had become trapped between stones in a rapid stream" (Perkins 1979).

Notionotus tricarinatus **Perkins, 1979**

Figs 3A–I, 6A–I, 11C, D, 14

Notionotus tricarinatus Perkins, 1979: 309.

Type material examined. *Holotype* (male): "PANAMA, C.Z./Albrook Forest Site/ground, 22-III-/1968, R.S. Hutton", Type No/76324/U S N M", "HOLOTYPE/Notionotus/tricarinatus/P.D. Perkins" (USNM).

Notionotus edibethae **García, 2000: 250. syn. nov.**

Type material examined. *Holotype* (male): "VENEZUELA. Trujillo/Mcpo. Rafael Rangel/La Guaira, Quebrada la/amarilla, 530 m./24-VIII-1997/Det. M. García, 199", "Col:/M. García/J. Camacho/E. Gomez", "Holotipo ♂/ Notionotus/edibethae/ Dcrip. M. García, 1997" (MALUZ). ***Paratypes* (2 exs.):** "VENEZUELA: Trujillo/ Mcpo. Rafael Rangel/ La Gira, Quebrada la/ amarilla, 530 m./ 24-VIII-1997/ Det. M. García, 199", "Col/ M. Garcia/ J. Camacho/", "Paratipo ♀/ Notionotus/ edibethae/ Dcrip. M. García, 1997" (1 ex. SEMC); "VENEZUELA, Trujillo,/ Mcpo. Rafael Rangel, La/ Gira, Qda. La Amarilla,/ 520 m 20–22 / V / 1995/ Trampa Interceptación/", "Colectores:/ J. Camacho/ M. García/", "Paratipo ♂ / Notionotus/ edibethae/ Dcrip. M. García, 1997" (1 ex., SEMC). The labeled holotype is an undissected male with the aedeagus visible and still attached to the abdomen. We also examined a permanent genitalia slide that had been presumed to be from holotype and is labeled as this species.

Notionotus nucleus **Perkins, 1979: 308. syn. nov.**

Type material examined. *Holotype* (male): "GUATE., Alta Verapaz/5 mi. W. La Tinta/small tropical brook/6-VI-1974, ME&PD Perkins", "Type No/76325/U S N M", "HOLOTYPE/Notionotus/nucleus/P.D. Perkins" (USNM).

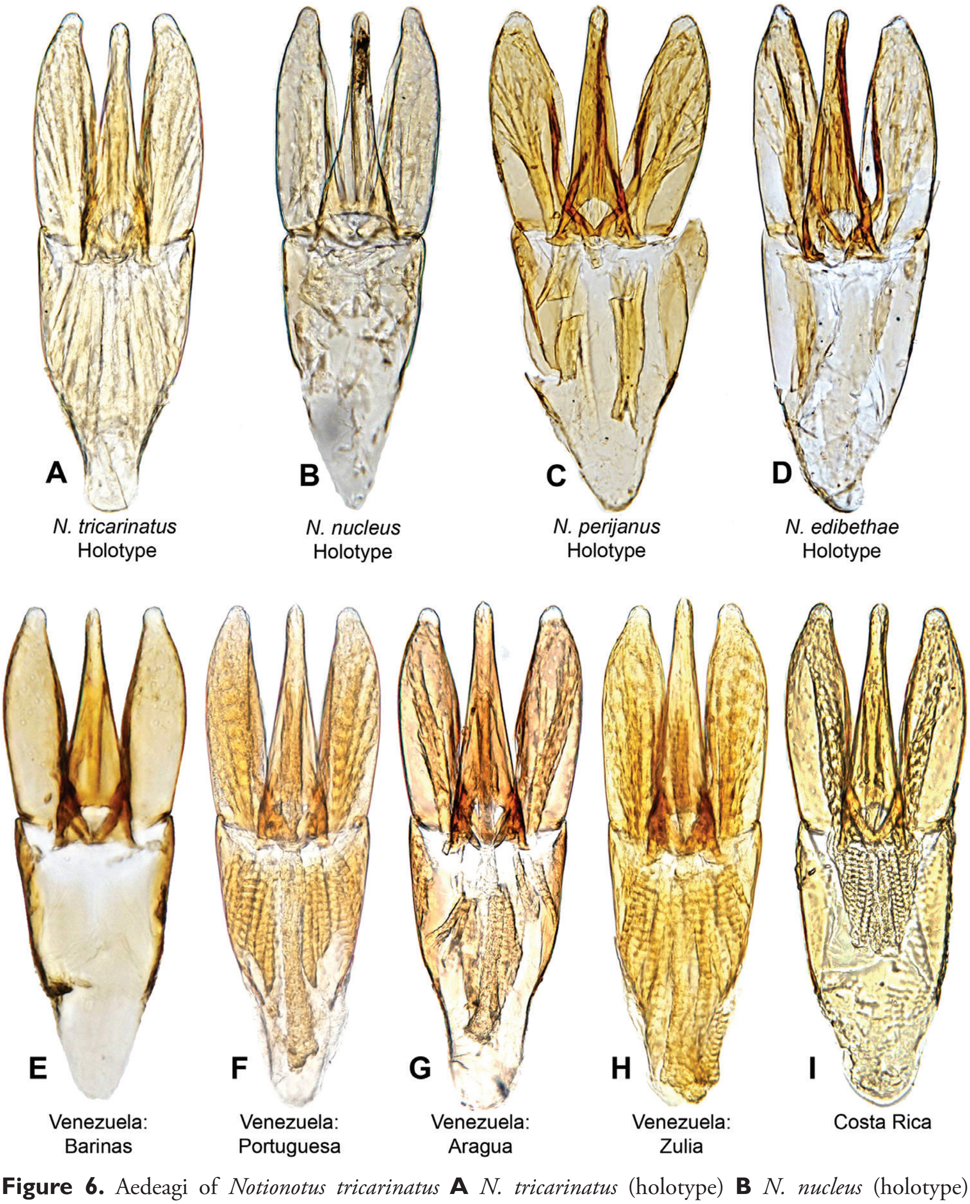

Figure 6. Aedeagi of *Notionotus tricarinatus* **A** *N. tricarinatus* (holotype) **B** *N. nucleus* (holotype) **C** *N. perijanus* (holotype) **D** *N. edibethae* (holotype) **E** specimen from Barinas State, Venezuela **F** specimen from Portuguesa State, Venezuela **G** specimen from Aragua State, Venezuela **H** specimen from Zulia State, Venezuela **I** specimen from Costa Rica.

Notionotus perijanus **García, 2000: 252. syn. nov.**

Type material examined. ***Holotype*** **(male):** [only the permanent slide mount of the aedeagus was examined] (MALUZ). As this species was described only from one male and one female specimen, we presume this slide is of the holotype specimen (Fig. 6C).

Additional material examined (173 exs.). Costa Rica: Cartago Province: Tapanti National Park, Building by Río Villegas, 29.v.2006, leg. A.E.Z. Short, HG-vapor light, AS-06-066 (5 exs., SEMC, INBio, including DNA voucher SLE2397). **Panama: Panama province:** Barrio Colorado, 9°11'N, 79°51'W, 40 m, 22–25-VI-2000, leg. S. Chatzimanolis, flight intercept trap, PAN1C00 022 (3 exs., SEMC); same data except PAN1C00 024 (5 exs., SEMC); same data except PAN1C00 025 (2 exs., SEMC); same data except PAN1C00 033 (1 ex., SEMC); same data except PAN1C00 0234 (1 ex., SEMC); same data except PAN1C00 014 (1 ex., SEMC); same data except 07-VI-1994, leg. D. Banks (2 exs., SEMC); same data except 08-VIII-1994, leg. D. Banks (1 ex., SEMC), same data except 08-VIII-1994, leg. D. Banks (1 ex., SEMC); same data except 04-VIII-1994, leg. D. Banks (1 ex., SEMC); same data except 01-VIII-1994, leg. D. Banks (1 ex., SEMC); Old plantation Rd. 6.9 km S Gamboa, 09°05'N, 79°40'W, 80 m, 04–07-VI-1995, leg. J, Ashe & R. Brooks, #137 flight intercept trap (1 ex., SEMC), same data except 07–22-VI-1995, #266 flight intercept trap (1 ex., SEMC); Colón, Parque Nacional Soberanía, Pipeline Rd km 6.1, 09°07'N, 79°45'W, 40 m, 07–21-VI-1995, leg. J, Ashe & R. Brooks, #265 flight intercept trap (2 exs., SEMC); Colón, Escobal & Piña Rds, 14 km N jct. 02–11-VI-1996, leg. J, Ashe & R. Brooks flight intercept trap PAN1AB96 181B (1 ex., SEMC). **Venezuela: Aragua State:** Henri Pittier Natural Park Río Cumboto, 10.39376°N, 67.79597°W, 130 m, 4.i.2009, leg. Short, García & Miller, river side pools, VZ09-0104-02B (18 exs., SEMC, including DNA voucher SLE2381); Río La Trilla 10.37319°N, 67.74250°W, 295 m, leg. Short, García & Miller, pools, VZ09-0104-01A (1 ex., SEMC). **Barinas State:** Río Santa Barbara, E. Santa Barbara. 7°50.028N, 71°11.188W, 177 m, 26.i.2012, leg. Short, Arias, Gustafson, sandy sidepool in floodplain, VZ12-0126-01B, (1 ex., SEMC). **Portuguesa State:** Trib. of Río Guanare, S. Biscucuy, 9°14.457'N, 69°55.994'W, 370 m, 19.i.2009, leg. Short, García & Miller, gravel stream, VZ09-0119-03X (15 exs., SEMC, including DNA vouchers SLE2391 and SLE2392). **Zulia State:** Perijá Natural Park Tukuko: Río Manantial, 9°50.490'N, 72°49.310'W, 270 m, 29.i.2009, leg. Short, García & Camacho, gravel margin, VZ09-0129-01A (91 exs., MIZA, SEMC, including DNA vouchers SLE1112 and SLE2371); same data except 29.i.2009, leg. Short, García & Miller, detrital pool, VZ09-0129-01B (1 ex., SEMC); same data except 22.ix.2007, leg. A.E.Z. Short, rock pools/margin, AS-07-020b (8 exs., SEMC); Toromo, 10°03.058'N, 72°49.974'W, 435 m, 31.xii.2005, leg. A.E.Z. Short, small stream and seep, AS-06-001 (6 exs., SEMC); same data except 28.i.2009, detrital pool, VZ09-0128-01A (3 exs., SEMC).

Differential diagnosis. See differential diagnosis for *Notionotus mexicanus*.

Description. ***Size and form*:** Body length 1.6–1.9 mm. Body form elongate oval, strongly convex in lateral view (Fig. 3A). ***Color and punctation*:** Dorsally yellow, head mostly pale brown or yellow, frons brown or dark brown; pronotum paler than elytra, with two small black round spots along posterior margin (Fig. 3A, D, G). Ventrally brown; maxillary palps, mouthparts, antennae yellow (antennal club slightly darker), legs pale brown (Fig. 3B, E, H). Clypeus and labrum with dense, fine, and weakly ground punctation (punctures separated by 2 × their width); pronotum and elytra ground punctation fine, weakly impressed and sparser than on head (punctures separated by 3 × their width). ***Head*:** Clypeus and labrum shallowly emarginate anteromedially, lateral margins of the labrum bearing setae. ***Thorax*:** Prosternum carinate medially, strongly raised, pointing anteriorly and acute. Elevation of mesoventrite with one transversal ridge, elevated medially, lateral sides concave; longitudinal ridge sharp and broadening posteriorly almost to the end, the point where the two ridges merged rounded and obtuse (e.g., Fig. 10A, B); elevation concave in lateral view; mesoventrite with triangular shape in ventral view. Metaventrite convex in the median region, pubescent with narrow glabrous patch on the medial and posterolateral area; anterior margin extending to mesoventrite elevation. Metafemora densely covered with hydrofuge pubescence on basal three-quarters (Fig. 3B, E, H). ***Abdomen*:** Abdominal ventrites very densely pubescent. Aedeagus (Fig. 6A–I) basal piece 1.2 × the length of a paramere. Parameres broad, base wider than the base of the median lobe, outer and inner margins convex, pinched at the apex, broad and rounded apex. Length of the median lobe can vary (median lobe as long as the parameres (Fig. 6F, I), slightly shorter (Fig. 6A, B) or longer than the parameres (Fig. 6H), median lobe with triangular shape, wide at base and gradually tapering to apical third, with rounded apex.

Distribution. Known from Guatemala, Costa Rica, Panama, and Venezuela (Fig. 14).

Life history. This species is found along the margins and in leaf packs of streams in the mountains and foothills of the Northern Andes and Central America. It prefers gravelly or rocky streams, especially in the foothills where it may sometimes be abundant (Fig. 11C, D).

Remarks. We examined more than 155 specimens from a dozen localities of this species from Guatemala to several chains of the Venezuelan Andes. Although there are subtle variations in the apex of the aedeagal parameres, this variation is relatively small and not correlated to geography, other morphological characters, or molecular data. These subtle variations in paramere shape likely explain why this species has been described four times, once each from Guatemala and Panama (Perkins 1979) and twice from Venezuela (García 2000). Three of these four species were described from single collecting events. However, with significantly more material available to us for this study from a range of additional localities, it is apparent these differences in paramere shape are more easily considered as intraspecific variation in a widespread, common species than as indicative of species boundaries. This hypothesis is also supported by available DNA evidence: we sequenced specimens from Costa Rica, the Serranía de Perijá, the Mérida Andes, as well as the Coastal mountains of Venezuela. All specimens form a clade (Fig. 1) with a maximum pairwise divergence in COI of 3.9% (although we only had COI data from specimens from several Venezuelan localities). However, 28S sequence data from specimens from Venezuela and Costa Rica are identical, further supporting the concept of a single, widespread species. In addition, specimens throughout its range were found in very similar habitats: leaf packs or detrital margins of streams with a gravel or rocky substrate

As both *N. nucleus* and *N. tricarinatus* were proposed in the same work (Perkins 1979), we use our authority as first revisors (ICZN article 24.2.2) to give precedence to *N. tricarinatus* as the valid name for this species.

***Notionotus vatius* sp. nov.**
http://zoobank.org/CD665789-B94F-4C19-AAE1-83B7ACCE9413
Figs 4H, 7C, 13B, 14

Type material. ***Holotype*** **(male):** "BRAZIL: Mato Grosso do Sul/ -20.72281°, -55.69127°; 225 m/Aquidauana (c. 27 km S) on/MS-174; leg. Hamada & team;/27. vi.2018; seepage & debris nr./stream margin; BR18-0627-01E" (INPA). ***Paratypes*** **(38 exs.): Brazil: Mato Grosso do Sul State:** Same data as holotype (19 exs., INPA, SEMC, including DNA Voucher 2324); Aquidauana on plateau (ca. 15 km E), -20.4509, -55.6218, 380 m, 22.vi.2018, leg. Hamada & team, detritus and washing roots at margin on rock, BR18-0622-03D (6 exs., SEMC, including DNA voucher SLE2327); Corumbá (ca. 27 km SE) by mountains, -19.28382, -57.57506, 146 m, 24.vi.2018, leg. Hamada & team, stream margin and leaf packs, BR18-0624-01A (1 ex., SEMC); Rio Bento Gomes (Pantanal), Campo Allegre I, 15°45'S, 56°33'W, 1993–1994, leg. E. Stuhr, spring-fed brook, (10 exs., NMW, SEMC). **Bahia:** Morro do Chapéu, Cachoeira Domingos Lopes, -11.55965, -40.90635, 675 m, 24.ii.2018, leg. Benetti & team, blackwater river and waterfall, BR18-0224-02A (1 ex., SEMC,

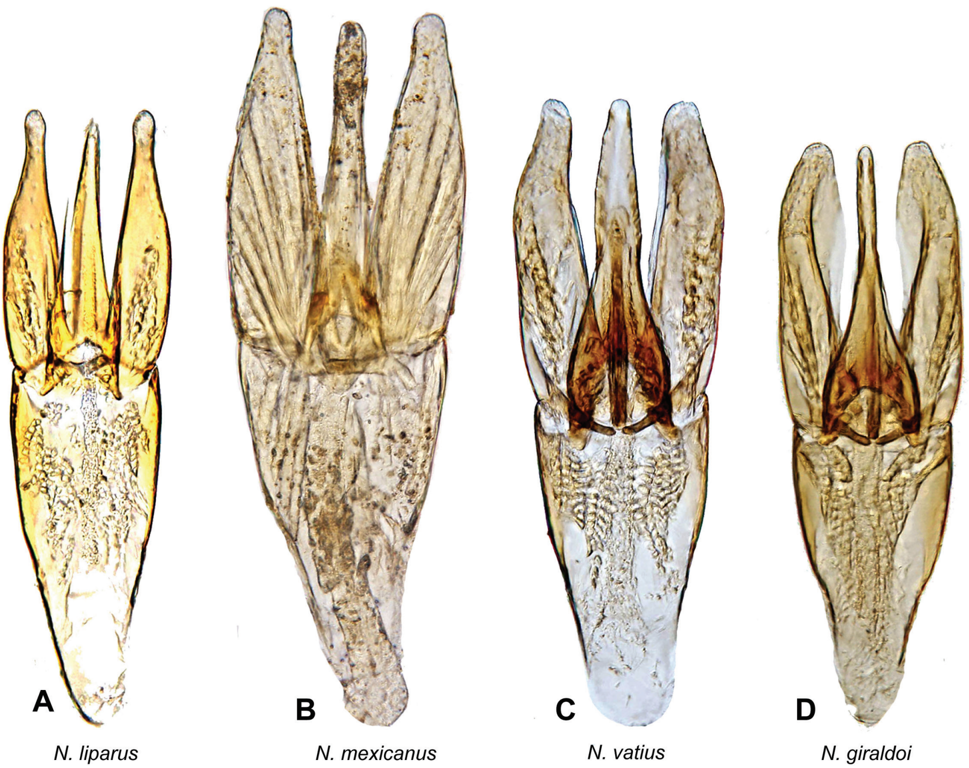

Figure 7. Aedeagi of *Notionotus liparus* species group **A** *N. liparus* (non-type specimen) **B** *N. mexicanus* (holotype) **C** *N. vatius* (holotype) **D** *N. giraldoi* (holotype).

DNA Voucher SLE2104); Livramento de Nossa Senhora, NE on BR-148, -13.6212, -41.81908, 536 m, 27.ii.2018, leg. Benetti & team, stream margins, BR18-0227-01A (1 ex., SEMC, DNA Voucher SLE2385).

Differential diagnosis. Among the species of *liparus* group, *Notionotus vatius* can be recognized by the brown dorsal coloration, and quite unique color pattern of the head frons and medial region of the clypeus dark brown, lateral side of the clypeus pale brown. In addition, the shape of aedeagus, especially the apex of the parameres is broad, blunt, and pointing slightly outwards, and the gonopore has rounded shape and it is situated at midlength of median lobe.

Description. ***Size and form*:** Body length 1.7–2.3 mm. Body form elongate oval, strongly convex in lateral view (Fig. 4H). ***Color and punctation*:** Dorsally brown, head mostly brown, frons and medial region of the clypeus dark brown, lateral side of the clypeus pale brown; pronotum pale brown with two small black round spots along posterior margin, elytra dark brown (Fig. 4H). Ventrally dark brown; maxilla, maxillary palps, antennae (antennal club slightly darker) yellow, legs pale brown. Clypeus and labrum with dense, fine, and weakly impressed ground punctation (punctures separated by 2 × their width); pronotum and elytra ground punctation fine, weakly impressed and sparser than on head (punctures separated by 3 × their width). ***Head*:** Clypeus and labrum shallowly emarginate anteromedially, lateral margins of the labrum bearing setae. ***Thorax*:** Prosternum carinate medially, strongly raised, pointing anteriorly and acute. Elevation of mesoventrite with one transversal ridge, elevated medially, lateral sides concave; longitudinal ridge sharp, the point where the two ridges merged rounded and obtuse (e.g., Fig. 10B); elevation flat in lateral view; mesoventrite with triangular shape in ventral view. Metaventrite convex in the median region, pubescent with narrow glabrous patch on the medial and posterolateral area, medial region patch drop-shaped; anterior margin extending to mesoventrite elevation. Metafemora densely covered with hydrofuge pubescence on basal three-quarters. ***Abdomen*:** Abdominal ventrites very densely pubescent. Aedeagus (Fig. 7C) with basal piece nearly the same length as a paramere. Base of the parameres slightly narrower than the base of the median lobe; outer and inner margins sinuate; apex of parameres wide and blunt, pointing outwards. Median lobe of the same length as the parameres, wide at basal region, narrowing in the midlength, then widening along at apical third, apex rounded; gonopore with rounded shape and situated at midlength of median lobe.

Etymology. The name is derived from the Latin word *vatius* meaning bent outwards, after the form of the parameres slightly pointing outwards of the aedeagus.

Distribution. This species is known from several localities in Bahia and Mato Grosso do Sul States in Brazil (Fig. 14).

Life history. This species was collected on seepages and along the margins of rocky streams (Fig. 13B).

Remarks. Although the known localities of this species are widely dispersed in Brazil, they are from similar habitats at similar elevations on the Brazilian Shield. Moreover, the specimens from Bahia and Mato Grosso do Sul states are less than 3% divergent in uncorrected pairwise distances in COI.

Notionotus lohezi species group

Diagnosis. The *lohezi* species group can be distinguishable by the presence of three ridges in the elevation of the mesoventrite, two transverse ridge and one longitudinal (Fig. 10C, D); the basal piece is shorter than the parameres, the length of the median lobe is shorter than the parameres.

Notionotus bicolor sp. nov.

http://zoobank.org/7954CB9D-66E9-492F-865E-90BA4991ADF3
Figs 4A, 8A, 10D, 12D, 15

Type material examined. ***Holotype*** **(male):** "SURINAME: Sipaliwini District/ 4.42313°N, 57.19198°W, 104 m/ Kabalebo Nature Resort/ Moi Moi Creek; 10–14.iii.2019/ leg Short & Baca small seeps/ SR19-0310-01F" (NZCS). ***Paratypes*** **(88 exs.): Suriname: Sipaliwini District:** Same data as holotype (8 exs., SEMC); Kabalebo Nature Resort: Charlie Falls, 4.38302°N, 57.21161°W, 174 m, 11.iii.2019, leg. Short, Baca and class, rocks pools in creekbed, SR19-0311-01A (55 exs., NZCS, SEMC, including DNA vouchers SLE1810 and SLE2120); same data except leg. Short, Seepage, SR19-0311-01B (14 exs., SEMC); same data except leg. Baca, side pools in gravel in creekbed, SR19-0311-01E (2 exs., SEMC); Kabalebo Nature Resort Moi Moi creek, 4.42313°N, 57.19198°W, 104 m, 10–14.iii.2019 leg. Short, Baca and class, margin of seepage, SR19-0310-01E (2 exs., SEMC); same data except leg. Baca, margin of stream pool with root mats, SR19-0310-01L (1 ex., SEMC); same data except leg. Short and class, small trickle on rocks w/detritus, SR19-0310-01M (4 exs., SEMC); CSNR: Tafelberg Summit, near Caiman Creek Camp, 3°53.942'N, 56°.10.849'W, 733 m, 19.viii.2013, leg. Short and Bloom, margins and leaf packs in Caiman Creek, SR13-0819-05D (2 exs., SEMC).

Differential diagnosis. *Notionotus bicolor* shares the bicolorous dorsal coloration that can also be observed in *N. garciae*, *N. patamona*, and *N. lohezi*. It can be recognized by the shape of the aedeagus, the median lobe is much shorter than in *N. insignitus* (Fig. 8B) and *N. patamona* (Fig. 8D), and slightly longer than in *N. lohezi* (Fig. 8F). The margins of the median lobe are sinuate with a widening in the middle length, this differs in the other species where the margins are slightly straight. Moreover, the apex is slightly narrow and rounded, this differs in *N. insignitus* with acute apex, *N. patamona* with rounded and wide apex and *N. lohezi* with blunt apex.

Description. ***Size and form*****:** Body length 1.7–2 mm. Body form elongate oval, moderately convex in lateral view (Fig. 4A). ***Color and punctation*****:** Dorsally bicolor, head brown, frons dark brown; pronotum yellow with two small black round spots along posterior margin; elytra dark brown, elytra margins paler (Fig. 4A). Ventrally brown; maxillary palps, mouthparts, and antennae yellow (antennal club slightly darker), pro legs yellow, meso and meta legs pale brown. Clypeus and labrum with dense, fine, and weakly impressed ground punctation (punctures separated by 2 × their

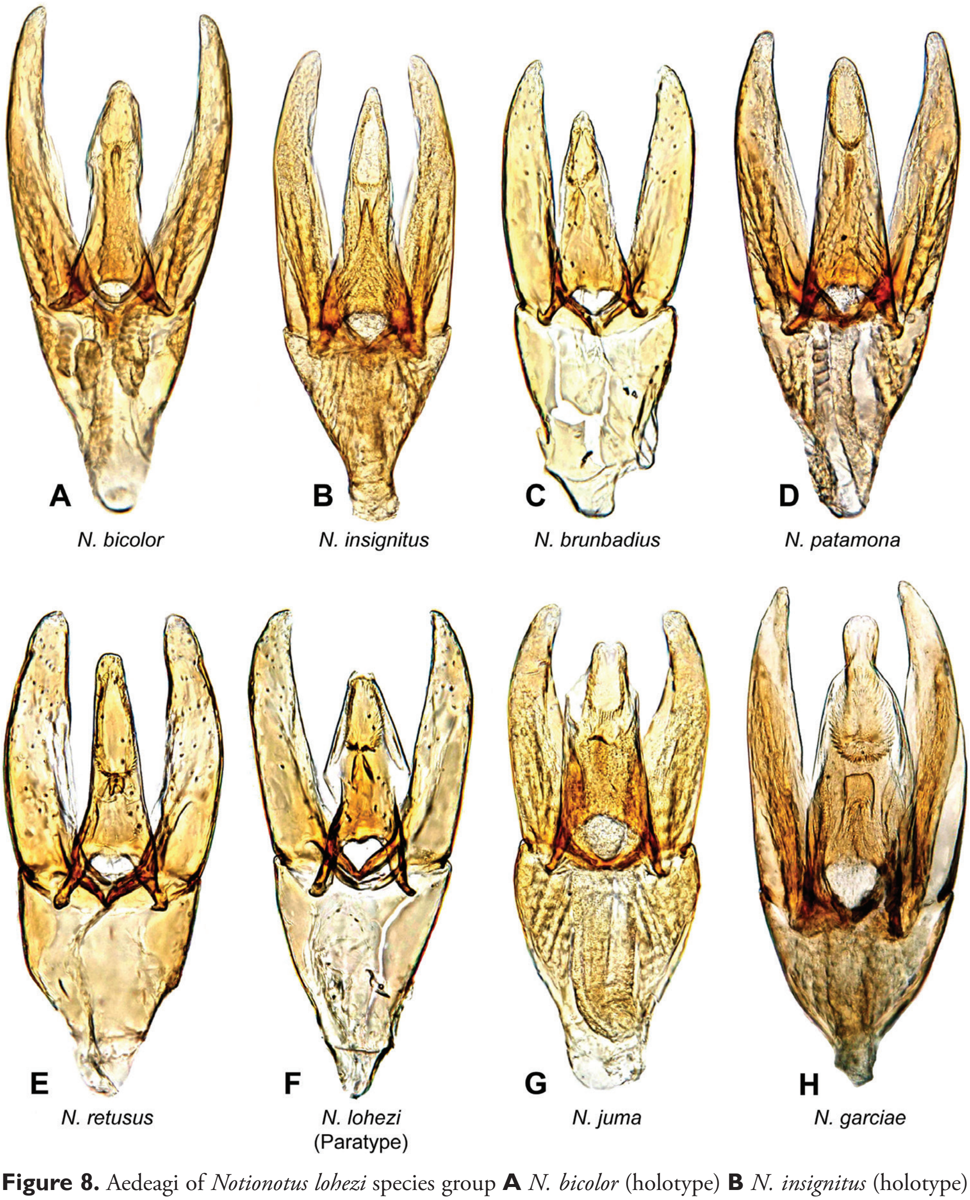

Figure 8. Aedeagi of *Notionotus lohezi* species group **A** *N. bicolor* (holotype) **B** *N. insignitus* (holotype) **C** *N. brunbadius* (holotype) **D** *N. patamona* (holotype) **E** *N. retusus* (holotype) **F** *N. lohezi* (paratype) **G** *N. juma* (holotype) **H** *N. garciae* (holotype).

width); pronotum and elytra ground punctation fine, weakly impressed and sparser than on head (punctures separated by 3–4 × their width). ***Head*:** Clypeus and labrum shallowly emarginate anteromedially, lateral margins of the labrum bearing setae. ***Thorax*:** Prosternum carinate medially, strongly raised, acute and pointing anteriorly. Elevation of mesoventrite with two transversal ridges, elevated medially, lateral sides concave; longitudinal ridge broad anteriorly and sharp posteriorly, the point where the three ridges merged wide and blunt (Fig. 10D); elevation flat in ventral view; mesoventrite with triangular shape in ventral view. Metaventrite convex in the median region, pubescent with narrow glabrous patch on the medial and posterolateral area; anterior margin extending to mesoventrite elevation. Metafemora with dense hydrofuge pubescence along basal three-quarters of the anterior margin and sparse pubescence along the entire basal posterior margin. ***Abdomen*:** Abdominal ventrites very densely pubescent. Aedeagus (Fig. 8A) with basal piece 0.7 × the length of a paramere. Base of the parameres slightly narrower than the base of the median lobe; outer margin convex, inner margins along basal two-thirds slightly convex, apical third straight; apex of parameres slightly acute, pointing inwards. Median lobe shorter than the parameres, wide at basal region, narrowing in the midlength, then sinuate, apex slightly acute; gonopore situated at the apex of median lobe.

Etymology. The name derived from the Latin words *bi* meaning two and *color* meaning hue, referring to the dorsal coloration of the species. This species has yellow coloration in the pronotum and black in the elytra.

Distribution. Known from two localities in central Suriname: Kabalebo and the summit of Tafelberg Tepui (Fig. 15).

Life history. At Kabalebo, this species was collected in several streams, including both along the margin, rock pools with detritus in the creek bed, and in seepage habitats (Fig. 12D). At Tafelberg, the species was collected along a rocky creek margin with detritus.

Notionotus bifidus **sp. nov.**

http://zoobank.org/AEAADA10-0A40-4AB9-B48E-FC27A126792B

Figs 4J, 9D, 12A, 14

Type material. ***Holotype*** **(male):** "VENEZUELA: Amazonas State/ 5°23.207'N, 67°36.922'W, 125 m/ Tobogan de la Selva; 8.viii.2008/leg. A. Short, M. García, L. Joly/ AS-08-080b; old "tobogancito"/on seepage area w/detritus" (MIZA). ***Paratypes*** **(54 exs.): Venezuela: Amazonas State:** Same data as holotype (18 exs., SEMC, including DNA voucher SLE1113); same data except 14.i.2009, leg. A. Short, clumps of wet leaves on rock, VZ09-0114-01D (15 exs., SEMC, including DNA voucher SLE2369); same date except 14.i.2009, leg. K. Miller, detrital rock pools, VZ09-0114-01E (1 ex., SEMC); same data except 14.i.2009, leg. Short & Miller partly shaded wet rock w/algae, VZ09-0114-01G (20 exs., MIZA, SEMC).

Differential diagnosis. *Notionotus bifidus* can be separated from all other species of *lohezi* group by being the only species in the group that present uniformly dorsal yellow coloration (Fig. 4J), the rectangular shape of the median lobe and its bifurcation at the apex, and the abrupt tapering of the parameres along apical third (Fig. 9D).

Description. ***Size and form*:** Body length 1.5–1.7 mm. Body form elongate oval, moderately convex in lateral view (Fig. 4J). ***Color and punctation*:** Dorsally yellow,

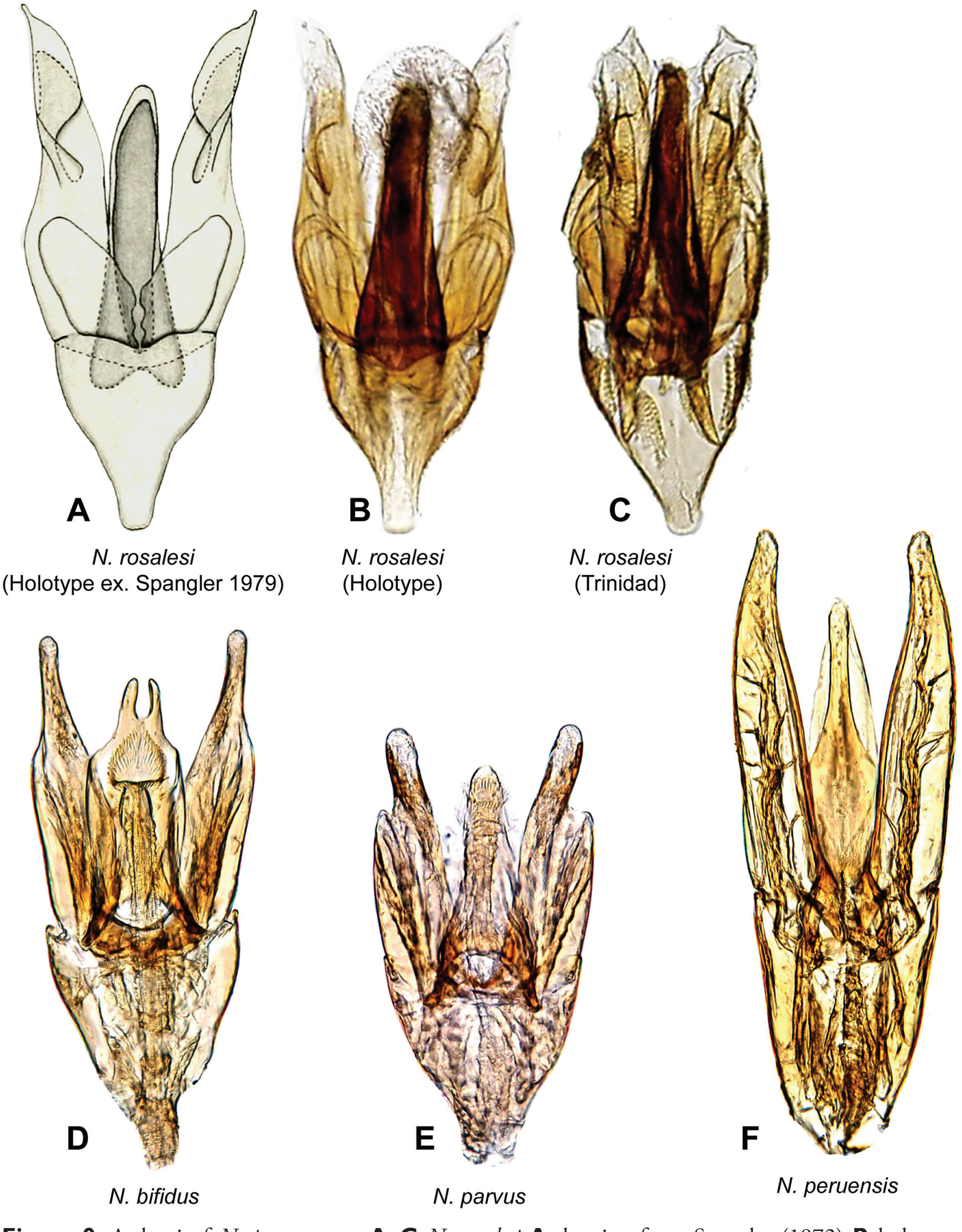

Figure 9. Aedeagi of *Notionotus* spp. **A–C** *N. rosalesi* **A** drawing from Spangler (1972) **B** holotype **C** specimen from Trinidad **D** *N. bifidus* **E** *N. parvus* **F** *N. peruensis*.

head mostly dark brown, frons and medial region of the clypeus dark brown, lateral sides of clypeus yellow; pronotum yellow with two small dark brown round spots along posterior margin; elytra yellow (Fig. 4J). Ventrally dark brown; maxillary palps, mouthparts, and antennae yellow. Pro legs yellow, meso and meta legs pale brown.

Clypeus and labrum with dense, fine, and weakly impressed ground punctation (punctures separated by 2 × their width); pronotum and elytra ground punctation fine, weakly impressed and sparser than on head (punctures separated by 3 × their width). ***Head*:** Clypeus and labrum shallowly emarginate anteromedially, lateral margins of the labrum bearing setae. ***Thorax*:** Prosternum carinate medially, strongly raised, acute and pointing anteriorly. Elevation of mesoventrite with two transversal ridges, elevated medially, lateral sides concave; longitudinal ridge broad anteriorly and sharp posteriorly, the point where the three ridges merged wide and blunt (e.g., Fig. 10C, D); elevation flat in ventral view; mesoventrite with triangular shape in ventral view. Metaventrite convex in the median region, pubescent with broad glabrous patch on the medial and

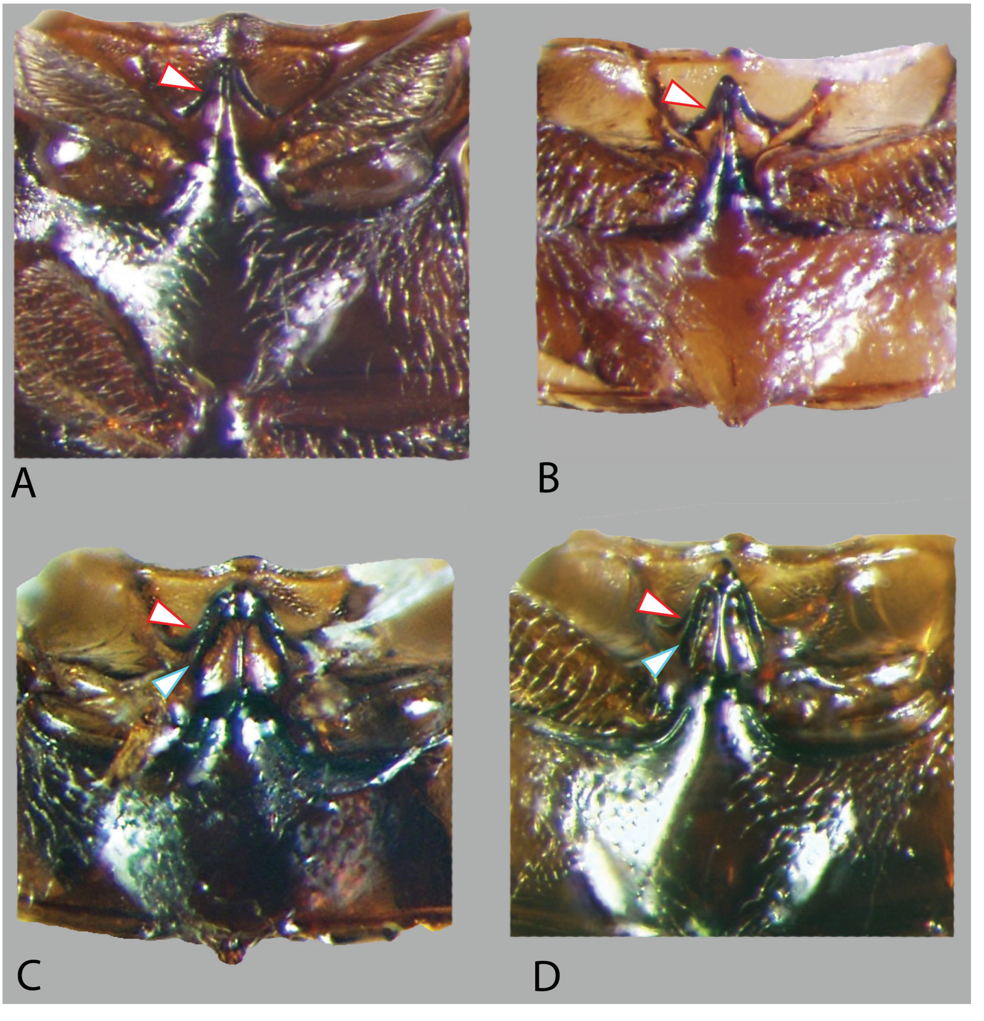

Figure 10. Mesoventral process of *Notionotus* spp. **A** *N. dilucidus* **B** *N. tricarinatus* **C** *N. insignitus* **D** *N. bicolor*. Red marks pointing to transverse ridge in **A–D** blue marks pointing to second transverse ridge in **C, D**.

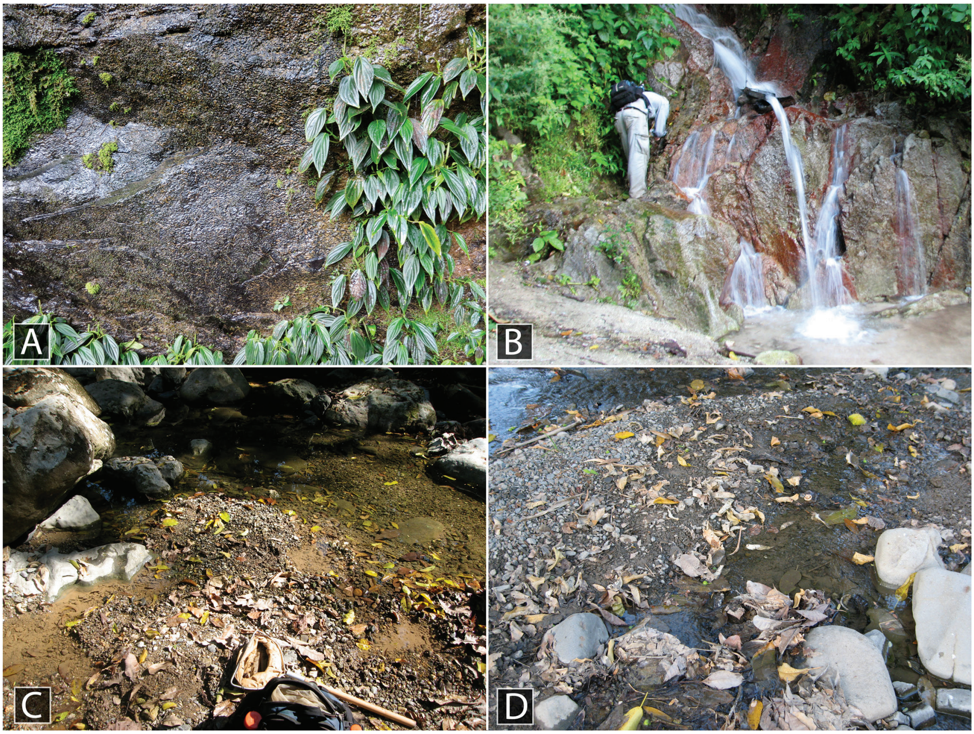

Figure 11. Habitat of *Notionotus* spp. in the Andean region of Venezuela **A** Venezuela, Barinas State, seepage habitat of *N. liparus* (collecting event VZ12-0124-02A) **B** Venezuela: Aragua, Henri Pittier National Park, seepage habitat of *N. liparus*, (collecting event AS-06-023) **C** Venezuela: Zulia, Rio Tukuko, habitat of *N. tricarinatus* (collecting event VZ09-0129-01A) **D** Venezuela, Portuguesa, tributary of the Rio Guanare, habitat of *N. tricarinatus* (collecting event VZ09-0119-03X).

posterolateral area; anterior margin extending to mesoventrite elevation. Metafemora with dense hydrofuge pubescence along basal three-quarters of the anterior margin and along basal one-quarter of posterior margin, then apical half of posterior margin with sparse setae. ***Abdomen*:** Abdominal ventrites very densely pubescent. Aedeagus (Fig. 9D) with basal piece 0.6 × the length of a paramere. Base of the parameres narrower than the base of the median lobe; outer margins straight along basal two-thirds, then narrowing abruptly along apical third, inner margins convex along basal two-thirds and then apically slightly concave; apex of parameres rounded. Median lobe shorter than the parameres, approximately rectangular, narrow along apical fifth, apex bifurcated; gonopore drop-shaped and situated at apical fourth of median lobe.

Etymology. The specific name comes from the Latin word *bifidus* meaning split into two parts, after the form of the median lobe "bifurcated apically" of the aedeagus.

Distribution. Known only from the type locality in Venezuela (Fig. 14).

Life history. This species was collected in seepage habitats that were covered with algae and detritus (Fig. 12A).

Notionotus brunbadius sp. nov.

http://zoobank.org/23615726-EDE5-40AD-B408-8ED24AC30EDC
Figs 4C, 8C, 12C, 15

Type material. ***Holotype* (male):** "BRAZIL: Amazonas, Manaus/-2.93079, -59.97514, 75 m/ Ducke Reserve/ leg. Short & team; stream margin/ & assoc. backwater swampy area/ 9–10.vi.2018; BR18-0609-03A", "DNA VOUCHER/ Extraction #/ SLE-1553" (INPA). ***Paratypes* (4 exs.): Brazil: Amazonas State:** Same data as holotype (2 exs., SEMC); same data except Igarape Barro Branco, muddy pools in swampy area adjacent to stream, BR18-0609-02B (1 ex., SEMC, DNA voucher SLE2102); same data except by unnamed stream, water in palm fronds, BR18-0609-03B (1 ex., SEMC).

Differential diagnosis. This species has a particular coloration pattern, dark reddish brown, which makes it easily distinguishable among the other species of the *lohezi* group. The shape of the parameres is slightly similar to *N. lohezi* (Fig. 8F) but the apex is less acute and bend much less inward. It can be separated by the triangular shape of the median lobe and acute apex (Fig. 8C).

Description. ***Size and form*:** Body length 1.7–1.9 mm. Body form elongate oval, moderately convex in lateral view (Fig. 4C). ***Color and punctation*:** Dorsally dark reddish brown, lateral margins of clypeus, pronotum and elytra yellow brown (Fig. 4C). Ventrally reddish brown, except for black abdominal ventrites; maxillary palps, mouth parts and antennae yellow (antennal club slightly darker). Clypeus and labrum with dense, fine, and weakly impressed ground punctation (punctures separated by 2 × their width); pronotum and elytra ground punctation fine, weakly impressed, and sparser than on head (punctures separated by 3–4 × their width). ***Head*:** Clypeus and labrum shallowly emarginate anteromedially, lateral margins of the labrum bearing setae. ***Thorax*:** Prosternum carinate medially, strongly raised, acute and pointing anteriorly. Elevation of mesoventrite with two transversal ridges, elevated medially, lateral sides concave; longitudinal ridge broad anteriorly and sharp posteriorly, the point where the three ridges merged wide and blunt (e.g., Fig. 10C, D); elevation flat in ventral view; mesoventrite with triangular shape in ventral view. Metaventrite convex in the median region, pubescent with narrow glabrous patch on the medial and posterolateral area; anterior margin extending to mesoventrite elevation. Metafemora with dense hydrofuge pubescence along three-quarters of the anterior basal margin and sparse pubescence along the posterior basal margin. ***Abdomen*:** Abdominal ventrites very densely pubescent. Aedeagus (Fig. 8C) with basal piece 0.7 × the length of a paramere. Base of the parameres narrower than the base of the median lobe; outer margins slightly convex, inner margins straight; apex of parameres acute and pointing outwards. Median lobe shorter than the parameres, approximately triangular, wide at the basal region, then slightly narrowing to the apex, apex acute, gonopore oval in shape and situated at the apex of the median lobe.

Etymology. The name is a combination of two Latin words *brun* meaning dark and *badius* meaning reddish brown, highlighting the distinguishable dark reddish brown color of this species.

Distribution. Known only from the type locality near Manaus, Brazil (Fig. 15).

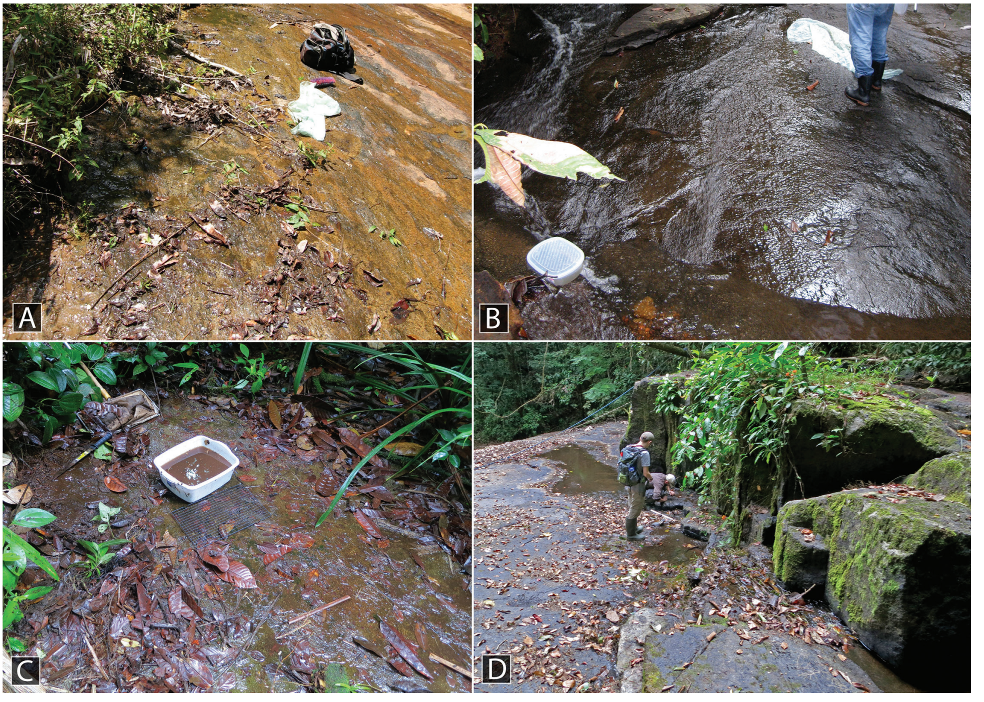

Figure 12. Habitat of *Notionotus* spp. **A** Venezuela: Amazonas State, type locality and habitat of *N. bifidus* (collecting event AS-08-080b) **B** Venezuela: Bolívar State: Type locality and habitat of *N. insignitus* (collecting event AS-08-058) **C** Guyana: Region 9: type locality and habitat of *N. patamona* (collecting event GY13-0318-01C) **D** Suriname: Kabalebo, habitat and type locality for *N. bicolor* (collecting event SR19-0310-01F).

Life history. The only known specimens were collected along the margin of a stream (Fig. 12C).

Notionotus garciae **sp. nov.**

http://zoobank.org/10EFC8E2-7C02-4F44-994B-54B3ABB388C8
Figs 4G, 8H, 13D, 15

Type material. ***Holotype*** **(male):** "BRAZIL: Amazonas: Manaus/ -2.93079, -59.97514, 75 m/ Ducke Reserve, stream nr./ transect trail; leg. Short & team/ stream margins & leaf packs/ 9.vi.2018; BR18-0609-01A" (INPA). ***Paratypes*** **(8 exs.): Brazil: Amazonas State:** Same data as holotype (3 exs., SEMC); same data except 9–10.vi.2018, stream margin and associate backwater swampy area, BR18-0609-03A (1 ex., SEMC); same data except Igarape Barro Branco, 6.vi.2018, shallow pools, BR18-0606-02D (1 ex., SEMC); same data except Igarape Barro Branco, margin of stream, 9.vi.2018, BR18-0609-02A (2 exs., SEMC); Presidente Figueiredo (ca. 57 km E) on AM-240, -1.98826, -59.51618, 80 m, airport stream, 19.vi.2018, leg. Short, margin of creek, (1 ex., SEMC, DNA voucher SLE1900).

Differential diagnosis. *Notionotus garciae* is very similar to *N. juma* in the bicolor dorsal coloration, the shape of the elevation of the mesoventrite and the pubescent area of the metafemora. It can be distinguished by the punctation of the pronotum, the elytra shallowly marked (in *N. juma* is moderately impressed, Fig. 8G), and the distinctive rounded and broad apex of the median lobe (Fig. 8H).

Figure 13. Habitat of *Notionotus* spp. **A** type locality and habitat of *N. giraldoi* (collecting event BR18-0710-02A) **B** type locality and habitat of *N. vatius* (collecting event BR18-0627-01A) **C** type locality and habitat of *N. brunbadius* (collecting event BR18-0609-03A) **D** type locality and habitat of *N. garciae* (collecting event BR18-0609-01A) **E** type locality and habitat of *N. juma* (collecting event BR18-0609-02B) **F** type locality and habitat of *N. retusus* (collecting event GY14-0311-02A).

Description. ***Size and form*:** Body length 1.7–1.8 mm. Body form elongate oval, convex in lateral view (Fig. 4G). ***Color and punctation*:** Dorsally bicolor, head mostly brown, frons dark brown, posteromedial margin of the clypeus pale brown and lateral sides and anterior margin yellow; pronotum yellow with two small black round spots along posterior margin; elytra brown, lateral and posterior side of the elytra yellow (Fig. 4G). Ventrally dark brown; maxillary palps, mouthparts, and antennae yellow. Pro and meso legs yellow, meta legs pale brown. Clypeus and labrum with dense, fine, and weakly impressed ground punctation (punctures separated by 2 × their width); pronotum and elytra ground punctation weakly impressed, fine, and sparser than on head (punctures separated by 3 × their width). ***Head*:** Clypeus and labrum shallowly emarginate anteromedially, lateral margins of the labrum bearing setae. ***Thorax*:** Prosternum carinate medially, strongly raised, acute and pointing anteriorly. Elevation of mesoventrite with two transversal ridges, elevated medially, lateral sides concave; longitudinal ridge broad anteriorly and sharp posteriorly, the point where the three ridges merged wide and blunt (e.g., Fig. 10C, D); elevation flat in ventral view; mesoventrite with triangular shape in ventral view. Metaventrite convex in the median region, pubescent with narrow glabrous patch on the medial and posterolateral area; anterior margin extending to mesoventrite elevation. Metafemora with dense hydrofuge pubescence along basal three-quarters of the anterior margin and sparse pubescence along the apical posterior margin. ***Abdomen*:** Abdominal ventrites very densely pubescent. Aedeagus (Fig. 8H) with basal piece 0.4 × the length of a paramere. Base of the parameres narrower than the base of the median lobe; outer margins nearly convex along basal two-thirds, then curved inwards along apex, inner margins nearly straight; apex of parameres acute. Median lobe shorter than the parameres, wide at basal region, narrowing in the midlength and then slightly broadening to apex, apex rounded and wide; gonopore ovate in shape and situated at apical fourth of median lobe.

Etymology. This species is named after Andrea Lorena García Hernández curator at the Colección de Insectos de la Universidad del Quindío (CIUQ) in recognition to her passion and contribution of the knowledge of the insects, specially hydrophilids in Colombia.

Distribution. This species is known from several collecting events at the Ducke Reserve near Manaus, Brazil (Fig. 15).

Life history. This species was collected along the margins of small streams in dense forest (Fig. 13D).

Notionotus insignitus **sp. nov.**
http://zoobank.org/9B5D9358-AC4A-49D1-B9F6-44490E2FAA7C
Figs 4D, 8B, 10C, 12B, 15

Type material. ***Holotype*** **(male):** "VENEZUELA: Bolívar State/ 6°2'10.5"N, 61°23'57.8"W, 630 m/ Along La Escalera; 31.vii.2008/ leg. A. Short, M. García, L. Joly/ AS-08-058; rocky stream" (MIZA). ***Paratypes*** **(14 exs.): Venezuela: Bolívar State:** same data as holotype (14 exs., SEMC, including DNA voucher SLE1115).

Differential diagnosis. See differential diagnosis for *Notionotus bicolor*. In addition, *N. insignitus* has a particular and unique color pattern in the elytra among the other congeners. The elytra are mostly dark brown, the posterior margins yellow and in the middle region has a characteristic yellow spot.

Description. ***Size and form*:** Body length 1.6–1.8 mm. Body form elongate oval, convex in lateral view (Fig. 4D). ***Color and punctation*:** Dorsally bicolor, head mostly brown, frons and middle region of the clypeus dark brown, lateral sides of the clypeus pale brown; pronotum yellow with two small black round spots along posterior margin; elytra dark brown, with a yellow spot on the anterior third of the elytra, lateral and posterior margins of the elytra yellow (Fig. 4D). Ventrally dark brown; maxillary palps, mouthparts, and antennae yellow (antennal club slightly darker). Pro and meso legs yellow, meta legs pale brown. Clypeus and labrum with dense, fine, and weakly impressed ground punctation (punctures separated by 2 × their width); pronotum and elytra ground punctation fine, weakly impressed and sparser than on head (punctures separated by 3 × their width). ***Head*:** Clypeus and labrum shallowly emarginate anteromedially, lateral margins of the labrum bearing setae. ***Thorax*:** Prosternum carinate medially, strongly raised, acute and pointing anteriorly. Elevation of mesoventrite with two transversal ridges, elevated medially, lateral sides concave; longitudinal ridge broad anteriorly and sharp posteriorly, the point where the three ridges merged wide and blunt (Fig. 10C); elevation flat in ventral view; mesoventrite with triangular shape in ventral view. Metaventrite convex in the median region, pubescent with narrow glabrous patch on the medial and posterolateral area; anterior margin extending to mesoventrite elevation. Metafemora with dense hydrofuge pubescence along basal three-quarters of the anterior margin and along basal one-quarter of the posterior margin, then anterior half of posterior margin with sparse setae. ***Abdomen*:** Abdominal ventrites very densely pubescent. Aedeagus (Fig. 8B) with basal piece 0.6 × the length of a paramere. Base of the parameres narrower than the base of the median lobe; outer margin straight along basal two-thirds, then apically slightly convex, inner margins convex along basal two-thirds and then apically straight; basal two-thirds of the parameres broad then apical third narrower; apex of parameres rounded and pointing inwards. Median lobe shorter than the parameres, approximately triangular, with acute apex; gonopore triangular and situated at apex of median lobe.

Etymology. The specific name comes from the Latin word *insignitus* meaning marked and refers to the distinctive yellow spot in the elytra of this species.

Distribution. Known only from the type locality in southeastern Venezuela (Fig. 15).

Life history. The only known series of this species was collected along the margin of a forested rocky stream (Fig. 12B).

Notionotus juma **sp. nov.**

http://zoobank.org/DA88A467-D7C8-4AE1-A8E2-4033D8AF3364

Figs 4E, 8G, 13E, 15

Type material. ***Holotype*** **(male):** "Brazil: Amazonas: Manaus/ -2.93079, -59.97514, 75 m/ Ducke Reserve, Igarape Barro/ Branco; Short & team; muddy/ pools in swampy

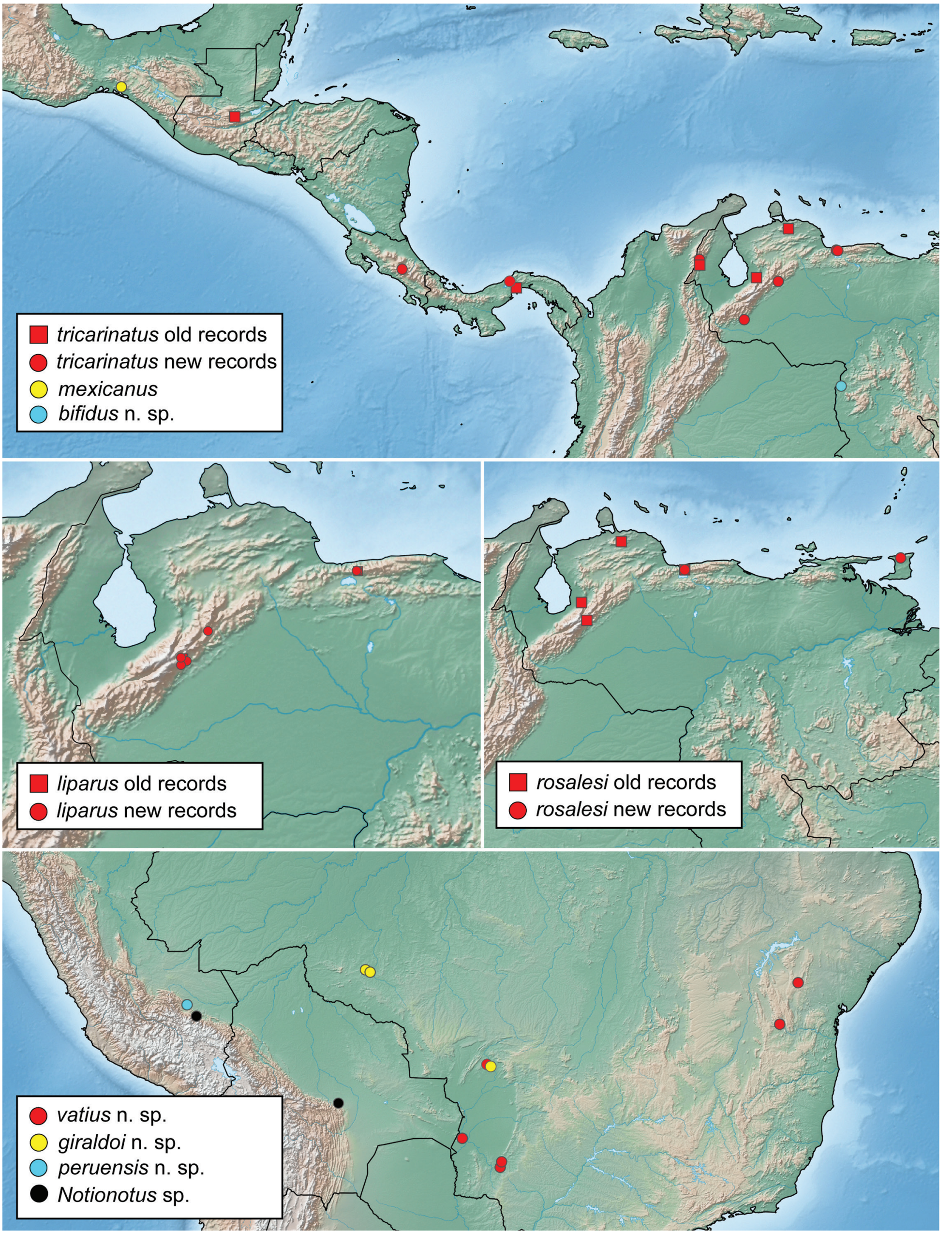

Figure 14. Distribution map of *Notionotus* spp.

area by stream/ 9.vi.2018; BR18-0609-02B" (INPA). ***Paratypes* (16 exs.): Brazil: Amazonas State:** Same data as holotype (13 exs., SEMC); same data except stream margins, 6.vi.2018, BR18-0606-02B (2 exs., SEMC, including DNA voucher SLE2100); Novo Airão Municipio, -2.68396, -60.93840, leg. Benetti, 9.vi.2017, densely vegetated margin of blackwater creek, BR17-0609-04A (1 ex., SEMC, DNA voucher SLE1269).

Differential diagnosis. See differential diagnosis for *Notionotus garciae*. In addition, the aedeagus of *N. juma* has an emargination in the apex of the medium lobe, being a particular feature among the species of the *lohezi* group.

Description. ***Size and form*:** Body length 1.6–1.9 mm. Body form elongate oval, convex in lateral view (Fig. 4E). ***Color and punctation*:** Dorsally bicolor, head pale brown, pronotum yellow with two small black round spots along posterior margin; elytra dark brown (Fig. 4E). Ventrally brown; maxillary palps, mouthparts, and antennae yellow (antennal club slightly darker). Pro and meso legs yellow, meta legs pale brown. Clypeus and labrum with dense, coarse, and moderately impressed ground punctation (punctures separated by 2 × their width); elytra and pronotum ground punctation coarse, moderately impressed and less dense than on head (punctures separated by 3 × their width). ***Head*:** Clypeus and labrum shallowly emarginate anteromedially, lateral margins of the labrum bearing setae. ***Thorax*:** Prosternum carinate medially, strongly raised, acute and pointing anteriorly. Elevation of mesoventrite with two transversal ridges, elevated medially, lateral sides concave; longitudinal ridge broad anteriorly and sharp posteriorly, the point where the three ridges merged wide and blunt (e.g., Fig. 10C, D); elevation flat in ventral view; mesoventrite with triangular shape in ventral view. Metaventrite convex in the median region, pubescent with narrow glabrous patch on the medial and posterolateral area; anterior margin extending to mesoventrite elevation. Metafemora densely covered with hydrofuge pubescence on basal three-quarters. ***Abdomen*:** Abdominal ventrites very densely pubescent. Aedeagus (Fig. 8G) with basal piece nearly the same length as a paramere. Base of the parameres as wide as the base of the median lobe; outer margins convex, then curved inwards along apex, inner margins convex along basal two-thirds, and concave at apical third; apex of parameres rounded. Median lobe shorter than the parameres, wide at basal region, slightly narrowing in the midlength, apex wide and emarginate medially; gonopore with an oval shape and situated at apex of the median lobe.

Etymology. This species is named after the Juma, an indigenous tribe located in the Açuã River, in the southern part of the state of Amazonas-Brazil.

Distribution. Known only from the Ducke Reserve near Manaus, Brazil (Fig. 15).

Life history. Specimens were collected in two habitats at the same forest reserve: in detrital pools in an area of shallowly flooded forest with detrital and mud substrate (Fig. 13E), and along the margins of a small stream.

Notionotus lohezi **Queney, 2010**

Figs 8F, 15

Notionotus lohezi Queney, 2010: 135.

Type material examined. ***Paratype*** **(male):** "♂", "*Notionotus lohezi*/ n. sp. PARATYPE/ P. QUENEY descr. 2010", "Guyane: Régina,/ Patawa, crique en/ forêt, 170 m,/ 13-IX-2009,/ leg. P. Queney" (SEMC). ***Paratypes*** **(5 exs.):** same data as the paratype dissected (5 exs., SEMC).

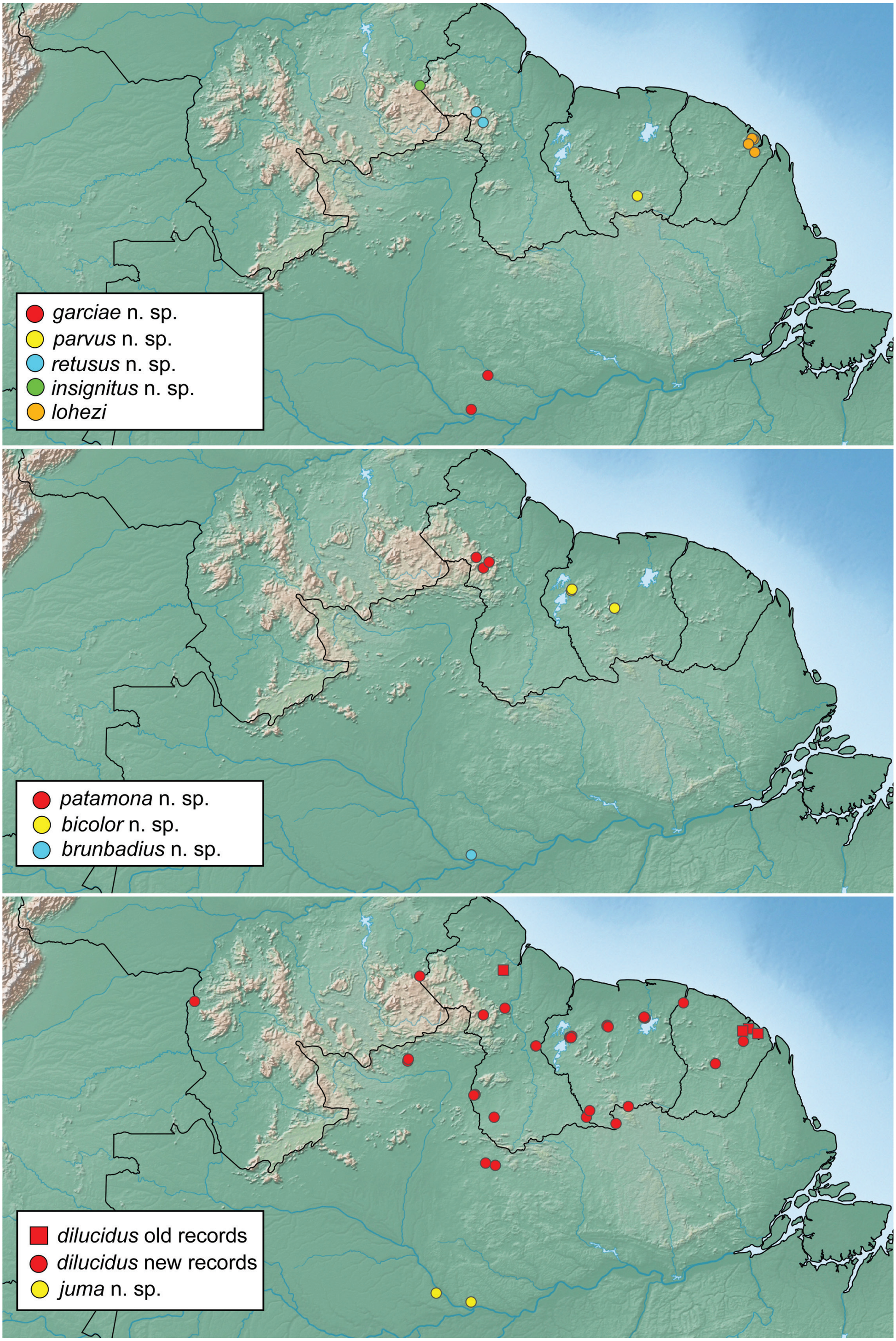

Figure 15. Distribution map of *Notionotus* spp.

Additional material examined (2 exs.). French Guiana: Savane Roche Virginie, near RN 2, 4.1883, -52.13982, 64 m, Crique Chauve-souris, leg. Short, 10.iii.2020, solid granite substrate, detritus along margins on granite, FG20-0310-01A (2 exs., SEMC, including DNA vouchers SLE2337 and 2387).

Differential diagnosis. See differential diagnosis for *Notionotus bicolor*.

Description. ***Size and form*:** Body length 1.6–1.8 mm. Body form elongate oval, convex in lateral view (e.g., Fig. 4A). ***Color and punctation*:** Dorsally bicolor, head bicolor, frons dark brown, clypeus yellow; pronotum yellow with two small black round spots along posterior margin; elytra dark brown, elytra margins paler (e.g., Fig. 4A). Ventrally dark brown; maxillary palps, mouthparts, and antennae yellow (antennal club slightly darker), legs brown. Clypeus and labrum with dense, fine, and weakly impressed ground punctation (punctures separated by 2 × their width); pronotum and elytra ground punctation fine, weakly impressed and sparser than on head (punctures separated by 3 × their width). ***Head*:** Clypeus and labrum shallowly emarginate anteromedially, lateral margins of the labrum bearing setae. ***Thorax*:** Prosternum carinate medially, strongly raised, acute and pointing anteriorly. Elevation of mesoventrite with two transversal ridges, elevated medially, lateral sides concave; longitudinal ridge broad anteriorly and sharp posteriorly, the point where the three ridges merged wide and blunt (e.g., Fig. 10C, D); elevation flat in ventral view; mesoventrite with triangular shape in ventral view. Metaventrite convex in the median region, pubescent with narrow glabrous patch on the medial and posterolateral area; anterior margin extending to mesoventrite elevation. Metafemora with dense hydrofuge pubescence along basal three-quarters of the anterior margin and along basal one-quarter of the posterior margin, then apical half of the posterior margin with sparse setae. ***Abdomen*:** abdominal ventrites very densely pubescent. Aedeagus (Fig. 8F) with basal piece 0.8 × the length of the paramere. Base of the parameres slightly narrower than the base of the median lobe, inner margins straight, then convex reaching the apex, outer margins convex, and rounded apex pointing inwards. Median lobe shorter than the parameres, approximately rectangular with apex blunt; gonopore situated at the apex of the median lobe.

Distribution. This species is only known from a few localities in French Guiana (Fig. 15).

Life history. This species was collected in rocky streams with detritus along margins.

Notionotus parvus **sp. nov.**

http://zoobank.org/08140DE3-8B15-42F9-ADA9-3A1F952C1D3D
Figs 4F, 9E, 15

Notionotus sp. 2 in Short, 2013: 88.

Type material. ***Holotype*** **(male):** "SURINAME: Sipaliwini District/ N 2.97731°, W 55.38500°, 200 m/ Camp 4 (low), Kasikasima; sandy/ stream on trail to METS camp/ 20.iii.2012; SR12-0320-02A/ leg. A. Short; 2012 CI-RAP Survey" (NZCS). ***Paratypes*** **(2 exs.): Suriname:** same data as holotype (2 exs., SEMC, including DNA voucher SLE2388).

Differential diagnosis. *Notionotus parvus* can be recognized by the pale reddish yellow color in the head and pronotum and reddish brown in the elytra (Fig. 4F). Furthermore, the aedeagus is quite unique, parameres tubular in shape with lanceolate appendages in the outer margin which are shorter than the length of the parameres, and gonopore with crown-shape located in the apical region of the median lobe (Fig. 9E).

Description. ***Size and form*:** Body length 1.7–1.9 mm. Body form elongate oval, convex in lateral view (Fig. 4F). ***Color and punctation*:** Dorsally reddish brown, head and pronotum pale reddish yellow; pronotum with two small black round spots along posterior margin; elytra dark reddish brown (Fig. 4F). Ventrally reddish brown; maxillary palps and mouthparts light yellow reddish, and antennae yellow (antennal club slightly darker). Pro and meso legs yellow, meta legs pale reddish brown. Clypeus and labrum with dense, fine, and weakly impressed ground punctation (punctures separated by 2 × their width); pronotum and elytra ground punctation fine, weakly impressed and sparser than on head (punctures separated by 3 × their width). ***Head*:** Clypeus and labrum shallowly emarginate anteromedially, lateral margins of the labrum bearing setae. ***Thorax*:** Prosternum carinate medially, strongly raised, acute and pointing anteriorly. Elevation of mesoventrite with two transversal ridges, elevated medially, lateral sides concave; longitudinal ridge broad anteriorly and sharp posteriorly, the point where the three ridges merged wide and blunt (e.g., Fig. 10C, D); elevation slightly convex in ventral view; mesoventrite with triangular shape in ventral view. Metaventrite convex in the median region, pubescent with narrow glabrous patch on the medial and posterolateral area; anterior margin extending to mesoventrite elevation. Metafemora with dense hydrofuge pubescence along basal three-quarters of the anterior margin and sparse pubescence along the apical posterior margin. ***Abdomen*:** Abdominal ventrites very densely pubescent. Aedeagus (Fig. 9E) with basal piece 0.5 × the length of a paramere. Base of the parameres narrower than the base of the median lobe; parameres tubular shape, outer margins sinuate and covered by lanceolate appendages that cover three-quarters of the margin; inner margins sinuate, apex of the parameres rounded. Median lobe shorter than the parameres, wide at basal region, narrowing apically, apex rounded and wide; gonopore crown-shaped and situated at apex of median lobe.

Etymology. The species name is derived from the Latin word *parvus* meaning little or small in reference to the small aedeagus size of this species.

Distribution. Only known from the type locality in southern Suriname (Fig. 15).

Life history. This species was collected along the margins of a small, sandy-bottomed stream.

Notionotus patamona **sp. nov.**

http://zoobank.org/B8AC3A70-8620-44E5-8665-709DCF4307AA

Figs 4B, 8D, 12C, 15

Type material. ***Holotype*** **(male):** "GUYANA: Region XIII [!sic: Region 8]/ 5°18.264'N, 59°50.257'W; 687 m/ Ayanganna Airstrip; trail from air-/ strip to Ayanganna; seepage area; over rocks in forest flowing into/ stream; leg. A. Short; 18.iii.2014/

GY14-0318-01C" (CBDG). ***Paratype*** **(12 exs.): Guyana: Region 8:** Same data as holotype (8 exs., SEMC); Upper Potaro Camp I (ca. 7 km NW Chenapau), Potaro margin trail, 5°0.660'N, 59°38.283'W, 484 m, 11.iii.2014, leg. Short, Baca, Salisbury and La Cruz, wet detritus in sandy area, GY14-0311-04A (1 ex., SEMC); top of falls on Potaro River, 5°0.730'N, 59°38.965'W, 585 m, 12.iii.2014, leg. Short, Salisbury and La Cruz, seeps with roots and algae, GY14-0312-01B (1 ex., SEMC); stream near camp, 5°0.673'N, 59°38.358'W, 500 m, 14.iii.2014, leg. Short, Salisbury and La Cruz, gravel/sandy stream w/ detritus, GY14-0314-01A (1 ex., SEMC); Kaieteur Natural Park, trail by guest house, 5°10.514'N, 59°28.970'W, 440 m, 21.iii.2014, leg. Short, Salisbury and La Cruz, forest pools, GY14-0321-01B (1 ex., SEMC).

Differential diagnosis. See differential diagnosis for *Notionotus bicolor*.

Description. ***Size and form*:** Body length 1.6–1.8 mm. Body form elongate oval, convex in lateral view (Fig. 4B). ***Color and punctation*:** Dorsally bicolor, head brown, frons dark brown, clypeus pale brown; pronotum yellow with two small black round spots along posterior margin; elytra dark brown, elytra margins paler (Fig. 4B). Ventrally brown; maxillary palps, mouthparts, antennae, and legs yellow. Clypeus and labrum with dense, fine, and weakly impressed ground punctation (punctures separated by 2 × their width); pronotum and elytra ground punctation fine, weakly impressed and sparser than on head (punctures separated by 3 × their width). ***Head*:** Clypeus and labrum shallowly emarginate anteromedially, lateral margins of the labrum bearing setae. ***Thorax*:** Prosternum carinate medially, strongly raised, acute and pointing anteriorly. Elevation of mesoventrite with two transversal ridges, elevated medially, lateral sides concave; longitudinal ridge broad anteriorly and sharp posteriorly, the point where the three ridges merged wide and blunt (e.g., Fig. 10C, D); elevation flat in ventral view; mesoventrite with triangular shape in ventral view. Metaventrite convex in the median region, pubescent with narrow glabrous patch on the medial and posterolateral area; anterior margin extending to mesoventrite elevation. Metafemora with dense hydrofuge pubescence along basal three-quarters of the anterior margin and along basal one-quarter of the posterior margin, then apical half of the posterior margin with sparse setae. ***Abdomen*:** Abdominal ventrites very densely pubescent. Aedeagus (Fig. 4B) with basal piece 0.7 × the length of a paramere. Base of the parameres narrower than the base of the median lobe; outer margins straight along basal two-thirds, then apically slightly convex, inner margins straight along basal two-thirds and then convex and tapering apically; apex of parameres rounded and pointing inwards. Median lobe shorter than the parameres, approximately triangular, gradually narrowing from the base, broad and rounded apex; gonopore oval-shaped and situated at apex of median lobe.

Etymology. This species is named after the Patamona, an indigenous tribe located in the mountainous region from which this species is known.

Distribution. Known from several closely situated localities in western Guyana (Fig. 15).

Life history. This species was collected at several a variety of stream-associated habitats, including along the margins of detritus and sandy-based streams, as well as in rock seepage habitats adjacent to streams (Fig. 12C).

***Notionotus retusus* sp. nov.**
http://zoobank.org/366A532F-DAAF-4521-9E0B-CD6AACA17266
Figs 8E, 13F, 15

Type material. *Holotype* (male): "GUYANA: Region XIII [!sic: Region 8]/ 5°0.730'N, 59°38.965'W, 585 m/ Upper Potaro Camp I (c. 7 km/ NW Chenapau), Ridge Trial/ leg. Short, Baca and Salisbury/ 11.iii.2014; GY14-0311-02A", "DNA VOUCHER/ Extraction #/ SLE-2110" (CBDG). ***Paratype* (1 ex.): Guyana: Region 8:** Ayanganna Airstrip, 5°18.264'N, 59°50.257'W; 687 m, trail from airstrip to Ayanganna, leg. A. Short, 18.iii.2014, seepage area over rocks in forest flowing into stream, GY14-0318-01C (1 ex., SEMC, DNA voucher 2372)

Differential diagnosis. The external characters of *Notionotus retusus* and *N. lohezi* are quite similar. The only way they can be separated is by the features of the aedeagus. In this species, the apex of the parameres is wide and rounded (acute in *N. lohezi*, Fig. 8F), the median lobe is much longer than in *N. lohezi* and the gonopore is elongated and oval (nearly rectangular in *N. lohezi*).

Description. *Size and form*: Body length 1.8 mm. Body form elongate oval, moderately convex in lateral view. ***Color and punctation*:** Dorsally bicolor, head mostly brown, frons brown, clypeus pale brown; pronotum yellow with two small black round spots along posterior margin; elytra dark brown. Ventrally brown; maxillary palps, mouthparts, antennae (antennal club slightly darker), legs brown. Clypeus and labrum with dense, fine, and weakly impressed ground punctation (punctures separated by 2 × their width); pronotum and elytra ground punctation fine, weakly impressed, and sparser than on head (punctures separated by 3 × their width). ***Head*:** Clypeus and labrum shallowly emarginate anteromedially, lateral margins of the labrum bearing setae. ***Thorax*:** Prosternum carinate medially, strongly raised, acute and pointing anteriorly. Elevation of mesoventrite with two transversal ridges, elevated medially, lateral sides concave; longitudinal ridge broad anteriorly and sharp posteriorly, the point where the three ridges merged wide and blunt (e.g., Fig. 10C, D); elevation flat in ventral view; mesoventrite with triangular shape in ventral view. Metaventrite convex in the median region, pubescent with narrow glabrous patch on the medial and posterolateral area; anterior margin extending to mesoventrite elevation. Metafemora with dense hydrofuge pubescence along basal three-quarters of the anterior margin and along basal one-quarter of posterior margin, then apical half of the posterior margin with sparse setae. ***Abdomen*:** Abdominal ventrites very densely pubescent. Aedeagus (Fig. 8E) with basal piece 0.7 × the length of a paramere. Base of the parameres nearly the same as the base of the median lobe; outer margins convex, inner margins nearly straight; apex of parameres broad, rounded and slightly pointing inwards. Median lobe shorter than the parameres, wide at basal region, narrowing in basal third, margins straight and apex rounded and nearly notched; gonopore with an oval shape and covering approximately two-thirds of the length of the median lobe.

Etymology. The specific name comes from the Latin word *retusus* meaning rounded and notched, after the form of the apex of the median lobe of the aedeagus.

Distribution. This species is only known from the type locality in western Guyana (Fig. 15).

Life history. This species was collected in detrital-filled pools in a shallow ravine with dense forest cover (Fig. 13F). Although the pools might not be considered a stream, the pools were part of a drainage network.

Notionotus rosalesi species group

Diagnosis. The species of this group can be recognized by the unique dorsal coloration, being almost yellow with a wide brown band in the third anterior of the elytra (Fig. 2G), the elevation of the mesoventrite with one transversal and longitudinal ridge (e.g., Fig. 10B), the shape of the genitalia is quite distinct, being the only one within all *Notionotus* species of the Neotropical region with the apical third of the parameres membranous (Fig. 9A–C).

Notionotus rosalesi Spangler, 1972

Figs 2G–I, 9A–C, 14

Notionotus rosalesi Spangler, 1972: 141

Type material examined. Holotype (male): "VENEZUELA/Arag., 10 Km S./Rancho Grande/II-14-1969/P.&P. Spangler", "TypeNo/71950/U S N M", "HOLOTYPE/Notionotus/rosalesi/P.J.Spangler" (USNM).

Additional material examined. Trinidad: Guanapo State: 4.1 km up Guanapo Valley, trib of Guanapo River, 460 ft, 11-VII-2005 (1 ex., SEMC); Verdant vale, Arima River, 10°42'N, 61°18'W, 570 ft, 9-VII-2005 (1 ex., SEMC). **Venezuela: Aragua:** Rancho Grande Biol. Stn. 1150 m, 10°21'N, 67°41'W, 25–28 II 1995, S. Marshall, yellow pan trap (1 ex., SEMC).

Differential diagnosis. *Notionotus rosalesi* can be distinguished by the wide brown band in the anterior third of the elytra, as well as, the unique shape of the genitalia, having many accessories at the base of the parameres, the apex of the parameres membranous and lanceolate.

Description. ***Size and form*:** Body length 1.8–1.9 mm. Body form elongate oval, moderately convex in lateral view (Fig. 2G). ***Color and punctation*:** Dorsally bicolor, head mostly brown, frons brown, medially region of the clypeus pale brown with lateral margins yellow; pronotum yellow with two small black round spots along posterior margin; elytra yellow except by a brown wideband on the anterior third of the elytra (Fig. 2G). Ventrally brown; maxillary palps, mouthparts, antennae, and legs yellow (antennal club slightly darker) (Fig. 2H). Clypeus and labrum with dense, fine, and weakly impressed ground punctation (punctures separated by 5 × their width); pronotum and elytra ground punctation fine, weakly impressed and sparser than on head (punctures separated by 3 × their width). ***Head*:** Clypeus and labrum shallowly emarginate anteromedially, lateral margins of the labrum bearing setae. ***Thorax*:** Prosternum carinate medially, strongly raised, pointing anteriorly and acute. Elevation of mesoventrite with one transversal ridge, elevated medially, lateral sides concave; longitudinal ridge narrowed anteriorly and broadening posteriorly, the point where the two ridges merged acute (e.g., Fig. 10B); elevation concave in lateral view; mesoventrite with triangular shape in ventral view. Metaventrite convex in the median region, pubescent with narrow glabrous patch on the medial and postero-lateral area; anterior margin extending to mesoventrite elevation. Metafemora with dense hydrofuge pubescence along basal three-quarters of the anterior margin and along basal half of the posterior margin. ***Abdomen*:** Abdominal ventrites very densely pubescent. Aedeagus (Fig. 9A–C) basal piece 0.4 × the length of a paramere; broad parameres, base of the parameres much wider than the base of the median lobe, base of the parameres with two accessories with ovate shape, outer margins of parameres strongly sinuate, inner margins slightly sinuate, with membranous acuminate apex, bending outwards; median lobe shorter than the parameres, approximately triangular, with apex rounded.

Distribution. Originally described from the Venezuelan states of Aragua and Barinas (Spangler 1972), it was later reported from the states of Trujillo and Falcón (García 2000). Here we report it for the first time from Trinidad (Fig. 14).

Life history. Although specific habitat information is limited, all specimens were collected in association with streams. Spangler (1972) characterized this species as a hygropetric specialist, although not all specimens known at that time were from seepages (the others were from a stream pool that "was in the bedrock and the bottom was covered with rotting leaves").

Remarks. The genitalia of the holotype appears to have some modest fungal growth on the median lobe (Fig. 9B), the circular "halo" at the tip of the median lobe appears to be unnatural and is not part of the original structure.

Notionotus peruensis species group

Diagnosis. The species of *peruensis* group can be diagnosed by the dorsal coloration completely yellow, the elevation of the mesoventrite with one transverse and one longitudinal (e.g., Fig. 10B), and by the shape of the genitalia (Fig. 9F).

Notionotus peruensis sp. nov.

http://zoobank.org/4E05420D-577E-4B12-8B2B-783B0C0BB101
Figs 4K, 9F, 14

Type material examined. ***Holotype*** **(male):** "PERU: Dept. Madre de/ Dios: Pantiacolla Lodge,/ Alto Madre de Dios R./ 12°39.3'S, 71°13.9'W 420 m/ 14–19-XI-2007 D. Brzoska/ ex. flight intercept trap/ PER1B07 004" (SEMC).

Differential diagnosis. *Notionotus peruensis* can be distinguished by the particular shape of the aedeagus, being nearly rectangular in the basal half and abruptly narrow in the apical half (Fig. 9F).

Description. ***Size and form*:** Body length 1.6 mm. Body form elongate oval, convex in lateral view (Fig. 4K). ***Color and punctation*:** Dorsally yellow, head mostly yellow and frons pale brown; pronotum with two small black round spots along posterior margin (Fig. 4K). Ventrally brown; maxillary palps, mouthparts, antennae (antennal club slightly darker) and legs yellow. Clypeus and labrum with dense, fine, and weakly impressed ground punctation (punctures separated by 2 × their width); pronotum and elytra ground punctation fine, weakly impressed and sparser than on head (punctures separated by 3 × their width). ***Head*:** Clypeus and labrum shallowly emarginate anteromedially, lateral margins of the labrum bearing setae. ***Thorax*:** Prosternum carinate medially, strongly raised, pointing anteriorly and acute. Elevation of mesoventrite with one transversal ridge, elevated medially, lateral sides concave; longitudinal ridge sharp, the point where the two ridges merged acute (e.g., Fig. 10B); elevation flat in lateral view; mesoventrite with triangular shape in ventral view. Metaventrite convex in the median region, pubescent with narrow glabrous patch on the medial and posterolateral area, medial region patch drop-shaped; anterior margin extending to mesoventrite elevation. Metafemora densely covered with hydrofuge pubescence on basal three-quarters. ***Abdomen*:** Abdominal ventrites very densely pubescent. Aedeagus (Fig. 9F) with basal piece 0.7 × the length of a paramere. Base of the parameres wider than the base of the median lobe; outer margins straight along basal two-thirds, then apically sinuate, inner margins straight along basal two-thirds and then convex and tapering apically; apex of parameres rounded and pointing outwards. Median lobe much shorter than the parameres, basal half rectangular, apical half narrowing abruptly, apex rounded.

Etymology. The species is named after Peru, the country where it was collected, as well as for being the first species described for the genus in this country.

Distribution. Known only from the type locality in Peru (Fig. 14).

Life history. The single specimen was collected at a flight intercept trap; nothing is known about its habitat.

***Notionotus* spp.**
Fig. 14

Material examined (2 exs.). Bolivia: Santa Cruz: Amboro National Park, Guarda Parque Mataracu, 21–27.xi.2004, malaise trap, leg. Robertson, García, & Vidaurre (1 female, UMSP). **Peru: Cusco:** Quispicanchi Province, streams 1 km N Quince Mil, 13°13.335'S, 70°46.035'W, 730 m, 9.i.2020, leg. Baca., Slow rivulets & pools w/ saturated detritus next to stream, PE20-0109-02A (1 female, SEMC, DNA voucher SLE2140).

Remarks. We examined two single female specimens from unique localities that we refrain from identifying or describing, due to the lack of male genitalia for comparison. The specimen from Peru likely represents an undescribed species, as suggested by its distant position in our DNA tree (Fig. 1). The single female from Bolivia is the first and only known record of the genus from that country.

Key to the species groups of *Notionotus* of the Neotropical Region

Although it is fairly straightforward to key specimens (especially males) to species group, identification to species within each group almost always requires examination of the aedeagus. For this reason, as well as the fact that there are no doubt many yet-to-be-described species, particularly in the southern Amazon region, we do not include a species key here.

1 Elevation of the mesoventrite composed by two ridges (one transverse and one longitudinal) (e.g., Fig. 10A, B)..**2**
– Elevation of the mesoventrite composed by three ridges (two transverse and one longitudinal) (e.g., Fig. 10C, D)............................ ***lohezi* species group**
2 Length of the parameres nearly the same as the length of the basal piece. Length of the median lobe almost the same as the parameres (e.g., *N. liparus*, Fig. 7A) ....***liparus* species group**
– Length of the parameres longer than the basal piece. Length of the median lobe almost the same as the parameres **3**
3 Outer margin of the parameres convex and tapering reaching the apex, rounded apex. Median lobe rectangular along basal half then tapering abruptly (e.g., *N. peruensis* sp. nov., Fig. 9F)......................***peruensis* species group**
– Outer margin of the parameres sinuate, apex of the parameres lanceolate. Median lobe wide and approximately triangular (e.g., *N. rosalesi*, Fig. 9F) .... ***rosalesi* species group**

Discussion

Since *Notionotus* was first described as a hygropetric genus from the Andean Region of Venezuela fifty years ago (Spangler 1972), our knowledge of the genus has substantially expanded. Within the Neotropical region, this present work expands the distribution throughout much of tropical South America, including the first records from Peru, Bolivia, and Brazil. We also find that while the originally described species do appear to prefer hygropetric habitats (especially *N. liparus*), most species are not found in seepages but prefer leaf packs and margins of forested streams. The vast majority of specimens have been collected at sites under 1000 meters in elevation, though *N. liparus* has been found as high as 1770 m. Although the highest density of known specimen records remains in the northern quarter of South America, particularly Venezuela and the Guiana Shield region, this is almost certainly an artifact of collecting effort, as aquatic beetles are in general less well known in the central and southern Amazon region. While many new species undoubtedly remain to be described, we also found that some species have quite expansive ranges (e.g., *N. dilucidus*, *N. tricarinatus*, *N. vatius*) and care should be taken to put even seemingly geographically distant new collections in context with existing species. The integration of DNA sequence data proved invaluable in helping to establish species limits in these widespread taxa.

Acknowledgements

We are grateful for the assistance and support of many colleagues during fieldwork, including Mauricio García (MALUZ), Jesús Camacho (MALUZ), Luis Joly (MIZA), Neusa Hamada (INPA), Cesar Benetti (INPA), Simon Clavier (ONIKHA, French Guiana), Vanessa Kadosoe (NZCS), and Paul Ouboter (NZCS). Charyn Micheli (USNM) provided continued access to type material in the Spangler collection. Stephen Baca is thanked for assisting with generating the molecular data. We are thankful to the assistance of Jennifer Girón with the dissection methodology of the specimens. Fieldwork in Suriname and Guyana was partly funded by Conservation International and WWF-Guianas respectively. Fieldwork in Brazil was partly funded by a Fulbright fellowship to AEZS and under SISBIO license 59961-1. We are grateful to the Office National des Forêts for the help provided during fieldwork in French Guiana. The expedition to Tafelberg was funded by grant #9286-13 from the National Geographic Society Committee for Research and Exploration to AEZS. This study was supported by the US National Science Foundation grant DEB-1453452 to AEZS.

References

García M (2000) Dos nuevas especies de *Notionotus* Spangler, 1972 (Coleoptera: Hydrophilidae: Hydrophilinae), de Venezuela, y nuevos registros para *N. rosalesi* y *N. liparus*. Boletín del centro de Investigaciones biológicas 34: 247–258.

Girón JC, Short AEZ (2017) Revision of the Neotropical water scavenger beetle genus *Quadriops* Hansen, 1999 (Coleoptera: Hydrophilidae: Acidocerinae). ZooKeys 705: 115–141. https://doi.org/10.3897/zookeys.705.19815

Hansen M (1991) The hydrophiloid beetles. Phylogeny, classification and a revision of the genera (Coleoptera: Hydrophilidae). Biologiske Skrifter 40: 1–367. https://books.google.bg/books?id=eWx1YOZrt6cC&lpg=PA1&dq=Hansen%20M%20(1991)%20The%20hydrophiloid%20beetles.%20Phylogeny%2C%20classification%20and%20a%20revision%20of%20the%20genera%20(Coleoptera%3A%20Hydrophilidae).%20Biologiske%20Skrifter%2040%3A%201%E2%80%93367.&lr&hl=es&pg=PA1#v=onepage&q&f=false

Hebauer F (2001) The genus *Notionotus* Spangler, 1972 in the Old World (Coleoptera: Hydrophilidae). Acta Coleopterologica 17(4): 9–14.

Hebauer F (2003) Another new *Notionotus* from southern India (Coleoptera: Hydrophilidae). Acta Coleopterologica 19(1): 63–66.

Jia FL, Short AEZ (2011) *Notionotus attenuatus* sp. n. from southern China with a key to the Old World species of the genus (Coleoptera: Hydrophilidae). Zootaxa 2830(1): 55–58. https://doi.org/10.11646/zootaxa.2830.1.5

Kohlenberg AT, Short AEZ (2017) Revision of the Neotropical water scavenger beetle genus *Tobochares* Short and García, 2007 (Coleoptera, Hydrophilidae, Acidocerinae). ZooKeys 669: 113–146. https://doi.org/10.3897/zookeys.669.11773

Lawrence J, Ślipiński A (2013) Australian Beetles: morphology, classification and keys. CSIRO Publishing, Melbourne, Australia, 576 pp. https://books.google.bg/books?id=xYMHA

QAAQBAJ&lpg=PP1&dq=Lawrence%20J%2C%20%C5%9Alipi%C5%84ski%20A%20(2013)%20Australian%20Beetles%3A%20morphology%2C%20classification%20and%20keys.%20CSIRO%20Publishing%2C%20Melbourne%2C%20Australia%2C%20576%20pp.&lr&hl=es&pg=PP1#v=onepage&q&f=false

Minh BQ, Nguyen MAT, von Haeseler A (2013) Ultrafast approximation for phylogenetic bootstrap. Molecular Biology and Evolution 30(5): 1188–1195. https://doi.org/10.1093/molbev/mst024

Nguyen L-T, Schmidt HA, von Haeseler A, Minh BQ (2015) IQ-TREE: A Fast and Effective Stochastic Algorithm for Estimating Maximum-Likelihood Phylogenies. Molecular Biology and Evolution 32(1): 268–274. https://doi.org/10.1093/molbev/msu300

Perkins PD (1979) Three new Middle American species of aquatic beetles in the genus *Notionotus* Spangler (Hydrophilidae: Hydrobiinae). Journal of the New York Entomological Society 87: 304–311.

Queney P (2010) Three new species of *Notionotus* Spangler from French Guiana and Guyana. Koleopterologische Rundschau 80: 129–137. https://www.zobodat.at/pdf/KOR_80_2010_0129-0137.pdf

Short AEZ (2013) Chapter 4. Aquatic Beetles of the Grensgebergte and Kasikasima Regions, Suriname (Insecta: Coleoptera). In: Alonso LE, Larsen TH (Eds) A Rapid Biological Assessment of the Upper Palumeu River Watershed (Grensgebergte and Kasikasima) of Southeastern Suriname. RAP Bulletin of Biological Assessment. Vol. 67. Conservation International, Arlington, VA, 79–89.

Short AEZ, Girón JC (2018) Review of the *Helochares* (Hydrobaticus) of the New World (Coleoptera: Hydrophilidae: Acidocerinae). Zootaxa 4407(1): 29–50. https://doi.org/10.11646/zootaxa.4407.1.2

Short AEZ, Kadosoe V (2011) Chapter 4. Aquatic Beetles of the Kwamalasamutu Region, Suriname (Insecta: Coleoptera). In: O'Shea BJ, Alonso LE, Larsen TH (Eds) A Rapid Biological Assessment of the Kwamalasamutu region, Southwestern Suriname. RAP Bulletin of Biological Assessment 63, Conservation International, Arlington, VA, 79–90.

Short AEZ, Salisbury S, La Cruz N (2017) Aquatic Beetles of the Upper Potaro Region, Guyana. BAT Survey Report No. 2. WWF-Guianas, Guyana Office. Georgetown, Guyana, 132–141. https://wwflac.awsassets.panda.org/downloads/bat_knp___upper_potaro__final_report_lowres_2.pdf

Short AEZ, Salisbury S, La Cruz N (2018) Aquatic Beetles of the Upper Berbice Region, Guyana. BAT Survey Report No. 3. WWF-Guianas, Guyana Office. Georgetown, Guyana, 128–135. https://wwfeu.awsassets.panda.org/downloads/biodiversity_assessment_survey_of_the_upper_berbice_region_2018.pdf

Shorthouse DP (2010) SimpleMappr, an online tool to produce publication-quality point maps. http://www.simplemappr.net [Accessed 10 January 2022]

Smith RR, Short AEZ (2020) Review of the genus *Chasmogenus* Sharp, 1882 of northeastern South America with an emphasis on Venezuela, Suriname, and Guyana (Coleoptera, Hydrophilidae, Acidocerinae). ZooKeys 934: 25–79. https://doi.org/10.3897/zookeys.934.49359

Spangler PJ (1972) A new genus and two new species of madicolous beetles from Venezuela (Coleoptera: Hydrophilidae). Proceedings of the Biological Society of Washington 85: 139–146.